Materials Reliability Program
Resistance to Primary Water Stress Corrosion Cracking of Alloys 690, 52, and 152 in Pressurized Water Reactors (MRP-111)

1009801

Materials Reliability Program
Resistance to Primary Water Stress Corrosion Cracking of Alloys 690, 52, and 152 in Pressurized Water Reactors (MRP-111)

1009801

Technical Update, March 2004

EPRI Project Manager

J. Hickling

C. King

EPRI • 3412 Hillview Avenue, Palo Alto, California 94304 • PO Box 10412, Palo Alto, California 94303 • USA
800.313.3774 • 650.855.2121 • askepri@epri.com • www.epri.com

DISCLAIMER OF WARRANTIES AND LIMITATION OF LIABILITIES

ORGANIZATION(S) THAT PREPARED THIS DOCUMENT

Framatome ANP

This is an EPRI Technical Update report. A Technical Update report is intended as an informal report of continuing research, a meeting, or a topical study. It is not a final EPRI technical report.

ORDERING INFORMATION

Requests for copies of this report should be directed to EPRI Orders and Conferences, 1355 Willow Way, Suite 278, Concord, CA 94520. Toll-free number: 800.313.3774, press 2, or internally x5379; voice: 925.609.9169; fax: 925.609.1310.

CITATIONS

This report was prepared by Framatome ANP

Principal Investigators

H. Xu and S. Fyfitch,
Framatome ANP, Inc.
3315 Old Forest Road
P.O. Box 10935
Lynchburg, VA 24506-0935

P. Scott
Framatome ANP, SAS
Tour AREVA
92084 Paris La Défense, France

M. Foucault
Framatome ANP, SAS
Porte Magenta – BP 181
71205 Le Creusot Cedex, France

R. Kilian and M. Winters,
Framatome ANP, GmbH
Freyeslebenstr. 1 – 91058
TGM – P.O. Box 3220 – 91050
Erlangen, Germany

The report is a corporate document that should be cited in the literature in the following manner:

Materials Reliability Program (MRP), Resistance to Primary Water Stress Corrosion Cracking of Alloys 690, 52, and 152 in Pressurized Water Reactors (MRP-111), EPRI, Palo Alto, CA: 2004. 1009801.

REPORT SUMMARY

Wrought Alloy 600 and its weld metals (Alloy 182 and Alloy 82) were originally used in pressurized water reactors (PWRs) due to the material's inherent resistance to general corrosion in a number of aggressive environments and because of a coefficient of thermal expansion that is very close to that of low alloy and carbon steel. Over the last thirty years, stress corrosion cracking in PWR primary water (PWSCC) has been observed in numerous Alloy 600 component items and associated welds, sometimes after relatively long incubation times. The occurrence of PWSCC has been responsible for significant downtime and replacement power costs.

Component repairs and replacements have generally utilized wrought Alloy 690 material and its compatible weld metals (Alloy 152 and Alloy 52), which have been shown to be highly resistant to PWSCC in laboratory experiments and have been free from cracking in operating reactors over periods already up to nearly 15 years. The challenge is to attempt to quantify the longevity of these materials with respect to aging degradation by corrosion in order to provide a sound technical basis for the development of future inspection requirements for repaired or replaced component items.

Approach

This document first reviews numerous laboratory tests, conducted over the last two decades, that were performed with wrought Alloy 690 and Alloy 52 or 152 weld materials under various test conditions pertinent to corrosion resistance in PWR environments. The main focus of the present review is on PWSCC, but secondary-side conditions are also briefly considered. Wherever possible, the existing laboratory test data have been evaluated to estimate the improvement factor of Alloy 690 relative to Alloy 600. In addition, Alloy 690 service experience in PWRs has been reviewed to augment the laboratory findings. The project team also worked to identify gaps in the existing database and suitable strategies to rectify these, as well as to provide a technical justification basis for future inspection requirements for these materials.

Results & Findings

It is concluded that wrought Alloy 690 and its weld metals (Alloys 52 and 152) are acceptable and highly corrosion-resistant replacement materials for Alloy 600 and its weld metals in PWRs, although limited, further testing is needed to examine some specific knowledge gaps that have been identified. Average improvement factors of at least 26 relative to Alloy 600MA material and 13 relative to Alloy 600TT material can be derived, but these numbers are clearly conservative, due to an absence of PWSCC in most Alloy 690 specimens within the test duration.

No stress corrosion degradation of the Alloy 690 materials has been observed in any replacement application to date. Service experience ranges from approximately10 to 14 years, depending upon the type of component considered.

The PWSCC inspection regimes developed in recent years for thick-walled components made of Alloys 600, 182, and 82 would be unnecessarily stringent if applied in exactly the same way to comparable component locations involving Alloy 690 and its weld metals. A separate inspection program, commensurate with the magnitude of improvement in PWSCC resistance already demonstrated, should be developed.

Applications, Values & Use

This report should be of interest to utility engineers and scientists concerned with all aspects of Alloy 600 cracking in PWR primary water, and especially to those involved in developing inspection regimes, making decisions on component replacement and dealing with plant aging issues. It will be of direct value in obtaining regulatory acceptance for the solutions adopted by the industry to deal with increasing incidences of PWSCC in thick-walled components of existing plants.

As part of an ongoing, comprehensive program involving utilities, reactor vendors and engineering/research organizations, this report will also help to ensure that corrosion degradation of nickel-base alloys does not limit service life and that full benefit can be obtained from improved designs for both replacement components and new reactors.

EPRI Perspective

The challenge facing the project team was first to gain access to a large amount of both published and unpublished data, and then to analyze and integrate the findings from very diverse experimental programs carried out over many years in a coherent way. EPRI was in a unique position to facilitate this exercise and benefited, in particular, from extensive previous experience gained in connection with related studies of steam generator tube degradation (see, e.g., TR 1003589 published in July, 2003). Together with consideration of field experience, this has resulted in a comprehensive status document addressing the issue of what factor of improvement can be expected when replacing PWSCC susceptible Alloy 600 materials in thick-walled components with Alloy 690 and its weld metals.

Some specific knowledge gaps were identified during the present review and will enable scant resources to be focused appropriately on future testing of Alloy 690 materials and monitoring of their service behavior. It is anticipated that this report will be updated and further refined as additional laboratory results and field inspection data become available.

Keywords

Alloy 600, Alloy 690, Alloy 52, Alloy 152, PWSCC, Material Degradation, Predictive Maintenance.

ABSTRACT

Over the last thirty years, stress corrosion cracking in PWR primary water (PWSCC) has been observed in numerous Alloy 600 component items and associated welds, sometimes after relatively long incubation times. Repairs and replacements have generally utilized wrought Alloy 690 material and its compatible weld metals (Alloy 152 and Alloy 52), which have been shown to be very highly resistant to PWSCC in laboratory experiments and have been free from cracking in operating reactors over periods already up to nearly 15 years. It is nevertheless prudent for the PWR industry to attempt to quantify the longevity of these materials with respect to aging degradation by corrosion in order to provide a sound technical basis for the development of future inspection requirements for repaired or replaced component items.

This document first reviews numerous laboratory tests, conducted over the last two decades, that were performed with wrought Alloy 690 and Alloy 52 or Alloy 152 weld materials under various test conditions pertinent to corrosion resistance in PWR environments. The main focus of the present review is on PWSCC, but secondary-side conditions are also briefly considered. Test media relevant to the primary circuit included high temperature de-aerated/hydrogenated water (with and without additions of zinc or some impurities), simulated primary water and hydrogenated steam (sometimes doped with contaminants).

The vast majority of the Alloy 690 specimens did not develop cracking after exposure time as long as 100,000 hours, whereas most of the Alloy 600 specimens in both MA and TT conditions developed PWSCC in the same studies, often after relatively brief periods. Occasional instances of shallow intergranular cracking in Alloy 690 material were more consistent with mechanical microfissuring than PWSCC, although the latter may be possible to a small extent in conjunction with abnormal heat treatments and unusual alloy microstructures or compositions. No PWSCC of the Alloy 152/52 weld metals has been identified to date, but investigations are limited and the resistance of the weld heat affected zone in the base metal does not appear to have been separately studied. Focused testing of Alloy 690 material and its weld metals should be carried out to fill in some specific knowledge gaps that have been identified in the present review.

Wherever possible, the existing laboratory test data have been evaluated to estimate the improvement factor of Alloy 690 relative to Alloy 600. Average improvement factors of at least 26 relative to Alloy 600MA material and 13 relative to Alloy 600TT material can be derived, but these numbers are clearly conservative, due to an absence of PWSCC in most Alloy 690 specimens within the test duration.

In addition, Alloy 690 service experience in PWRs has been reviewed to augment the laboratory findings. Based on both laboratory and field data, it is concluded that Alloy 690 and its weld metals Alloys 52 and 152 are very unlikely that PWSCC would develop during extended PWR

plant lifetimes (60+ years). Hence, the PWSCC inspection regimes developed in recent years for thick-walled component items made of Alloys 600, 182, and 82 would be unnecessarily stringent if applied in exactly the same way to comparable component item locations involving Alloy 690 and its weld metals. A separate inspection program, commensurate with the magnitude of improvement in PWSCC resistance already demonstrated, should be developed. It is anticipated that this could be further refined as additional laboratory results and field inspection data become available.

CONTENTS

List of Figures

List of Tables

List of Acronyms

ALARA – As low as reasonably achievable

APFIM – Atom probe field ion microscope (microscopy)

ATEM – Analytical transmission electron microscope (microscopy)

ASME – American Society of Mechanical Engineers

ASTM – American Society for Testing and Materials

AWS – American Welding Society

AVT – All Volatile Treatment

CEA – Commisariat à l`Énergie Atomique (the French Atomic Energy Commission)

CL – Constant Load

CLT – Constant load test

CEDM – Control element drive mechanism

CERT – Constant extension rate test, also known as slow strain rate test (SSRT)

CRDM – Control rod drive mechanism

DCB – Double cantilever beam specimen

EdF – Electricité de France (the French national electric utility)

EFPH – Effective full power hours

EFPY – Effective full power years

EPRI - Electric Power Research Institute

GTA – Gas tungsten arc (welding)

HAZ – Heat-affected zone

ID – Inside diameter

IG – Intergranular

IGA – Intergranular attack

IGSCC – Intergranular stress corrosion cracking

LTCP – Low temperature crack propagation

MA – Mill annealed

OD – Outside diameter

OTSG – Once-through steam generator

ppm – Parts per million

ppb – Parts per billion

PWR – Pressurized water reactor

PWSCC – Primary water stress corrosion cracking

RUB – Reverse U-Bend stress corrosion cracking specimens made from split half steam generator tubing, hence also known as split tube U-Bend specimens

SCC – Stress corrosion cracking

SEM – Scanning electron microscope (or microscopy)

SG – Steam generator

SSRT – Slow strain rate test, also known as constant extension rate test (CERT)

STEM – Scanning transmission electron microscope (or microscopy)

TEM – Transmission electron microscope (or microscopy)

TGSCC – transgranular stress corrosion cracking

TT – Thermal treatment

XPS – X-ray photoelectron spectroscopy

1 INTRODUCTION

1.1 Background

Wrought Alloy 600 and its weld metals (Alloy 182 and Alloy 82) were originally used in pressurized water reactors (PWRs) due to the material's inherent resistance to general corrosion in a number of aggressive environments and because of a coefficient of thermal expansion that is very close to that of low alloy and carbon steel. Over the last thirty years, primary water stress corrosion cracking (PWSCC) has been observed in Alloy 600 component items and Alloy 82/182 welds such as steam generator tubes and plugs, pressurizer heater sleeves and welds, pressurizer instrument nozzles, reactor vessel closure head nozzles and welds, reactor vessel outlet nozzle welds, and more recently in a lower reactor vessel head instrumentation nozzle and weld. Table 1-1 provides a synopsis of the Alloy 600 PWSCC experience in commercial PWRs. This table identifies the first commercially observed occurrence of PWSCC for each particular component item in a PWR and lists the approximate service life (in calendar years) at the time PWSCC was identified at that particular location. PWSCC was first observed at very highly stressed locations in the hot leg of steam generators in the 1970s. Pressurizer nozzles, which operate at the highest temperature in PWRs, were the next locations to have leakage and failures identified. Currently, PWSCC has been observed on nozzles and welds at nearly all locations where it is utilized throughout the reactor coolant system.

The occurrence of PWSCC has been responsible for significant downtime and replacement power costs at PWRs. Notable examples of equipment failures include extended outages and repairs or replacements at Calvert Cliffs, V.C. Summer, Oconee Nuclear Station, Davis-Besse, and North Anna. Repairs and replacements since the late 1980s have generally utilized wrought Alloy 690 material and its weld metals (Alloy 152 and Alloy 52), which have been shown to be considerably less susceptible, if not immune, to PWSCC for all practical purposes under normal operating conditions. Nevertheless, U.S. NRC Bulletin 2002-02, "Reactor Vessel Head and Vessel Head Penetration Nozzle Inspection Programs," dated August 9, 2002 does not indicate that inspection credit will currently be given for upgraded replacement reactor vessel heads, using Alloy 690 wrought and weld materials, over existing head penetrations using Alloy 600 wrought and weld materials that have < 8 effective degradation years.[1]

1.2 Causes of Alloy 600 PWSCC

Stress corrosion cracking of metals and alloys is caused by the synergistic effects of environment, material condition, and stress. In a PWR primary water environment, intergranular stress corrosion cracking of wrought Alloy 600 material and its weld metals (Alloy 182 and

[1] An effective degradation year (EDY) is a means for assessing the potential for PWSCC cracking at a plant. It accounts for the amount of time a plant has operated and the temperatures at which it has operated.

Alloy 82) is commonly referred to as PWSCC. The occurrence of stress corrosion cracking of Alloy 600 in high-purity water has been extensively studied since the first reported observation of cracking in laboratory tests by Coriou, et al.[1] in 1959. The mechanism of this cracking phenomenon is not completely understood, and prediction of crack initiation time has proven to be very difficult due to the uncertainty of numerous contributory variables including metallurgical condition, cold work, and residual stress. Although the crack initiation time can vary tremendously from heat to heat, wrought Alloy 600 material and its weld metals are susceptible to PWSCC when the total stress level is close to or in excess of the yield strength.

PWSCC is a thermally-activated mechanism that can be correlated with a Svante Arrhenius relationship (exponential) and is very temperature dependent. The vast majority of PWSCC of steam generator roll expansion transitions has occurred first on the hot leg side of the tube sheet due the 50-70^{o}F (27-38^{o}C) higher temperatures. However, failures of Alloy 600 material have also been reported in France to have occurred in reactor vessel upper head nozzle material at a temperature of approximately 554^{o}F (290^{o}C).[2] On at least one other occasion PWSCC has been cited on a component item at a significantly lower water temperature of 423^{o}F (217^{o}C) although the details leading to this conclusion have not been independently verified by the authors of this report.[3]

The susceptibility of Alloy 600 depends on several factors including the chemical composition, metallurgical condition during manufacture of the material, heat treatment during fabrication of the component item, and its operating parameters.[4] The carbon and chromium contents appear to be the most important chemical composition variables. These, in turn, affect the chromium carbide precipitation during thermal-mechanical processing. Microstructural conditions such as grain size and location relative to carbide precipitation also are important variables that determine the susceptibility of a material to PWSCC. Finally, fabrication parameters and heat treatment determine the overall yield strength and degree of cold work. Alloy 600 that has been low temperature mill-annealed, with grain boundaries poorly decorated with carbides, and has relatively high yield strength (due to some degree of remaining cold work) is generally observed to be the most susceptible to PWSCC.

Tensile stresses, resulting from both residual and operating stresses, can be significant for some Alloy 600 component items. A stress close to the material yield strength is generally necessary for PWSCC to occur. Operating stresses arise from mechanical (pressure) and thermal loading, while residual stresses are generated as a result of fabrication, installation, and welding processes. Residual stresses are more difficult to quantify than operating stresses and, in many instances, are of a higher magnitude and usually a major factor leading to premature failure.

In summary, PWSCC requires three key factors to be present simultaneously: an environment that promotes intergranular stress corrosion cracking, susceptible material, and significant, prolonged tensile stress. Eliminating any one of these three factors will mitigate cracking in principle, although in practice it is prudent to attack all of these factors at once, wherever feasible.

Based on the excellent test results and field performances, Alloy 690 has become the replacement material of choice for degraded Alloy 600 component items in PWRs. This

document provides a systematic evaluation of field and laboratory data on potential corrosion mechanisms, particularly PWSCC, and provides a technical basis or justification for development of future inspection requirements for these materials.

1.3 Purpose and Scope

Existing data suggest that the effects of corrosion, particularly PWSCC concerns, are minimal with Alloy 690/52/152 materials. Within the EPRI PWR Materials Reliability Program (MRP), the Mitigation Working Group of the Alloy 600 Issue Task Group (ITG) has initiated this effort to demonstrate and quantify the margin of improvement resulting from use of the replacement materials (Alloys 690/152/52). The scope of this document is to:

1. Evaluate both field and laboratory data on the behavior of Alloys 690/152/52 exposed to actual or simulated PWR primary water (including off-chemistry conditions and accelerated testing), taking into account the effects of material condition (e.g., thermal processing history, microstructure, cold work) and mechanical stress levels (applied and residual).

2. Analyze the data by comparison with the known behavior of Alloy 600 and its weld materials so as to generate a technical report describing, as far as currently possible, the margins of improvement in resistance to PWSCC expected from use of the replacement alloys.

3. Identify gaps in the existing database and suitable strategies to rectify these.

4. Provide a technical justification basis for development of future inspection requirements for these materials.

Table 1-1 First Reported Occurrence of Alloy 600 PWSCC for Various PWR Component Items

Component Item	Date PWSCC Initially Observed	Service Life[a] (Calendar Years)
Steam Generator Hot Leg Tubes	1971	2
Pressurizer Instrument Nozzles	1986	2
Steam Generator Cold Leg Tubes	1986	18
Pressurizer Heaters and Sleeves	1987	5
Steam Generator Channel Head Drain Pipes	1988	1
Pressurizer Heater Diaphragm Plate Weld	1989	16
Control Rod Drive Mechanism Nozzles	1991	12
Hot Leg Instrument Nozzles	1991	5
Power Operated Relief Valve Safe End	1993	22
Pressurizer Nozzle Welds (Repair)	1994	1
Steam Generator Tubesheet Plate Cladding	1995	13
Cold Leg Piping Instrument Nozzles [b]	1997	13
Hot Leg Nozzle Welds	2000	13
Reactor Vessel Hot Leg Nozzle Buttering/Piping Welds	2000	17
Pressurizer Instrumentation Nozzle Welds	2000	27
Control Rod Drive Mechanism Nozzle/RV Head Welds	2000	27
Surge Line Nozzle Welds [c]	2002	21
Reactor Vessel Lower Head In-Core Instrumentation Nozzles/Welds	2003	14

(a) This listing identifies the first reported occurrence of identified cracking for each component item. Leakage has occurred in some component items in less than one year of service life and in other component items after nearly 30 years of service.
(b) One plant identified “suspect” visual evidence of boric acid leakage around two nozzles during a visual inspection; nozzles were preventively repaired without investigating whether leakage had in fact occurred.
(c) Crack-like flaw indications have not been confirmed as PWSCC at this time.

2 ALLOY 690 PROPERTIES AND METALLURGY

2.1 Material Specifications

Alloy 690 and its predecessor Alloy 600 were first developed by Inco Alloys International under the trade names Inconel Alloy 690 and Inconel Alloy 600.[5, 6] Alloys 82 and 182 were first introduced by Inco Alloys International under the trade names Inconel Filler Metal 82 and Inconel Welding Electrode 182 for welding Alloy 600 component items. Alloys 52 and 152 were introduced by Inco Alloys International under the trade names Inconel Filler Metal 52 and Inconel Welding Electrode 152 and are now used for welding Alloy 690 component items. The present owner of the trade name of Inconel is Special Metals Corporation. Currently, all these alloys have been adopted by ASTM (American Society for Testing and Materials), ASME (American Society of Mechanical Engineers), and other international materials societies. Even though these alloys are listed under the UNS (Unified Numbering System) numbers in ASTM or ASME standards (see Table 2-1), these alloys are generically referred to as Alloy 600, Alloy 690, Alloy 82, Alloy 182, Alloy 52 or Alloy 152 in the nuclear power industry.

Table 2-1 provides a summary of the most commonly used product forms in the ASME Boiler and Pressure Vessel Code Section II material specifications for the wrought Alloy 690 materials, and the corresponding weld metals Alloys 52 and 152. Because Alloy 690, Alloy 52, and Alloy 152 were developed for replacing their predecessors Alloy 600, Alloys 82, and Alloy 182 for light water nuclear power reactors, they are listed in the same ASME material specifications. It is noted that modified versions of Alloy 152/52 with improved weldability are currently being developed. For example, the Inconel Filler Metal 52M (also called Alloy 52M), offered by Special Metals Corporation, contains boron and zirconium to minimize the tendency for ductility-dip cracking and added resistance to oxide "floaters" and inclusions. Alloy 52M has been proposed to AWS (American Welding Society) and is listed in AWS A5.14 as ERNiCrFe-7A.[7] Inconel Welding Electrode 152M, a modified Alloy 152, is also being offered by Special Metals Corporation.

Table 2-2 lists the chemical composition requirements for Alloys 690/600, 152/182, and 52/82. The ASME chemical composition requirements for these alloys remain identical to the original specification developed by the Inco Alloys International. However, stricter requirements on chemical composition, mechanical properties, and heat treatment process are imposed on Alloy 600 or 690 by utilities and vendors for applications in PWRs. For Alloy 690 bars, plates, and heavy section tubing, the carbon content is routinely specified to be in a range between 0.010% and 0.040% or narrower, instead of the max. 0.050% carbon specified in ASME Section II. For Alloy 690 SG tubing, the EPRI Guidelines require the carbon content to be between 0.015% to 0.025%.[8] The lower limit ensures continuous or semi-continuous intergranular carbide precipitation while the upper limit keeps intragranular carbide precipitation to a minimum upon thermal heat treatment. Alloy 690 has higher yield and tensile strengths than Alloy 600 due to

the increased Cr content. Therefore, the lowered carbon level does not affect the allowable stresses for Alloy 690.

Table 2-3 lists the room temperature properties of Alloys 690/600, 152/182, and 52/82. However, ASME properties for the weld metals are not listed, which may be due to the fact the welds are less homogenous (e.g., dilution or mixing with the base metals) and their properties are anisotropic due to the directional solidification structure in welds. Table 2-4 lists the ASME properties of Alloys 690 and 600 at elevated temperatures. Such properties are used in the design of Alloy 600 and 690 component items for repair or replacement and calculating the operating stress.

2.2 Phase Diagram of Alloy 690

The first comprehensive study of Alloy 690 was published by Sedriks et al.[9] of Inco Alloys International, Inc. in 1979. This was the time that Alloy 690 began to be introduced for fabricating steam generator tubing in PWRs. The physical metallurgy and properties of Alloy 690 from this study and other sources are summarized below.

Figure 2-1 shows the Ni-Cr-Fe phase diagram with the location of the $\gamma/\gamma+\alpha'$ solvus line indicated from 816 to 1260°C (1500 to 2300°F). The lowest temperature at which the $\gamma/\gamma+\alpha'$ solvus has been determined is 816°C (1500°F). The locations of Alloys 690 and 600 compositions are marked on the diagram and are both well within the austenite field (γ). The range of melting temperatures is 2450-2510 °F[6] (1343-1377 °C) for Alloy 690 and 2470-2575°F[5] (1354-1413°C) for Alloy 600. The α' phase is a chromium-rich phase, which is very similar to the iron-chromium σ phase both in morphology and hardness. The α' phase can cause embrittlement when precipitated during prolonged high temperature exposure in alloys whose compositions lie in the two-phase $\gamma+\alpha'$ field. Precipitation of α' phase is a mechanism of aging embrittlement of austenitic stainless steel welds or castings containing small amounts of δ ferrite and of martensitic precipitation-hardenable stainless steel when exposed to elevated operating temperatures in PWRs.[10] Since Alloys 600 and 690 are both stable austenitic solid solution alloys from room temperature to the melting temperature, precipitation of α' phase is not expected nor has ever been found in Alloys 600 and 690.

K. Smith et al. evaluated the possible occurrence of an "ordered" Ni_2Cr phase in Alloy 690.[11] This concern was raised due to the fact that the Ni/Cr (atomic) ratio for an alloy with 70%Ni-30%Cr wt% is about 2.1 to 1, which is very close to that of Ni_2Cr. The brittle and hard intermetallic Ni_2Cr phase is stable below 580°C (1076°F) and could have a similar embrittling effect as the iron-chromium σ intermetallic phase in austenitic alloys. However, K. Smith's research found that iron has an inhibiting effect on the formation of Ni_2Cr phase and that the minimum specified iron content in Alloy 690 was high enough to inhibit any Ni_2Cr formation. Later, Larsson et al. performed extensive testing for the same phenomenon including hardness tests, tensile tests, transmission electron microscopy (TEM), differential scanning calorimetry (DSC), and differential thermal analysis (DTA) on commercially produced Alloy 690TT that had been thermally aged for 3000 hours at 400 and 500°C (752 and 932°F) and an Alloy 690 corrosion specimen exposed at 365°C (689°F) for 32,961 hours.[12] The study confirmed that no evidence of long range ordering of type Ni_2Cr was found in the thermally aged Alloy 690.

Nevertheless, vendors specify higher minimum iron contents than the ASME Code allowed minimum in order to provide a significant margin against formation of an ordered Ni_2Cr phase in Alloy 690.

The microstructure of Alloy 690 is similar to Alloy 600, i.e., an austenitic matrix with the secondary phases being predominantly chromium carbides precipitated both intergranularly and intragranularly. The other minor secondary phases in Alloys 600 and 690 are titanium nitrides, titanium carbides, and carbonitrides. Because the austenitic matrix phase is stable up the melting temperature, both alloys are non-heat treatable via phase changes (such as the austenite to martensite transformation in carbon and low alloy steels) and cannot be hardened through secondary phase precipitation (such as through γ' precipitation in Alloy X-750 or Alloy 718).

2.3 Carbide Solubility

The extent of intragranular and intergranular carbide precipitation depends on the thermal mechanical history and carbon content. Most research efforts on Alloys 690 and 600 have been focused on the grain boundary microstructure, especially due to observations of generally higher PWSCC resistance of Alloy 600 with a microstructure containing continuous intergranular carbides and few intragranular carbides.[13] The intergranular carbide precipitates are found to be both M_7C_3 and $M_{23}C_6$ types in Alloy 600 and mostly globular $M_{23}C_6$ type in Alloy 690.[14, 15]

It is generally recognized that the solubility of carbon in Alloy 690 is lower than that in Alloy 600. This is due to the higher Cr content which lowers the solubility while increasing the propensity for carbide precipitation. The carbon solubility curve of Alloy 690 was investigated by Sarver et al.[16] The Alloy 690 heats used are listed in Table 2-6. The results are shown in Figure 2-2 with the Alloy 690 solubility line drawn to separate the specimens having no visible carbides from the specimens having visible carbides. Figure 2-2 also shows the comparison of carbon solubility curves for Alloy 690 and Alloy 600. The equations fitted to these curves are:

Alloy 690

$$^{o}F = 2647.5 + 120\ Ln(\%C) \quad \textbf{(Eq. 2-1)}$$

$$^{o}C = 1453.1 + 66.9\ Ln(\%C)$$

Alloy 600

$$^{o}F = 2640 + 234.5 Ln(\%C) \quad \textbf{(Eq. 2-2)}$$

$$^{o}C = 1449 + 130.3\ Ln(\%C)$$

It should be noted that thermo-mechanical processing of both of these materials may cause grain boundaries to move by recrystallization after all the available carbon has precipitated as carbides on the old grain boundaries, thus creating a "ghost" grain boundary carbide network. Coring or non-equilibrium solidification of the original ingot can also manifest itself in the form of carbide banding. Solution heat treatments at temperatures above the carbon solubility curves for prolonged periods followed by rapid quenches can minimize the observed effects, but cannot eliminate them. Prohibitively long solution heat treatment would be required to dissolve the carbides and allow the carbon to diffuse away from the original sites in order to prevent the carbon from re-precipitating at the old sites during carbide precipitation heat treatment.

2.4 Intergranular Carbide Precipitation and Sensitization

The time-temperature chromium carbide precipitation curves for Alloy 600 and Alloy 690 determined by Yonezawa et al. are shown in Figure 2-3.[17] The highest precipitation rate (the nose of the C-curves) is at approximately 850-950°C (1550-1750°F). The Alloy 690 and Alloy 600 heats were annealed at 1100°C (2012°F) and contained 0.03% carbon but the exact chemical composition was not listed. From Figure 2-3, chromium carbides precipitate first at the grain boundaries followed by precipitation inside the grains. In addition, carbide precipitation is faster in Alloy 690 than in Alloy 600 due to the higher chromium content of Alloy 690. For Alloy 600, the precipitation of the grain boundary carbides is complete after a short period of time at 1300°F (704°C). However, an extended 10-15 hours period is required to fully replenish the Cr-depleted grain boundary with Cr from the bulk of the grains to avoid a "sensitized" microstructure.[18, 19] It was reasoned that since Alloy 690 has a much higher Cr content, full replenishment of the grain boundaries is not necessary and a 4 to 5 hour thermal treatment should be adequate.[20]

Sedriks et al. [9] found that if the carbon content is kept to 0.02% or below, Alloy 690 cannot be "sensitized" as defined by the Huey test, i.e., the boiling nitric acid test per ASTM A 262 Practice C[21]. This means the Cr level near the grain boundary was sufficiently high in Alloy 690 containing ≤ 0.02% carbon after intergranular carbide precipitation to prevent intergranular attack by boiling nitric acid. In the Huey test, specimens are placed in boiling 65%wt nitric acid, typically for five 48-hour periods, with a fresh nitric acid solution being used in each period. It should be noted that the Huey test for sensitization is normally used for detecting susceptibility to intergranular attack in austenitic stainless steels, not for high-nickel alloys such as Alloy 690 or Alloy 600. "Sensitization" usually refers to grain boundary chromium depletion in austenitic stainless steels such as Type 304 and Type 316 exposed to 800-1500°F (427-816 °C) for a prolonged period of time that varies with carbon content. Precipitation of chromium carbides along the grain boundaries causes the Cr depletion near the grain boundaries, which are preferentially attacked under certain oxidizing environmental conditions (for example in nitric acid or in the normal oxygenated water chemistry used in Boiling Water Reactors).

For Alloy 600 steam generator tubing, a modified Huey Test (25% HNO_3 with two 24-hour boiling periods) is often used, instead of the 65% HNO_3 with five 48-hour boiling periods specified in ASTM A 262, Practice C. Due to the higher resistance of Alloy 690 to sensitization, Sarver et al. used 65% HNO_3 for sensitization testing of several heats of Alloy 690 with varying carbon contents and heat treatments. The time-temperature-sensitization diagrams plotted by Sarver et al. are shown in Figure 2-5 to Figure 2-7.[16] Figure 2-5 shows very low corrosion rates for heat NX4459HG (0.06%C) with a 1900°F (1038°C) anneal before the sensitization treatment. The corrosion rate was highest (1.7 mil/month) after a sensitization treatment of 1000°F (538°C) for 100 hours. Figure 2-6 shows the corrosion rates for heat NX9217H (0.01%C), which was milled annealed at 1900°F (1038°C) for one hour. The corrosion rate was also low except when sensitized at 1000°F (538°C) for 20-100 hours. Figure 2-7 shows the results for heat NX9780H, also containing 0.01%C, but a slightly higher Cr content than NX9217H (29.20% vs. 27.27%). Heat NX9780H also showed a very low corrosion rate even when sensitized at 1000°F (538°C) for 10-20 hours. The highest degree of sensitization for Alloy 690, as defined by the Huey test, is produced by heat treatment at 1000°F for 20 to 100 hours. The complete chemical compositions of heats NX4459HG, NX9217H, and NX9780H studied by Sarver et al. are summarized in Table 2-6. It should be noted that for Alloy 600 a sensitized microstructure with continuous

intergranular carbides and grain boundary Cr depletion is more resistant to PWSCC than the same heat without intergranular carbides and grain boundary Cr depletion. Similarly, the same "sensitization" heat treatment also enhances PWSCC resistance of Alloy 690.

Sarver et al. also investigated the effect of carbon content, annealing temperature, and one-hour precipitation heat treatments on the carbide morphology. The results are shown in Table 2-7. The annealing temperature and carbon level both affected the temperature at which heavy intergranular carbide precipitation occurred. Depending upon the desired annealing temperature and carbon content, a one-hour heat treatment could be chosen to produce heavy intergranular carbide precipitation. The high carbon (0.03%C) material was much more likely to show intragranular carbides than the lower carbon (0.01%C) material although intergranular precipitation occurred equally in both materials. Although heavy intergranular carbide precipitation was produced by many heat treatments, no significant intergranular sensitization occurred except with the 0.03% carbon material annealed at 2100°F (1149°C) and heat treated at 1200 and 1300°F (649 and 704°C), as shown by the Huey test. Corrosion rates in the Huey tests were 3.3 and 1.7 mil/month (1.0 and 1.5 mm/year), respectively. For all other heat treatments, rates were less than 1.2 mil/month (0.4 mm/year).

2.5 Effect of Elevated Temperature Exposure

Figure 2-4 shows the results of short-time tensile tests performed on annealed Alloy 690 at temperature ranging from room temperatures up to 1800°F (982°C).[6] The curves represent average values for both cold-worked and hot-worked products in the annealed condition. Figure 2-4 shows that annealed Alloy 690 retains more than 90% of its room temperature tensile properties (yield and tensile strengths and elongation) up to 800°F (427°C). Only at temperatures over 1000°F (540°C) does the tensile strength start to decline substantially. The retention of room temperature tensile properties and the long-term high temperature stability are reflected in the ASME design stress intensity values for Alloy 690 and Alloy 600 (see Table 2-4).

Table 2-5 lists the room temperature tensile results of annealed Alloy 690 after exposure to elevated temperatures for various periods of time.[6] The long-term high temperature stability of Alloy 690 was demonstrated by Charpy impact testing of Alloy 690 after long periods at 566 to 760°C (1050 to 1400°F). This range of temperatures is similar to that of post weld stress relieving heat treatment (PWHT) temperatures for carbon and low alloy steel vessels or piping in PWRs. Table 2-5 shows the room temperature Charpy impact energy (189 J un-aged) was virtually unchanged after 12,000 hours or 500 days at elevated temperatures. The room temperature Charpy impact energy is found to be a very sensitive indicator of the precipitation of α' or σ phases for alloys with an austenitic matrix. For example, aging at 400°C (752°F) for 10,000 hours or 417 days reduced the Charpy impact energy from ~220 J to 50 J of a CF-8 casting austenitic stainless steel (the equivalent of wrought Type 304 stainless steel) containing 24% δ ferrite.[22]

Hence, it can be concluded that thermal aging embrittlement is not a concern for Alloy 690 and Alloy 600 component items from exposure to high temperatures during fabrication or repair welding or PWHT heat treatment at 800-1300°F, or from long-term exposure to PWR operating temperature of up to 650°F (343 °C).

Table 2-1 ASME Specifications of Alloys 690/600, 152/182, and 52/82

Specification	Alloy	Product Form
ASME SB-163 [23]	UNS N06690 (Alloy 690) UNS N06600 (Alloy 600)	Seamless Tubing
ASME SB-166 [24]	UNS N06690 (Alloy 690) UNS N06600 (Alloy 600)	Rod, Bar, Wire
ASME SB-167 [25]	UNS N06690 (Alloy 690) UNS N06600 (Alloy 600)	Seamless Pipe and Tube
ASME SB-168 [26]	UNS N06690 (Alloy 690) UNS N06600 (Alloy 600)	Plate, Sheet, Strip
ASME SFA-5.11 [27]	ENiCrFe-7, UNS W86152 (Alloy 152) ENiCrFe-3, UNS W86182 (Alloy 182)	Coated welding electrode
ASME SFA-5.14 [28]	ERNiCrFe-7, UNS N06052 (Alloy 52) ERNiCr-3, UNS N06082 (Alloy 82)	Bare welding electrode and rod

Table 2-2 ASME Chemical Composition Requirement (wt%) [23-28]

Alloy	Ni	Cr	Fe	C	Mn	Si	S	Ti	Nb + Ta	Cu	P	Al	Mo	Other
690	58.0 min	27.0-31.0	7.0-11.0	0.05 max	0.50 max	0.50 max	0.015 max	--	--	0.50 max	--	--	--	--
600	72.0 min	14.0-17.0	6.0-10.0	0.15 max	1.0 max	0.50 max	0.015 max	--	--	0.50 max	--	--	--	--
152 (a)	Bal.	28.0-31.5	7.0-12.0	0.05 max	5.0 max	0.75 max	0.015 max	0.50 max	1.0-2.5	0.50 max	0.03 max	0.50 max	0.50 max	0.50 max
182	59.0 min	13.0-17.0	10.0 max	0.10 max	5.0-9.5	1.0 max	0.015 max	1.0 max	1.0-2.5	0.50 max	0.03 max	--	--	0.50 max
52 (a)	Bal.	28.0-31.5	7.0-11.0	0.04 max	1.0 max	0.50 max	0.015 max	1.0 max	0.10 max	0.30 max	0.02 max	1.10 max	0.50 max	0.50 max
82	67.0 min	18.0-22.0	3.0 max	0.10 max	2.5-3.5	0.50 max	0.015 max	0.75 max	2.0-3.0	0.50 max	0.03 max	--	--	0.50 max

(a) It is noted that modified versions of Alloy 152/52 with improved weldability are currently being developed.

Table 2-3 ASME Room Temperature Properties

		Alloy 690	Alloy 600	Alloy 152	Alloy 182	Alloy 52	Alloy 82
Density	lb/in^3	0.293 (a)	0.300 (a)	NA	NA	NA	NA
	kg/cm^3	8.11 (a)	8.30 (a)				
Poison's Ratio	--	0.29 (b)	0.29 (b)	NA	NA	NA	NA
Min. Tensile Strength	ksi	85 [25]	80 [25]	80 [29]	80 [29]	80 [29]	80 [29]
	MPa	586 [25]	550 [25]	552 [29]	552 [29]	552 [29]	552 [29]
Min. Yield Strength	ksi	30 [25]	30 [25]	NA	NA	NA	NA
	MPa	205 [25]	205 [25]	NA	NA	NA	NA
Min. Elongation	%	35 [25]	35 [25]	30 [29]	30 [29]	30 [29]	30 [29]

(a) From Table NF-2 of Ref. 30.
(b) From Table NF-1 of Ref. 30.

Table 2-4 ASME Elevated Temperature Properties for Alloy 690 and Alloy 600 [30]

Temp	Young's Modulus $E^{(a)}$, $x10^6$ ksi		Coefficient of Thermal Expansion $\alpha^{(b)}$, $x10^{-6}$ in/in/ °F		Design Stress Intensity (c) S_m, ksi		Yield Strength (d) S_y, ksi		Tensile Strength (d) S_u, ksi	
°F	690	600	690	600	690	600	690	600	690	600
70	30.3	31.0	7.7	6.8	23.3	23.3	35.0	35.0	85.0	80.0
100	30.1 (a)	30.8	7.8	6.9	23.3	23.3	35.0	35.0	85.0	80.0
200	29.5	30.2	7.9	7.1	23.3	23.3	31.7	32.0	85.0	80.0
300	29.1	29.8	7.9	7.3	23.3	23.3	29.8	31.2	84.0	80.0
400	28.8	29.5	8.0	7.5	23.3	23.3	28.6	30.7	82.0	80.0
500	28.3	29.0	8.1	7.6	23.3	23.3	27.9	30.3	80.8	80.0
600	28.1	28.7	8.2	7.8	23.3	23.3	27.6	29.9	80.2	80.0
650	27.9 (a)	28.5	8.2	7.8	23.3	23.3	27.5	29.7	80.0	80.0
700	27.6	28.2	8.3	7.9	23.3	23.3	27.5	29.4	79.8	80.0

(a) From Table TM-4 of Ref. 30. Values of Young's modulus for 100°F and 650°F are obtained by linear interpolation.
(b) Mean coefficient of thermal expansion going from 70°F to the indicated temperature, from Table TE-4 of Ref .
(c) From Table 2B of Ref. 30. For annealed Alloy 690 and Alloy 600 of SB-163, SB-166, SB-167, and SB-168; some exception exists see Table 2B of Ref. 30 for details.
(d) From Table Y-1 of Ref. 30. For annealed Alloy 690 and Alloy 600 of SB-163, SB-166, SB-167, and SB-168; some exception exists see Table Y-1 of Ref. 30 for details.

Table 2-5 Effect of Thermal Aging on Room Temperature Properties of an Annealed Alloy 690 [9]

Exposure Temperature		Aging Time	Yield Strength		Tensile Strength		Elong.	Charpy Impact Energy	
°F	°C	hour	ksi	MPa	ksi	MPa	%	ft-lb.	J
N/A	N/A	Not Aged	41.0	283	103.5	714	48	140	190
1050	565	1,000	48.5	334	105.0	727	45	115	156
		4,000	47.0	324	105.5	724	45	126	171
		12,000	45.5	314	105.5	727	44	121	164
1100	595	1,000	62.5	431	107.0	738	45	144	195
		4,000	46.5	321	106.0	731	43	125	170
		13,248	45.5	314	105.5	727	44	125	170
1200	650	1,000	46.8	323	105.5	727	46	146	198
		4,000	48.5	334	106.0	731	54	132	179
		12,000	46.1	318	108.5	748	41	127	172
1400	760	1,000	50.0	345	107.0	738	44	158	214
		4,000	44.4	306	103.5	714	44	148	201
		12,000	46.5	321	103.5	714	46	136	184

Table 2-6 Chemical Composition (wt%) of Alloy 690 Heats used by Sarver et al.[16]

Heat	Ni	Cr	Fe	C	Mn	Si	S	Ti	Nb + Ta	Cu	P	Al	Mo
Intergranular Carbide Precipitation Study													
NX9217H	Bal	27.27	10.22	0.01	0.15	0.10	0.003	0.25		0.15		0.17	
NX9780H	Bal	29.20	8.85	0.01	0.33	0.43	0.001	0.46		0.12		0.26	
NX4459HG	Bal	28.25	8.86	0.06	0.20	0.10	0.004	0.32		0.04		0.17	
NX4401H	Bal	29.25	10.22	0.01	0.21	0.25	0.001	0.28		0.26		0.15	
Carbon Solubility Study													
EXP 1	Bal	28.7	9.2	<0.001	0.02	0.001	0.001			0.03			
EXP 2	Bal	28.8	9.8	0.01	0.06	0.06	0.003			0.02			
NX4458H	Bal	27.9	9.8	0.016	0.19	0.10	0.002			0.26			
EXP 3	Bal	29.9	9.6	0.02	0.03	0.05	0.003			0.01			
EXP 4	Bal	28.7	9.3	0.02	0.02	0.001	0.001			0.03			
NX05E1H	Bal	29.9	9.5	0.021	0.21	0.39	0.001			0.28			
NX10C1H	Bal	29.8	9.4	0.039	0.15	0.15	0.008			0.30			
EXP 5	Bal	29.0	9.1	0.04	0.02	0.001	0.002			0.02			
EXP 6	Bal	29.1	9.1	0.058	0.02	0.001	0.001			0.02			
EXP 7	Bal	29.4	10.3	0.06	0.03	0.06	0.003			0.03			
EXP 8	Bal	29.5	9.8	0.06	0.01	0.05	0.003			0.02			
Heat Treatment Study													
NX4401H	Bal	29.25	10.22	0.01	0.21	0.25	0.001	0.28		0.26		0.15	
NX4588H	Bal	29.92	9.49	0.03	0.18	0.21	0.001	0.27		0.24		0.21	
NX2184H	Bal	28.82	8.98	0.01	0.18	0.24	0.001	0.26		0.24		0.30	
NX4308 (Alloy 600)	Bal	15.11	7.60	0.03	0.35	0.21	0.007	0.26		0.29		0.50	

Table 2-7 Effect of heat treatment on Alloy 690 carbide precipitation, after Ref. 16.

		0.01%C NX4401H				0.03%C NX4588H			
		Initial Anneal Temp, 20 minutes				Initial Anneal Temp, 20 minutes			
		1800°F	1900°F	2000°F	2100°F	1800°F	1900°F	2000°F	2100°F
Carbide Precipitation Temp, 1 hour	1200°F	VL	VL	L	VL	VL	H	H Intra	L
	1300°F	VL	L	H Intra	L	L	H	H Intra	L
	1400°F	H	H	H	H	L Intra	L	H Intra	H Intra
	1500°F	VL	H	H	H	L Intra	L Intra	H Intra	H

(a) Heat treatment code:
VL – very light intergranular carbides; L – light intergranular carbides
H – heavy intergranular carbides; Intra – intragranular carbides

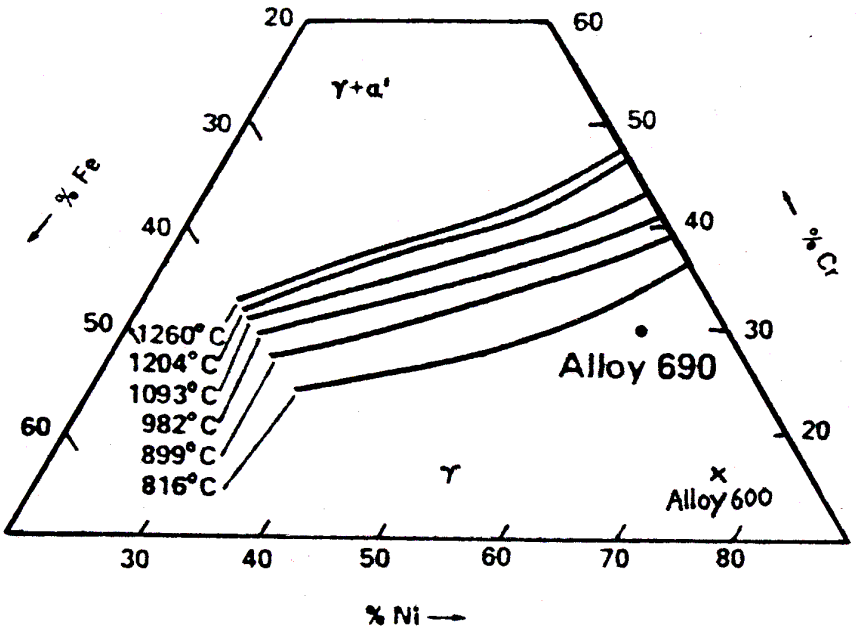

Figure 2-1 The Ni-Cr-Fe phase diagram showing the location of the γ/γ+α' solvus at elevated temperatures from 816 to 1260°C (1500 to 2300°F). The locations of Alloy 690 and Alloy 600 composition are marked on the diagram.[9]

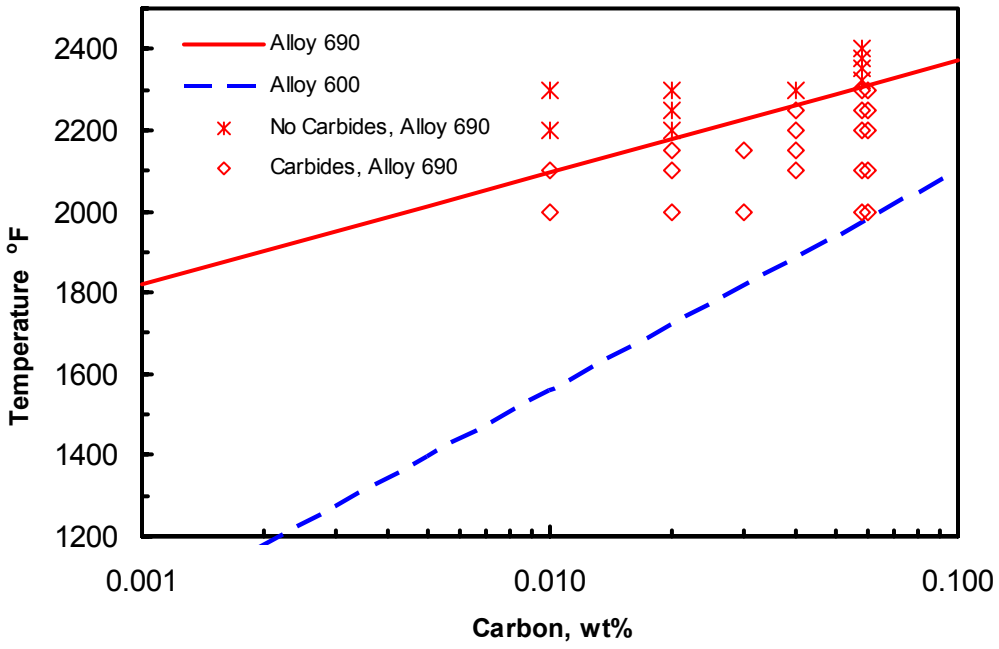

Figure 2-2 Carbon solubility diagram for Alloy 690 and Alloy 600, after Ref. 16.

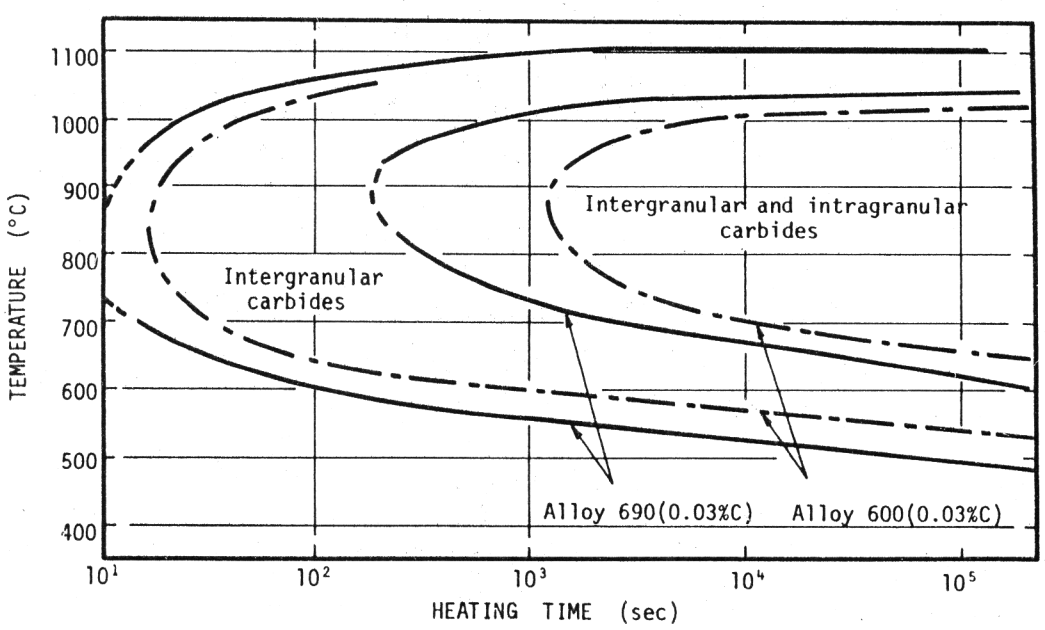

Figure 2-3 Precipitation of chromium carbides in Alloy 690 and Alloy 600, which were solution annealed at 1100°C (2012°F).

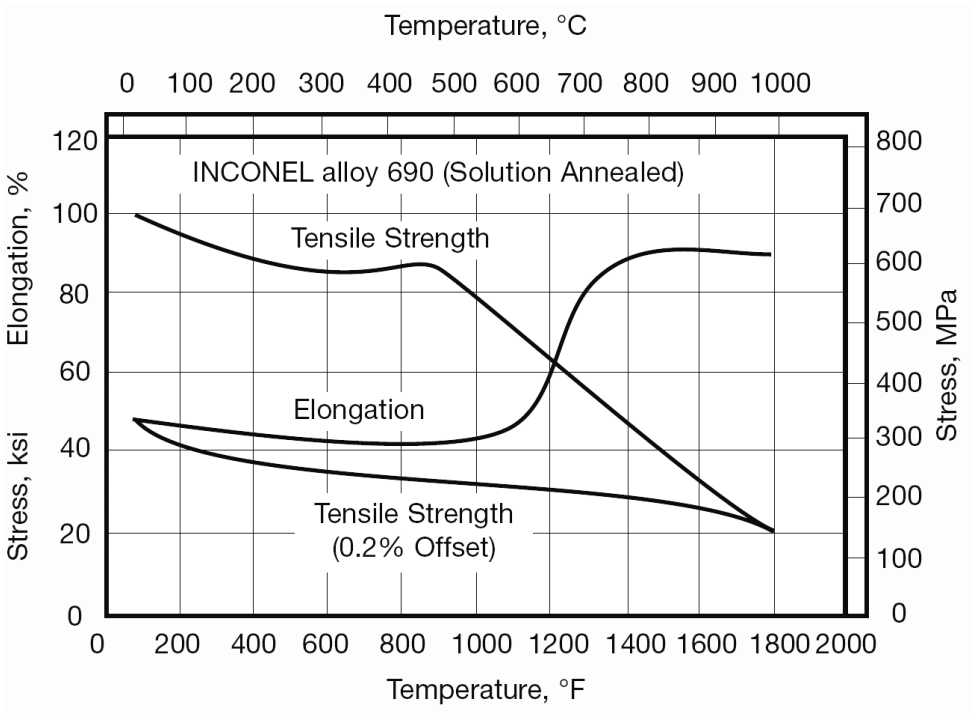

Figure 2-4 High-temperature tensile properties of annealed Alloy 690. Data a composite of cold worked and hot worked products in the annealed condition.[6]

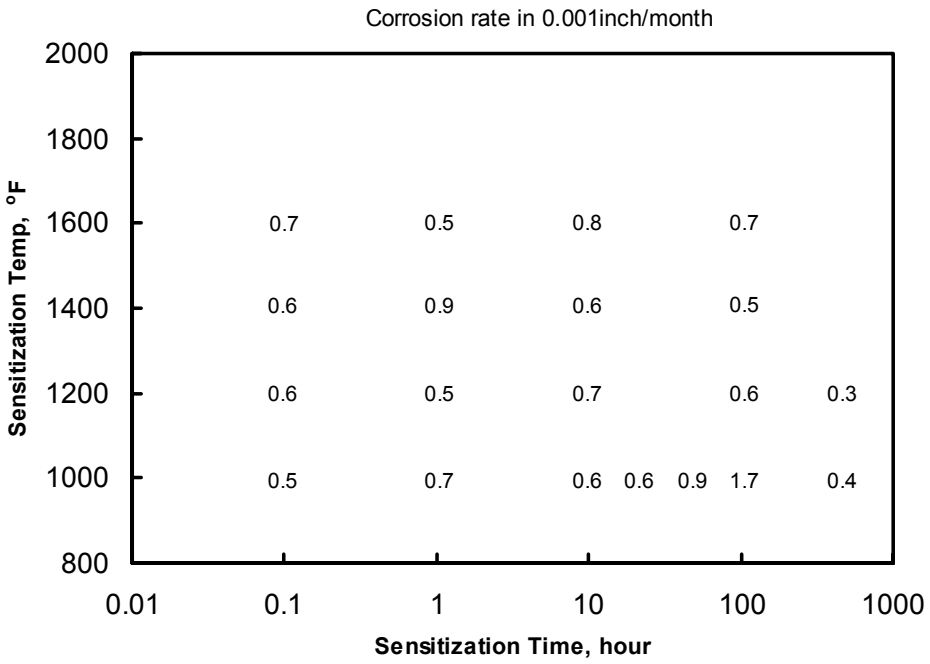

Figure 2-5 Time-Temperature-Sensitization diagram by Modified Huey Test, Alloy 690 Heat NX4459HG (0.06%C), after Ref. 16.

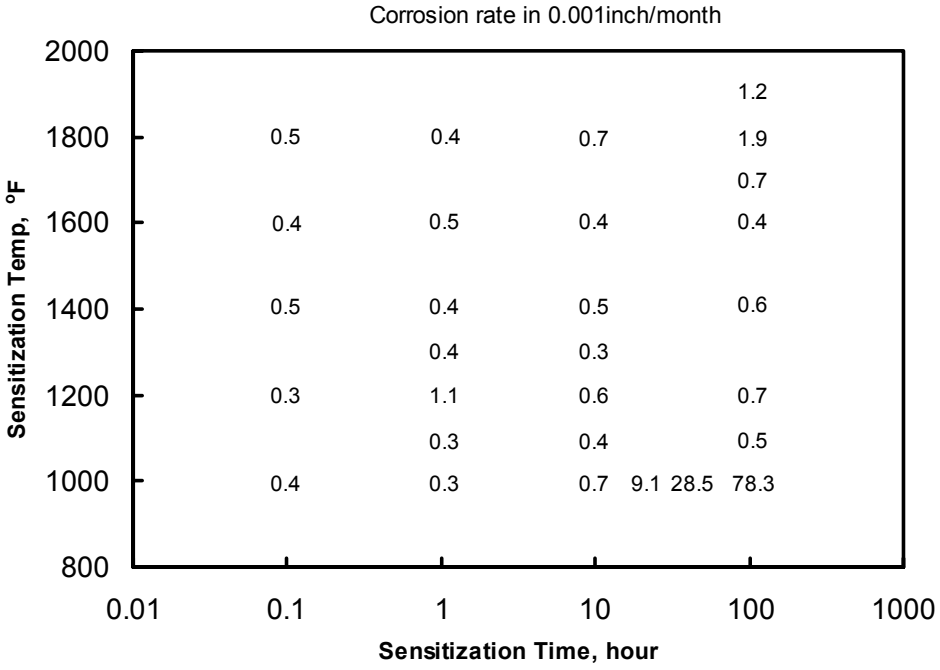

Figure 2-6 Time-Temperature-Sensitization diagram by Modified Huey Test, Alloy 690 Heat NX9217H (0.01%C), after Ref. 16.

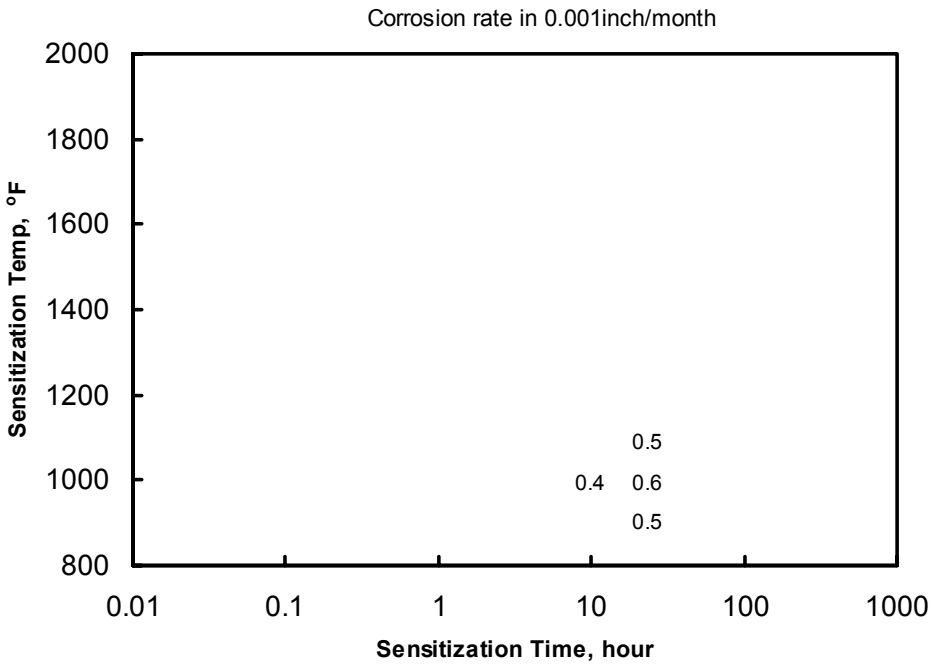

Figure 2-7 Time-Temperature-Sensitization diagram by Modified Huey Test, Alloy 690 Heat NX9780H (0.01%C), after Ref. 16.

3 CORROSION IN PRIMARY WATER

3.1 General Corrosion Tests in Primary Water

This section summarizes the results of a comprehensive review of the available laboratory test data pertinent to general corrosion of Alloy 690 in PWR primary water. General corrosion can be defined as uniform deterioration of a metal surface by chemical or electrochemical reaction with the environment. Nickel-base Alloy 600 and Alloy 690 are essentially immune to general corrosion in a PWR environment due to the formation of an adherent Cr-rich oxide on the surface. The general corrosion rate of Alloy 690 in flowing primary water is of particular interest for PWR steam generator tubing materials. Material lost to the stream can become radioactive by coming in contact with the reactor core and then redeposit on the surfaces of the primary loop. Hence, the metal release rate has a strong implication for a plant's "ALARA" practice – to keep the total neutron dose to a level as low as reasonably achievable.

3.1.1 SG Tubing by Sedricks et al. 1979

Sedriks et al. evaluated Alloy 690 general corrosion in two simulated PWR primary water environments using a high velocity test loop.[9] Borated water was added to simulate the primary side of the steam generator tubing and ammoniated water was used to adjust the pH value to simulate a secondary water environment. The loop test conditions and simulated PWR water chemistry are listed in Table 3-1. The Alloy 690 test specimens were fabricated from heat Y24A7L, with a composition listed in Table 3-2. The heat number and composition of the control specimens were not reported. The Alloy 690 test specimens and Alloy 600 and Alloy 800 control specimens were heat treated for ½ hour at 980°C (1800°F) followed by air cooling. The surfaces were prepared by grinding on a wet 120 grit silicon carbide belt to a 0.75 μm finish. The specimens were weighed and then exposed to the borated water for 2,250 hours and to the ammoniated water for 1,000 hours at 18 ft/sec (5.5 m/sec). After exposure, the specimens from the ammoniated water tests were descaled by cathodic charging in 5% H_2SO_4 inhibited with quinoline ethiodide. The specimens from the borated water tests were descaled by the alkaline permanganate acid method. The terminology and reporting method followed NACE standard TM-02-74, covering the following terms:

1. "Descaled metal loss" (metal consumed): the difference between initial weight and weight after removal of adherent corrosion film.

2. "Corrosion film weight" (adherent corrosion film): the difference between the weight before descaling and the weight after descaling.

The difference between the descaled metal loss and the corrosion film weight represents the base metal lost to the stream. Alloys showing the least loss of material to the stream would be expected to produce the lowest activity levels in the PWR primary coolant system. The metal

loss to the stream from the test is shown Figure 3-1. For the three alloys tested, Alloy 600, Alloy 690, and Alloy 800, Figure 3-1 shows that the general corrosion rate decreases with an increasing Cr content. Alloy 690, having the highest Cr content of the three, lost the least amount of material to the high velocity simulated PWR water. The observed corrosion films formed on Alloy 690 after the borated and ammoniated exposures were of the thin tarnish type and appeared to be extremely adherent to the base metal. The study reported a standard experimental error of about 25% and suggested Figure 3-1 should be used as an guide rather than precise corrosion rate measurements in a high temperature PWR water environment.

3.1.2 SG Tubing by K. Smith et al. 1985

K. Smith et al. investigated the corrosion rate and metal release rate of Alloy 690 and Alloy 600 SG tubing in flowing simulated PWR primary water.[11] The Alloy 690 specimens were fabricated from the full length SG tubes (also called "pre-series" tubes) that were produced by an established industrial route. The three pre-industrial production Alloy 690 heats were intentionally chosen to span the limits of the specification requirements for C and Cr content. The chemical composition and mechanical properties of these three heats are listed in Table 3-3. The Alloy 690 specimens for the general corrosion tests were in the mill annealed condition (MA) as no difference between the MA and the thermally treated (TT) condition was expected. However, it was not reported which heats were used for fabricating the Alloy 690MA corrosion specimens. The chemical composition also was not provided for the Alloy 600 control materials. In addition, the detailed test conditions such as water flow rate and test temperature were not listed.

Weight changes before and after chemical de-filming were used to calculate the amount of total corrosion from the SG tube I.D. and the amount released to the stream. The corrosion rate and metal release rate curves shown in Figure 3-2 were constructed by fitting a regression equation to the data. The test results show that Alloy 690's general corrosion rate and metal release rate was reduced by a factor of 2 to 4 compared to Alloy 600 material.

3.1.3 SG Tubing by Yonezawa et al. 1985

Yonezawa et al. investigated the weight loss of Alloy 690, Alloy 600, and Alloy 800L SG tubing in simulated PWR primary water chemistry.[17] The test coupons were made from split SG tubes. The test was conducted at 360°C (680°F) for up to 4,000 hours. The composition and heat treatment of the test material are listed in Table 3-4. The test condition and water chemistry are listed in Table 3-5. Results of the tests are shown in Table 3-6. Even though the data was scattered and the test duration was limited, the results showed that the general corrosion behavior of Alloy 690 and Alloy 600 in primary water is about the same.

3.1.4 Esposito et al. 1991

Esposito et al. investigated corrosion rate and metal release rate of Alloy 690 and Alloy 600 in a simulated PWR primary water environment with and without Zn addition (Zn was used in other tests to assess effectiveness of Zn in mitigating PWSCC initiation) at 330°C (626°F).[31] The test conditions and autoclave water chemistry are summarized in Table 3-7. Test coupons were fabricated from Type 304, Type 316, Alloy 600MA, Alloy 600TT, Alloy 690TT, Alloy 750, and Stellite. The heat information and chemical composition were not reported. The test coupons

were suspended in the autoclave and exposed for times up to 2,500 hours with or without adding zinc borate. Unlike in the general corrosion rate studies for SG tubing, the test coupons in this study were not subjected to any significant rate of coolant flow. At the conclusion of the test, some samples were descaled to a constant weight by cathodically stripping the oxide film.

The metal corrosion and corrosion release are calculated from the coupon weight change measurements.

Total metal corroded = $W_0 - W_d$
Oxide film weight = $W_a - W_d$
Metal release = $(W_0 - W_d) - 70\%*(W_a - W_d)$

Where: W_0 = original sample weight
W_a = weight after coupon exposure
W_d = weight after descaling
70% is the assumption that metals in the oxide corrosion film represent 70% of the total film weight.

The above values are then divided by the specimen area to obtain the corrosion release per unit area. The average corrosion rate and corrosion release rate after 2,500 hours of exposure with and without zinc addition are listed in Table 3-8. The detailed general corrosion data from each specimen examined are listed Table 3-9. The test results clearly show that the Alloy 690TT has the lowest general corrosion rate among all the materials tested in PWR primary water both with and without zinc addition. The results also confirm that the general corrosion rate of Fe-Cr-Ni alloys in primary water environment decreases with increasing Cr content. In addition, the test results also indicate that zinc addition could significantly reduce the general corrosion rate of most commonly used materials in the PWR primary coolant system.

3.2 Stress Corrosion Cracking Tests in Primary Water Relevant Conditions

This section summarizes the results of a comprehensive review of the available laboratory test data pertinent to SCC in primary water relevant conditions for Alloy 690/152/52 materials. Most testing has been performed with Alloy 690 wrought materials with very few tests having been identified for Alloy 52 or Alloy 152 weld materials. Numerous investigations have been performed under a variety of PWR-relevant environmental conditions:

1. High temperature de-oxygenated (deaerated) water
2. Additions of boron, lithium, and hydrogen
3. Hydrogenated steam
4. Steam doped with chloride, fluoride, and sulfate anions
5. Additions of zinc

The various test conditions cited in this report include temperatures to 680°F (360°C) water, dissolved oxygen levels < 20 ppb, tests in doped and undoped 752°F (400°C) steam, lithium concentrations up to 3.5 ppm, boron concentrations up to 1800 ppm, hydrogen concentrations up to 100 cc/kg H_2O, and with the additions of chlorides and zinc. Even though the wording "simulated primary water conditions" was often used by the authors, it is clear, from the test conditions listed, that some test conditions employed were outside the normal range of primary water chemistry.

Accelerated testing has been performed on double U-bend (simulating crevice conditions), reverse U-bend (RUB), constant load tests (CLTs), four-point bend, and steam generator tubing mock-up specimens. The literature review is divided into four groups:

1. Deaerated water
2. Deaerated water with additions of boron and lithium
3. Steam with the addition of hydrogen
4. Steam with the addition of hydrogen and other impurities ("doped steam")

Section 4 provides an evaluation of these test data and a quantitative or semi-quantitative assessment of Alloy 690/152/52 material's PWSCC resistance improvement relative to Alloy 600/82/182 material.

3.2.1 Deaerated Water Testing

3.2.1.1 Double U-Bend Tests by Sedricks et al. 1979

Sedriks et al. reported the results of double U-bend autoclave testing of Alloy 690 for resistance to stress corrosion cracking in a deaerated water environment at temperatures between 600 °F (316°C) and 680°F (360°C) using Alloy 600 as the control material.[9] The test conditions and water chemistry are listed in Table 3-10. The Alloy 690 heats used are listed in Table 3-2. The Alloy 600 control specimen heat number and composition were not reported. Alloy 690 and Alloy 600 specimens with both MA and TT heat treatments were tested. Details of the Alloy 600 and Alloy 690 product form, the double U-bend specimen size, design, and the loading stress were not reported.

None of the Alloy 690 specimens cracked under any of the test conditions listed in Table 3-10. Table 3-11 and Table 3-12 show that a wide variety of heat treatments, cold work, welding, and the presence of crevices were further evaluated at 600°F (316°C) under the test conditions of Test 1a and Test 3. None of the Alloy 690 specimens (creviced double U-bend) cracked while some Alloy 600 control specimens cracked under identical test conditions. Table 3-13 shows that increasing the test temperature to 650°F (360°C) and exposure time to 60 weeks (~10,000 hours) (Test 1b) did not produce cracking in any Alloy 690 U-bend specimens.

3.2.1.2 C-Ring Test by A. Smith et al. 1989-1991

A. Smith et al. reported stress corrosion tests on commercially produced Alloy 690 SG tubes.[32, 33] C-ring stress corrosion test specimens were fabricated per ASTM G 38[34] from Alloy 690 tubes "A" and "E", which were annealed at 1040°C (1904°F) and thermally treated at 715°C (1319°F) for 12 hours. The chemical composition of tubes "A" and "E" and their mechanical properties are summarized in Table 3-15. The C-ring specimens were tested in a variety of environmental conditions at 340°C (644°F), including pure deaerated water. In the pure water tests, the autoclave was pressurized to 10 bar (1 MPa or 145 psi) with hydrogen and then depressurized to 2 bar. No intergranular attack or stress corrosion cracking was noted after 1,500 hours of exposure. However, intergranular attack (IGA) was found in the C-ring specimens tested in caustic environments. Details of caustic IGA in Alloy 690 C-ring specimens by A. Smith et al. are provided in Section C.2.

3.2.1.3 RUB by Norring et al. 1987-1991

Norring et al. reported stress corrosion tests on reverse U-bend (RUB) specimens fabricated from Alloy 690 and Alloy 600 steam generator tubing in hydrogenated high temperature water.[35, 36, 37] The testing materials given by Ref. 35 and 36 are the following:

1. Alloy 690TT (thermally treated). Six tubes from two heats. The annealing heat treatment was 1 minute at either a low temperature of 900°C (1650°F) or a high temperature of 1090°C (1994°F). The thermal heat treatment was 12 hours at 715°C (1320°F). The measured Vickers microhardness value was between 143 and 226 HV.

2. Alloy 690MA (mill annealed). Five tubes from the same heats as Alloy 690TT. One of the tubes was annealed at a low temperature of 900°C (1650°F). The measured Vickers microhardness values were between 160 and 220 HV.

3. Alloy 600TT. One tube. The annealing heat treatment was at 990°F (1814°F)/1 minute and it was given a thermal heat treatment of 1320°F/12 hours.

4. Alloy 600MA SG tubes removed from Ringhals 2, 3, and 4. Three tubes from each unit.

5. Alloy 600 tubes from heats NX1991 and NX2650, which were known to be susceptible to intergranular stress corrosion cracking.

6. Special production tubes of Alloy 600 from EPRI, which were produced from materials from three different vendors and annealed at 927°C (1700°F) or 1024°C (1875°F).

Carbide Precipitation

Table 3-16 lists the heat chemical composition of selective elements for a few of the Alloy 690 and Alloy 600 materials used for fabricating RUB specimens. For these heats of materials, the grain boundary precipitation and chemistry were investigated by using analytic transmission

electron microscopy (ATEM) and atom probe field ion microscopy (APFIM). Their findings are summarized below.

The precipitates observed by ATEM in Alloy 690TT and Alloy 690MA were exclusively the globular $M_{23}C_6$ type. The intergranular $M_{23}C_6$ precipitates showed a cube-face coincidence with one of the abutting grains. The intragranular $M_{23}C_6$ precipitates were often large and incoherent with the surrounding matrix. The intergranular carbide density was much higher in the Alloy 690TT than Alloy 690MA. M_7C_3 type intergranular and intragranular precipitates were always observed by ATEM in all Alloy 600 materials. The M_7C_3 type precipitates were usually globular, but elongated intergranular M_7C_3 precipitates were also found in the Alloy 600. Some intergranular $M_{23}C_6$ precipitates were also sometimes observed in Alloy 600. Energy dispersive X-ray analysis (EDX) indicates that grain boundary Cr level was lowered by 3% in the Alloy 690MA and 6% in the Alloy 690TT.

The atom probe technique identified four different types of grain boundary precipitates, M_7C_3, $M_{23}C_6$, M(CN), and MB. The types of intergranular carbides identified by APFIM and their density are listed in Table 3-17.[37] The $M_{23}C_6$ precipitates in Alloy 690 were much richer in Cr than the same precipitates in Alloy 600. Grain boundary Cr depletion was found to be less in Alloy 600 than in Alloy 690. Cr depletion in Alloy 600 was found only at grain boundaries decorated with $M_{23}C_6$ type precipitates. For example, the grain boundary Cr was lowered by ~2% from the bulk concentration of 15.8% in the BH material. No Cr depletion was found at grain boundaries decorated only with M_7C_3 type precipitates in Alloy 600.

Alloy 690 RUB Test Results

The testing was performed using RUB specimens regardless of the original tube diameter which ranged from 1/2" to 7/8". The distance between the legs of the specimens was kept constant at 25.4 mm (1"). The testing was performed at 365°C (689°F) in two once-through autoclaves, whose environment conditions are listed in Table 3-18. Slightly different autoclave hydrogen levels were reported in the references cited.

A total of 67 Alloy 690 RUB specimens from 11 tubes (including both TT and MA) were tested at 365°C (689°F). The breakdown of the Alloy 690 RUB specimens and test duration are listed in Table 3-19. Most of the Alloy 690 RUB specimens were tested up to 25,000 hours. However, Ref. 37 indicates the test was finally terminated after an accumulated 33,000 hours with none of them cracked. After 20,000 hours of exposure, some Alloy 690 RUB specimens were removed to verify that they did not contain microcracks. The examination showed that no such cracks existed. Based on a crack initiation activation energy of 50 kcal/mole, the 33,000 hours at 365°C (689°F) is equivalent to 20 times the 33,000 hours or 75 years at 320°C (608°F) using an Arrhenius temperature-activation relationship.

Alloy 600 RUB Test Results

A total of 106 Alloy 600 RUB specimens from 106 tubes were tested at 365°C (689°F). The breakdown of the Alloy 600 RUB specimens, test duration, and results is listed Table 3-20. Each of the mill annealed (MA) and some of the thermally treated (TT) Alloy 600 RUB specimens

developed cracks with a Weibull characteristic time to cracking (63.2% probability of cracking) ranging from 800 to 13,000 hours.

3.2.1.4 CERT Tests of Alloy 690 and Alloy 600 by Angeliu et al. 1991

Angeliu et al. reported CERT (constant extension rate test, also known as slow strain rate test or SSRT) results of high purity laboratory heats of Alloy 600 and Alloy 690 in argon and high purity deaerated water at 360°C (680°F).[38, 39] The tensile specimens were fabricated from a cast ingot swaged to a 3.05 (0.12") mm rod stock. Cold work was introduced into all of the specimens using a two-step compression process. The gage section (2.2 mm dia. and 14.3 mm gage length) was compressed in the thickness direction by a two-step compression to produce a 30% reduction in thickness. The first compression step flattened the 2.2 mm dia. cylindrical gage section to a rectangular cross section of 1.7 mm thick. The specimens were then annealed to dissolve all carbon into solution and heat treated to produce approximately 100 μm size grains (ASTM grain size 3.5). After annealing, a second compression step reduced the thickness from 1.7 mm to 1.2 mm, or about a 30% thickness reduction. After final cold work, each specimen was ground and polished through 1 mm diamond paste. This type of deformation is known to enhance intergranular stress corrosion cracking (IGSCC) susceptibility in high temperature water.

The autoclave water chemistry and CERT testing conditions are provided in Table 3-22. After testing, the specimens were examined with a scanning electron microscope (SEM). The percentage of the fracture surface showing intergranular cracking was determined from SEM photographs at 60 to 80X magnifications. The nominal chemical composition, the annealing time and temperature, and the CERT test results in the argon atmosphere and in high temperature deaerated water are listed in Table 3-23 and Table 3-24, respectively.

The CERT results showed that the high temperature deaerated water enhanced the IG cracking susceptibility in the Alloy 600 (as opposed to behavior in argon) while having no effect on the Alloy 690. The propensity to IG fracture was reduced with Cr content increasing from 5%, to 16%, and to 30% and carbon content increasing from 0.001% to 0.03% when tested in high temperature water. The improvement was attributed to an increase in creep resistance from increasing Cr content and a small amount of carbon in solution. The improvement from a carbon addition in Alloy 690 was less noticeable due to the improvement from Cr. The results show that Alloy 690 and Alloy 600 containing 0.03% carbon are both highly resistant to IG cracking (0% IG) in the CERT test either in argon or deaerated water at 360°C (680°F). However, a slight amount of IG cracking (2%) was detected in the Alloy 690 specimens containing very low carbon (0.002%) tested both in argon and deaerated water at 360°C (680°F). Since the same small amount of (2%) IG cracking was found in both argon and deaerated water environments, the intergranular cracking in Alloy 690 in this study should not be considered as an indication of Alloy 690 potential susceptibility to PWSCC. Angeliu et al. claimed this was the first reported instance of intergranular cracking of Alloy 690 material (albeit an ultra low carbon high purity laboratory grade) produced in deaerated environments. However, it is noted that Nakayama et al. reported intergranular cracking of Alloy 690 single U-bend specimens tested in hydrogen saturated water containing lithium and boric acid (see Section 3.3).

In addition to CERT tests, Angeliu et al. also investigated surface oxide formation in the test coupons (the same as used for the CERT tests) after ~100 hour exposure to deaerated high temperature water. The test coupons, measuring 10 mm x 6 mm by 0.5 mm, were obtained by rolling the 3.05 mm rod stock to 0.5 mm thickness. The coupons were then solution annealed as was used for the CERT specimens. Unlike the CERT specimens, these coupons were not cold worked after the solution anneal. The coupons were ground with SiC paper and one side was polished to a mirror smooth finish. After exposure, the surface was cleaned and examined by X-ray photoelectron spectroscopy (XPS) and scanning transmission electron microscopy (STEM). The surface oxide film was found to be a mixture of Cr_2O_3 and $Ni(OH)_2$ phases. The oxide film thickness and predominant phase in the oxide film are summarized in Table 3-25. The ultra low carbon Alloy 600 (0.002% carbon) was found to have a very thin Cr_2O_3 rich surface film. Increasing the carbon content from 0.002% to 0.03% caused the Alloy 600 film thickness to grow from 38 nm to 281 nm, consisting mostly the $Ni(OH)_2$ phase. The surface oxide film thickness in Alloy 690 contained predominantly fine grained Cr_2O_3 . Increasing the carbon content from 0.002% to 0.03% caused the Alloy 690 film thickness to increase only slightly, from 46 nm to 58 nm. It has been found that as the Cr content increases in high-nickel alloys, the repassivation rate (formation of Cr_2O_3) and IGSCC resistance are all increased. On the other hand, a thicker but less dense $Ni(OH)_2$ film is more likely to contain defects, hence more likely to rupture and expose the metal underneath to environmental attack. In some instances, the hexagonal $Ni(OH)_2$ plates were found to have grown into the grain boundary, offering the potential for intergranular crack nucleation.

3.2.2 Deaerated Water With Li/B Testing

3.2.2.1 RUB Tests by K. Smith et al. 1985

K. Smith et al. reported stress corrosion tests on reverse U-bend (RUB) specimens fabricated from Alloy 690 and Alloy 600 SG tubing in a simulated PWR primary water environment.[11] The Alloy 690 RUB specimens were fabricated from full length SG tubes of three pre-industrial production heats. The full length SG tubes (also called “pre-series” tubes) were produced by an established industrial route. The three pre-industrial production Alloy 690 heats were intentionally chosen to span the limits of the specification requirements for C and Cr content. The chemical composition and mechanical properties of these three heats are listed in Table 3-3. The SG tube diameter was not listed. The chemical composition also was not provided for the Alloy 600 control heats.

The Alloy 690 and Alloy 600 were both tested in the MA and TT conditions for up to 16,000 hours at 360°C (680°F). Two kinds of autoclave water chemistry were used to simulate the beginning and end of fuel cycle PWR primary water chemistry. The autoclave water chemistry is listed in Table 3-14. The number of RUB specimens for each alloy condition was 10. The test results are shown Figure 3-3. None of the Alloy 690 (TT or MA) RUB specimens developed cracks after 13,000 hours exposure under the beginning of fuel cycle condition and 16,000 hours under the end of fuel cycle condition. Alloy 600 RUB specimens of both TT and MA developed cracks under both the beginning and end of fuel cycle conditions. As expected, the Alloy 600 in

the TT condition was evidently much more resistant to cracking than Alloy 600 in the MA condition.

3.2.2.2 RUB and Constant Load Test by Yonezawa et al. 1985

Yonezawa et al. conducted stress corrosion tests on reverse U-bend specimens fabricated from Alloy 690 and Alloy 600 SG tubing in both the TT and MA heat treatment conditions and shot-peened Alloy 800L in simulated PWR primary water environment.[17] The test was conducted at 360°C (680°F) for up to 12,000 hours. The composition and heat treatment of the test materials are listed in Table 3-4. The test condition and water chemistry are listed in Table 3-5. The diameter of the SG tubes used to fabricate the RUB specimens was not reported. RUB specimen testing stress levels, measured by X-ray diffraction analysis, were between 70 and 130 ksi. Figure 3-4 shows the measured stress vs. the crack detection time. Intergranular cracking was observed in the 20% pre-strained Alloy 600MA specimens after 300 hours of exposure and in the Alloy 600TT specimens after 800 hours of exposure. However, no cracking was observed in Alloy 690 and shot-peened Alloy 800 specimens after 12,000 hours of exposure time. It is noteworthy that the X-ray diffraction measured stresses in the Alloy 690 RUB specimen were higher than that of the cracked Alloy 600TT and MA specimens. The minimum stress level vs. minimum time-to-cracking curves were drawn for Alloy 600TT and Alloy 600MA on Figure 3-4. As expected, Alloy 600TT had a higher resistance to stress corrosion cracking than Alloy 600MA in the primary water.

In addition, Yonezawa et al. reported constant load (CL) stress corrosion cracking (SCC) test results at the same testing temperature and in the same primary water environment as for the RUB specimens. No details of the CL specimen geometry were provided. The constant load test results are shown in Figure 3-5, which indicates the loading stress was between approximately 60 and 90 ksi. Alloy 600MA developed SCC after 1,100 hours of exposure. However, no failure was observed of the Alloy 690TT CL specimens after approximately 7,000 hours of exposure.

3.2.2.3 U-Bend Test of Alloy 690 by Nakayama et al. 1987

Nakayama et al. performed single U-bend tests of Alloy 600, Alloy 690, and Alloy 800 in hydrogen saturated water.[40] Various heats of Alloy 600, Alloy 690, and Alloy 800 SG tubing were melted in a vacuum induction furnace and the resulting ingots were reduced to plates of 4-mm thickness by forging and hot rolling. The chemical compositions of the Alloy 600 and the Alloy 690 SG tubing used are listed in Table 3-26. Single U-bend specimens of the dimension 2 mm x 14 mm x 65 mm were machined from the 4-mm plates of Alloy 690 and 600 in both solution annealed (MA) and thermally treated (TT) conditions. In addition, the specimens were given aging treatment at 500°C (932°F) for 24 and 100 hours to simulate 24 and 100 years of exposure at 300°C (572°F) based on the Larson-Miller equation. Details of Alloy 600 and Alloy 690 heat treatment and aging treatment are listed in Table 3-27.

The single U-bend specimens were tested in hydrogen saturated water containing 1000 ppm boron and 2 ppm lithium at 330°C (626°F) for 3000 hours. The solution was renewed every 250 hours. The test results (measured maximum crack depths) are listed in Table 3-28. Slight intergranular cracking was detected in two out of the four Alloy 690 conditions tested. The maximum intergranular crack depth was 70 μm in Alloy 690TT with a 24-hour aging treatment

and 30 μm in Alloy 690MA with a 100-hour aging treatment. Cracking was more severe in Alloy 600 specimens while no Alloy 800 specimens developed cracks. In addition, SEM microscopy (the authors reported that SEM microscopy was used) showed that the intergranular cracks in Alloy 690TT (70 μm max. depth) were at the tips of dislocation pile-ups.

3.2.2.4 CERT Test of Psaila-Dombrowski et al. 1995-1997

Psaila-Dombrowski et al. reported the results of CERT tests in simulated primary water at 343°C (650°F).[41, 42] The CERT test specimens were machined from Alloy 690 plate and Alloys 82, 182, and 152 welds. The studies investigated the corrosion performance of welds connecting a steam generator divider plate to the weld buildup in a welded-in divider plate (WIDP) design. This weld region was believed to be possibly susceptible to primary water stress corrosion cracking due to a lack of post-weld stress relieving.

A number of weld build-ups and a composite plate were manufactured. The weld samples were fabricated in a manner consistent with SG fabrication practices in which Alloy 52 is used to attach the Alloy 690 plate to the Alloy 82 buildup. The mock-up composite plate began as a 60 mm (2.36") thick A 508 carbon steel plate. One edge of the A 508 plate was overlaid with a 5 mm thickness of Alloy 82 and then stress relieved. The test block was completed by making a modified double V-groove weld between the 5.5 mm thick Alloy 690 plate and the Alloy 82 overlay using Alloy 152. The plate was not stress relieved following the welding. The overall length of the composite weld plate was ~1,000 mm. CERT specimens were machined from Alloy 82, Alloy 152 and the heat affected zones (HAZ) between Alloy 82 and Alloy 152, and Alloy 152 and Alloy 600 (see Figure 3-6). The size and geometry of the CERT specimens are shown in Figure 3-7. The specimens were machined parallel to the fusion line. This would allow all the materials in the specimens to be evaluated for SCC susceptibility. If the specimens had been machined perpendicular to the fusion line, only the weakest material would undergo plastic deformation and hence be evaluated for SCC susceptibility. However, information on the chemical composition of the Alloy 82 and 152 weld metals and Alloy 690 plate and heat treatment condition of Alloy 690 were not reported.

The CERT tests were performed in an inverted 7.5 liter Alloy C-276 autoclave. The autoclave environment was to simulate a typical PWR Water Chemistry according to EPRI's PWR Primary Water Chemistry Guidelines. In addition, CERT tests were also performed in a faulted primary water chemistry. The faulted water had 150 ppb of chloride by adding NaCl to the feed tank. The CERT tests were performed at a constant strain rate of either 5×10^{-8} or 10^{-6} sec^{-1}. The water chemistry and test parameters are listed in Table 3-29. During the tests, the autoclave pressure preloaded the specimens to approximately 155 MPa (22.5 ksi). This was not believed to affect the test results as this stress level was below 50% of the room temperature yield stress. After the test, the specimen fracture surface was examined by SEM for evidence of SCC.

The CERT test results are summarized in Table 3-30. During the Phase 1 tests at a strain rate of 10^{-6} sec^{-1}, no evidence of SCC was found in any of the CERT specimens including those tested in the faulted water chemistry containing 150 ppb chloride. The fracture surfaces examined by SEM were dimpled indicating ductile failure. In addition, specimens containing two different materials did not have step failures indicating failures at different times. However, SCC cracking was detected only

in Alloy 82 in the CERT specimen containing both Alloy 82 and 152 weld metals when tested at the lower strain rate of $5x10^{-8}$ sec^{-1} in normal primary water (see Figure 3-8). No SCC cracking was observed in the Alloy 152 (also see Figure 3-9) and Alloy 690 specimens.

3.2.2.5 RUB Test and Constant Load Test by Ogawa et al. 1997

Ogawa et al. reported the results of reverse U-bend (RUB) tests and constant load tests on Alloy 600MA & TT and Alloy 690TT SG tubes.[43] The Alloy 600 and Alloy 690 SG tube size, material composition and heat treatment information are summarized in Table 3-31. The number of specimens and test temperature are summarized in Table 3-32.

RUB Test

The RUB test temperature was 320°C (608°F) for the Alloy 600MA & TT materials, and 360°C (680°F) for the Alloy 690TT material. However, the RUB specimens were tested in slightly different primary water chemistries. The test results are summarized in Table 3-33.

In Phase 1, the RUB specimens were tested in the so-called optimum pH water chemistry (pH 7.3 at 285°C or 545°F, 280 ppm B, and 2.0 ppm Li) and in the reference pH water chemistry (pH 7.1 at 285°C or 545°F, 500 ppm B, and 2.0 ppm Li). The tests in Phase 1 lasted up to 10,000 hours and the occurrence of PWSCC cracking was checked after 3000, 4190, 5000, 7000, and 10,000 hours. PWSCC was observed for the Alloy 600MA material prestrained at 20%, 15%, 10%, and 5% under both pH conditions. PWSCC was also observed for the Alloy 600TT material prestrained at 20%, 15%, and 10% under the reference pH and for the 20% and 15% prestrain under the optimum pH environment. No PWSCC was observed for the 20% prestrained Alloy 690TT specimens tested at a higher temperature than the Alloy 600MA & TT specimens.

In Phase 2, the RUB specimens were tested in the candidate water chemistry (pH 6.86 at 285°C or 545°F, 1600 ppm B, and 3.5 ppm Li) and in the reference water chemistry (pH 6.61 at 285°C or 545°F, 1600 ppm B, and 2.0 ppm Li). The tests in Phase 2 lasted up to 10,015 hours and the occurrence of PWSCC cracking was checked after 1356, 3000, 5005, 7,000, 8536 and 10,015 hours. The results were similar to those obtained in Phase 1. Both the prestrained Alloy 600MA and 600TT specimens cracked although the Alloy 600TT material was more resistant to PWSCC than the Alloy 600MA material. Again, no PWSCC was observed for the 20% prestrained Alloy 690TT specimens tested at a higher temperature than the Alloy 600MA & TT specimens.

Constant Load Test

The constant load specimens (uniaxial tensile specimens) were cut from the SG tube wall. The specimens were all loaded to 85 ksi. The test temperatures were 320°C (608°F) and 340°C (644°F) for the Alloy 600MA & TT specimens, and 360°C (680°F) for the Alloy 690TT specimens. The constant load specimens were tested in primary water chemistries identical to the ones used for the RUB specimens. The test results are summarized in Table 3-33.

None of the Alloy 600 specimens (10 each for MA & TT condition) exhibited PWSCC at 320°C (608°F) regardless of the water condition used after 10,000 hours exposure. In contrast, all of the

Alloy 600 specimens (10 each for MA & TT condition) exhibited PWSCC when tested at 340°C (644°F) under both water conditions at the end of 10,000 hours exposure. None of the Alloy 690 specimens developed PWSCC after 10,000 hours at 360°C (680°F). Based on the 50 kcal/mole activation energy commonly used for Alloy 600 PWSCC initiation, the crack initiation time at 340°C (644°F) is only 25% of that at 320°C (608°F). Similarly, the 10,000 hour exposure at 360°C (680°F) for Alloy 690 specimens would be equivalent to 36,600 hour exposure at 340°C (644°F). These results confirmed that PWSCC is a thermally-activated mechanism and Alloy 690 has a much higher PWSCC resistance compared to Alloy 600 of either MA or TT condition.

3.2.2.6 RUB Tests by Angell et al. 1999

Angell et al. performed RUB stress corrosion tests on Alloy 600 and Alloy 690 SG tubes in primary water chemistry both with and without zinc additions.[44] The Alloy 600 and Alloy 690 SG tube information are listed in Table 3-36. The tests were performed at 350°C (662°F) in two phases with each phase lasting 7500 hours. Phase 1 was to simulate beginning of cycle primary water for a 12-month fuel cycle and Phase 2 was to simulate beginning of cycle primary water for an 18-month fuel cycle. Zinc was added in the form of zinc acetate to a level of 40 ppb to assess the effectiveness of such addition on PWSCC initiation.

The test conditions and test results are summarized in Table 3-37. The descriptions on the RUB specimen I.D. were vague and could not be associated directly with the chemical composition of the Alloy 600 and Alloy 690 SG tubes listed. Hence, the specimen heat number in Table 3-37 includes some guesswork. None of the Alloy 690 RUB specimens cracked either with or without the zinc additions while some of the Alloy 600 specimens cracked both with and without the zinc addition. Zinc addition seems to slightly improve cracking resistance of the Alloy 600 specimens while having no apparent affect on the already resistant Alloy 690 specimens. Phase 2 included some uncracked specimens carried forward from Phase 1. However, for the Alloy 600 specimens, it was not mentioned if the cracked ones included the ones from Phase 1. For the Alloy 690 specimens, the maximum exposure time without failure was 15,000 hours.

3.2.2.7 Studies by CEA and EdF

A large research study was undertaken by the CEA in collaboration with EdF starting in 1987 to determine using accelerated testing the long term resistance of Alloy 690TT to SCC in PWR primary water. This followed a decision taken in France, as elsewhere, at the beginning of the 1980's to replace Alloy 600 in certain PWR component items with Alloy 690TT. The following summary of this French work on Alloy 690TT is taken from the following proprietary reports; a CEA review written in 2002[45], an EdF state of the art review in December 1995[46], and two additional complementary EdF reports written in 1997[47] and 2002[48]. English language reviews of much of this French work also appeared in the open literature in 1999[49] and 2003[50]. An EDF proprietary report[51] on a study of nickel-base weld metals including Alloys 152 and 52 is also summarized here.

3.2.2.7.1 CEA Technical Report RT-SCCME 618 Rev. A [45] - 2002

Sixteen heats of Alloy 690 conforming to the French RCC-M 4105 standard (1988) were tested of which three were pre-production heats for R & D purposes. A list of the materials tested in this program is given in Table 3-38; the chemical compositions are given in Table 3-39. All except one were made by Imphy, the remaining one being supplied by Huntington. One of the pre-series heats, WE092, was on the limit of the then current RCC-M specification with 30.9%Cr, 0.037%C and a low iron content of 7.3%Fe. Another pre-production heat, WE094, had high carbon, 0.031%C, and low iron, 8.5%Fe, while the remainder contained about 29%Cr, 10%Fe and carbon contents between 0.015 and 0.025%C.

All sixteen heats of Alloy 690 were formed into 19.05 mm diameter SG tubes of wall thickness 1.09 mm by Valinox Nucléaire. The mill anneal (MA) in cracked ammonia of the pre-production heats WE092 and WE094 was initially performed at 980°C (1796°F) for 2 minutes and were then thermally treated (TT) at 700 to 730°C (1292 to 1346°F). However, the mechanical properties were in excess of the specification requirements and so these two pre-production heats were mill annealed again at 1040 and 1070°C (1904 and 1958°F) followed by a thermal treatment at 700 to 730°C (1292 to 1346°F). The other industrial heats were mill annealed between 1040 and 1070°C (1904 and 1958°F) also for 2 minutes and thermally treated under vacuum at 700 to 730°C for 5 hours. Tube straightening was then performed to ensure linearity was within specification and followed by internal sand blasting with corundum and external surface polishing with an abrasive band.

The unusual thermal history of the two pre-production heats WE092 and WE094 with the higher carbon contents was probably responsible for the small grain sizes of ASTM 10 to 11 and 9 to 10 respectively. On the internal surface of the two pre-production heats, the grain size was even smaller at ASTM 12 to 13. These figures should be compared with ASTM 7 to 9 for the bulk material of the other heats and ASTM 10 to 12 on the internal surface. The internal surface layer with smaller grain size on the tube internal surfaces could be up to 30 μm thick.

The metallurgical characterization of the SG tubes revealed a high degree of grain boundary carbide coverage (i.e., apparently continuous at a magnification of 1000X) with the exception of the two pre-production heats with high carbon, WE092 and WE094, where it was classified as having a low linear density (less than 1 carbide in 10 μm or 0.0039 inch). The low grain boundary carbide density of the two heats was considered to result from the unusual thermal history with the initial mill anneal at 980°C (1796°F). The intragranular carbide density of these two heats was classified as medium (i.e., between $2x10^{-4}$ and 10^{-2} μm^{-2}) whereas for the others, with four exceptions, it was classified as low ($<2x10^{-4}$ μm^{-2}). Of the four exceptions, three were judged as having medium density of intragranular carbides and one, WF786, as having a high density of intragranular carbides ($>10^{-2}$ μm^{-2}).

The residual stress and level of cold work were measured by X-rays on the internal surfaces of tubes from two heats, WE092 and another representative industrial heat. The level of cold work on the internal surface of both was observed to be about 15%. The internal surface stresses were compressive at -300 MPa (-43.5 ksi) for WE092 and -180 (-26.1ksi) to -280 MPa (40.6 ksi) for the other (with an estimated uncertainty of ±65 MPa or ±9.4 ksi).

Bulk 0.2% offset yield strengths were measured at room temperature on tensile specimens taken from the tubes. All were in specification (275 to 470 MPa in RCC-M 4105) being typically between 300 and 360 MPa except the pre-production heat, WE092, at 499 MPa before its repeated heat treatment. Heat WE094 was just in specification at about 50MPa lower than WE092. After the two pre-production heats were given their second mill anneal at 1040 to 1070°C (1904 to 1958°F) followed by a second thermal treatment, the yield strength was 464 MPa for WE092 and about 50MPa lower for WE094.

During preparation of the RUB specimens for the SCC tests, surface defects appeared where the deformation was greatest in the surface cold worked layers with low ductility. The deformation of the apex of a RUB is typically between 30 to 40%. Thus the inner tube surface layer that was previously in compression would be transformed into very high tension due to the prior cold work. All measured surface stresses at the apex of the RUB specimens were above 1000 MPa (145 ksi) and up to 1230±30 MPa (178.4±4.4 ksi), the precise value depending on the heat of material. The surface defects were orientated mainly, but not exclusively, in the axial direction of the original tube, and were 5 to 100 μm long and up to 20 μm deep. The largest surface defects were found on specimens made from the pre-production heats WE092 and WE094. Due to the small grain size and magnification of the optical micrographs it is difficult to assert that the defects were definitely intergranular. An experiment was conducted in which RUB specimens were made after a surface layer 40 μm thick was removed by electropolishing. These specimens did not show any surface defects, thus proving that the modified fine grain surface layer was at the origin of the defects formed on RUB specimens from the as-manufactured tubes. The surface stresses on the RUB specimens formed from the electropolished tubes were only about 5 to 10% lower than those from the as-manufactured tubes.

SCC testing was carried out in PWR primary water at 360°C (680°F) and 20 MPa pressure in a static autoclave with the hydrogen concentration in the liquid phase controlled to between 23 and 35 ml/kg using a Pd/Ag thimble. The SCC tests lasted 90,000 hours in total but regular examinations (at intervals between 2,000 and 7,500 hours) of the RUB specimens in an SEM did not show any IGSCC or any propagation of the pre-formed mechanical surface defects. The trapped hydrogen content of the Alloy 690 specimens was measured and was usually about 2±0.5 ppm. (Similar concentrations of hydrogen were measured in several RUB specimens of Alloy 600 that were tested at the same time and that typically cracked within 5,000 hours. Other related studies have typically measured 2 to 5 ppm hydrogen, which may be compared with those from slow strain rate tests of up to 35 ppm.)

Measurements of the surface residual stress on RUB specimens from seven of the sixteen heats of Alloy 690 showed that it reduced rapidly at the beginning of the SCC tests and stabilized at about 30 to 70% of the original value depending on the heat of material concerned. The largest percentage relaxation occurred in the pre-production heats WE092 and WE094. Below the surface, the stresses remained high between 600 and 800 MPa, again the precise value depending on the heat of material.

The hardness of each Alloy 690 specimen was measured during the exposure tests at 360°C (680°F) and specimens were examined by TEM for any evidence of short range ordering to form Ni_2Cr, particularly in heats at the bottom end of the iron specification of 7%Fe. Note that some literature data suggest that after 100,000 hours at 360°C some short range ordering may occur at

7%Fe. In the present study, although a statistically significant slight increase in hardness of up to ~30HV did occur, there was no evidence of Ni_2Cr formation found by TEM. However, those heats with the highest Ni/Cr atomic ratio and lowest Fe contents, heats WE092 and WE094, showed the highest increase (of ~30HV) in hardness.

No attempt was made in this CEA report to assess the practical implications of any of the experimental observations with regard to the suitability or longevity of Alloy 690TT for PWR service.

3.2.2.7.2 EDF Report HT-44/95/013/A, 1995[46]

In order to quantify the resistance of Alloys 690TT (and 800) to SCC in PWR primary water, various types of laboratory tests were conducted in hydrogenated pure water at 325 and 360°C (617 and 680°F) and in PWR primary water at 360°C on specimens of steam generator tubing plus a lesser number of specimens of Alloy 690TT typical of upper head CRDM nozzles (Table 3-40 and Table 3-41). Chemical compositions and mechanical properties of the various heats of Alloy 690TT are given in Table 3-42 and Table 3-43 respectively.

As in the case of the parallel tests performed by the CEA, three categories of Alloy 690TT SG tube were tested; 4 experimental tubes from 3 heats supplied by Huntington, 5 pre-production tubes from 3 heats of which 2 were supplied by Imphy (WE092 and WE094) and one by Huntington, and 9 industrial tubes from 9 heats of which 2 were from Huntington and the remainder from Imphy/Tecphy. Various combinations of mill anneal conditions between 980 and 1070°C (1040 to 1070°C in the case of the industrial tubes), mill anneal atmospheres (cracked ammonia or hydrogen) and final thermal treatment (700°C or 1292°F for 16 or 5 hours) were present among the 18 SG tubes available for the study. All tubes were straightened prior to the thermal treatment where required. Many of the early tubes were sand blasted on the internal surface, and all were polished with an abrasive band on the external surface. The practice of sand blasting the internal tube surface with the objective of removing a nitrided layer from the cracked ammonia was discontinued in 1989 and subsequently a hydrogen atmosphere was adopted for the mill anneal. The tube diameters were mainly 19.05 mm (0.750") with a 1.1 mm (0.043") thick wall but some for replacement bundles for 900 MWe stations were 22.2 mm diameter with a 1.27 mm (0.050") wall thickness. One of the Alloy 690 tubes was discovered to be contaminated during tube drawing by a phosphorus containing lubricant resulting in localized formation of a Cr_3P eutectic up to 15 μm (0.0006") deep and occasionally 40 μm (0.0016") deep.

The Alloy 690TT specimens from forged CRDM nozzles came from one experimental and one industrial heat both supplied by Tecphy. Both products were subjected to a laboratory heat treatment at 715°C (1319°F) for 5 hours.

Concerning the chemical compositions, as noted earlier for the CEA study, one of the Alloy 690 heats, WE092, was deliberately fabricated with the carbon and chromium at the high end of the specification and iron at the low end of the specification for a study of short range ordering during thermal aging. The iron content of the two CRDM nozzle heats was relatively high at 10.5%Fe.

The mechanical properties of the Alloy 690TT SG tubes were within the RCC-M 4105 specification with the exception of one pre-production heat that was initially mill annealed at 980°C (1796°F) prior to thermal treatment, as noted in the earlier summary of the CEA work. However, both pre-production Imphy heats WE092 and WE094 formed into tubes by Vallourec had 0.2% offset yield strengths significantly exceeding the EPRI recommended maximum of 379 MPa (55.0 ksi) even when mill annealed at 1040 or 1060°C (1904 or 1940°F) prior to thermal treatment. Two of the industrial tubes had 0.2% offset yield strengths close to the minimum limit recommended by EPRI.

The grain size and carbide morphologies of all heats were characterized. The intergranular carbide decoration was generally classified as "medium". The microstructures of two French pre-production heats WE092 and WE094 have already been described above in the companion CEA study (CEA Report RT618). Additional details concerning tubes mill annealed in cracked ammonia show that nitrided layers up to 20 μm (0.0008") thick were formed. The removal of these layers on the internal surface by sand blasting generated the cold work that then resulted in recrystallization during thermal treatment to form the tiny grains observed on the internal surface. The nitriding of the external surface disappeared during final polishing step. This whole problem was then circumvented with the adoption of hydrogen for the protective atmosphere during mill annealing although some occasional surface carburization was observed.

Concerning the two Alloy 690TT CRDM nozzles, the grain size varied between ASTM 3 and 6 and there was a tendency for the grain size to increase towards the internal surface. The carbide precipitation was entirely intergranular and attributed to a high solution anneal temperature of 1050 to 1080°C (1922 to 1976°F).

Stress corrosion experiments were performed either in pure water at 325 or 360°C with an overpressure of 3 bar hydrogen or in PWR primary water (1000 ppm B, 2 ppm Li and 0.16 to 0.5 bar hydrogen) at 360°C (680°F). RUB specimens were prepared from the steam generator tubes with initial stresses that varied between 850 and 1050 MPa (, as measured by X-rays at 20°C (68°C). Similar 19 mm (0.748") diameter tubes were elecro-discharge machined (EDM) from the wall thickness of the CRDM nozzles and, after removal of the fused surface layer by electropolishing, were split longitudinally in half to be formed also into RUB specimens. In this case, the measured peak stresses were between 700 and 860 MPa (102 and 125 ksi). SSRT and constant load tests on the SG tube materials were carried out using planar tensile specimens machined by EDM. In most cases for SSRT, but not constant load, these specimens were also electropolished to remove the fused layer as well as the surface layer of small grains present on the original internal surfaces of some tubes. Round gage SSRT and constant load specimens were machined from the CRDM nozzle materials, the surface cold worked layer in this case being removed by electropolishing only for the SSRT.

Each Alloy 690TT RUB specimen was inspected every 3000 to 4000 hours during the SCC tests along with a RUB of Alloy 600 that was inserted into each phase of testing; the latter Alloy 600 RUB typically cracked between 500 and 2,000 hours. Specimens of the experimental tubes were tested for a total of 38,000 hours in hydrogenated pure water at 325°C (617°F)and 46,000 hours in primary water at 360°C. (Note that some preliminary tests in hydrogenated steam at 400°C were not pursued beyond 6,000 hours.) The specimens from the pre-production tubes were tested for 10,000 hours in hydrogenated pure water at 360°C and in PWR primary water for 25,000 hours at 360°C

(and in the preliminary study in hydrogenated steam at 400°C for 6,000 hours). The specimens from the industrial production tubes had reached 10,000 hours in hydrogenated water at 360°C (680°F) and 35,000 hours in primary water at 360°C when the EdF report was written in 1995 (and 2600 hours in hydrogenated steam at 400°C in the preliminary study). The Alloy 690 RUB specimens prepared from the CRDM nozzles were tested for 12665 hours at 360°C in PWR primary water.

No SCC initiation was noted in any Alloy 690 RUB nor was any propagation detected of surface defects created when forming RUBs from a few of the SG tube materials, as described for the CEA study. In certain high magnification pictures of the pre-formed surface defects in the perturbed surface layers on Alloy 690TT, these pre-formed defects definitely appear to be predominantly intergranular. The surface stresses on the RUB specimens were observed to relax rapidly to between 30 and 70% of the starting value, as also noted in the CEA study (CEA Report RT618). The stress relaxation of the RUB specimens of Alloy 690 was more marked than was the case for Alloy 600.

Slow strain rate tests were performed in argon and in PWR water at 360°C with a strain rate of $5x10^{-8}$ sec^{-1}. No test in argon on electropolished Alloy 690TT specimens gave rise to any cracking but those heats of SG tubing with the retained perturbed inner surface layers showed surface fissures up to 10 μm deep.

In PWR primary water, all SSRT on the same heats, with two exceptions, gave rise to short intergranular cracks 5 to 20 μm (0.0002" to 0.0008") deep independent of the surface preparation. This included the industrial production tubes of which the one with surface phosphorus contamination was not notably worse. The two exceptions were specimens from the pre-production heat WE092 and one of the industrial production heats. From multiple specimen tests on WE092, intergranular cracks in the necked region up to 45 μm (0.0018") deep were observed when electropolished and up to 120 μm (0.0047") deep from the as-received internal tube surface, whereas the depth of cracking outside the necked region varied from 10 to 65 μm (0.0004" to 0.0026"). The other exception was an industrial heat, WG592, of which only 2 specimens were tested, one electropolished and one where the industrial surface (sandblasted before thermal treatment) was retained. Cracking to a depth of 35 μm (0.0014") from the industrial sandblasted surface involved intergranular penetration throughout a very fine-grained recrystallized surface layer plus ~ 1 normal size grain depth thereafter. In the case of the electropolished surface of WG592, the observed crack depth of 20 μm (0.0008") was equivalent to only ~ 1 normal grain size. Note that 1 grain-depth penetrations were also observed in other cases (including Alloy 800), so that it is thus debatable whether the observed intergranular separations for Alloy 690TT were truly representative of PWSCC. For comparison, similar SSRTs on Alloy 600MA showed 80 μm (0.003") deep cracks from electropolished surfaces and 500 μm (0.020") deep from as-received surfaces.

The SSRT specimens from the CRDM nozzles showed intergranular cracks that did not exceed one grain depth, in this case 70 μm (0.0028") maximum, independent of initial surface condition. This was judged to indicate that no significant SCC had occurred.

It was concluded by the EdF authors from all these SSRT results that IGSCC had been provoked to a limited extent in Alloy 690TT but resistance was clearly very high. It can be deduced from the results that the resistance of Alloy 690TT was usually more than an order of magnitude better than

Alloy 600MA, with the exception of the Alloy 690TT heat with the out-of-specification carbon content, small grain size and poor intergranular carbide decoration, WE092, as described in the previous section.

Constant load tests in PWR primary water at 360°C (680°F) showed no cracking typical of SCC even on the worst pre-production Alloy 690TT tube (heat WE092) when loaded up to a nominal stress of 684 MPa (99.2 ksi) for 10,900 hours. The same was true of Alloy 690 samples from the CRDM nozzles for periods up to 18,500 hours at a nominal stress of 580 MPa (84.1 ksi).

3.2.2.7.3 EDF Report HT-44/97/020/A, 1997[47]

This EDF report is in fact a copy of the PhD thesis of J-D Mithieux that was examined on October 29, 1997 at the Institut National Polytechnique de Grenoble. The objective of the work was to try to understand why Alloy 690 has such good resistance to stress corrosion in PWR primary water and to quantify its limits. In this context, the literature review by Mithieux cited a prior EdF supported PhD thesis by J. F. Kergaravat at the Institut National Polytechnique de Grenoble in which an Alloy 690TT steam generator tube was heat treated at 1100°C (2012°F) to take the carbides back into solution followed by a rapid quench. This material was observed to crack in PWR primary water, apparently during a slow strain rate test but with otherwise unspecified test conditions.

Since degradation of a protective film is generally considered an essential step for the development of stress corrosion, an experimental investigation of repassivation kinetics and substrate deformation behavior was undertaken. Repassivation kinetics of Alloys 600MA and 690TT were measured by a potential step technique in PWR primary water at 360°C and the macroscopic and intergranular creep rates were determined between 325°C and 400°C. These were then correlated with results of RUB and SSRT experiments on the same heats. The essential results from this work were published in the open literature in 1999[49].

The materials selected for the study were in the form of steam generator tubes from six heats of Alloy 600 steam generator tubes and five heats of Alloy 690TT, the latter including the French pre-production heat WE092 (with high carbon and chromium and low iron and the double heat treatment history). An additional forged bar of Alloy 690 was also studied. All the Alloy 600 heats and one experimental Alloy 690 heat were received in the mill annealed condition and were given thermal treatments, as necessary. Another heat treatment, 1100°C for 20 minutes followed by a water quench, was also used in some cases to ensure that the carbides were taken back into solution. The carbide morphologies (intergranular and intragranular) of all the heat/heat treatment combinations were examined and classified according to a standard EDF system described earlier.

The corrosion experiments were carried out in three different autoclave systems depending on whether the objective was electrochemical measurements, slow strain rate tests or long term exposure of RUB specimens. It should be noted that the hydrogen concentration was not the same in each system, being around 23 and 25 ml/kg for the first two types of test and 167 ml/kg for the experiments with RUB specimens (see Table 3-45). The hydrogen concentration was only fixed at the beginning of each test by a given overpressure at 125°C (257°F) and was apparently not measured continuously during the experiments at temperature in this particular work.

For the electrochemical experiments, an external Ag/AgCl reference electrode was employed. The specimens in the potential step experiments were first cathodically polarized at ECP-310mV (after correction for a considerable IR drop in the comparatively low conductivity PWR primary water) for 300 seconds and then forced back rapidly to the original ECP in order to measure the repassivation current and its decay with time. When the re-oxidation transients were measured, it included a contribution from re-oxidation of adsorbed hydrogen on the surface produced during the preceding step. However, control experiments on platinum suggested a contribution of only 10% to the anodic current from hydrogen oxidation obtained on the nickel alloy surfaces. (Note, however, that the pre-existing oxidized surface cannot be completely reduced at -310mV relative to the free corrosion potential since chromium containing oxides are still stable and it seems possible therefore that the re-oxidation transients may only have concerned an outer layer of nickel ferrite). The repassivation currents decreased with increasing hydrogen overpressure as expected. The decrease in repassivation rate between Alloy 600 and Alloy 690TT was found to be only a factor of two and it was concluded that it could not alone explain the difference in their susceptibility to stress corrosion.

The creep studies allowed a primary creep law to be quantified as a function of temperature from 325 to 400°C, stress from 450 to 650 MPa, and material characteristics. Secondary creep does not occur at the temperatures of interest in PWRs. Grain boundary sliding was observed with the aid of scratches made with 4000 grade abrasive paper on a previously electropolished surface. The sliding of several tens of grains was observed on each specimen tested and averaged. The uncertainty in the average was up to 50% because of the variability observed in sliding rates depending on grain boundary orientation relative to the principal tensile stress.

The primary macroscopic creep rate in air for the mill annealed and thermally treated versions of Alloy 600 and 690TT followed the same parabolic law with the strain rate proportional to $t^{-0.47}$. For the solution annealed materials the strain rate was proportional to t^{-1}, the difference being linked to the concentration of carbon in solution and the increased grain size. The activation energy for primary creep was observed to be 180 kJ/mole for both the mill annealed and thermally treated Alloys 600 and 690TT. Thermal treatment of Alloys 600 and 690 caused the creep rate to increase by a factor between 3 and 9 depending on the heat (presumably due to the reduction in amount of interstitial carbon) although, for similar thermal mechanical treatments, the creep rate decreased with increasing density of grain boundary carbides. The increase in chromium content between 15 and 30% between Alloys 600 and 690 caused a decrease in macroscopic primary creep rate by about a factor of two for similar grain sizes and degrees of grain boundary decoration by carbides. Additional experiments were also carried out in PWR water at 360°C. An increase in the creep rate by a factor of three relative to argon was observed and was interpreted as either an effect of hydrogen or of vacancy injection from surface oxidation.

In parallel, the intergranular creep resistance was measured and expressed in terms of intergranular viscosity, which is inversely proportional to the intergranular sliding rate. The intergranular viscosity increased strongly with the density of intergranular (carbide) precipitation. For example, the grain boundary sliding rate decreased by a factor of up to 20 between the same heats of Alloy 600 in the mill annealed and thermally treated conditions. However, the intergranular viscosity was only slightly affected by the chromium content. A parameter called the fraction of intergranular deformation, defined by the ratio of the intergranular to total creep rate, was correlated with

exponential functions of the observed density of intergranular carbides. In reality, the observed favorable effect of thermal treatment in increasing intergranular viscosity was more complex than simply an effect of intergranular carbides because at the same time the reduction in dissolved carbon also resulted in a change from homogeneous planar sliding to intense localized planar slip. The latter deformation greatly exceeded any contribution from grain boundary sliding.

A parametric equation was derived to evaluate intergranular viscosity as a function of easily measured microstructural parameters:

- the fractional grain boundary coverage by intergranular carbides divided by a constant for Alloy 600 or 690TT,

- the constant of proportionality for Alloy 600 or 690TT in the equation relating the macroscopic creep rate to stress, yield stress, temperature and time,

- the grain size.

The observed correlation between predicted and observed grain boundary sliding rates was satisfactory but with a scatter band of up to an order of magnitude. If the second parameter in the above list was not available experimentally, an alternative estimation was proposed based on the grain size and a characteristic constant for mill annealed Alloy 600, or thermally treated Alloy 600 or thermally treated Alloy 690.

Crack propagation rates measured during slow strain rate tests (SSRT) at a strain rate of $5x10^{-8}$ sec^{-1} in PWR primary water at 360°C (calculated from the total test time – 500h, the assumed time to initiation at that strain rate) were correlated with the resistance of the material to intergranular sliding (Figure 3-10 and Figure 3-11). The observed correlation ($da/dt=5.7x10^{4}\eta^{-0.76}$) over two orders of magnitude of crack growth rates between $5x10^{-3}$ and $2x10^{-1}$ μm/h was deemed satisfactory, albeit with two outliers corresponding to two solution annealed heats (of Alloy 600 and 690). (It may be noted that a correlation derived from the Alloy 690 points, taken alone above the detection limit for crack growth in Figure 3-10, would give rise to a steeper slope.) The correlation was, nevertheless, significantly better than that between the crack growth rate and the fractional grain boundary coverage by carbides, for example. Beyond 20% coverage of grain boundaries by carbides, crack growth rates were below $5x10^{-3}$ μm/h, which corresponds to the apparent "threshold" for cracking defined by the smallest detectable intergranular crack of 10 μm in experiments lasting up to 2000 hours. However, cracking of one mill annealed and two thermally treated Alloy 690 heats above this "threshold" was observed, one of which being the pre-production heat WE092 extensively cited earlier. It is noted that the rates of crack propagation between $2x10^{-2}$ and 10^{-1} μm/h in these three cases were calculated from intergranular crack extensions of 20 to 120 μm (0.0008" to 0.0047"). The author concluded that there is a comparatively weak effect of chromium content and strong effect of intergranular precipitates on stress corrosion (propagation) susceptibility.

The same type of correlation but with more scatter between stress corrosion initiation times and intergranular viscosity ($t_i=3.07x10^{-2}\eta^{-0.57}$) was derived from results obtained using RUB specimens of Alloy 600 in PWR primary water at 360°C (680°F), (but note the very high hydrogen in these

tests mentioned earlier). No crack initiation was observed in the case of Alloy 690TT after between 16,000 and 27,000 hours of test for the thermally treated heats and 52,000 hours for the mill annealed heat, despite having similar intergranular sliding rates to Alloy 600 with comparable intergranular carbide morphology. This difference in initiation resistance was attributed to an important effect of chromium content on crack initiation, the hypothesis being that less hydrogen entered the higher chromium material, particularly in the absence of dynamic straining. Thus Mithieux concluded with the opinion that understanding the role of chromium content on resistance to stress corrosion initiation under static loading in PWR primary water required significant further work, notably on hydrogen/metal interactions.

3.2.2.7.4 EDF Report HT-29/02/001/A, 2002[48]

Although not explicitly stated in the EDF report, the text appears to be that of the PhD thesis of J-P Saulay [48] following the preceding study by J-D Mithieux. Again, the goal was to understand and quantify the margin against the occurrence of stress corrosion cracking in Alloy 690TT compared to Alloy 600 in PWR primary water under very severe test conditions. The essential results from this work were published in the open literature in 2003.[50]

The work was divided into two parts of which the first addressed the effects of shot peening and cold forming on the resistance of Alloy 690TT to stress corrosion cracking in PWR primary water. In the second part, a quantitative estimation of the margin against stress corrosion occurring in Alloy 690TT was made. To this end, an attempt was made to define the conditions under which Alloy 690TT may stress corrode in PWR primary water.

The materials selected for study were from the same batch (of steam generator tubes) as those described in the PhD thesis of J-D Mithieux.[47] Three heats of Alloy 600 and three heats of Alloy 690TT were used of which the latter included the pre-production heat WE092, the industrial heat WG592 with a poor intergranular carbide structure that had showed 35 μm of cracking in the work of Mithieux, and one industrial heat WE799 with an acceptable carbide structure (see Table 3-40 to Table 3-43). One of the Alloy 600 heats, which was mill annealed, also had a very well developed intergranular carbide structure and it too had not cracked significantly in the work of Mithieux, whereas the other two Alloy 600TT heats selected had cracked in the previous study. Cold worked surface layers were reported to be present on the internal and external layers of all the steam generator tube samples although data were shown only for one of each alloy type with the comment that the cold worked layers were twice as thick at up to 100 μm on the Alloy 600 tube compared to the Alloy 690TT tube of heat WE092. These cold worked layers were removed by electropolishing in some cases prior to stress corrosion tests, however.

Tensile specimens were machined from the steam generator tubes by EDM; the fused layer was presumably also removed by electropolishing although this was not explicitly stated. Some were shot peened on one or both sides with glass beads to an Almen intensity of 27N, which resulted in compressive layers between 150 and 250 μm (0.0059” and 0.098”) thick and peak compressive stresses between -800 and -1000 MPa (-145 ksi). Other specimens were cold formed to create a V-shaped hump of height 6.5 mm in the middle of the gage section; the so-called "Smialowska" specimen. Two radii for the apex of the V-shaped hump of 1 and 2 mm were used. The microhardness was measured on the hump with peak values as high as 400-450HV.

The initial results of Saulay concerned the effects of shot peening on the stress corrosion resistance in PWR primary water at 360°C of the pre-production heat of Alloy 690TT (WE092). The same system of fixing the hydrogen overpressure at 125°C (257°F) before each SSRT was used as before in the work of Mithieux, which gave a dissolved hydrogen concentration of about 30 ml/kg (See Table 3-48). The strain rate was $2.5x10^{-7}$ or $5x10^{-8}$ sec^{-1}. Tests were conducted on specimens of WE092 either with the as-received steam generator tube surfaces, or electropolished, or shot peened. Typically, two tests per condition were conducted at $2.5x10^{-7}$ and $5x10^{-8}$ sec^{-1} of which one was interrupted at a quarter to half of the test period of the companion test to specimen failure. Crack growth rates were calculated from each pair of results, and were usually based on observed crack depths between 10 and 120 μm (Figure 3-11). (It is noteworthy that the crack depths observed at the lower strain rate were usually 10 to 30% deeper and certainly not several times deeper, as might have been expected.) Based on all the tests the author concluded that the cold worked layer present on tubes of heat WE092 caused the crack growth rate to be multiplied by a factor of 1.3 by comparison with an electropolished surface.

Shot peening on both sides of the specimens was concluded to decrease the resistance of the pre-production heat WE092 to stress corrosion cracking, based, it seems, on two cracked areas being observed rather than one on the as-received material, but the deduced growth rates were essentially the same. For the specimens of WE092 shot peened on one side, it was concluded that the crack depth increased by a factor of 2 due to shot peening compared to the as-received condition but this conclusion is difficult to support after examining the quantitative results. Two tests were also carried out on the industrial heat of Alloy 690TT (WG592) with intermediate quality carbide morphology from which it was deduced that the crack propagation rate in the intermediate quality Alloy 690 heat was nearly the same as in WE092 despite being "more resistant". Thus, prior shot peening had no effect on the stress corrosion resistance of the industrial production heat of Alloy 690 with intermediate intergranular carbide quality. The so-called rapid propagation phase was not observed on any shot peened specimen of Alloy 690TT in contrast to most similar tests on Alloy 600MA. These results may be compared with those for a rather resistant heat of Alloy 600TT where shot peening was observed to increase crack growth rates by a factor of 5 to 6 compared to electropolished surfaces and by a factor of 3 relative to the as-received steam generator tube surfaces. In addition, transition to the rapid propagation phase was also observed.

Five SSRT experiments were conducted at $5x10^{-8}$ sec^{-1} using the cold deformed specimens with the V-shaped hump, of which four were on the three heats of Alloy 690TT and one was on a nominally resistant heat of Alloy 600TT. Of the three heats of Alloy 690TT with a radius at the apex of the V-shaped hump of 1 mm, the two heats with unacceptable or marginal intergranular carbide structure showed intergranular cracks to twice the depth (maximum of 225 μm) observed on the normal test specimens. On the other hand, the third industrial Alloy 690TT heat with good intergranular carbide morphology cracked to about a third of the depth of the other two, whereas the Alloy 600TT specimen with a V-shaped hump cracked almost all the way through the thickness. Thus, use of a cold deformed test specimen modified the observed stress corrosion behavior of Alloy 690TT in such a way that the authors concluded that no heat of Alloy 690TT could be considered completely immune to stress corrosion, although it was still very much better than even a rather resistant heat of Alloy 600TT.

The second part of the study allowed a diagram showing lifetime to cracking of the experimental heat of Alloy 690TT (WE092) to be drawn as a function of strain rate, as published at the Environmental Degradation conference at Skamania Lodge in 2003.[50] It is based on an approach published previously by Boursier for Alloy 600, the advantage of which was stated to be the ability to present both SSRT and constant load stress corrosion data on the same unified diagram (as a function of strain rate). Note that the development of stress corrosion in Alloy 600 is viewed as proceeding in three phases; crack initiation, "slow crack propagation" and "fast crack propagation" about an order of magnitude faster. The last of these steps is consistent with data obtained under linear elastic conditions using fracture mechanics specimens but is not always observed in SSRT using small tensile specimens. Thus SSRT specimen lifetimes usually tend to be dominated by a combination of "initiation" and "slow propagation".

In the present case, two domains in the development of cracking during SSRT were distinguished for certain heats of Alloy 690TT; initiation of a crack to a defined depth of 10 μm (0.0004") and a second phase of "slow propagation". The SSRT data used to construct the failure diagram for Alloy 690 were those obtained on the pre-production heat WE092 together with a single observation on the same heat at constant load interrupted after 10915 hours of exposure at 360°C (680°F) and a stress of 680 MPa (98.6 ksi). The latter result is treated as a long term creep test with a primary creep rate at the 10915 hours point of 3.6×10^{-10} sec^{-1}, as calculated from the study by Mithieux, and an assumption that a crack of 10 μm was present at the end of the test. On a log-log plot of deformation rate versus time, loci or isodamage lines representing the same depth of stress corrosion cracking were added, for example at 10 μm (representing initiation) and 100 μm (Figure 3-12). To these loci are added the mechanical ductile rupture locus. In this way, the life of a component to a given crack depth, or rupture, can be predicted if the applied strain rate is known or from the primary creep rate at a given point during its decay at constant load.

For the constant load case, it was necessary to show, given the variable strain rate history during primary creep decay, that it was reasonable to use the creep rate at the point in time when the damage is comparable to that which would have been observed if that same (lower) strain rate had been maintained constant throughout life. With the aid of a slow strain rate test at two successive different strain rates (2×10^{-7} and 4×10^{-9} sec^{-1}) maintained for times (63 and 1800 hours respectively) that were insufficient to traverse the locus defining the 10 μm crack depth marker of "initiation", it was shown that the exposure times for each step could be simply added together as if they were all at the lower strain rate. In other words, there was no perceived "history" effect in the specimens due to the preceding periods of dynamic strain not exceeding the total required to initiate a 10 μm (0.0004") crack. In a second test at the two selected strain rates where the period at the faster strain rate exceeded that required to initiate a 10 μm crack, a crack initiated in the first step then continued to propagate in the second step at the lower strain rate. Thus, once the effective initiation limit of 10 μm was crossed, further stress corrosion damage was cumulative and crack propagation followed the isodamage lines drawn on the failure diagram (Figure 3-12).

3.2.2.7.5 Results Reported by Vaillant et al. 1999[49]

Vaillant et al. reported RUB and CERT results on Alloy 600MA & TT and Alloy 690MA & TT SG tubes in primary water.[49] The carbon content and the heat treatment conditions of the six Alloy 600 tubes and five Alloy 690 SG tubes are listed in Table 3-44. The RUB and CERT test

conditions are listed in Table 3-45. The number of test specimens for each heat or heat treatment was not reported.

RUB Results

The RUB test was performed in a static autoclave at 360°C (680°F) with 100 cc H_2/kg H_2O. The X-ray measured true stress level at the Alloy 600 specimen apex was between 750 and 1000 MPa (109 and 145 ksi). Some shallow cracks (10 μm or 0.0004" deep) appeared at the apex of the Alloy 690 RUB specimens after bending, but before immersion inside the autoclave. So the stress measured at the Alloy 690 RUB specimen apex surface was not well-defined. However, the stress level measured after removing the 10 μm or 0.0004" deep crack was the same as for the Alloy 600 RUB specimens. Hence, the stress at the tip of the short crack caused by bending is at least as high as the apex surface stress of the Alloy 600 RUB specimens.

The RUB specimens were removed periodically for inspection (every 500 hours for the Alloy 600 and an interval between 3000 to 6000 hours for the Alloy 690). If cracks were observed or suspected, the specimens were cut for metallurgical examination. Otherwise, the specimens were returned for continued testing. The test results shown on Figure 9 of Ref. 49 are summarized in Table 3-46. Except for 6E specimen, all the Alloy 600 RUB specimens developed cracks within 3,500 hours. The Alloy 600 6E specimen did not develop cracks even after 36,000 hours of exposure. Within each Alloy 600 heat, the TT condition had a higher crack resistance than the MA condition. None of the Alloy 690 specimens tested cracked after 16,500, 25,000, or 54,000 hours of exposure. Results for the Alloy 690 heat 9.754 were not reported.

CERT Results

Vaillant et al. considered the CERT test to be a test measuring the stress corrosion crack growth rate. The CERT tests were conducted at a strain rate of $5x10^{-8}$ sec^{-1}. Significant intergranular cracking was observed on three Alloy 690 SG tubes that did not crack during the RUB tests. The reported depth of the intergranular cracks are listed in Table 3-46, which also lists the average crack growth rate (CGR) estimated from Ref. 49. The crack growth rates are also summarized in Figure 3-10. The CERT results from the Alloy 600 6E specimen and the Alloy 690TT 9.799 specimen did not crack. (Note: It is inferred that no intergranular cracking was observed on the two CERT specimens, even thought the report did not specifically use the word "intergranular cracking" or "environmental assisted cracking".) This was attributed to the high degree of intergranular carbide precipitation in these two SG tubes. Based on Figure 3-10, Vaillant et al. concluded that Alloy 690 did not necessarily have a lower CGR than Alloy 600. Vaillant et al. suggested that the CGR obtained in the CERT tests is mainly dependent on the grain boundary carbide precipitation and the creep rate while the crack initiation time in the RUB tests was mainly a function of Cr contents. The results and conclusions by Vaillant et al. are further discussed in Section 4.1.2.

3.2.2.7.6 Results Reported by Boursier et al. 2003[50]

The investigation by Boursier et al. was an extension of an earlier study by Vaillant et al. in Ref. 49 with additional CERT tests.[50] Boursier et al. investigated the effect of surface condition, strain rate, and localized strain on the SCC cracking of the CERT specimens in primary water at

360°C (680°F). The chemical composition and heat treatment conditions of the six Alloy 600 tubes and five Alloy 690 SG tubes are listed in Table 3-47. These tubes were among the ones used for RUB and CERT tests in Ref. 49. The crack growth rates from the previous CERT tests are summarized in Figure 3-10. The CGR numbers are also listed in Table 3-46.

Boursier et al. performed the CERT tests at a strain rate between 5 x 10^{-9} and 2.5 x 10^{-7} sec^{-1} and the constant load tests at a load between 603 and 684 MPa (87 and 99 ksi). The cross section of the specimens was 3.5 mm x 1.1 mm. To evaluate the surface condition on PWSCC, the specimens were tested in the as-received surface, electropolished surface, shot peened either on one side (surfaces) or on both sides (surfaces). In addition, some specimens were pressed to a hump (Smialowska-type specimens). The test environmental conditions are listed in Table 3-48. For the CERT tests, true stress and elongation were measured as a function of time. For the constant load tests, the elongation was measured. After the tests, the failed specimens' crack depth was measured by SEM. All failed CERT and constant load specimens tested in water exhibited the presence of a similar intergranular cracking morphology on the fracture surface (as-received condition specimens, peened specimens, or pressed hump specimens). In contrast, tests conducted in an inert (argon or helium) environment showed entirely ductile fracture.

The CERT results of the experimental heat of Alloy 690 (690 Exp) are summarized in Table 3-49. The extent of the cracking in the specimens shot-peened on both surfaces was equivalent to that of the as-received condition. On the contrary, specimens shot-peened on one side had an increase of the stress corrosion cracking depth and a reduction of the test time. Similar results were also reported at lower strain rates. It was deduced that the cold work layer strongly influenced the slow propagation phase. The crack propagation rate measured in the shot peened state (0.9 μm/h) was higher than that measured in the as-received condition (0.3 μm/h). The effect of cold work on the initiation phase is more difficult to establish. It seemed that the surface cold work slightly increased the initiation time. The electropolishing removed the superficial surface cold worked layer from the SG tube fabrication process (straightening and grinding outer surface). Hence, the electropolished specimens were slightly better than the as-received condition specimens. Boursier et al. noted that there was no effect of shot-peening on the industrial Alloy 690 (690 Ind) as the same corrosion resistance was observed on the as-received material and the shot-peened specimens. However, as discussed in the previous (Vaillant et al.) section, the same concern should be raised as whether crack propagation rate estimated from CERT can be used to rank Alloy 690 or Alloy 600 PWSCC crack growth rate.

The effect of strain rate on the CERT results of the experimental heat of Alloy 690 (690 Exp) is shown in Figure 3-11. The crack growth rate increased with increasing applied strain rate in the CERT test. Table 3-49 also shows the effect of cold work on cracking of the CERT specimens. In the as-received condition, the industrial Alloy 690 (690 Ind.) and the high resistant heat Alloy 600 (600 Ref) showed much less cracking (shallower crack depth and longer cracking time) than the experimental Alloy 690 (690 Exp 1). The cold work caused more severe cracking in the pressed hump specimens, especially in the Alloy 600 (600 Ref. heat) which showed good cracking resistance in the as-received condition. [0]The humped specimen (i.e. with bulk cold work) from the industrial heat Alloy 690 (690 Ind.) had a cracking depth of 70 μm. No descriptions or micrographs were provided to confirm that the cracking was intergranular. Based on Table 3-48, Alloy 690 Ind. (coded as 9.799 in Table 3-48) had an ASTM grain size of No. 6

to 7, or 32 to 45 μm. Hence, the cracking depth is about 2 grains or less. Several Alloy 690 corrosion studies reviewed in this document (see Section 4.1.1) have shown that Alloy 690 is prone to shallow intergranular splitting from excessive mechanical straining. Hence, it may be possible that the shallow cracking in the Alloy 690 Ind. humped specimen could come from the pressing strain rather than being caused by IGSCC.

3.2.2.7.7 EDF Report HT-44/98/016/A, 1998[51]

EDF has studied since 1993 the stress corrosion resistance of Alloys 52 and 152 in PWR primary water and compared the results to those obtained on various other nickel base weld deposits with chromium contents between 14.5% Cr (Alloy 182) and 26% Cr. Their resistance to stress corrosion in hydrogenated PWR primary water at 360°C was examined using very severe tests.[51]

The welds used in this work were fabricated using Alloy 182 coated electrodes, Alloy 82 TIG wire, Soudometal 22%Cr, Alloy 625, Soudometal 26% Cr, Inco Alloy 152, Soudometal 30%Cr, and Alloy 52 TIG wire. Several of these welding products were experimental alloys and, at the time, only Alloys 182, 82 and 625 were considered to be industrial products. Initial fears of a reduction in the toughness of welds with 30% Cr proved to be unfounded whereas the main welding problem encountered at such high Cr levels was hot cracking. Some variations of chemical composition as-welded by comparison with the target values were observed, the most notable among them being a Cr content of the Alloy 52 weld of 25.5% instead of 30%. The mechanical properties were all to specification. The samples for stress corrosion testing were machined from weldments that were not stress relieved.

The as-welded microstructures were studied. The Soudometal 22%Cr weld showed some iron rich nodules resulting probably from a welding anomaly. For the products with 30%Cr, hot cracks up to 0.5 mm in length were reported. However, the example of Alloy 52 here was not apparently affected by hot cracking whereas the other two products with 30%Cr were strongly affected. Based on comparisons with a previous study of hot cracking in Alloy 182, the presence of traces of low melting phases detectable by SEM, rounded grain edges, and absence of secondary crack branches was judged to be sufficient to distinguish hot cracks from stress corrosion cracks. However, it should be noted that today it is known such features may not necessarily always be present since one form of hot cracking in Alloy 52 is definitely linked to ductility dip cracking where no low melting point phase is involved.[51]

RUB specimens for stress corrosion testing were fabricated by EDM machining a half section of tube across the welding direction and then bending it like half a steam generator tube to form a RUB with the weld metal at the apex. Electropolishing was used to eliminate any surfaces resulting from EDM machining. Longitudinal stresses of 700 to 860 MPa were measured by X-rays while the circumferential stresses were lower between 500 and 600 MPa. The tensile specimens for constant load tests and SSRT had round gage sections with the long dimension along the length of the weld. These specimens were also electropolished to eliminate any cold worked layers from machining. All testing was carried out in static autoclaves, the deaeration and hydrogen overpressure being established at 125°C (Table 3-45). For the RUB tests, the hydrogen concentration as measured via a Pd/Ag thimble was >100 ml/kg and for the SSRT 25 ml/kg. The residual hydrogen at the end of test was also measured but not reported.

Using RUB specimens, Alloy 182 (14.5% Cr) was observed to be very susceptible to stress corrosion cracking and Alloy 82 (18-20% Cr) was only slightly less sensitive. Cracks appeared in one of the Alloy 182 specimens at the first test interruption after 500 hours and the second was cracked after 1500 hours. The first specimen of Alloy 82 cracked after 2000 hours and all were cracked at 6500 hours. For chromium contents between 21 and 22% Cr, no stress corrosion crack initiation was observed, as was also the case for Alloys 52 and 152 in tests lasting between 18,000 and 27,000 hours. This general behavior was confirmed by constant load tests (450 to 514 MPa or 0.8 to 0.9 of the UTS) on Alloys 182, 82 and 152. Two out of three specimens of Alloy 152 failed by creep rupture after 13,000 to 27,000 hours at 360°C, however.

Slow strain rate tests at $5x10^{-8}$ sec^{-1} (after 50 hours initial exposure without applied stress) confirmed the high susceptibility of Alloy 182 to stress corrosion and the somewhat less severe susceptibility of Alloy 82. An interrupted test on Alloy 182 revealed no initiation at 0.9% strain but rapid growth at about 20 to 40 μm/h along the dendrite direction between 1 and 3.4% strain. The rate of propagation deduced for Alloy 82 was 0.6 to 0.7 μm/h. The resistance to stress corrosion cracking as measured by SSRT improved for chromium contents between 21 and 22% Cr but susceptibility was nevertheless still significant. Cracking remained possible up to 25-26% Cr. On the other hand, the test program to date on Alloy 152 has shown no stress corrosion cracking despite the presence of welding defects (hot cracks) in the tested specimens. This conclusion does, however, depend strongly on the interpretation of the fractography and the ability to distinguish hot cracking from stress corrosion cracking. A companion study cited in the report refers to the testing of precracked DCB (double cantilever beam) specimens (by ETH) where stress corrosion crack growth in Alloy 182 was clearly observed but not in Alloy 152 after 4300 hours at 350°C in PWR primary water.

A more detailed study of the various stress corrosion properties of the weld deposit materials studied enabled the following deductions to be made:

- A chromium content greater than 22% is very beneficial as regards resistance to stress corrosion crack initiation under static load or constant deformation and at 30% in alloys 52 and 152 complete resistance was found.

- Nevertheless, depending on elements other than chromium and possibly the microstructure, a chromium content equal or greater than 21-22% and up to 26%Cr cannot guarantee the absence of stress corrosion propagation from pre-existing defects, although in the case of Alloy 152 (30%Cr) no propagation was observed.

The report concludes by saying that a better understanding of the good performance of nickel base weld deposits with 30% Cr would necessitate a similar approach to that developed by EdF for the Alloy 690 base metal.

3.2.2.8 SG Tube Mock-Up Test in Hydrogenated Water by Framatome ANP, France (Appendix B)

Framatome ANP (France) performed a comparative study of the resistance of Alloy 690TT and Alloy 600MA and TT to PWSCC using mock-ups representative of the tube expansion zones in

the tubesheet of recirculating PWR steam generators. Several different types of manufacturing anomalies were reproduced in the mock-ups, over-size tube / tubesheet gaps, over-rolling, skip rolls in the tubesheet, and excessive kiss-rolling. The mock-ups were tested in the form of heated capsules containing deaerated, hydrogenated and demineralized water at 360°C (680°F).

SG Tube Mock-Up Material

The Alloy 600 tubes were ¾" diameter (WD281, MA & TT) and 7/8" diameter (NX3335 MA). The Alloy 690 (WE094 TT) tubes were ¾" diameter tubes manufactured in a pre-production run. The Alloy 690TT tubes were heat treated at 1040°C (1904°F) for 3 min + 700°C (1292°F) for 5 hours. Both the Alloy 600 and Alloy 690 tubes were typical of manufacturing practice about 16 years ago. The chemical composition and the mechanical properties are listed in Table 3-56.

The grain size of the Alloy 690 at mid-thickness was aproximately10 μm but a perturbed layer was detected on the inner surface of the tube. This layer was characterized by a finer grain size of about 2μm, the presence of dense carbide precipitates and a higher hardness. Microhardness measurements indicate that this perturbed surface layer is about 100 microns thick. This structure was typical of the pre-series heats, which were the only ones available when the mock-ups were manufactured. Since then, Alloy 690TT tubes used in steam generators have much more rigorous quality control and the inner surfaces are free of such perturbed layers.

SG Tube Mock-Up Fabrication

The mock-ups were manufactured by Framatome-ANP in Chalon sur Saône using the same tools and procedures as those used for PWR steam generators. Each mock-up consisted of a SG tube section and a thick carbon-steel cylinder representing the top side of the tubesheet. The tube section was expanded into holes drilled in the carbon steel cylinder representing the tubesheet using a mechanical rolling tool. Four rolling steps were needed inside each carbon steel cylinder. A kiss-rolling step was then carried out on each side of the carbon steel cylinder. Thus, two roll transition zones were available on each mock-up, as represented in the Figure 3-17, which shows a cross section view of the standard mock-up design. In addition, between the two roll transition zones, several non-conformities such as a lack of overlap between two rolling steps or a skipped roll step were introduced in some cases. Such fabrication non-conformities were known to be extremely detrimental for primary water side cracking of tubes in the case of steam generators with Alloy 600 tube bundles.

The total number of roll transition zones manufactured from Alloy 690TT was 16 whereas 40 were manufactured from the Alloy 600 heats. The mock-ups (each comprising two roll transition zones) were identified with a number between 1 and 21 for the Alloy 600 mock-ups and between 501 and 508 for Alloy 690TT mock-ups. A letter (H or B) was also added to the identification number for each transition zone. An Alloy 600 plug was manual metal arc welded into each end of the mock-ups in order to form a capsule. During this operation, the tube was cooled in order to maintain the residual stresses in the roll transition zones introduced by the roll expansion. Each mock-up (capsule) was equipped with a small stainless steel tubing to allow the test environment to be introduced, a high pressure valve, a manometer and an external thermocouple inserted in the carbon steel sheet.

Test Procedure

The test environment was high purity deaerated water with a hydrogen overpressure. This environment was chosen to facilitate good control of the test environmental parameters and also knowing that hydrogenated pure water is slightly more aggressive from the stress corrosion view point than PWR primary water that also contains lithium hydroxide and boric acid in varying concentrations throughout any given fuel cycle. The mock-ups were introduced into a furnace whose temperature was subsequently controlled at 360°C (680°F).

Throughout the exposure period at 360°C (680°F) the conductivity of the aqueous environment was less than 1 μS/cm. After, the first and the sixth test periods of about 10,000 hours, the water from several mock-ups was sampled and analyzed. The results are given in Table 3-56. During the first 17 000 hours of the exposure period, no hydrogen was injected in the mock-ups. Subsequently, an over pressure of hydrogen of 15 bar was added at the beginning of each test period and was renewed every 2 months when half of the over-pressure was lost by diffusion. Testing of the Alloy 690TT mock-ups lasted 100,000 hours at 360°C (10 periods of 10,000 hours) and an internal total pressure between 210 and 230 bar was maintained. No leak occurred during this entire test duration on any mock-up. One mockup, 506, was extracted for destructive examination after 60,000 hours of test.

Alloy 690TT SG Tube Surface Microcracks

SEM surface examinations of non-flattened Alloy 690TT half tube revealed some tiny cracks on the inner tube surface in the transition zones of the kiss rolling. Their length was about 1.5 mm and their width 2 μm, on each side of the roll transition. Examination of the flattened half tube revealed the presence of many microcracks, some of the opened microcracks corresponded to those which were also observed before flattening but numerous others were new ones opened or created during the mechanical flattening operation. This type of flaw was also observed on parts of the tube which were not rolled, that is remote from the rolled zone. The microcracks were fully characterized by metallographic examination with SEM. They were intergranular and their length was always limited to the thickness of the perturbed surface layer on the internal surface of the tube (about 10 μm thick in this case). The microcracks are concluded to be strain induced by rolling and are limited to the hard perturbed surface layer already present on the inside surface of the tube in the as-received condition. These microcracks were intergranular but did not propagate in the tube during exposure to hydrogenated water at 360°C (680°F) during 60,000 hours exposure. The same shallow intergranular splitting was also noticed by Miglin et al. in Alloy 690 RUB specimens tested in all-volatile treated (AVT) water. Miglin et al. concluded that these defects were due to mechanical strain rather than due to IGSCC (see Section C.1 for detail).

Results

Eight mock-ups (16 different roll transition zones) were manufactured with Alloy 690TT tubing and tested in the same conditions as the Alloy 600 mock-ups. None of the Alloy 690TT mock-ups cracked even after exposure times extending up to 100,000 hours. Non-destructive and destructive examinations showed that no stress corrosion crack initiation or propagation had occurred, despite the simulated manufacturing anomalies that had caused such severe detrimental effects on PWSCC resistance of similar Alloy 600 mock-ups. Metallurgical examinations of the

Alloy 690TT mock-ups confirmed that even when some mechanically-induced intergranular cracks were initiated by severe straining of a hard perturbed internal surface layer, such cracks did not propagate in hydrogenated water at 360°C (680°F) after exposure times up to 100,000 hours.

The results of the Alloy 600 mock-up are summarized in Table 3-57 and Table 3-58. The first leaks due to through-wall cracking appeared on the Alloy 600 MA mock-ups after exposure times as short as 800 hours. Alloy 600TT tubes seemed to have better resistance to PWSCC in the case of severe non conformities such as over-sized tube / tube sheet gaps but with normal roll transition parameters, no effect of the thermal treatment was observed. Nevertheless, there was a marked heat to heat effect on PWSCC (as is characteristic of field Alloy 600 PWSCC behavior) independent of roll transition fabrication characteristics.

Almost all the Alloy 600 mock-ups cracked. Of the 40 different roll transition zones that were tested, two were withdrawn without any leakage after short exposure times and four zones survived 30,000 hours (the maximum exposure time of the Alloy 600 mock-ups) without any leakage occurring. All the other roll transition zones cracked. The average time to leakage of the Alloy 600 mock-ups was 8,350 hours with a standard deviation equal to 6,600 hours. The most susceptible zones were roll transition zones with over-size tube / tube sheet gaps and / or with skip rolls inside the tube sheet (independent of the tube / tube sheet gap if skip rolls were present).

3.2.3 Hydrogenated Steam Testing

3.2.3.1 RUB Test in Hydrogenated Steam by Sui et al. 1997

Sui et al. reported the results of RUB stress corrosion tests on Alloy 600 and Alloy 690TT materials.[52, 53] The tests were performed in a hydrogen/steam mixture at 380°C (716°F) in a static autoclave. The Alloy 600 and Alloy 690 tube size, chemical composition, mechanical properties, and heat treatment information are listed in Table 3-34. The Alloy 600 and Alloy 690 SG tubes were cut into 96 mm lengths then split longitudinally into halves and holes were drilled at each end of the half tube for securing the bolts. The split half tubes were bent outward to form a radius of about 15 mm. They were cleaned with methanol and boiling pure water immediately before testing.

The static autoclaves used for the tests had an internal volume of 1.3 liters. In the initial experiments, the test specimens were loaded into the autoclave with 100 ml of deionized water and purged with hydrogen to achieve a low oxygen level. The autoclave was then pressurized to 0.3 MPa absolute (0.2 MPa gauge) with hydrogen at room temperature, and then heated to 380°C (716°F). The operating pressure at 380°C (716°F) was 15.2 MPa (2,205 psi) giving an estimated H_2/H_2O partial pressure ratio of 0.04. The specimens were removed from the autoclave at various times for examination, and then returned for further testing, unless they were cracked. The specimen examination was performed using a binocular optical microscope and a scanning electron microscope.

The RUB test results are summarized in Table 3-35. Alloy 600 EPRI 1 and 2 heats were more susceptible to cracking than Heat 2682. Four of the five Alloy 600 specimens developed cracks in 2,578 hours of exposure. The specimen from Heat 2682 (in the as-received condition) did develop

cracking after 2,578 hours. In contrast, the three Alloy 690TT specimens did not develop cracks after 3,000 hours of exposure. However, eventually, two specimens from Alloy 690 Heat B, which was deliberately mill annealed at unusually low temperature before the thermal treatment, developed intergranular cracking after 13,824 hours of exposure even though no cracks were observed after 12,600 hours. The cracks initiated on the I.D. surface of the split tube and propagated along the longitudinal axis of the tube. The largest crack was about 2 mm long and almost through the tube wall thickness (0.97 mm). Figure 3-13 shows the cracks observed in Alloy 690 specimen 5R from heat B without aging at 550°C (1022°F).

None of the eight specimens from Alloy 690 Heat A developed any cracks. However, Figure 3-14 shows a short crack generated by flattening at room temperature one of the Alloy 690 RUB specimens from heat A after 13,824 hours exposure. Sui et al. attributed this short crack to embrittlement of grain boundaries near the surface from the exposure. Further, Sui et al. suggest such a short crack to be indications of embrittled zones or "pre-damage zones" ahead of the intergranular crack tips.

Both heats of Alloy 690 were thermally treated at ~715°C (1319°F) for 15 hours. However, the cracked Alloy 690 Heat B was deliberately treated mill annealed at an unusually lower temperature than the un-cracked Alloy 690 Heat A (1769°F for Heat B vs. 1958°F for Heat A). The lower mill anneal temperature resulted in less dissolved carbon available to precipitate in the grain boundaries upon the thermal heat treatment. The grain boundaries in Heat A were covered almost continuously by carbides, which were determined to be the $M_{23}C_6$ type by TEM. In contrast, the grain boundaries in Heat B were essentially free of intergranular carbide coverage. Heat B also had a higher content of Al, which tend to result in a finer grain size and therefore a lower density of intergranular carbides in Heat B even further. The average grain size was 25 μm (ASTM No. 7.5) for Heat A and 15 μm (ASTM No. 9.0) or less for Heat B. The small grain size of Heat B was reflected in its higher room temperature yield strength. The strain distributions in the RUB specimens were measured by grids engraved on the inner and out surfaces of the specimens. Although Alloy 690 had a smaller tube diameter, both RUBs were bent with the tooling designed to fit Alloy 600 SG tubes. As a result, the Alloy 690 RUB specimens were stretched to a higher strain level in the transverse direction (normal to the tube axis). The RUB results by Sui et al. suggest that Alloy 690 could be susceptible to IGSCC in a hydrogenated steam environment if the final mill anneal temperature is too low to cause intergranular carbide precipitation upon the subsequent thermal heat treatment.

3.2.3.2 RUB Test in Hydrogenated Steam by Framatome ANP, Germany (Appendix A)

Framatome ANP (Germany) performed accelerated RUB tests in 400°C (752°F) hydrogenated steam. The hydrogen partial pressure was 1.1 bar (16 psi) at a total pressure of 200 bar (2900 psi). The chemical composition and mechanical properties of the Alloy 690 TT and Alloy 600 MA SG tubes used are summarized in6 Table 3-53. To simulate a malfunctioning rolling tool, 50% of the RUB specimens (three specimens per material) were deliberately scored with actual tools used during manufacturing. These surface marks were introduced into the internal surfaces of split tube sections prior to bending. The scores were shaped in the form of longitudinal and circumferential grooves with a width of approximately 1 mm (0.04") and a depth ranging from

20% to a maximum of 40% of the tube's wall thickness. The scoring process and the actual depth of grooves were controlled with surface profilometry.

The RUB test in the hot hydrogenated steam lasted up to 405 days (9,720 hours) with inspection intervals after 14, 30 and 60 days. The inspections were performed visually using a stereomicroscope at magnifications ranging from 25X to 40X. The level of detection for crack indications using a stereomicroscope at the above mentioned magnifications is approximately 150µm (0.006"). The first inspection after 14 days revealed that all scored and non-scored Alloy 600MA RUBs had developed cracking. The cracking exhibited a multi-directional nature and occurred predominantly in an area associated with the apex of the RUB specimens. After cracking was observed in Alloy 600MA RUBs, the specimens were removed and testing was resumed with Alloy 690TT specimens only. None of the Alloy 690TT RUB specimens revealed any crack indications, even after a total exposure time of 405 days (9,720 hours). Table 3-54 summarizes the results obtained during the hot steam test for both materials in the scored and non-scored condition. After the RUB tests, metallographic examination of a scored and non-scored specimen of each material was conducted. Vickers microhardness measurements (100g load – HV0.1) were conducted at selected locations.

The Alloy 600MA specimens exhibited PWSCC on numerous locations, which appeared independent of the presence of surface marks/scores. The crack progression occurred in an intergranular manner normal to the tube surfaces. Some locations exhibited through-wall defects. Vickers microhardness readings in the Alloy 600MA ranged from 290HV to 307HV. Immediately adjacent to the mechanically-induced scores the microstructure yielded hardness ranging from 337HV to 345HV.

The Alloy 690TT's microstructure appeared as expected to be, a semi-continuous to a continuous network of grain boundary precipitates as a result of mill annealing and the subsequent thermal treatment. The grain size was determined according to ASTM E 112 and showed relatively large variations since it ranged between 5 and 7. No crack indications were found in this material confirming the findings from visual inspection. Vickers microhardness readings ranged from 260HV to 278HV, approximately 30 points lower than that for the Alloy 600MA. Locations immediately adjacent to the scores yielded numbers ranging from 327HV to 335HV, which is only 10 points lower than that of the Alloy 600MA.

PWSCC in Alloy 600MA tubing was observed in row 1 U-bends of actual SGs after approximately one year of plant operation. The configuration of a RUB specimen is comparable to a row 1 U-bend tube. However, the tighter bend radius and the split-tube configuration of the RUB specimens accelerate the time necessary to initiate cracking by a factor of 2 to 3, if compared to an actual row 1 U-bend. Thus, the time necessary to initiate cracking in an actual row 1 U-bend under hot steam test conditions is 14 to 21 days. Based on the geometry of a row 1 U-bend, the conclusion can be drawn that one year of plant operation corresponds to approximately 20 days under hot steam test conditions. The 405 days test duration without cracking corresponds to approximately 20 years of plant operation for a row 1 U-bend.

3.2.4 Doped Steam Testing

3.2.4.1 Four-Point Bend Tests of Alloys 52M, 182, and 600 in Doped Hydrogenated Steam by Jacko et al. 2003

Jacko et al. performed accelerated test of Alloys 52M, 182 and 600 weld mock-ups at 400°C (752°F) in steam-plus-hydrogen doped with fluoride, chloride and sulfate anions.[54] The objective of the test was to demonstrate the adequacy of the weld repair made to the reactor vessel outlet nozzle-to-pipe safe-end weld at Ringhals 4 in 2002. The Alloy 52M used for the repair is an improved version of Alloy 52 as used for the fusion welding of Alloy 690 component items. It is stated by Jacko et al. that the composition is modified from that of Alloy 52 by lowering Al and Ti and increasing the Nb+Ta concentration; this is done to avoid slag and oxide inclusions in the multipass weldments. The chemical composition of the Alloys 52M, 182, and 600 used for the test mockups is summarized in Table 3-50.

A schematic drawing of the cross section of the Alloy 52M test specimens prepared to simulate the repair is shown in Figure 3-15. The right side of the specimen represents the AISI Type 316 safe end, while the left side represents the AWS Type 308-clad ASME SA-508 steel nozzle. The rectangular outline indicates the location of the specimen removed by machining for the accelerated corrosion testing. The Alloy 182 weld metal mockups for the companion tests were prepared in a slightly different manner. These specimens were removed from a full section mockup; that is, an 895-mm OD pipe with 80-mm thick wall. A number of different heats of Alloy 182 welding electrodes were used to make this full-scale nozzle weld. Table 3-50 lists the composition of a typical Alloy 182 heat used. Control specimens of Alloy 600 were fabricated from archived sections of a CRDM nozzle. This material was from Heat WF 147. This heat of Alloy 600 was noted by Jacko et al. as having exhibited moderate resistance to stress corrosion cracking in a previous test program.

The specimens were prepared as flat plates and bolt-loaded in specially designed four-point bending fixture as shown in Figure 3-16. The Alloy 182 weld specimens and the Alloy 52M weld specimens have the same dimensions. They were 180-mm long x 40-mm wide x 9-mm thick plates in which the welds were transverse to the long dimension. The Alloy 600 specimens were 102-mm long x 19-mm wide x 3.8-mm thick strips. The specimens were taken at locations of varying depths from the surface. The microstructure has been observed to vary through the wall of the nozzle. This permits the possibility that the SCC response may be influenced by heterogeneity of the microstructure or possible differences in the manufacturing-related deformation. Two strain/stress levels were tested in this program.

1. The lower level was 0.35% strain. This corresponds to the strain at approximately the 0.2% offset yield strength of the material because residual stresses associated with welds are typically around the yield strength.

2. The second strain/stress level was intended to exaggerate the strain conditions in order to represent a situation where the use of multiple weld passes might contribute to cyclic hardening of the material. Thus a strain level of 1% was selected and cyclic compression/tension loading was used. These specimens were first strained in

compression to -1% total strain by bending. The specimens were then deformed back to the original configuration and restrained in tension to +1% strain.

In a four-point bend specimen configuration (Figure 3-16), the stresses and strains are constant between the inner supports. With the bent beam configuration, the entire weld and all microstructural features can be located within the inner supports, ensuring that the strain (and stress) is uniform, and that SCC is less likely to initiate at a location unique to the test article configuration. The stresses measured for these specimens at various stages in the test program are summarized in Table 3-51. These elastic stresses were calculated, using the 400°C elastic modulus of Alloy 600 (195.3 GPa), from the strains released as the specimens were unloaded. The "low" stress values are approximately equal to the yield strengths of the test materials, typically in the range from 320 to 440 MPa. These stresses remained, even at the completion of the autoclave exposures; stress relaxation did not appear to be a significant factor. The residual stresses for the "high" stress specimens averaged 431 to 456 MPa for the Alloy 600 and Alloy 52M specimens. Significantly higher stresses, 568 to 586 MPa, were measured for the Alloy 182 specimens, related perhaps to the higher yield strength and higher initial work-hardening rate for this weld metal.

A 400°C high-pressure steam-plus-hydrogen environment was selected for the accelerated corrosion test environment. To enhance the aggressiveness of this environment, the steam is raised from water that is "doped" with 30 ppm each of the anions Cl^-, F^- and SO_4^{-2}, each of which is added as sodium salts. The hydrogen partial pressure is controlled at approximately 75 kPa with the total steam pressure at 20 MPa. This environment has been used for over fifteen years as a means to accelerate the simulated PWSCC of nickel-base alloys. In a recent accelerated test program, 400°C doped steam tests were performed on Alloy 600 CRDM nozzle penetrations removed from Ringhals 2.[55] The cumulative SCC initiation probability statistics from this experiment were compared to those for the initial PWSCC observed in service at Ringhals 2. This analysis indicated that the degradation observed after 89,000 effective full-power hours (EFPH) at 317°C (603°F) was essentially duplicated in 289 hours of exposure to 400°C (752°F) doped steam, an acceleration factor of 308 relative to primary water at 317°C (603°F). The Ringhals 4 reactor outlet nozzle operates at 322.8°C (613°F). Hence, the acceleration factor for the 400°C doped steam relative to this service temperature has to be adjusted to 195 to recognize this temperature difference (using Q = 55 kcal/mole [55]). Thus, a cumulative exposure time of 1800 hours - on the order of eleven weeks of cumulative autoclave exposure time- is equivalent to 40 effective full-power years (EFPY) of operation of the Ringhals 4 nozzle. Regular inspections of the specimens were performed at convenient intervals. During these inspections, specimens were ultrasonically cleaned and given a fluorescent dye-penetrant examination. Post-test examinations of the specimens included dye-penetrant inspections and inspections of the surfaces by optical microscopy. Metallographic examinations were used to further characterize cracking or other features of interest.

The four-point bend test results are summarized in Table 3-52. After a cumulative exposure of 2051 hours (equivalent to 45.6 EFPY), no environmental degradation was detected on the surface of any of the Alloy 52M welds. In the inspection after a cumulative exposure of 1343 hours, short (0.16 and 0.20-mm in length) indications were observed on the surface of the two high-strain Alloy 52M specimens. These indications did not change in subsequent exposures.

Metallographic cross-sectioning indicated these to be shallow hot-microfissures that were present from the weld preparation, but were not clearly identified in the earlier examinations.

In addition to the Alloy 52M specimens, four Alloy 182 weld specimens were tested; two at low strain and two at high strain, Table III. After a cumulative exposure of 214 hours, a number of cracks were observed in both of the high-strain specimens. These cracks ranged from as short as 0.25 mm to 3.0 mm in length. The low-strain specimens first exhibited stress corrosion cracking at the 450-hour interim inspection. During a subsequent 148-hour exposure, these cracks grew to a maximum length of 4.0 mm. The initial cracking was observed after 214 hours, with a subsequent exposure of approximately 150 hours more. The total crack depth is on the order of 1.4 mm.

Six Alloy 600 specimens were also tested. Four of these were exposed in the autoclave containing the Alloy 52M weld specimens, and two were exposed in the autoclave containing the Alloy 182 weld specimens. Two specimens were strained to 0.35%, whereas the remaining four were strained to 1%. The four specimens exposed with the Alloy 52M specimens accrued a total exposure of 1801 hours (equivalent to 40.1 EFPY). The two low-strain specimens and one of the four high-strain specimens did not crack; the remaining high-strain specimen exhibited a short SCC crack at 598 hours. After a total of 1343 hours, this crack had grown to a length of 5 mm, at which time the specimen was removed for characterization, including destructive metallographic sectioning. One of the high-strain Alloy 600 specimens exposed with the Alloy 182 weld specimens was cracked after 301 hours; a 5-mm long array of cracking was seen. The other high-strain specimen in this autoclave showed a similar, but smaller (2.7-mm long) crack array after 450 hours.

As noted above, the only indications found in the simulated Alloy 52M weld repairs were two microfissures, apparently residual from the specimen manufacturing process. Such microfissures are not unusual for austenitic nickel-base alloy welds. Visual and dye-penetrant inspections are generally successful in identifying these features, but they are typically classified as non-relevant through NB 5350 of ASME Code Section III. In general, these small microfissures are not observed to participate in the initiation or propagation of environmental cracking. Cracking of the Alloy 600 specimens was limited to three of the four specimens strained 1%. The archived heat of CRDM nozzle from which this material was taken exhibits moderate resistance to SCC in laboratory tests; hence, these results are reasonable. Even though the cracking was less severe than in the Alloy 182 weld specimens, the cracks initiated in times (214, 365 and 598 hours) that were only a fraction of the 2051-hour cumulative exposure time of the Alloy 52M weld specimens, which did not crack.

3.3 Low Temperature Crack Propagation (LTCP)

Brown and Mills investigated fracture behavior of Alloys 690 and 600 and their weld metals EN82H (Alloy 82) and EN52 (Alloy 52) in low and high temperature hydrogenated and alkali treated water.[56, 57, 58] EN82H and EN82 are military specifications of Alloy 82. EN82H contains a higher content of carbon than EN82. The chemical compositions of the materials tested are listed in Table 3-59. The carbon content of the EN82H heats tested was ~0.04%, which was within the ASME Section II limit of 0.10% max. for Alloy 82 (see Table 2-2). Fracture toughness tests were performed on deeply precracked cracked compact (CT) specimens. The CT

specimens were machined from a 50.8 mm (2 inch) thick Alloy 600MA plate and a 76.2 mm (3 inch) dia. Alloy 690TT bar. The Alloy 600MA plate was annealed at 982°C (1800°F) and the Alloy 690TT was annealed at 1074°C (1965°F) and thermally treated at 718°C (1324°F) for 10 hours. The EN82H and EN52 weld metals were fabricated using a manual gas-tungsten arc (GTA) weld process to join 25.4-mm (1-inch) thick Alloys 600 and 690 plates or to join 50.8-mm (2-inch) thick plates. Welds were fabricated by three manufacturers using a pure argon shield gas or an argon-hydrogen shield gas. The weld CT-specimens were machined and tested for fracture resistance in the as-welded condition.

The fracture toughness tests were performed at 54°C (129°F) and 338°C (640°F) in air and in alkali-treated deionized water with a hydrogen concentration ranging from 15 to 200 cc H_2/kg H_2O. All test materials exhibited excellent fracture toughness at 338°C (640°F) undergoing ductile failure. The fracture toughness of Alloy 600 was mostly unaffected in the 54°C (129°F) water and maintained a ductile failure mechanism. Alloy 690, EN82H, and EN52 showed dramatic decreases in fracture toughness in 54°C (129°F) water transitioning from ductile tearing to intergranular cracking. This intergranular cracking was reproduced in hydrogen-precharged specimens tested in air. The low temperature embrittlement was attributed to hydrogen buildup in the crack tip, causing embrittlement which changed the crack propagation mechanism from ductile dimple rupture to intergranular. Such an embrittlement phenomenon was termed “low temperature crack propagation (LTCP). The main conclusions of the studies are summarized below:

1. The high hydrogen concentration in the water does not affect the J value in high temperature water since the high temperature facilitates hydrogen diffusion, hence avoiding a build-up of hydrogen at the crack tip.

2. The high hydrogen concentration in the water at low temperatures appears to affect the J value, due to a hydrogen embrittlement type phenomenon. As the hydrogen concentration is lowered, the J values increase.

3. There appears to be a large scatter in the data, particularly for tests at 54°C (129°F), apparently attributable to weld manufacturer.

4. High loading rates in 54°C (129°F) water yield similar J values compared to low loading rates in 338°C (640°F) water. This indicates that diffusion and accumulation of hydrogen at the crack tip is the cause of embrittlement at low temperature.

5. Modest toughness and ductility is nevertheless retained at low temperatures in Alloy 690. As a result, LTCP is not a primary design concern for Alloy 690.

It should be noted that LTCP is not considered a crack initiation mechanism but is rather a potential mechanism for an existing crack to propagate. No LTCP related failures of Alloy 690 or its weld metals have ever been reported in PWRs or in any actual field applications. Based on these results, LTCP could only become operative at temperatures below approximately 149°C (300°F). LTCP is not considered to be a concern under normal PWR operating conditions due to

the operating temperature of 550°F to 650°F. Furthermore, the hydrogen concentration used in the above mentioned studies was four to five times the normal hydrogen concentration found in primary water. LTCP is probably not a concern under shutdown conditions due to the significantly lower hydrogen concentrations present, when compared to the hydrogen level used in the studies.

Symons studied the effect of hydrogen charging on Alloy 690 plate.[59] Both solution annealed and thermally treated Alloy 690 subsize tension specimens and compact tension (CT) specimens were charged in pure hydrogen autoclave at 337°C (639°F) for four weeks. The hydrogen concentration was measured at 38 to 60 ppm (wt%). The tensile specimens were tested at a strain rate 4 x 10^{-4} sec^{-1} at room temperature and the CT specimens were tested according to ASTM E 819-89 at room temperature. The test results showed that hydrogen addition reduced Alloy 690 ductility and fracture toughness. The degree of embrittlement was more severe for the thermally treated Alloy 690 than solution annealed Alloy 690. The increased embrittlement was attributed to a combination of an elevated local hydrogen concentration (hydrogen trapping) by grain boundary carbides and an increased stress level at the carbides/matrix interface due to larger carbide precipitates. Intergranular cracking was more extensive in precracked CT specimens than in tensile specimens. The hydrostatic stress, which increases the intergranular cracking tendency, is much higher in CT specimens than in tensile specimens.

Lenartova studied Alloys 600, 690, 800 and Type 321 stainless steel cathodically charged with hydrogen to 30 or 115 ppm.[60] The charged tensile specimens were tested at a strain rate of 10^{-7} sec^{-1} at room temperature. The solution annealed Alloys 690, 800 and Type 321 did not show any intergranular cracking but Alloy 600 did show some sensitivity to IG hydrogen embrittlement even without grain boundary carbides. When carbides were precipitated on grain boundaries (accompanied by phosphorus segregation as reported by the author) of Alloys 600, 690 and Type 321 stainless steel, intergranular cracking was observed to increase with increasing hydrogen content and could be suppressed by extracting the hydrogen. However, Alloy 800 did not show any intergranular cracking whatever the heat treatment or state of precipitation on grain boundaries. The critical concentration for mainly intergranular hydrogen cracking in the nickel alloys and stainless steel with GB carbides was about 30 ppm whereas below 5 ppm the ductility and fracture surfaces were very similar to those of the as-received condition. Note that in PWR primary water the average hydrogen concentration attained in austenitic metals is < 2 ppm.

It is clear from other studies of low temperature cracking of Alloy 600 in PWR primary water or after cathodic hydrogen charging that the grain boundary carbide morphology of such benefit to PWSCC resistance has exactly the opposite effect on low temperature hydrogen embrittlement.[60] Considerable benefit from improved grain boundary carbide morphology is obvious from practical operating experience to date with thermally treated Alloy 600 and Alloy 690 whereas the opposite effect would have occurred if LTCP had been a dominant failure mode. Thus, it is concluded that LTCP is unlikely to become a practical concern for Alloy 690, and Alloy 152, and Alloy 52 weld metals.

3.4 Corrosion Fatigue

Psaila-Dombrowski et al. performed S-N fatigue tests for Alloy 690 plate and Alloys 82, 182, and 152 weld metals in air and in simulated primary water at 315°C (600°F) and fatigue crack growth rate tests for Alloys 82 and 52 weld metals in simulated primary water at 315°C (600°F).[42] The simulated primary water chemistry is listed in Table 3-29. A number of weld build-ups and a composite plate were manufactured. The weld samples were fabricated in a manner consistent with SG fabrication practices in which Alloy 52 is used to attach the Alloy 690 plate to the Alloy 82 buildup. The mock-up composite plate began as a 60 mm (2.36") thick A 508 carbon steel plate. One edge of the A 508 plate was overlaid with a 5 mm thickness of Alloy 82 and then stress relieved. The test block was completed by making a modified double V-groove weld between the 5.5 mm thick Alloy 690 plate and the Alloy 82 overlay using Alloy 152. The plate was not stress relieved following the welding. The overall length of the composite weld plate was ~1,000 mm. However, information on the chemical composition of the Alloy 82 and 152 weld metals and Alloy 690 plate and heat treatment condition of Alloy 690 were not reported.

A modified tensile specimen (see Figure 3-18) was used to conduct the low cycle fatigue tests. The orientation of the specimens was such that the axes of the specimens were perpendicular to the direction of welding. In all cases, the gauge sections of the specimens contained only the test material of interest. The tests were conducted in a 76 liter autoclave using a load frame with high lateral stiffness to maintain alignment of the specimen during testing. Most fatigue tests were completed using a strain range of 0.008 and a mean strain of 0. However, several tests were performed at different strain levels to expand the data base. With one exception, all tests in the simulated primary water were performed at a strain rate of 0.001 sec^{-1}. Higher strain rates were used in the air tests because no effect of frequency was expected in an air environment.

The fatigue test results (see Table 3-60 and Figure 3-19) showed that the Alloy 690 fatigue life in the primary water decreased by about 40% compared to the fatigue life in air. However, it was still well above the ASME design curve. The fatigue properties of Alloy 690 in the primary water and in air were in good agreement with predictions made using the following model for Alloy 600 at 150 to 350°C (302 to 662°F).[61]

$$\text{In air,} \qquad \ln(N_{25}) = 6.94 - 1.776 \ln(\varepsilon_a - 0.12) + 0.498 \qquad \textbf{(Eq. 3-1)}$$

$$\text{In water,} \qquad \ln(N_{25}) = 6.94 - 1.776 \ln(\varepsilon_a - 0.12) + 0.498 - 0.401 \qquad \textbf{(Eq. 3-2)}$$

Where, N_{25} – the fatigue life defined as the number of cycles for the peak tensile stress to drop 25% from its initial value

ε_a – the applied strain amplitude in %

Figure 3-19 also shows that the Alloy 82 weld metal exhibited the highest fatigue life among the four materials tested in air. In primary water, all four materials exhibited similar fatigue lives, which were all well above the ASME design curve. Thus, it appears that the primary water has a measurable influence on fatigue life at the strain range and rates used in the study. However, additional fatigue data under other test conditions should be obtained to provide a more complete characterization.

The fatigue crack growth rate tests used standard ASTM precracked 1T compact tension (CT) specimens. The specimens were fabricated with an orientation where crack growth was normal to the welding direction. The results of the test were presented as crack growth rate as a function of stress intensity range (ΔK) and loading frequency as shown in Table 3-61 and Figure 3-20. The test data showed that the cycle-based crack growth rate varied inversely with loading frequency for both Alloy 52 and Alloy 82 weld metals, but the variation was higher for Alloy 82 than Alloy 52. In evaluating the crack growth data for the Alloy 82 at $\Delta K = 36$ ksi$\sqrt{\text{in}}$, it was evident that the data separated into two groups. One group exhibited crack growth rates somewhat higher than the other group. The group of higher growth rates was obtained from a second Alloy 82 specimen taken very near the location of the first Alloy 82 specimen. The reason for the difference in crack growth rate was not clear, but it might indicate that a measurable degree of variation exists in the crack growth properties as a function of locations in the weld. Alloy 52 exhibited a better fatigue crack growth resistance than Alloy 82 in the primary water, but the magnitude of the difference was observed to vary as a function of specimen orientation. Thus, it was not clear if the difference was statistically significant. Compared to the available fatigue crack growth rates in air, the fatigue crack growth rates were typically accelerated by factors of 5 to 20 in the primary water.

Table 3-1 High Velocity Loop Test Conditions by Sedricks et al. [9]

Loop Test Conditions			PWR Steam Generator
Temperature	600°F (316°C)		~610°F
Pressure	2000 psig (13.8 MPa)		~2200 psig
Flow Rate	18 ft/sec (5.5 m/sec)		~20ft
Loop Water Chemistry			
	Borated Water	Ammoniated Water	EPRI Guidelines, Primary Water[62]
Hydrogen	25 cc STP H_2 /kg H_2O	25 cc STP H_2 /kg H_2O	25 - 35 cc STP H_2 /kg H_2O
Oxygen	0 – 15 ppb	0 – 15 ppb	<5 ppb
H_3BO_3	1500 ppm	--	0 – 10,000 ppm
LiOH	0.7 ppm	--	3.5 ppm
pH	5.5	9.5 – 10.9 by ammonia	pH > 6.9 at 77°F
Loop Volume	8.5 gal (32.3 liter)	8.5 gal (32.3 liter)	--

Table 3-2 Chemical Composition of Alloy 690 Heats (wt%) Used by Sedricks et al. [9]

Heat	Ref	Ni	Cr	Fe	C	Mn	Si	S	Ti	Nb + Ta	Cu	P	Al	Mo
Y24A7L	9	Bal.	29.9	8.7	0.02									
NX10C1H	9	Bal.	30.8	9.6	0.03									
NX4458H	9	Bal.	27.9	8.8	0.01									
NX20C4H	9	Bal.	30.2	9.0	0.02									
NX4460H	9	Bal.	28.3	8.9	0.06									
T-57177	9	Bal.	29.3	10.1	0.05									
T-99016	9	Bal.	29.3	11.4	0.07									
T-53176	9	Bal.	28.8	12.4	0.07									
T-53838	9	Bal.	28.3	12.1	0.07									
T-61540 filler	9	Bal.	29.3	11.7	0.06									

Table 3-3 Chemical Composition (wt%) of Alloy 690 Heats Used by K. Smith et al. [11]

Heat	Ni	Cr	Fe	C	Mn	Si	S	Ti	Nb + Ta	Cu	P	Al	Mo	Co
Heat 1	58.8	28.9	10.2	0.016	0.15	0.24	0.001	0.33		0.17	0.011	0.31		0.04
Heat 2	61.2	29.1	8.6	0.028	0.24	0.30	0.002	0.25		0.01	0.005	0.28		0.01
Heat 3	60.4	30.9	7.2	0.038	0.28	0.32	0.002	0.25		0.01	0.005	0.33		0.01

Mechanical Properties: Mill annealed at 1040°F (1904°F) + thermally treated at 700°C (1292°F) for 5 hours

Heat	Room Temp 0.2% Yield Strength		Room Temp Tensile Strength		350°C (662°F) 0.2% Yield Strength	
	MPa	ksi	MPa	ksi	MPa	ksi
Heat 1	344	49.9	739	107.2	269	39.0
Heat 2	438	63.5	814	118.0	364	52.8
Heat 3	444	64.4	829	120.2	357	51.8

Table 3-4 Chemical Composition (wt%), Heat Treatment of Specimens Used by Yonezawa et al. [17]

Heat	Ni	Cr	Fe	C	Mn	Si	S	Ti	Nb + Ta	Cu	P	Al	Mo	Co
Alloy 690	59.86	30.10	8.94	0.020	0.34	0.23		0.24						
Alloy 600	74.50	15.90	8.51	0.027	0.30	0.35		0.19						
Alloy 800L	33.65	21.20	42.9	0.020	0.62	0.49		0.42						

	Annealing Temp	Thermal Treatment	Other
Alloy 690MA	950°C (1742°F)	----	----
Alloy 690TT	1075°C (1967°F)	700°C (1292°F) for 15 hours	----
Alloy 600MA	975°C (1787°F)	----	----
Alloy 600TT	920°C (1688°F)	700°C (1292°F) for 15 hours	----
Alloy 800L	925°C (1697°F)	----	Slight cold worked & shot peened.
Alloy 800L	925°C (1697°F)	----	----

Table 3-5 Test Condition for General Corrosion and RUB Specimens by Yonezawa et al. [17]

Temperature	360°C (680°F)
Hydrogen	30 cc/kg H_2O STP
Oxygen	< 5 ppb
H_3BO_3	500 ppm
LiOH	1 – 2 ppm
pH	Not listed

Table 3-6 General Corrosion by Yonezawa et al. [17]

	Weight Loss (mg/cm^2) after 1000 hours at 360°C (680°F)	Weight Loss (mg/cm^2) after 4000 hours at 360°C (680°F)
Alloy 690MA	Not tested	0.02
Alloy 690TT	0.07	0.02
Alloy 600MA	0.10	0.03
Alloy 600TT	0.13	0.02
Alloy 800L	0.13	0.03

Table 3-7 Autoclave Test Conditions Used by Esposito et al. [31]

	Without Zinc	With Zinc
Temperature	330°C (626°F)	330°C (626°F)
Pressure	2600 psi (17.9 MPa)	2600 psi (17.9 MPa)
Hydrogen	25 cc/kg H_2O	25 cc/kg H_2O
Oxygen	Not listed	Not listed
H_3BO_3	1200 ppm	1200 ppm
LiOH	2.2 ppm	2.2 ppm
pH	Not listed	Not listed
Feed rate from make-up tank	300 cc/hour	300 cc/hour
Zinc Borate	None	50 ppb

Table 3-8 General Corrosion Rate in Primary Water by Esposito [31]

	Corrosion Rate, 2500 hour Average mg/dm^2/month		Metal Release Rate, 2500 hour Average mg/dm^2/month	
	With Zinc	Without Zinc	With Zinc	Without Zinc
304 SS	1.1	3.5	0.1	1.3
316 SS	1.3	3.5	0.1	1.4
600MA	1.5	2.6	0.3	0.8
600TT	0.5	2.1	0.2	0.9
690TT	0.2	1.3	0.1	0.6
X-750	0.6	2.6	0.2	1.2
Stellite	0.4	14.7	0.1	12.0

Table 3-9 General Corrosion Data in PWR Primary Water by Esposito et al. [31]

	Without Zinc Addition				With Zinc Addition			
Material	Exposure Time (hour)	Metal Loss (mg/dm^2)	Oxide Remaining (mg/dm^2)	Metal Release (mg/dm^2)	Exposure Time (hour)	Metal Loss (mg/dm^2)	Oxide Remaining (mg/dm^2)	Metal Release (mg/dm^2)
304 SS	500	4.04	3.37	1.68	500	1.70	1.81	0.43
304 SS	2500	13.64	11.48	5.61	2500	3.75	4.77	0.41
304 SS	2500	11.05	11.17	3.23	---	---	---	---
316 SS	2500	12.37	10.66	4.91	2500	4.34	5.53	0.47
600MA	500	4.26	5.41	0.47	---	---	---	---
600MA	2500	7.61	7.46	2.39	2500	6.66	7.50	1.42
600MA	2500	10.49	10.32	3.27	2500	3.77	4.43	0.66
600MA	2500	10.83	10.33	3.60	---	---	---	---
600MA	2500	6.88	6.39	2.41	---	---	---	---
600TT	500	1.00	1.50	-0.05	500	0.33	0.03	0.10
600TT	1300	6.66	6.66	2.00	1300	1.33	1.66	0.17
600TT	2500	7.16	5.83	3.10	2500	1.83	1.66	0.67
690TT	500	0.81	1.29	-0.09	500	0.50	1.00	-0.20
690TT	1300	3.28	3.44	0.87	1300	0.49	1.31	-0.40
690TT	2500	4.50	3.33	2.17	2500	0.81	1.93	-0.50
X-750	2500	8.93	7.06	3.99	2500	2.00	1.87	0.69
Stellite	---	---	---	---	800	1.98	1.85	0.69
Stellite	2500	61.80	16.00	50.60	2500	3.68	3.82	1.00
Stellite	2500	74.90	25.50	57.10	2500	1.22	1.22	0.37

Table 3-10 Double U-Bend Test Conditions Used by Sedricks [9]

Autoclave Test	Test 1a	Test 1b	Test 2	Test 3	Test 4
Alloy 690 Heat	Y24A7L	NX4458H, NX4460H	Not reported	Y24A7L	Not reported
Test Time	48 weeks	60 weeks	96 weeks	48 weeks	18 weeks
Temperature	600°F (316°C)	680°F (360°C)	620°F (326°C)	600°F (316°C)	600°F (316°C)
Water source	Distilled-deionized water, receptivity > 1 MΩ-cm		Add 60 ppm Na_2HOP_4	Distilled-deionized water	Add 10g lead for 1.8 liter water
pH	pH 10 adjusted with NH_4OH			pH unadjusted	pH unadjusted
Deaeration Method	Ar pressurizing-aspirating; bubbling Ar	H_2 and catalyst N_2H_4	Bubbling N_2, hydrazine	Ar pressurizing-aspirating; Steaming	Ar pressurizing-aspirating
Oxygen	~20 ppb	< 20 ppb	10 – 20 ppb	0 – 5 ppb	~20 ppb
Flow Rate	No flow	0.3 gal/hour	No flow	No flow	No flow
Hydrogen	None	Not reported	Not reported	None	None
H_3BO_3	None	None	None	None	None
LiOH	None	None	None	None	None

Table 3-11 Double U-Bend (creviced) Test Results Under Test 1a Condition in Table 3-10

	Heat Treatment Code [(a)]	Number of Specimens	Test duration (week)	No. cracked Specimens / No. destructively examined	Max. Attack Depth
Alloy 690, Heat No. Y24A7L	MA	2	48	0/2	0
	MA+L	2	48	0/2	0
	MA+A1	2	48	0/2	0
	CR	2	48	0/2	0
	A1+L	2	48	0/2	0
	A3+L	2	48	0/2	0
	A2+W (1/2")	2	18	0/2	0
	A2+W (1")	2	18	0/2	0
Alloy 600, One heat. Heat No. not listed.	CR+A1	2	48	0/2	0
	MA+CR	2	18	1/2	2.79 mm
	Not listed	2	48	0/2	0
	A1+L	2	48	0/2	0
	A3+L	2	48	0/2	0

(a) Heat treatment code:
MA – Mill annealed
CR – cold rolled 40%
A1 – 1 hour at 2000°F/water quench
A2 – 1 hour at 2100°F/water quench
A3 – 1 hour at 2200°F/water quench
L – 2 hours at 1200°F/air cool
W (thickness) = manual gas tungsten-arc welded at indicated thickness with matching filler.

Table 3-12 Double U-Bend (creviced) Test Results Under Test 3 Condition in Table 3-10

	Heat Treatment Code [(a)]	Number of Specimens	Test duration (week)	No. cracked Specimens / No. destructively examined	Max. Attack Depth
Alloy 690, Heat No. Y24A7L	MA	4	48	0/4	0
	MA+L	4	48	0/4	0
	A1	4	48	0/4	0
	A2	6	48	0/6	0
	A1+L	4	48	0/4	0
	A3+L	4	48	0/4	0
	CR	4	48	0/4	0
	A2+W (1/2")	4	48	0/4	0
	A2+W (1")	2	48	0/2	0
Alloy 600, One heat. Heat No. not listed.	MA	4	48	1/4	2 mil (0.05 mm)
	A1	4	48	1/4	5 mil (0.12 mm)
	A1+L	4	48	0/4	0

(a) Heat treatment code:
MA – Mill annealed
CR – cold rolled 40%
A1 – 1 hour at 2000°F/water quench
A2 – 1 hour at 2100°F/water quench
A3 – 1 hour at 2200°F/water quench
L – 2 hours at 1200°F/air cool
W (thickness) = manual gas tungsten-arc welded at indicated thickness with matching filler.

Table 3-13 Double U-Bend (Creviced) Test Results Under Test 1b Condition in Table 3-10

	Heat Treatment Code [(a)]	Heat No.	Number of Specimens	Test duration (week)	No. cracked Specimens / No. destructively examined	Max. Attack Depth
Alloy 690	M	NX4458H, NX 4460H	4	60	0/4	0
	A4	One of the above two heats	2	60	0/2	0
	A4+L4	One of the above two heats	2	60	0/2	0

(a) Heat treatment code:
M – 0.5 hour at 1850°F/air cool
A4 – 1 hour at 2050°F/water quench
L4 – 1 hour at 1250°F/air cool

Table 3-14 SG Tubing Reverse U-Bend Test Conditions Use by K. Smith et al. [11]

	Beginning of Fuel Cycle	End of Fuel Cycle
Temperature	360°C (680°F)	360°C (680°F)
Hydrogen	3.8 ppm dissolved H_2 (240KPa over pressure)	3.8 ppm dissolved H_2 (240KPa over pressure)
Oxygen	Not listed	Not listed
H_3BO_3	1200 ppm	200 ppm B
LiOH	2.0 ppm	0.5 ppm
pH	Not listed	Not listed

Table 3-15 Chemical Composition (wt%) of Alloy 690 Heats Used by A. Smith et al. [32]

Heat	Ni	Cr	Fe	C	Mn	Si	S	Ti	Nb + Ta	Cu	P	Al	Mo	Co
Tube A	60.	30.	9.0	0.022	0.35	0.25	0.003	0.38		0.01	0.01	0.03		0.01
Tube E	60.	29.	10.	0.015	0.36	0.28	0.001	0.36		0.01	0.01	0.13		0.02
Tube F	60.	30.	9.2	0.019	0.35	0.35	0.003	0.36		0.01	0.01	0.02		0.01

Mechanical Properties:
Tubes A and E: Milled annealed at 1040°F (1904°F) + thermally treated at 715°C (1319°F) for 12 hours
Tube F: Milled annealed at 1070°F (1958°F) + thermally treated at 725°C (1337°F) for 15 hours
Tubes A and E tested in deaerated water; Tubes A, E, and F tested in deaerated caustic water.

Heat	0.2% Yield Strength		Tensile Strength		Grain Size		Vickers Hardness Number [(b)] (VHN)
	MPa	ksi	MPa	ksi	μm [(a)]	ASTM [(a)]	
Tube A	357	51.8	771	112	27.66	7.5	197
Tube E	320	46.4	724	105	28.35	7.5	193
Tube F	335	48.6	736	107	30.50	7.0	179

(a) Unit of grain size was not listed; μm is judged to be the only plausible unit.
(b) Load used not reported.

Table 3-16 Chemical Composition (wt%) of Alloys 600 and 690 Use by Norring et al. [35, 36, 37]

Matl. [a] Heat Code	Material	Heat Treatment Condition	C%	Cr%	P%	B%	0.2% off-set yield	
							MPa	ksi
BL	Alloy 600MA	927°C (1700°F)/3-5 min	0.038	15.8	0.012	0.0026	389	56.4
BH	Alloy 600MA	1024°C (1875°F)/3-5 min	0.038	15.8	0.012	0.0026	292	42.4
BH-RUB[b]	Alloy 600MA	1024°C (1875°F)/3-5 min + 365°C for 13,500 hours	0.038	15.8	0.012	0.0026	292	42.4
E	Alloy 600	See Note (c)	0.022	16.6	0.004	<0.0002	322	46.7
IP	Alloy 600TT	990°C (1814°F)/1 min + 725°C (1319°F) /12hours	0.026	16.6	0.004	<0.0002	313	45.4
PP	Alloy 690TT	1080°C (1976°F)/1 min + 725°C (1319°F) /5hours	0.020	29.9	0.006	<0.0002	318	46.1
F	Alloy 690MA	1060°C (1940°F)/1min	0.023	29.9	0.005	<0.0002	380	55.1

(a) The same heats were also used for RUB testing. See Tables Table 3-19, Table 3-20, and Table 3-21.
(b) BH–RUB was identical to BH, except it was removed after testing at 365°C (689°F) for 13,500 hours.
(c) Records indicate that "E" is thermally treated. However, its microstructure is found to be indicative of a mill annealed material (990°C or 1814°F for 1 minute).

Table 3-17 Grain Boundary Chemical and Precipitates Evaluation [37]

Matl. [a] Heat Code	Material	Heat Treatment Condition	Weibull Crack Initiation time	Grain Boundary Carbide Type by Atom Probe	Grain Boundary Carbide Density (1/μm)
BL	Alloy 600MA	927°C (1700°F)/3-5 min	1,050 hours [d]	MB	0 – 0.1
BH	Alloy 600MA	1024°C (1875°F)/3-5 min	12,000 hours [d]	M(CN)	0.5 – 2
BH-RUB[b]	Alloy 600MA	1024°C (1875°F)/3-5 min + 365°C for 13,500 hours	12,000 hours [d]	Not listed	0.5 – 2
E	Alloy 600	See Note (c)	10,500 hours	Not listed	0 – 0.1
IP	Alloy 600TT	990°C (1814°F)/1 min + 725°C (1319°F) /12hours	2 out of 4 specimens cracked after 23,000 hours	$M_{23}C_6$	3 – 8
PP [f]	Alloy 690TT	1080°C (1976°F)/1 min + 725°C (1319°F) /5hours	>23,000 hours [e]	$M_{23}C_6$, M_7C_3	3 – 8
F	Alloy 690MA	1060°C (1940°F)/1min	>33,000 hours [e]	Not listed	0.1 – 1

(a) The same heats were also used for RUB testing. See Tables Table 3-19, Table 3-20, and Table 3-21.
(b) BH–RUB was identical to BH, except it was removed after testing at 365°C for 13,500 hours.
(c) Records indicate that "E" is thermally treated. However, its microstructure is found to be indicative of a mill annealed material (990°C or 1814°F for 1min).
(d) The numbers 1050 hours and 12,000 hours appear to be rounded from the same materials in Table 3-21.
(e) None of the RUB specimens were cracked at the termination of the testing.
(f) PP was listed twice with different type of grain boundary carbides in the reference.

Table 3-18 SG Tubing Reverse U-Bend Test Conditions Use by Norring et al.

Reference [(a)]	Ref. 35	Ref. 37
Temperature	365°C (689°F)	365°C (689°F)
Hydrogen	4 – 5 ppm (Activity 4 – 5 kPa)	50 cc H_2/kg H_2O (Activity 5.9kPa)
Oxygen	< 5 ppb	<5 ppb
Outlet	0.09 – 0.15 μs/cm	0.08 – 0.11 μs/cm
Impurities	Not listed	SO_4^{2-} <20ppb Cl^- <15 ppb F^- < 20 ppb

(a) For the same investigation, the test condition reported was slightly different in the referenced papers.

Table 3-19 Alloy 690 Reverse U-Bend Test Results by Norring et al.[36, 37]

Matl. Heat Code	Tube Dia.	Specimen Number	Anneal Temp	TT or MA	Duration (hours) [(a)]	Test Result
A	3/4"	8	>1000°C (1832°F)	TT	25,000	No IGSCC
B	3/4"	7	>1000°C (1832°F)	TT	25,000	No IGSCC
D	3/4"	8	>1000°C (1832°F)	TT	25,000	No IGSCC
PP	3/4"	6	>1000°C (1832°F)	TT	**23,000**	No IGSCC
C	3/4"	6	<1000°C (1832°F)	TT	25,000	No IGSCC
I	3/4"	6	<1000°C (1832°F)	TT	25,000	No IGSCC
F	3/4"	6	>1000°C (1832°F)	MA	**33,000**	No IGSCC
H	3/4"	6	>1000°C (1832°F)	MA	25,000	No IGSCC
G	3/4"	6	<1000°C (1832°F)	MA	25,000	No IGSCC
Y	1/2"	4	<1000°C (1832°F)	MA	20,500	No IGSCC
Z	1/2"	4	<1000°C (1832°F)	MA	20,500	No IGSCC

(a) The test duration is based on Figure 1 of Ref. 36, except for "PP" and "F" which is based on Ref. 37. The 23,000 hours for "PP" and 33,000 hours for "F" are the total accumulated test time at the termination of the test. Hence, it is probable that many other Alloy 690 RUB specimens listed in the table also accumulated 33,000 hours at the test termination without cracking.

Table 3-20 Alloy 600 Reverse U-Bend Test Results by Norring et al. [36]

Matl. Heat Code	Tube Dia.	Specimen Number	Anneal Temp	TT or MA	Duration (a) (hours)	Test Result
V	7/8”	7	Not listed	MA	2,500	IGSCC
W	7/8”	3	Not listed	MA	1,600	IGSCC
K	7/8”	4	Removed from PWR	MA	800	IGSCC
L	7/8”	4	Removed from PWR	MA	1,200	IGSCC
M	7/8”	4	Removed from PWR	MA	1,500	IGSCC
N	3/4"	5	Removed from PWR	MA	7,000	IGSCC
O	3/4"	3	Removed from PWR	MA	6,500	IGSCC
P	3/4"	5	Removed from PWR	MA	7,000	IGSCC
R	3/4"	5	Removed from PWR	MA	5,500	IGSCC
S	3/4"	5	Removed from PWR	MA	7,500	IGSCC
T	3/4"	5	Removed from PWR	MA	3,500	IGSCC
EB	3/4"	2	Removed from PWR	MA	6,800	IGSCC
EC	3/4"	2	Removed from PWR	MA	6,800	IGSCC
ED	3/4"	2	Removed from PWR	MA	3,600	IGSCC
EL	3/4"	4	<1000^{o}C (1832^{o}F)	MA	7,700	IGSCC
SL	3/4"	7	<1000^{o}C (1832^{o}F)	MA	4,700	IGSCC
HL	3/4"	7	<1000^{o}C (1832^{o}F)	MA	3,000	IGSCC
BL	3/4"	7	<1000^{o}C (1832^{o}F)	MA	**1,051**	IGSCC
SH	3/4"	3	>1000^{o}C (1832^{o}F)	MA	13,000	IGSCC
HH	3/4"	3	>1000^{o}C (1832^{o}F)	MA	11,800	IGSCC
BH	3/4"	3	>1000^{o}C (1832^{o}F)	MA	**11,920**	IGSCC
VA	7/8"	4	>1000^{o}C (1832^{o}F)	TT	15,500	No IGSCC
E	3/4"	8	>1000^{o}C (1832^{o}F)	TT	10,500	IGSCC
EA	3/4"	2	Removed from PWR	TT	12,000	No IGSCC
EE	3/4"	2	Removed from PWR	TT	12,000	No IGSCC

(a) For Alloy 600 specimens that developed IGSCC, the time is the Weibull scale parameter. Both the Weibull scale parameter or test time is estimated from Figure 1 of Ref. 36, except for BL and BH which were listed.

Table 3-21 Alloy 600 Crack Initiation Time from Reverse U-Bend Test by Norring [35]

Alloy 600 SG Tube source	Tube Diameter	Weibull crack initiation time (hour)
PWR Ringhals 2	7/8”	910
PWR Ringhals 3	3/4"	5,620
PWR Ringhals 4	3/4"	4,590
Alloy 600MA	7/8”	1,440
Alloy 600TT	3/4"	8,060
EPRI Provided B&WTP	Not listed	740
EPRI Provided Huntington	Not listed	2,480
EPRI Provided Sandvik	Not listed	3,490

Table 3-22 CERT Test Conditions Use by Angeliu et al.[38]

	Hydrogenated water	High Purity Argon
Strain rate	$3x10^{-7}$ sec^{-1} Initial	$3x10^{-7}$ sec^{-1} Initial
Temperature	360°C (680°F)	360°C (680°F)
Hydrogen	16 cc H_2/kg H_2O or 0.1 MPa	--
Oxygen	< 10 ppb	--
Outlet	0.09 – 0.15 μs/cm	--
Impurities	18 mΩ	--

Table 3-23 CERT Results (Tested in Argon) by Angeliu et al.[38]

Type	Chemical Composition	Annealing Temp (a)	Ultimate Tensile		Elong. %	% IG Fracture	Hours to Failure
			MPa	ksi			
	Ni-5%Cr-9%Fe-0.0001%C	900°C (1652°F)	416	60	8.9	20	77
Alloy 600	Ni-16%Cr-9%Fe-0.001%C	1100°C (2012°F)	524	76	11.4	14	106
Alloy 600	Ni-16%Cr-9%Fe-0.002%C	1100°C (2012°F)	610	88	10.0	<3	93
Alloy 600	Ni-16%Cr-9%Fe-0.03%C	1100°C (2012°F)	642	93	21.9	0	186
Alloy 690	Ni-30%Cr-9%Fe-0.002%C	1050°C (1922°F)	580	84	11.6	2	105
Alloy 690	Ni-30%Cr-9%Fe-0.03%C	1200°C (2192°F)	678	98	14.5	0	157

(a) Annealing time was 20 minutes for all specimens. Annealing was performed before introducing the 30% cold work.

Table 3-24 CERT Results (Tested in Deaerated Water) by Angeliu et al.[38]

Type	Chemical Composition	Annealing Temp (a)	Ultimate Tensile		Elong. %	% IG Fracture	Hours to Failure
			MPa	ksi			
	Ni-5%Cr-9%Fe-0.0001%C	900°C (1652°F)	374	54	6.8	42	66
Alloy 600	Ni-16%Cr-9%Fe-0.001%C	1100°C (2012°F)	494	72	12.9	21	125
Alloy 600	Ni-16%Cr-9%Fe-0.002%C	1100°C (2012°F)	570	83	9.2	14	78
Alloy 600	Ni-16%Cr-9%Fe-0.03%C	1100°C (2012°F)	612	89	25.1	0	219
Alloy 690	Ni-30%Cr-9%Fe-0.002%C	1050°C (1922°F)	579	84	14.5	2	137
Alloy 690	Ni-30%Cr-9%Fe-0.03%C	1200°C (2192°F)	655	95	NA	0	180

(a) Annealing time was 20 minutes for all specimens. Annealing was performed before introducing the 30% cold work.

Table 3-25 Oxide Film on Coupons Exposed to 680°F Deaerated Water for ~100 hours [38]

Type	Chemical Composition	Annealing Temp (a)	Ion Implantation	Film Thickness (nm)	Predominant Phase in the Oxide Film
Alloy 600	Ni-16%Cr-9%Fe-0.002%C	1100°C (2012°F)	None	38	Cr_2O_3
Alloy 600	Ni-16%Cr-9%Fe-0.03%C	1100°C (2012°F)	None	281	$Ni(OH)_2$
Alloy 690	Ni-30%Cr-9%Fe-0.002%C	1050°C (1922°F)	None	46	Cr_2O_3
Alloy 690	Ni-30%Cr-9%Fe-0.03%C	1200°C (2192°F)	None	58	Cr_2O_3

(a) Annealing time was 20 minutes for all specimens. Coupon surface was ground and polished after annealing and before exposure to high temperature deaerated water.

Table 3-26 Chemical Composition of Alloys 600 and 690 SG Tubing Used by Nakayama et al. [40]

Heat	Ni	Cr	Fe	C	Mn	Si	S	Ti	Nb + Ta	Cu	P	Al	Mo	Co
No. 15, 600	Bal.	15.26	8.22	0.025	0.51	0.30	0.0035	0.20		0.09	0.010	0.32		0.002
No. 16, 600	Bal.	15.73	8.35	0.038	0.50	0.27	0.0036	0.20		0.10	0.009	0.29		0.078
No. 17, 690	Bal.	29.65	9.50	0.034	0.40	0.38	0.0097	0.40		0.10	0.009	0.39		0.079
No. 18, 690	Bal.	29.34	9.20	0.034	0.40	0.37	0.0027	0.79		0.10	0.009	0.40		0.078

Table 3-27 Heat Treatment of Alloys 600 and 690 SG Tubing Used by Nakayama et al. [40]

Heat	Solution Heat Treatment	Thermal Treatment	Aging
Alloy 600MA	0.5-hour at 1050°C (1922°F), water quench	--	24, 100 hours at 500°C (932°F), and 1000 hours at 350°C (662°F)
Alloy 600TT	0.5-hour at 950°C (1742°F), water quench	15-hour at 700°C (1292°F)	
Alloy 690MA	0.5-hour at 1100°C (2012°F), water quench	--	24, 100 hours at 500°C (932°F)
Alloy 690TT	0.5-hour at 1100°C (2012°F), water quench	15-hour at 700°C (1292°F)	

Table 3-28 Single U-Bend Test Results in Hydrogen Saturated Water by Nakayama et al. [40]

Heat	Max. Crack Depth, μm		
	100 hours at 500°C (932°F)	24 hours at 500°C (932°F)	1000 hours at 350°C (662°F)
Alloy 800 (0.3%Ti)	0	0	0
Alloy 600MA	130	90	170
Alloy 600TT	90	30	60
Alloy 690MA	30	0	--
Alloy 690TT	0	70	--

Table 3-29 Test Conditions Use by Psaila-Dombrowski et al.[41, 42]

	Primary water chemistry for CERT, S/N fatigue test, and fatigue crack growth rate test	Faulted primary water chemistry for CERT only
Strain rate for CERT	$5x10^{-8}$ or 10^{-6} sec^{-}	$5x10^{-8}$ or 10^{-6} sec^{-1}
Temperature	343°C (650°F) for CERT 315°C (600°F) for fatigue tests	343°C (650°F)
Hydrogen	> 20 cc H_2/kg H_2O	> 20 cc H_2/kg H_2O
Oxygen	Not listed	Not listed
LiOH	2.2 ppm +/- 0.1 ppm	2.2 ppm +/- 0.1 ppm
B (H_3BO_3)	1000 ppm +/- 25 ppm (~5700 ppm)	1000 ppm +/- 25 ppm (~5700 ppm)
pH, room temp	6.5 +/- 0.2	6.5 +/- 0.2
		150 ppb chloride

Table 3-30 CERT Test Results by Psaila-Dombrowski et al.[41, 42]

Water	Strain Rate	Results	Alloy 82 Weld [(a)]	82/152 HAZ	Alloy 152 Weld	152/690 HAZ
Phase 1, Normal	10^{-6} s^{-1}	Max. stress, MPa (ksi)	586 (85)	552 (80)	552 (80)	621 (90)
		Time to failure, hour	135	125	140	130
		SCC	No	No	No	No
Phase 1, Normal	10^{-6} s^{-1}	Max. stress, MPa (ksi)	586 (85)	565 (82)	655 (95)	620 (90)
		Time to failure, hour	155	125	100	150
		SCC	No	No	No	No
Phase 1, Faulted	10^{-6} s^{-1}	Max. stress, MPa (ksi)	572 (83)	552 (80)	586 (85)	572 (80)
		Time to failure, hour	140	140	140	140
		SCC	No	No	No	No
Phase 2, Normal	$5x10^{-8}$ s^{-1}	Max. stress, MPa (ksi)	467 (68)	483 (70)	591 (86)	427 (62)
		Time to failure, hour	Did not fail[(b)]	Did not fail[(b)]	Did not fail[(b)]	Did not fail[(b)]
		SCC	Yes, secondary cracks	Yes, cracks in Alloy 82	No	No

(a) Average value of two specimens.
(b) These specimens did not fail during the 4122 hours of test duration.

Table 3-31 Alloy 690 and Alloy 690 SG Tubing Used by Ogawa et al. [43]

	SG Tub Size		Heat Treatment	
	I.D. dia. (mm)	Wall Thickness (mm)	Solution Heat Treatment /Mill Anneal	Thermal Treatment
600MA	22.23 mm	1.27	925°C (1697°F)	--
600TT	22.23 mm	1.27	925°C (1697°F)	700°C (1292°F)/15 hours
690TT	22.23 mm	1.27	1075°C (1967°F)	700°C (1292°F)/15 hours

Heat	Ni	Cr	Fe	C	Mn	Si	S	Ti	Nb + Ta	Cu	P	Al	Mo	Co
600MA&TT	74.30	16.35	8.2	0.028	0.30	0.33	0.001			0.0 (a)				
690TT	60.15	30.35	Bal.	0.021	0.33	0.35	0.001			0.01				

(a) 0.0% was the number listed for Cu in the reference.

Table 3-32 RUB and Constant Load Specimens Used by Ogawa et al. [43]

	Reverse U-Bend	Uniaxial Constant Load
Alloy 600MA	Tested at 320°C (608°F), 10 RUB specimens for each prestraining level of 0, 5%, 10%, 15%, 20%	Stressed to 85 ksi, tested at 320°C (608°F) and 340°C (644°F), 10 specimens each temp
Alloy 600TT	Same as for Alloy 600MA	Same as for Alloy 600MA
Alloy 690TT	Tested at 360°C (680°F), 10 RUB specimens for prestraining level of 20%	Stressed to 85 ksi, tested at 360°C (680°F), 5 specimens

Table 3-33 RUB and Constant Load Test Results by Ogawa et al. [43]

Phase 1 RUB Results

	Temp	Prestrain	Ref. pH (500 ppm B, 2.0 ppm Li)					Optimum pH (280 ppm B, 2.0 ppm Li)				
		hours	3000	4190	5000	7000	10000	3000	4190	5000	7000	10000
600MA	320°C (608°F)	20%	3/10	4/10	5/10	9/10	10/10	2/10	3/10	4/10	7/10	10/10
		15%	1/10	2/10	4/10	8/10	10/10	0/10	1/10	2/10	5/10	8/10
		10%	0/10	0/10	3/10	7/10	9/10	0/10	1/10	2/10	4/10	6/10
		5%	0/10	0/10	0/10	1/10	3/10	0/10	0/10	0/10	0/10	2/10
		0	0/10	0/10	0/10	0/10	0/10	0/10	0/10	0/10	0/10	0/10
600TT	320°C (608°F)	20%	0/10	1/10	2/10	5/10	10/10	0/10	0/10	0/10	2/10	6/10
		15%	0/10	0/10	0/10	1/10	6/10	0/10	0/10	0/10	1/10	4/10
		10%	0/10	0/10	0/10	0/10	1/10	0/10	0/10	0/10	0/10	0/10
		5%	0/10	0/10	0/10	0/10	0/10	0/10	0/10	0/10	0/10	0/10
		0	0/10	0/10	0/10	0/10	0/10	0/10	0/10	0/10	0/10	0/10
690TT	360°C (680°F)	20%	0/10	0/10	0/10	0/10	0/10	0/10	0/10	0/10	0/10	0/10

Phase 2 RUB Results

	Temp	Prestrain	Reference pH (1600 ppm B, 2.0 ppm Li)						Candidate pH (1600 ppm B, 3.5 ppm Li)					
		hours	1356	3000	5005	7000	8536	10015	1356	3000	5005	7000	8536	10015
600MA	320°C (608°F)	20%	0/10	8/10	10/10				0/10	6/10	7/10	8/10	8/10	8/10
		15%	0/10	2/10	9/10	10/10			0/10	4/10	8/10	9/10	9/10	9/10
		10%	0/10	1/10	5/10	7/10	8/10	9/10	0/10	0/10	5/10	7/10	7/10	8/10
		5%	0/10	0/10	0/10	1/10	1/10	2/10	0/10	0/10	0/10	0/10	2/10	3/10
		0	0/10	0/10	0/10	0/10	0/10	0/10	0/10	0/10	0/10	0/10	0/10	0/10
600TT	320°C (608°F)	20%	0/10	0/10	3/10	5/10	7/10	9/10	0/10	0/10	3/10	4/10	7/10	9/10
		15%	0/10	0/10	1/10	6/10	9/10	9/10	0/10	0/10	1/10	4/10	5/10	6/10
		10%	0/10	0/10	0/10	0/10	0/10	0/10	0/10	0/10	0/10	0/10	0/10	0/10
		5%	0/10	0/10	0/10	0/10	0/10	0/10	0/10	0/10	0/10	0/10	0/10	0/10
		0	0/10	0/10	0/10	0/10	0/10	0/10	0/10	0/10	0/10	0/10	0/10	0/10
690TT	360°C (680°F)	20%	0/10	0/10	0/10	0/10	0/10	0/10	0/10	0/10	0/10	0/10	0/10	0/10

(a) x/10 – x is the accumulated number of specimens cracked. 10 is the total number of RUB specimens tested.

Phase 1 Constant Load Test Results, Tested up to 10,000 hours

	Temp.	Specimens Number [b]	Ref. pH (500 ppm B, 2.0 ppm Li)	Optimum pH (280 ppm B, 2.0 ppm Li)	Reference pH (1600 ppm B, 2.0 ppm Li)	Candidate pH (1600 ppm B, 3.5 ppm Li)
Alloy 600MA	320°C (608°F)	10	None cracked	None cracked	None cracked	None cracked
	340°C (644°F)	10	All cracked	All cracked	All cracked	All cracked
Alloy 600TT	320°C (608°F)	10	None cracked [c]	None cracked	None cracked	None cracked
	340°C (644°F)	10	All cracked	All cracked	All cracked	All cracked
Alloy 690TT	360°C (680°F),	5	None cracked	None cracked	None cracked	None cracked

(b) Number of specimens tested under each water condition.
(c) “None cracked” indicate no PWSCC observed in any specimens after 10,000 hours.

Table 3-34 Alloy 690 and Alloy 690 SG Tubing Used by Sui et al. [52]

	SG Tub Size		Material Processing History in the As-Received Condition		
	I.D. dia. (mm)	Wall Thickness (mm)	Intermediate Mill Annealing	Final Mill Anneal	Thermal Treatment
600 (2682)	15.10	1.00	Unknown	Unknown	Unknown
600 (EPRI 1)	15.10	1.00	Unknown	1025°C (1877°F)	Unknown
600 (EPRI 2)	15.10	1.00	Unknown	925°C (1697°F)	Unknown
690 (A)	14.97	0.97	1100°C (2012°F)/3 min.	1070°C (1958°F)/2 min.	725°C (1337°F)/15 hours
690 (B)	14.97	0.97	Unknown	965°C (1769°F)/4 min.	715°C (1319°F)/15 hours

Heat	Ni	Cr	Fe	C	Mn	Si	S	Ti	Nb + Ta	Cu	P	Al	Mo	Co
600 (2682)	74.36	15.50	9.29	0.024	0.25	0.30	0.001			0.28				
600 (EPRI 1)	75.0	15.8	8.0	0.039	0.26	0.31	0.002			0.01				
600 (EPRI 2)	75.0	15.8	8.0	0.038	0.26	0.32	0.001			0.01				
690 (A)	59.5	30.0	9.2	0.019	0.35	0.35	0.003			0.01		0.02		
690 (B)	59.7	28.9	10.2	0.019	0.36	0.32	0.001			0.02		0.14		

Room Temperature Mechanical Properties

Heat	0.2% Yield Strength		Tensile Strength		Elongation
	MPa	ksi	MPa	ksi	%
600 (2682)	365	53	744	108	36
600 (EPRI 1)	292	42	679	98	47
600 (EPRI 2)	389	56	737	107	37
690 (A)	335	49	736	107	42
690 (B)	452	66	798	116	40

Table 3-35 RUB Test Results in Hydrogen/Steam at 716°F by Sui et al. [52, 53]

C – Cracked; NC – Not cracked; IG – Slight intergranular cracking; SA – Slight intergranular attack

Alloy 600 RUB Test Results

Specimen	Heat	Heat Treatment in addition to the listed in Table 3-34	Result After Hours of Exposure					
			552	625	905	1416	2026	2578
Autoclave 1								
1U	2682	As-received		NC	NC	NC	NC	NC
2U	2682	925°C (1697°C)/ 4-min.		NC	NC	NC	NC	C
3U	2682	5% Elong., 925°C (1697°C)/ 4-min.		SA	IG	IG	IG	C
4U	2682	10% elongation + 925°C (1697°F)/ 4-min		SA	IG	IG	IG	C
5U		15% Elong., 925°C (1697°C)/ 4-min.		SA	IG	IG	IG	NC
6U	EPRI I	As-received		NC	NC	C		
7U	EPRI 1	5% Elong., 925°C (1697°C)/ 4-min.		NC	NC	C		
8U	EPRI 2	As-received		NC	NC	C		
9U	EPRI 2	5% Elong., 925°C (1697°C)/ 4-min.						
Autoclave S2								
10U	EPRI I	450°C (842°F) / 60 hours	NC					
11U	EPRI 2	450°C (842°F) / 60 hours	C					

Alloy 690 RUB Test Results, Autoclave S1

	690 Heat	Heat Treatment in addition to the listed in Table 3-34	Examination after Hours of Exposure									
			500	1000	1500	2000	3000	4000	4500	7000	12600	13824
1R	A	As-received	NC	NC	NC	NC	NC	NC	NC	NC	NC	NC
2R	A	550°C (1022°F) /30 hours	NC	NC	NC	NC	NC	NC	NC	NC	NC	NC
3R	A	10% Elong., 925°C (1697°C)/4-min.	NC	NC	NC	NC	NC	NC	NC	NC	NC	NC
4R	A	10% Elong., 925°C (1697°C)/4-min. + 550°C (1022°F) /30 hours	NC	NC	NC	NC	NC	NC	NC	NC	NC	NC
5R	**B**	As-received	NC	NC	NC	NC	NC	NC	NC	NC	NC	**C**
6R	**B**	550°C (1022°F) /60 hours	NC	NC	NC	NC	NC	NC	NC	NC	NC	**C**

Alloy 690 RUB Test Results, Autoclave S2

	690 Heat	Heat Treatment in addition to the listed in Table 3-34	Examination after Hours of Exposure						
			500	1500	2500	3000	5500	11000	12324
7R	A	10% Elong., 925°C (1697°C)/4-min. + 550°C (1022°F) /10 hours	NC	NC	NC	NC	NC	NC	NC
8R	A	10% Elong., + 550°C (1022°F)/100 hours	NC	NC	NC	NC	NC	NC	NC
9R	A	Same as 7R	NC	NC	NC	NC	NC	NC	NC
10R	A	Same as 8R	NC	NC	NC	NC	NC	NC	NC

Table 3-36 Alloy 690 and Alloy 690 SG Tubing Used by Angell et al. [44]

Heat	Ni	Cr	Fe	C	Mn	Si	S	Ti	Nb + Ta	Cu	P	Al	Mo	Co
96834 Alloy 600	74.91	15.83	8.09	0.038	0.26	0.3	0.001			0.01				0.02
752246 Alloy 690	59.4	30.1	9.23	0.02	0.35	0.37	0.003			0.01	0.009			0.01

Room Temperature Mechanical Properties

Heat	Size	Heat Treatment	0.2% Yield Strength		Tensile Strength		Elongation
			MPa	ksi	MPa	ksi	%
96834, Alloy 600MA	19.1mm O.D. dia.	Mill Anneal	390	57	737	107	37
752246, Alloy 690TT	17.5 mm O.D. dia.	Thermally Treated	326	47	747	108	37

Table 3-37 RUB Test Conditions and Results(662°F) by Angell et al. [44]

	Phase 1, simulating beginning of cycle water for a 12-month fuel cycle		Phase 2, simulating beginning of cycle water for an 18-month fuel cycle	
	Without zinc	With zinc	Without zinc	With zinc
Zinc	--	40 ppb	--	40 ppb
Temperature	350°C (662°F)		350°C (662°F)	
Hydrogen	25 – 50 cc H_2/kg H_2O or 0.1 MPa		25 – 50 cc H_2/kg H_2O or 0.1 MPa	
B	1200 mg/kg B as H_3BO_3		1800 mg/kg B as H_3BO_3	
Li	2.2 mg/kg Li as LiOH		3.5 mg/kg Li as LiOH	
pH	6.75 at 292°C and 7.10 at 350°C		6.75 at 292°C and 7.10 at 350°C	

Specimen I.D.	Heat	Phase 1		Phase 2			
		Without zinc	With zinc	Without zinc		With zinc	
		7500 hours	7500 hours	5500 hours	7500 hours	5500 hours	7500 hours
Alloy 600 Studsvik	96834, [(c)] Alloy 600MA	1/6	2/6	3/6 [(a)]	3/6 [(a)]	1/6 [(a)]	1/6 [(a)]
Alloy 690 Studsvik	752246, [(c)] Alloy 690TT	0/6	0/6	0/4 [(a)]	0/4 [(a)]	0/4 [(a)]	0/4 [(a)]
Alloy 600 Westinghouse	Not listed	--	--	0/4	3/4	0/4	2/4

(a) Include two uncracked specimens carried forward from Phase 1. However, for Alloy 600, it was not mentioned if the cracked ones in Phase 2 included the ones from Phase 1. For Alloy 690, the maximum specimen exposure time without failure was 15,000 hours.
(b) x/y – x is the accumulated number of specimens cracked; y is the total number of RUB specimens tested.
(c) The descriptions on the RUB specimen I.D. were vague and could not be associated directly with the chemical composition of the Alloy 600 and Alloy 690 SG tubes listed. Hence, the specimen heat number was an educated guess.

Table 3-38 Origin and thermal treatments of Alloy 690 materials tested by the CEA [45]

Tube*	Manufacturer	Heat number	Final Heat Treatment (atmosphere NH_3)
Pre-series SG tube	Imphy	WE 092**	980°C 2 min + 700-730°C 5 h
Pre-series SG tube	Imphy	WE 092**	1040-1070°C 2 min + 700-730°C 5 h
Pre-series SG tube	Imphy	WE 094**	980°C 2 min + 700-730°C 5h
Pre-series SG tube	Imphy	WE 094**	1040-1070°C 2 min + 700-730°C 5 h
Pre-series SG tube	Huntington	NX 3238	1040-1070°C 2 min + 700-730°C 5 h
Industrial SG tube	Imphy	WF 754	1040-1070°C 2 min + 700-730°C 5 h
Industrial SG tube	Imphy	WF 771	1040-1070°C 2 min + 700-730°C 5 h
Industrial SG tube	Imphy	WE 773	1040-1070°C 2 min + 700-730°C 5 h
Industrial SG tube	Imphy	WF 779	1040-1070°C 2 min + 700-730°C 5 h
Industrial SG tube	Imphy	WF 783	1040-1070°C 2 min + 700-730°C 5 h
Industrial SG tube	Imphy	WF 786	1040-1070°C 2 min + 700-730°C 5 h
Industrial SG tube	Imphy	WF 793	1040-1070°C 2 min + 700-730°C 5 h
Industrial SG tube	Imphy	WF 816	1040-1070°C 2 min + 700-730°C 5 h
Industrial SG tube	Imphy	WF 825	1040-1070°C 2 min + 700-730°C 5 h
Industrial SG tube	Imphy	WF 826	1040-1070°C 2 min + 700-730°C 5 h
Industrial SG tube	Imphy	WF 833	1040-1070°C 2 min + 700-730°C 5 h
Industrial SG tube	Imphy	WF 837	1040-1070°C 2 min + 700-730°C 5 h

*: All tubes straightened, sand blasted on ID and OD polished.
** Heats WE 092 and WE 094 were originally heat treated at 980°C + 700°C before the heat treatment indicated in the table.

Table 3-39 Chemical Compositions of Alloy 690 Materials Tested by the CEA [45]

Heat Number	Materials analyzed	Ni	Cr	Fe	C	Mn	Si	S	P	Cu	Co	Al	Ti	N
RCCM 4105 specification		≥58	28-31	7-11	0.01-0.04	•0.50	•0.50	•0.015	•0025	•0.50	•0.10	•0.50	•0.50	-
WE 092	sample	60.4	30.9	7.3	0.037	0.28	0.32	0.002	0.005	-	-	-	0.22	-
WE 094	sample	61.1	29.2	8.5	0.028	0.24	0.32	0.002	0.005	0.01	0.01	0.39	0.24	-
NX 3238	sample	58.8	28.9	102	0.016	0.15	0.24	0.001	0.011	0.17	0.04	0.31	0.33	-
WF 754	ingot top	59.9	28.9	10.2	0.016	0.30	0.31	0.001	0.008	0.014	0.014	0.19	0.31	0.026
	ingot base	59.9	28.8	10.2	0.016	0.30	0.34	0.001	0.008	0.014	0.014	0.16	0.40	
WF 771	sample	59.7	28.5	10.7	0.025	0.33	0.30	0.005	0.009	0.005	0.016	0.16	0.27	-
WF 773	sample	60.4	28.4	10.3	0.020	0.24	028	0.005	0.005	0.014	0.009	0.16	0.17	-
WF 779	ingot top	59.6	28.9	10.5	0.021	0.32	0.26	0.001	0.009	0.008	0.014	0.11	0.25	0.034
	sample	60.6	28.5	10.2	0.022	0.30	0.28	0005	0.008	0.005	0.011	0.19	0.15	
	ingot base	59.6	28.8	10.5	0.024	0.31	0.26	0.001	0.010	0.009	0.014	0.14	0.35	
WF 783	ingot top	59.5	29.7	9.8	0.019	0.33	0.29	0.001	0.008	0.012	0.010	0.09	0.27	0.041
	sample	60.4	29.1	9.5	0.016	0.29	0.31	0.005	0.005	0.005	0.009	0.14	0.17	
	ingot base	59.5	29.7	9.8	0.020	0.32	0.26	0.001	0.008	0.007	0.011	0.09	0.28	
WF 786	ingot top	59.6	29.1	10.3	0.021	0.26	0.24	0.001	0.008	0.016	0.012	0.10	0.27	0.044
	sample	60.3	28.6	10.2	0.018	0.23	0.27	0.005	0.005	0.014	0.010	0.12	0.14	
	ingot base	59.6	29.1	10.3	0.021	0.27	0.26	0.001	0.008	0.016	0.011	0.12	0.29	
WF 816	ingot top	59.4	29.1	10.5	0.022	0.33	0.29	0.001	0.008	0.007	0.011	0.11	0.24	0.037
	ingot base	59.5	29.0	10.5	0.025	0.33	0.26	0.001	0.009	0.011	0.011	0.12	0.30	
WF 825	ingot top	59.4	28.9	10.6	0.021	0.35	0.30	0.001	0.008	0.010	0.011	0.12	0.25	0.036
	ingot base	59.5	28.8	10.6	0.022	0.34	0.25	0.001	0.009	0.005	0.012	0.14	0.30	
WF 826	sample	59.4	29.1	10.6	0.019	0.31	0.28	0.005	0.006	0.006	0.014	0.14	0.17	-
WF 833	ingot top	59.4	29.0	10.6	0.021	0.33	0.29	0.001	0.009	0.005	0.012	0.10	0.26	0.035
	sample	59.7	28.9	10.4	0.020	0.31	0.31	0.005	0.008	0.006	0.014	0.16	0.24	
	ingot base	59.4	28.9	10.6	0 023	0.33	0.26	0 001	0.009	0.008	0.012	0.15	0.31	
WF 837	ingot top	59.1	29.1	10.8	0.022	0.31	0.27	0001	0.007	0.005	0.011	0.09	0.22	0.029
	sample	59.2	29.0	10.7	0.020	0.35	0.26	0.005	0.006	0.006	0.014	0.10	0.29	
	Ingot base	59.2	29.0	10.8	0.019	0.32	0.23	0.001	0.009	_ 0.009	0.012	0.12	0.27	

Table 3-40 Origins and heat treatments of Alloy 690 SG tube materials tested by EdF [46]

Alloy 690	Manufacturer	Process	Heat number	Tube Maker	Final heat treatment (Mill anneal atmosphere)	Diameter / thickness (mm)
Experimental SG tube**	Huntington	AOD ?	NX 4458 H	Huntington	1095°C	12.7/1.35
	Huntington	VAR	NX 40C5 HS	Westinghouse/ Vallourec	1040°C (H_2) 1040°C + 16 h x 700°C	22.2/1.27
	Huntington	AOD	NX 9780 H	Westinghouse/ Vallourec	1045°C (H_2) 1045°C + 16 h x 700°C	22.2/1.27
	Huntington	AOD	NX 9780 H	Westinghouse/ Vallourec	980°C (H_2) 980°C + 16 h x 700°C	22.2/1.27
Pre-series SG tube**	Huntington	-	NX 3238	Vallourec	1040°C (NH_3) +5hx700 C	19.07/1.1
	Imphy	ESR	WE 094	Vallourec	1040°C (NH_3) + 5 h x 700°C	19.07/1.1
	Imphy	ESR	WE 092	Vallourec	980°C (NH_3) + 5 h x 700C	19.05/1.1
	Imphy	ESR	WE 092	Vallourec	1060°C (NH_3) + 5 h x 700°C	19.05/1.1
	Imphy	ESR	WE 092	Vallourec	1040°C (NH_3) + 5 h x 700°C	19.05/1.1
Industrial SG tube**	Imphy	ESR	WF 511	Vallourec	1040°C to 1070°C (NH_3) + 5 h x 700C	19.05/1.1
	Imphy	ESR	WF 517	Vallourec	1040 to 1070°C (NH_3) + 5 h x 700°C	19.05/1.1
	Imphy	ÉSR	WF 754	Vallourec	1040 to 1070°C (H_2) + 5 h x 700°C	19.05/1.1
	Imphy	ESR	WF 816	Vallourec	1040 to 1070°C (H_2) + 5 h x 7001C	19.05/1.1
	Huntington	-	NX 4814	Vallourec	1040 to 1070°C (NH_3) + 5 h x 700°C	19.05/1.1
	Huntington	-	NX 4817	Vallourec	1040 to 1070°C (NH_3) + 5 h x 700°C	19.05/1.1
	Tecphy	ÉSR	WH 799	Valinox	1060 to 1080°C (H_2) + 5 h x 700°C	22.2/1.27
	Tecphy	ESR	WG 592	Valinox	1040 to 1080°C (H_2) + 5 h x 700°C	19.05/1.1
	Tecphy	ÉSR	WJ 741	Valinox	1060 to 1080°C (H_2) + 5 h x 700°C	22.2/1.27*

s : AOD : Argon Oxygen Decarburization -VAR: Vacuum Arc Remelting - ESR : Electroslag Remelting.
s* :Tube surface contaminated with phosphate during fabrication.
**: All tubes straightened, sand blasted on ID (except NX 4817 and WH 799) and OD polished.

Table 3-41 Origins and Heat Treatments of Alloy 690 CRDM Nozzles Tested by EdF [46]

CRDM nozzles	Manufacturer	Process	Heat Number	Tube maker	Extrusion temperature (°C)	Solution anneal and heat treatment temperatures		Diameter / thickness (mm)
Experimental	Tecphy	ESR	WJ 151	Valinox	1110-1230	1050 + 5 h x715°C	- Pre-straighten in a press 1 straightening pass with hyperbolic rolls	109/21,5
Industrial	Tecphy	ESR	WJ 172	Valinox	1110-1210	1080 + 5 h x 715°C	- Pre-straighten in a press - 2 straightening passes with VALTI rolls	110/23

Table 3-42 Chemical compositions of Alloy 690 materials tested by EdF [46]

	C	Si	Mn	S	P	Cr	Ni	Co	Ti	Cu	Al	N	Fe
RCCM 4105 specification 1988 edition	0.010-0.040	•0.50	•0.50	•0.015	• 0.025	28.00 - 31 00	≥58.00	•0.10 Target max 0.05	•0.50	•0.50	•0.50		7.00-11.00
NX 4458 H	0.021	0.12	0.16	0.002	0.007	27.9	62.2	0 02	0.17	0.03	0.12	0.023	9.00
NX 40C5 HS	0.028	0.23	0.31	0.003	0.006	28.7	61.3	0.02	0.30	< 0.01	0.23	0.032	9.2
NX 9780 H	0.012	0.42	0.30	< 0.001	0.010	29.1	60.2	0.03	0.49	0.10	0.26	0.027	8.9
NX 3238	0.016	0.24	0.15	0.001	0.011	28.9	58.8	0.04	0 3 3	0.17	0.31	-	10.2
WE 092	0.041	0.36	0.33	0.001	0.004	30.7	60.4	<001	0.29	<0.01	0.27	0.098	7.2
WE 094	0.029	0.34	0.31	0.001	0 004	28 7	bal	< 0.01	0.29	< 0.01	0.24	0.083	8.4
WF 511	0.017	0.36	0.30	< 0.001	-	29.2	59.4	< 0.01	0.27	< 0.01	0.13	0.040	10.1
WF 517	0.016	0.35	0.27	< 0.001	-	29.2	59.5	< 0.01	0.26	< 0.01	0.17	0.040	10.3
WF 754	0.015	0.31	0.30	< 0.001	0.009	29.0	bal	< 0.01	0.31	< 0.01	0.25	0.041	10.0
WF 816	0.021	0.30	0.34	< 0.001	0.006	29.2	bal	< 0.01	0.23	< 0.01	0.17	0.040	10.4
NX 4814	0.022	0.18	0.08	< 0.001	-	29.0	59.7	< 0.01	0.31	0.03	0.23	0.046	10.6
NX 4817	0.021	0.18	0.08	< 0.001	-	29.0	59.6	< 0.01	0.30	0.11	0.21	0.045	10.5
WH 799	0.018	0.32	0.34	0.002	0.004	28.90	bal	< 0.01	0.23	< 0.01	0.13	0.030	10.95
WG 592	0.023	0.38	0.42	0.002	0.006	29.15	bal	< 0.01	0.23	< 0.01	0.16	0.030	9.60
ATU 240	0.021	0.30	0.33	< 0.001	0.006	29.05	bal	0.01	0.32	< 0.01	0.20	-	10.25
WJ 151	0.023	0.26	0.33	<0.001	0.009	29.04	59.10	0.012	0.20	<0.01	0.11	-	10.67
WJ 172	0.024	0.36	0.30	<0.001	0.007	28.95	59.40	0.013	0.17	0.007	0.11	-	10.66

Table 3-43 Mechanical properties of Alloy 690 materials tested by EdF [46]

Heat Number	Mill anneal temperature (°C)	Tensile properties at 20°C			Tensile properties at 350°C		
		$Rp_{O.2}$ (MPa)	R_m (MPa)	El (%)	Rp_{02} (MPa)	R_m (MPa)	El (%)
RCC-M 4105 + FM 684		275 • 470	≥ 630	≥30	≥ 230	-	-
NX 3238	1040	325	758	46	259	631	44
WE 094	1040	419	825	37	358	723	36
WE 092	980	499	957	40	417	732	36
WE 092	1060	447	849	36	391	709	34
WE 092	1040	464	880	36	398	750	30
WF 511	1040 to 1070	324	744	51	-	-	-
WF 517	1040 to 1070	308	720	53	-	-	-
WF 754	1040 to 1070	304	727	46	232 to 244	589 to 616	-
WF 816	1040 to 1070	360	755	42	280	626	38
NX 4814	1040 to 1070	359	778	45	-	-	-
NX 4817	1040 to 1070	355	776	47	-	-	-
WH 799	1060 to 1080	307 305	708 705	49 51	246 244	590 586	- 45
WG 592	1040 to 1080	331 329	750 747	43 44	271 273	637 637	36 39
ATU 240	1060 to 1080	307 313	708 716	49 49	253 249	595 592	46 44
WJ 151	-	230 228	607 610	57 57	180 179	502 501	59 57
WJ 172	-	347 347	678 681	45 44	292 287	557 554	44 46

Table 3-44 Alloy 690 and Alloy 690 SG Used by Vaillant et al. [49]

Heat	%C	Heat Treatment	YS 20°C	YS 350°C	UTS 350°C	Elong 350°C	GB Carbide	Grain Size
			MPa	MPa	MPa	%	%	ASTM
6E Alloy 600	0.033	1070°C	340	280	670	48	24	8
		1070°C + 700°C	315	360	610		25	
6P Alloy 600	0.016	980°C	340	300	680	40	10	9
		980°C + 700°C	330	255	650		14	
6L Alloy 600	0.026	980°C	380	330	710	35	4	10
		980°C + 700°C	365	290	680		8	
6.242 Alloy 600	0.030	930°C	333	290	680	42	7	10
		930°C + 700°C					11	
6.285 Alloy 600	0.033	940°C	310	263	670	42	7	9
		940°C + 700°C					10	
6.287 Alloy 600	0.034	900°C	325	275	680	40	6	9
		900°C + 700°C					8	
9G Alloy 690	0.012	980°C	410	330	690	40	3	3
9.092 Alloy 690	0.041	980°C + 700°Cx5hours and 1060°C + 700°Cx5hours	447	391	709	34	12	10
9.592 Alloy 690	0.023	1040/1080°C + 700°C	330	272	673	38	13	9-10
9.754 Alloy 690	0.015	1040/1070°C + 700°C	304	238	608		23	6
9.799 Alloy 690	0.018	1060/1080°C + 700°C	306	245	588	45	34	6-7

9G = NX 9780 H
9.092 = WE 092
9.592 = WG 592
9.754 = WF 754
9.799 = WH 799

Table 3-45 RUB and CERT Test Conditions by Vaillant et al. [49]

	RUB	CERT
Temperature	360°C (680°F)	360°C (680°F)
Hydrogen	100 cc H_2/kg H_2O	25-30 cc H_2/kg H_2O
B	1000 ppm B as H_3BO_3	1000 ppm B as H_3BO_3
Li	2 ppm Li as LiOH	2 ppm Li as LiOH
pH	Not reported	Not reported
		$5x10^{-8}$ sec^{-1} strain rate

Table 3-46 RUB and CERT Test Results by Vaillant et al. [49]

		RUB Test		CERT Test	
Heat	Material	Hours (a)	Results	Intergranular Crack Depth	CGR, μm/hour (b)
6E	600TT	36,000	Not cracked	No intergranular cracking	4.49E-03 (c)
6P	600MA	3,000	Cracked	Yes, depth not listed	2.15E-02
6P	600TT	3,500	Cracked	Yes, depth not listed	1.11E-02
6L	600MA	1,000	Cracked	Yes, depth not listed	6.02E-02
6L	600TT	3,000	Cracked	Yes, depth not listed	9.86E-02
6.242	600MA	500	Cracked	Yes, depth not listed	1.45E-01
6.242	600TT	1,500	Cracked	Yes, depth not listed	8.30E-02
9.092	690TT	25,000	Not cracked	120 μm (0.0047”)	1.42E-01
9.592	690TT	16,500	Not cracked	20–35 μm (0.0008” – 0.0014”)	2.15E-02
9.799	690TT	16,500	Not cracked	No intergranular cracking	2.92E-03 (c)
9G4	690MA	54,000	Not cracked	20–35 μm (0.0008” – 0.0014”)	1.81E-02

(a) Test hours is based on Ref. 49.
(b) Average crack growth rate (CGR) is estimated based on Ref. 49.
(c) Below the detection limit of 10 μm in 2000 hours or 5.00 E-03.

Table 3-47 SG Tubes Used by Boursier et al. [50]

SG Tubes [a]	Note[b]	Eq. of Ref. 49 [a]	Heat Treatment	%Cr	%Fe	%C
690 Exp1	Experiment heat	9.092 Alloy 690TT	980°C + 700°C and 1060°C + 700°C x 5-hour	30.7	7.2	0.041
690 Exp2	Experiment heat	9.092 Alloy 690TT	980°C + 700°C and 1040°C + 700°C x 5-hour			
690 Ind	Industrial (commercial)	9.799 Alloy 690TT	1060°C + 700°C x 5-hour	28.9	10.95	0.018
600 A, ref.	Reference heat, (high resistant heat)	6E Alloy 600MA	1070°C	16.3	7.82	0.033
600 B, sensitive	PWSCC sensitive (low resistant heat)	6.242 Alloy 600MA	930°C	16.05	9.20	0.030

SG Tubes [a]	SG Code in Ref. 49 [a]	YS 20°C	UTS 20°C	Elong 20°C	YS 350°C	UTS 350°C	Elong 350°C
		MPa	MPa	%	MPa	MPa	%
690 Exp1	9.092 Alloy 690TT	447	849	36	391	709	34
690 Exp2	9.092 Alloy 690TT	464	880	36	398	750	30
690 Ind	9.799 Alloy 690TT	305	705	50	245	588	45
600 A, ref.	6E Alloy 600MA	340	710	38	280	670	48
600 B, sensitive	6.242 Alloy 600MA	333	716	42	290	680	42

(a) These SG tube were also used in Ref. 49, but were referred by different codes.
(b) Based on the results from Ref. 49, Alloy 690 Ind has a higher PWSCC resistance than Alloy 690 Exp. Alloy 600 A is a very PWSCC resistant heat while Alloy 600 B is a low resistant heat.

Table 3-48 CERT and Constant Load Test Conditions by Boursier et al. [50]

	CERT Test	Constant Load Test
Temperature	360°C (680°F)	360°C (680°F)
Hydrogen	30 cc H_2/kg H_2O	30 cc H_2/kg H_2O
B	1000 ppm B as H_3BO_3	1000 ppm B as H_3BO_3
Li	2 ppm Li as LiOH	2 ppm Li as LiOH
pH	Not reported	Not reported
	5×10^{-9} – 2.5×10^{-7} sec^{-1} strain rate	603 to 684 MPa (87 to 99 ksi)

Table 3-49 Alloy 690 CERT Test Results by Boursier et al. [50]

360°C (680°F) Primary water, Strain rate 2.5 x 10^{-7} sec^{-1}

Surface condition	As-received		Electropolished		1-Side Shot Peened		2-Side Shot Peened	
	Hours to cracking	Crack depth μm	Hours to cracking	Crack depth μm	Hours to cracking	Crack depth μm	Hours to cracking	Crack depth μm
690 Exp 1	291	90	286	40	--	--	250	74
690 Exp 2	307	47	--	--	258	105	250	50

360°C (680°F) Primary water, Strain rate 5 x 10^{-8} sec^{-1}

Surface condition	As received		Cold Pressed Hump (R=1)	
	Hours to cracking	Crack depth μm	hours to cracking	Crack depth μm
690 Exp 1	1341	120	669	225
690 Ind	2202	5	934	70
600 A	2208	10	343	1087

Exp 1 and Exp 2 = WE 092 (solution annealed at 1060 and 1040°C respectively before TT at 700°C),
Ind= WH 799

Table 3-50 Alloys 52M, 182, 600 Used by Jacko et al. [54]

Alloy	Ni	Cr	Fe	C	Mn	Si	S	Ti	Nb + Ta	Cu	P	Al	Mo	Other
52M [(a)] Y9570	60.10	30.13	8.50	0.020	0.92	0.03	0.001	0.22	0.93	0.03	0.003	0.08	0.02	<0.50
182 [(b)] WC46F5	68.90	13.95	8.04	0.042	6.63	0.43	0.002	0.47	1.41	0.01	0.004			<0.50
600 WF 147	73.07	15.65	9.65	0.033	0.78	0.29	0.001			0.02	0.009			

(a) Heat number Y9570, batch 50249/1. Additional elements: B – 0.004%, Zr – 0.006%.
(b) Additional element: Co – 0.18%.

Table 3-51 Calculated Stress in the Four-Point Bend Specimens Used by Jacko et al. [54]

Alloy		Residual Stress, MPa (a)		
		Pre-test after furnace relief	Mid-test	Post-test
Alloy 52M	High	n/a	n/a	431
	Low	433	384	398
Alloy 182	High	586	n/a	568
	Low	433	n/a	441
Alloy 600	High	456	436	452
	Low	326	392	326

(a) Stresses calculated from measured strains using E at 400°C of Alloy 600) = 195.3 GPa.

Table 3-52 Four-Point Bend Test Results by Jacko et al. [54]

Autoclave Exposure	Equivalent Exposure (a)	Alloy 52M		Alloy 182		Alloy 600	
Hours	EFPY	Low Strain	High Strain	Low Strain	High Strain	Low Strain	High Strain
124	2.8	0/2	0/2	0/2	0/2	0/2	0/4
214	4.8	0/2	0/2	--	2/2	--	--
269	6.0	0/2	0/2	0/2	2/2	0/2	1/4
418	9.3	0/2	0/2	--		0/2	1/4
450	10.0	0/2	0/2	2/2		--	2/4
598	13.3	0/2	0/2	2/2		0/2	3/4
889	19.8	0/2	0/2			0/2	3/4
1343	29.9	0/2	0/2			0/2	3/4
1801	40.1	0/2	0/2			0/2	3/4
2051	45.6	0/2	0/2			--	--

(a) Equivalent EFPYs for the Ringhals 4 outlet nozzle temperature of 322.8°C (613°F) relative to hours at the 400°C doped steam to this service.

(a) x/y – x is the accumulated number of specimens cracked; y is the total specimen number.

Table 3-53 Alloys 690TT and 600MA Used by Framatome ANP, Germany [App. A]

Alloy	Ni	Cr	Fe	C	Mn	Si	S	Ti	Nb + Ta	Cu	P	Al	Mo	Other
Alloy 690TT, 754380	59.40	29.95	9.45	0.019	0.32	0.35	0.001	0.30		0.010	0.008	0.025	0.01	
Alloy 600MA, 752677	72.7	16.55	9.19	0.027	0.80	0.29	0.003	0.29		0.010	0.008	0.14	N/A	

(a) Additional element: Co – 0.012% for Alloy 690TT, 0.011% for Alloy 600MA. N – 0.025% for Alloy 690.

	0.2% Yield Strength	Tensile Strength	Elongation (2”)	outer diameter	wall thickness
Alloy 690TT heat 754380	349 MPa (51 ksi)	746 MPa (108 ksi)	44 %	19.05 mm (3/4”)	1.09 mm (0.043”)
Alloy 600MA heat 752677	399 MPa (58 ksi)	715 MPa (104 ksi)	42 %	22.23 mm (7/8”)	1.27 mm (0.05”)

Table 3-54 RUB Test Results by Framatome ANP, Germany [App. A]

Material	scored surface	total No. of specimens	cracked RUBs after 14 days	cracked RUBs after 30 days	cracked RUBs after 60 days	cracked RUBs after 405 days
Alloy 690TT heat 754380	yes	3	0/3	0/3	0/3	0/3
	no	3	0/3	0/3	0/3	0/3
Alloy 600MA heat 752677	yes	3	3/3	-	-	-
	no	3	3/3	-	-	-

Table 3-55 Alloys 690TT and 600MA&TT Used by Framatome ANP, France [App. B]

Alloy	Ni	Cr	Fe	C	Mn	Si	S	Ti	Nb + Ta	Cu	P	Al	Mo	Other
Alloy 600, WD281	73.40	16.03	8.89	0.035	0.81	0.33	0.001	0.21		0.01	0.010	0.25		
Alloy 600, NX3335	75.11	15.76	8.45	0.03	0.14	0.16	< 0.005	0.10		0.11	0.010	0.081		
Alloy 690, WE094	61.29	28.99	8.75	0.027	0.23	0.28	0.002	0.25		0.01	0.005	0.17		

(a) Additional element: Co – 0.013% for WD2810, 0.036% for NX3335, and 0.01% for WE094. N – 0.0158% % for WE094.

	0.2% Yield Strength, MPa		Tensile Strength, MPa		Elongation, %	
	20°C	343°C (650°F)	20°C	343°C (650°F)	20°C	343°C (650°F)
Alloy 600, WD281	339	262	723	675	41.7	39.1
Alloy 600, NX3335	329	266	721	623	41.3	36.1
Alloy 690, WE094	419	358	825	723	37	36

Table 3-56 Chemical analysis of the aqueous environment in the mock-ups after the 6th test period of 10,000 hours [App. B]

Mock-up	501+503+504+507		502+505+506+508	
	1st period	6th period	1st period	6th period
Cl^- (mg/kg)	0.7	0.46	0.4	0.57
F^- (mg/kg)	0.08	0.56	0.25	0.05
Na^+ (mg/kg)	0.19	0.43	0.14	0.10
SiO_2 (mg/kg)	0.71	4.3	0.43	4.8

Table 3-57 Results for all mock-ups fabricated from Alloy 600 heat WD281 [App. B]

Mock-up	Heat treatment	T/TS Gap (mm)	Kiss rolling (mm)	Skip roll	Intended Over-roll (mm)	Measured Over-roll (mm)	Duration (h)	Result
1B	MA	0.4	0	no	+3	+10	14 400	RTZ
1H					- 1.5	0	20 250	RTZ
2B	MA	0.4	0	no	-	-	-	-
2H					+ 6	+ 6	22 800	RTZ
3B	TT	0.4	0.15	no	+ 20	-	10 000	RTZ
3H					- 1.5	+1	18 400	RTZ
5B	MA	0.4	0.15	yes	+20	+8	1 500	SR
5H					-1.5	4	10 600	RTZ
6B	MA	0.4	0.15	yes	-1.5	0	1 900	SR
6H			0.30		+20	+23		
7B	TT	0.4	0.30	yes	+20	+26	11 100	OZ
7H					-1.5	+3	11 000	SR
8B	MA	0.4	0.30	no	+20	+23	11 750	RTZ
8H					-1.5	+2	12 850	RTZ
10B	TT	0.4	0.30	no	+1.5	-	34 000	No leak
10H					-1.5	-		
11B	TT	0.4	0.30	no	+20	+22	10 750	RTZ
11H					+20		10 500	RTZ
12B	MA	0.4	0.30	no	+20	+24	20 000	RTZ
12H					+1.5	-	30 000	No leak
14B	MA	0.95	0.15	no	+1.5	+1.5	1 300	RTZ
14H					-1.5	+2	800	RTZ
15B	MA	0.95	0.15	no	+20	+23	3 800	RTZ
15H					+20	+23	4 050	RTZ
16B	TT	0.95	0.15	no	+1.5	+7	3 500	OZ
16H					-1.5	+2		
17B	TT	0.95	0.15	no	+20		5 400	RTZ
17H					+20	+23	5 900	RTZ
18B	MA	0.95	0.30	no	+20	+23	4 000	No leak
18H					+20	+23		RTZ
19B	MA	0.95	0.30	no	-1.5	+1	1 600	OZ
19H					+1.5	+6		
20B	TT	0.95	0.30	no	+1.5		1 800	RTZ
20H					-1.5	+2	1 500	RTZ
21B	MA	0.95	0.30	yes	+20	+25	3 800	RTZ
21H					+1.5	+2		No leak

Table 3-58 Results for all mock-ups fabricated from Alloy 600 heat NX3335 [App. B]

Mock-up	Heat treatment	T/TS Gap (mm)	Kiss rolling (mm)	Skip roll	Intended Over-roll (mm)	Duration (h)	Result
4B	MA	0.4	0.30	No	+20	19 600	RTZ
4H					+1.5	27 000	RTZ
9B	MA	0.95	0.30	No	+20	11 300	RTZ
9H					+20	12 150	RTZ

Note: RTZ : cracked in roll transition zone - SR : cracked in skip roll - OZ : cracked in overlap zone

Table 3-59 Chemical Composition of Alloys 600, 690, 82, and 52 Tested by Brown and Mills [56, 57]

Heat	Ni	Cr	Fe	C	Mn	Si	S	Ti	Nb + Ta	Cu	P	Al	Mo	Co
EN82, heat 1	73.2	18.7	1.5	0.007	2.4	<0.1	0.0007	0.4		0.006	<0.001	0.09		<0.1
EN82H, heat 2	76.3	19.93	0.68	0.037	2.73	0.06	0.001	0.32	2.44	0.11	0.014			0.02
EN82H, heat 3	72.9	20.00	1.10	0.04	2.90	0.06	0.002	0.41	2.52	0.02	0.003			
EN82H, heat 4	73.6	19.75	0.73	0.04	2.93	0.09	<0.001	0.30	2.51	0.07	0.004			
EN82H, heat 5	73.7	19.54	0.77	0.04	2.92	0.18	0.001	0.30	2.49	0.02	0.002			
EN82H, heat 6	72.8	19.8	1.31	0.041	2.87	0.07	0.004	0.28	2.5	0.07	0.003			
EN52	60.4	28.97	8.98	0.03	0.23	0.17	<0.001	0.56		<0.01	0.004	0.63		0.01
Alloy 600, plate	75.4	15.54	7.76	0.07	0.25	0.29	<0.001	0.35		0.11	0.007	0.17		0.04
Alloy 690, bar	59.8	29.54	8.25	0.026	0.29	0.01	0.0005	0.32		0.01	0.001	0.31		<0.001

(a) EN82 heat 1 is the as-welded chemistry. All other EN82 and EN52 were the filler metal chemistry.

Table 3-60 Low Cycle Fatigue Test Results by Psaila-Dombrowski et al. [42]

Alloy 690, Alloys 82, 52, and 152 Weld Metals, tested at 600°F

I.D.	Env.	Strain Rate	Strain Range %	Strain Amp. %	Life Cycles (1000s)	I.D.	Env.	Strain Rate	Strain Range %	Strain Amp. %	Life Cycles (1000s)
690-11	Air	0.016	0.4	0.2	>221.3	82-13	Air	0.048	1.2	0.6	21.1
690-12	Air	0.016	0.4	0.2	120.0	82-9	Air	0.032	0.8	0.4	40.3
690-15	Air	0.001	0.4	0.2	>203.7	82-10	Air	0.032	0.8	0.4	77.24
690-7	Air	0.048	1.2	0.6	8.75	82-2	Water	0.001	0.9	0.45	11.32
690-8	Air	0.048	1.2	0.6	7.49	82-3	Water	0.001	0.8	0.4	15.4
690-14	Air	0.048	1.2	0.6	7.15	82-4[(a)]	Water	0.001	0.8	0.4	14.61
690-9	Air	0.032	0.8	0.4	16.04	82-5	Water[(b)]	0.0001	0.8	0.4	9.61
690-10	Air	0.032	0.8	0.4	19.1	52-1	Air	0.016	0.8	0.4	24.12
690-13	Air	0.032	0.8	0.4	16.45	52-2	Air	0.016	0.8	0.4	10.15
690-1	Water	0.001	0.8	0.4	10.17	52-3	Air	0.016	0.8	0.4	18.17
82-15	Air	0.024	0.6	0.3	552.8	52-4	Water	0.001	0.8	0.4	10.14
82-8	Air	0.024	0.6	0.3	>633.0	52-5	Water	0.001	0.8	0.4	8.17
82-14	Air	0.048	1.2	0.6	10.8	152-4	Air	0.032	0.8	0.4	13.4
82-12	Air	0.048	1.2	0.6	21.65	152-1	Water	0.001	0.8	0.4	11.6

(a) Test conducted at 59°C (138°F).
(b) Li (0.2 ppm) and pH (5.62) in the autoclave effluent did not meet chemistry specification.

Table 3-61 Fatigue Crack Growth Rate Test Results by Psaila-Dombrowski et al. [42]

Alloys 82 and 52 Weld Metals

Specimen I.D.	ΔK (ksi√in)	Stress Ratio (R)	Frequency	CGR (in/cycle)	Specimen I.D.	ΔK (ksi √in)	Stress Ratio (R)	Frequency	CGR (in/cycle)
82	20	0.5	1	1.0E-5	82	36	0.1	0.001	4.0E-5
82	20	0.5	0.1	1.4E-5	82CT2	36	0.1	0.01	8.6E-5
82	20	0.5	0.01	1.6E-5	82CT2	36	0.1	0.001	1.1E-4
82	20	0.5	0.0018	2.1E-5	82CT2	36	0.1	0.0001	3.1E-4
82	20	0.5	0.00018	4.8E-5	52CT1	36	0.1	1	2.0E-5
82	36	0.1	1	3.2E-5	52CT1	36	0.1	0.1	2.1E-5
82	36	0.1	0.1	3.9E-5	52CT1	36	0.1	0.01	2.1E-5
82	36	0.1	0.01	4.0E-5	52CT1	36	0.1	0.001	2.5E-5

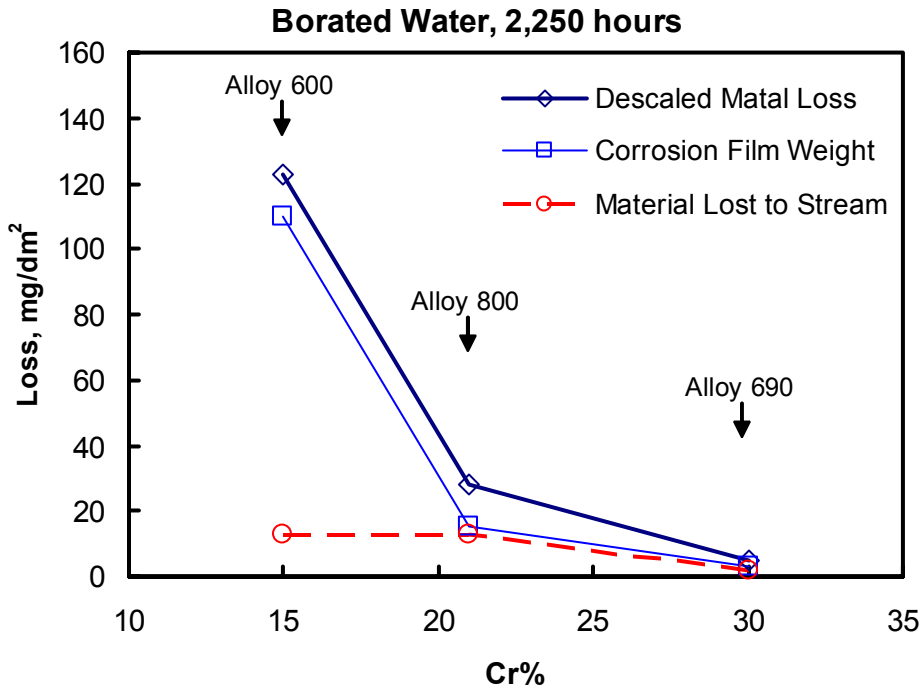

Figure 3-1 Comparison of material lost to stream in 316°F (600°F) deaerated water flowing at a velocity of 18 ft/sec (5.5 m/sec). After Ref. 9.

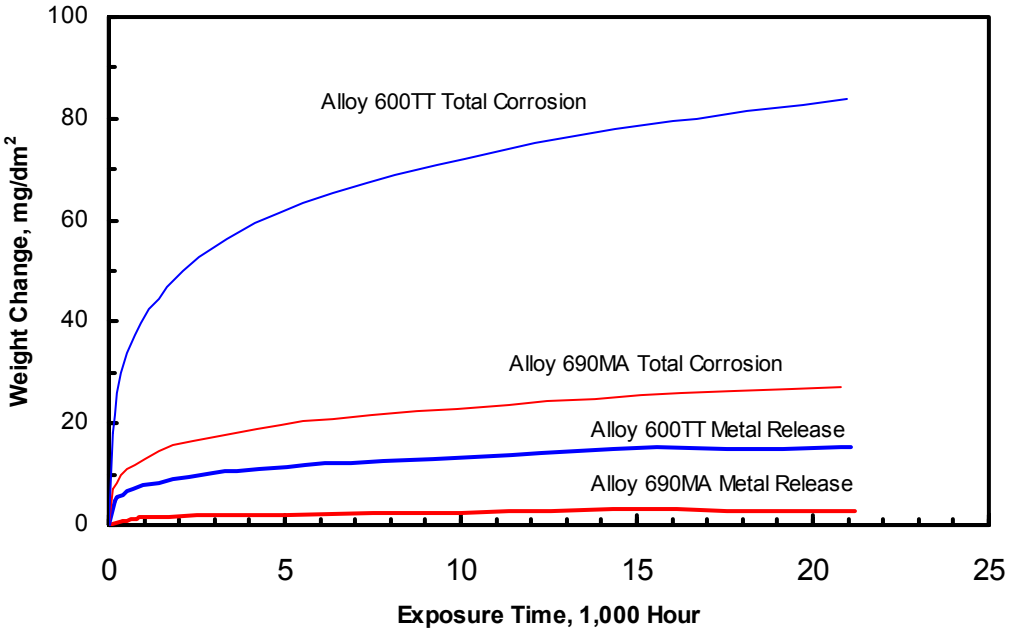

Figure 3-2 Comparison of general corrosion and material release to stream in simulated high temperature PWR primary water. After Ref. 11.

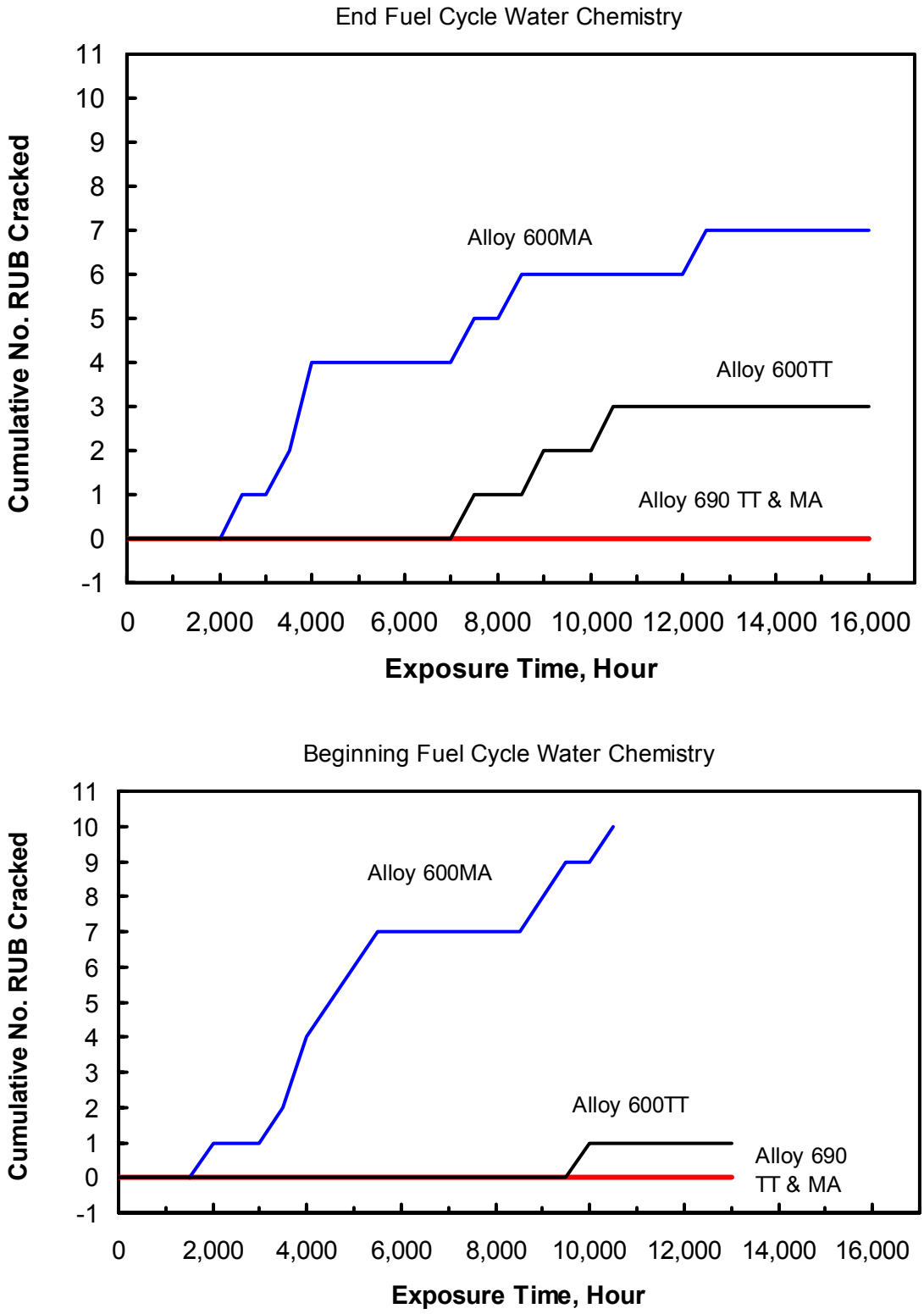

Figure 3-3 Cumulative number of RUB specimens cracked as function of test time by K. Smith. None of the Alloy 690 TT and MA cracked. The number of RUB specimens for each series is 10. [11]

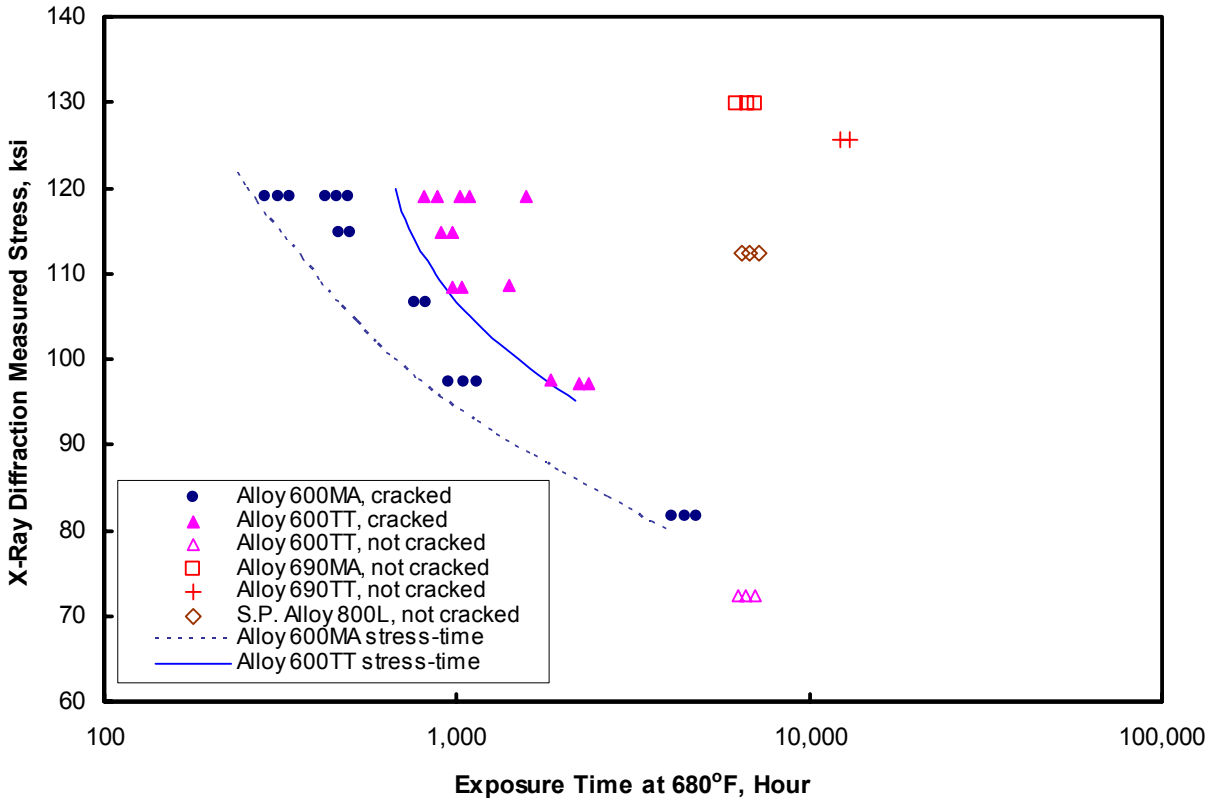

Figure 3-4 Testing of RUB Specimens in simulated primary water at 680°F (360°C). The stress was measured by X-ray diffraction. After Ref. 17.

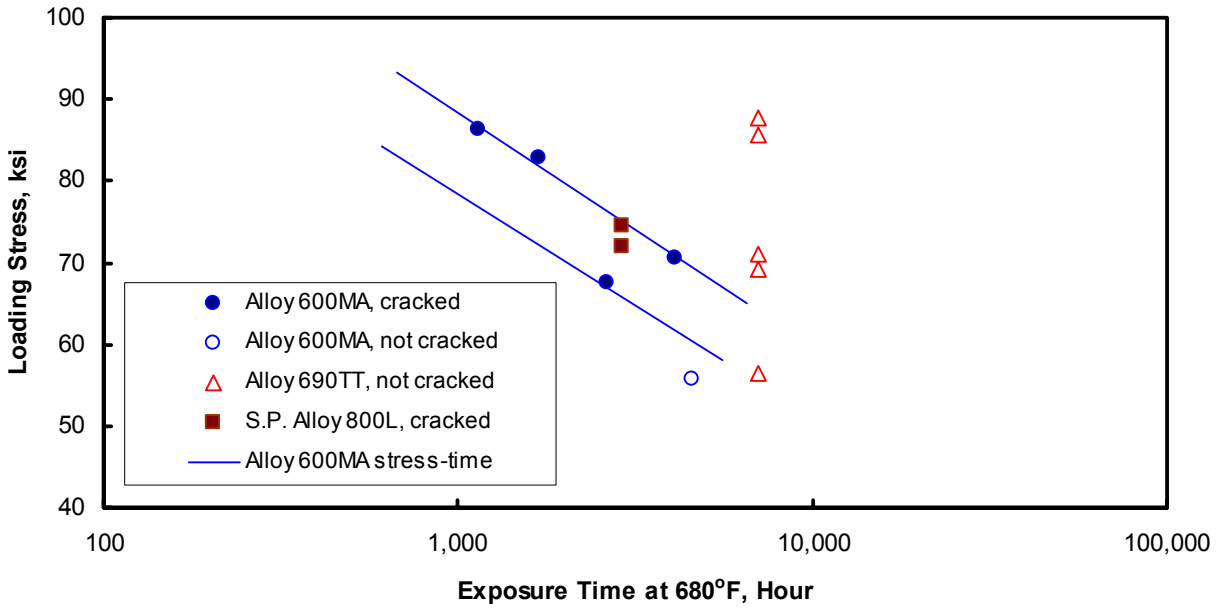

Figure 3-5 Constant load test (CLT) in simulated primary water at 680°F (360°C). The stress level was measured by X-ray diffraction. After Ref. 17.

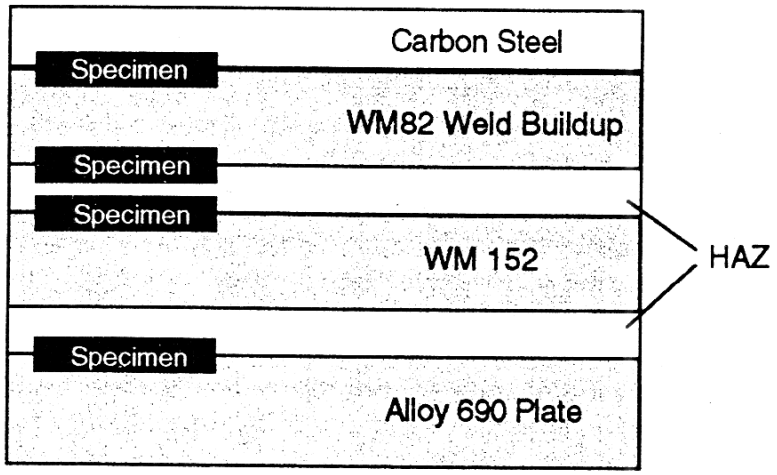

Figure 3-6 Schematic of weld mock-up block indicating the location and orientation of CERT specimens.[42]

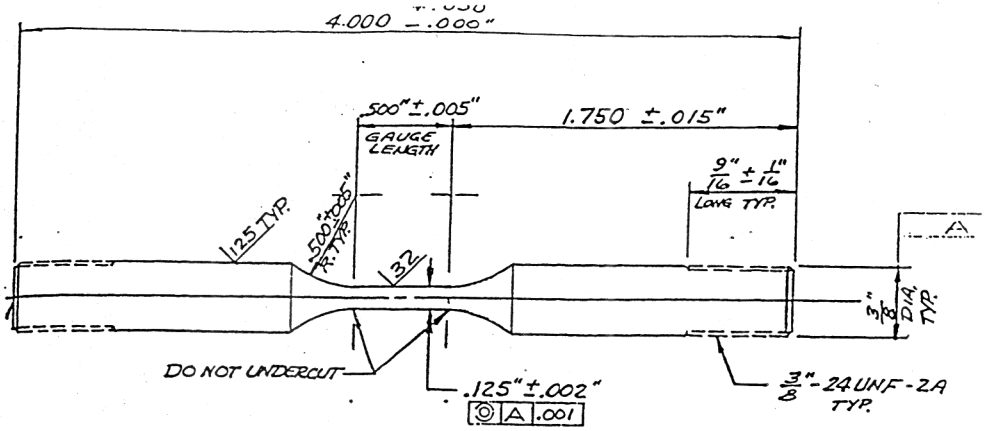

Figure 3-7 CERT specimen design.[42]

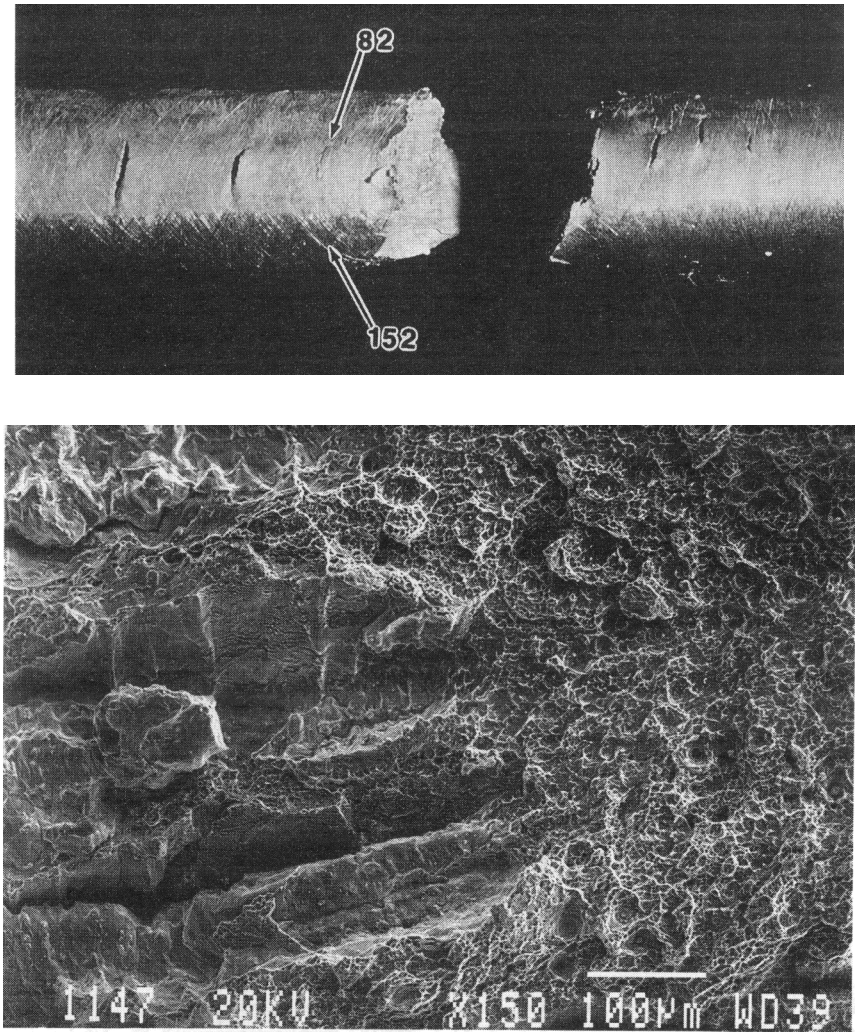

Figure 3-8 Above, Alloy 82/Alloy 152 CERT specimen surface after testing in water showed several cracks in Alloy 82. Below, SEM micrograph of the final fracture surface showed a ductile dimpled fracture surface in Alloy 152 and a brittle intergranular crack surface in Alloy 82.[42]

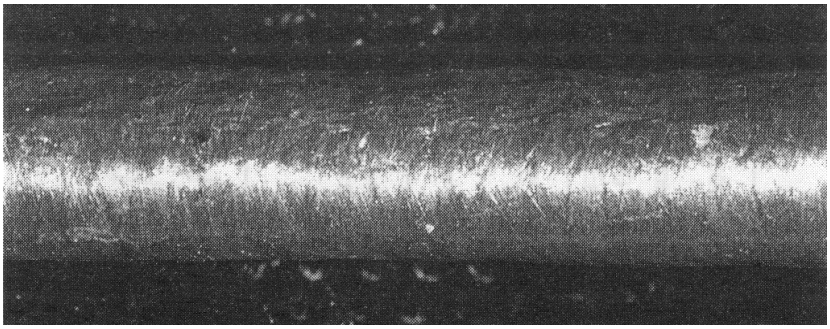

Figure 3-9 Alloy 152 CERT specimen surface after testing in water. No cracks were seen.[42]

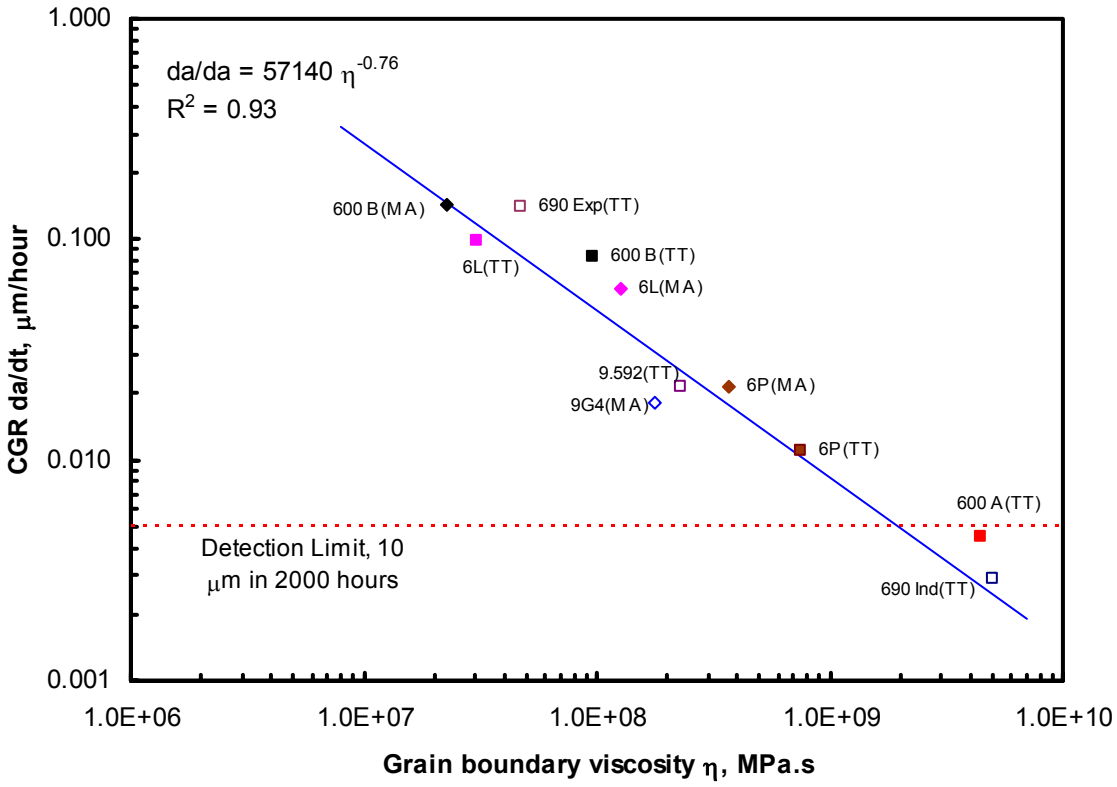

Figure 3-10 PWSCC crack growth rate (CGR) in CERT tests at 360°C (680°F) versus the grain boundary (creep) viscosity. After Figure 1 of Ref. 50.

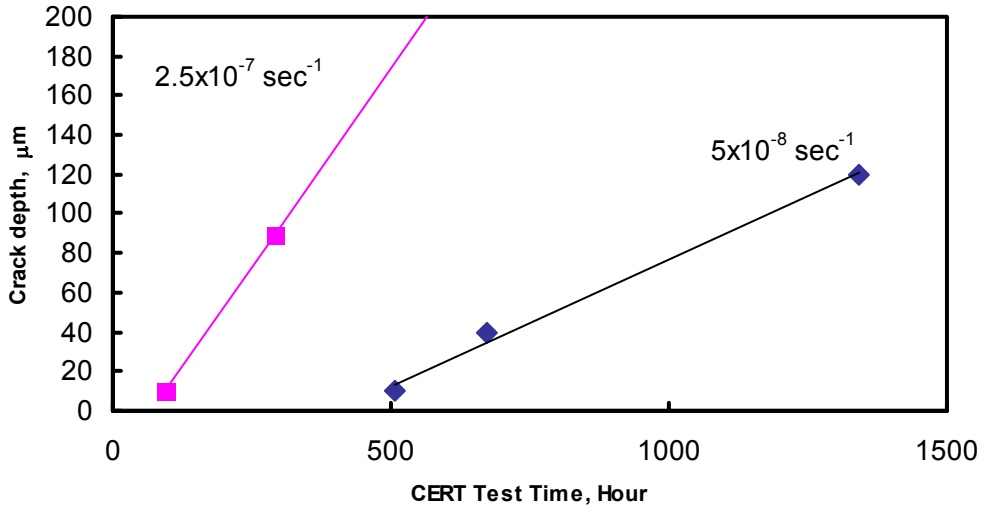

Figure 3-11 PWSCC crack depth in CERT test of Alloy 690 Exp 1 material at 360°C (680°F). After Figure 4 of Ref. 50.

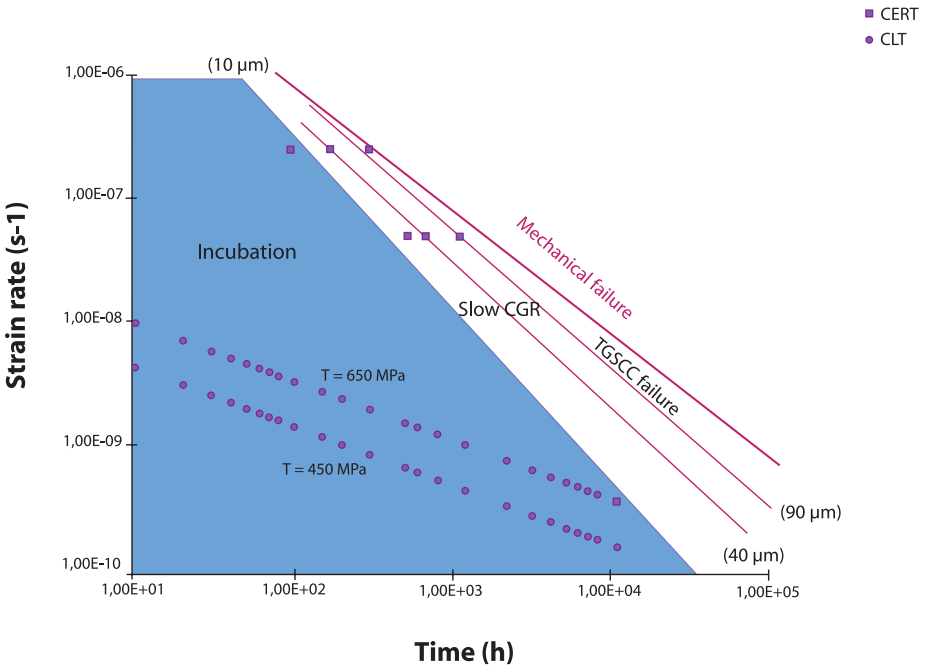

Figure 3-12 Fields of cracking for CERTs and constant load tests as a function of time and strain rate (Experimental alloy 690 in the as-received condition, hydrogenated PWR primary water at 360 °C).[50]

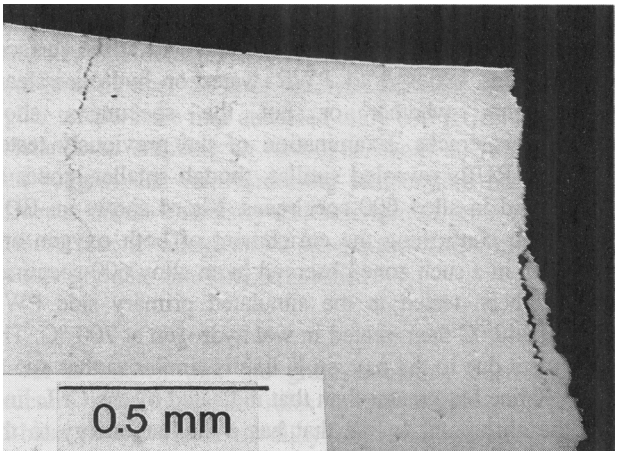

Figure 3-13 Cracks observed in Alloy 690 RUB specimen 5R (from Heat B) after 13,824 hours exposure in hydrogenated steam at 380°C (716°F).[52]

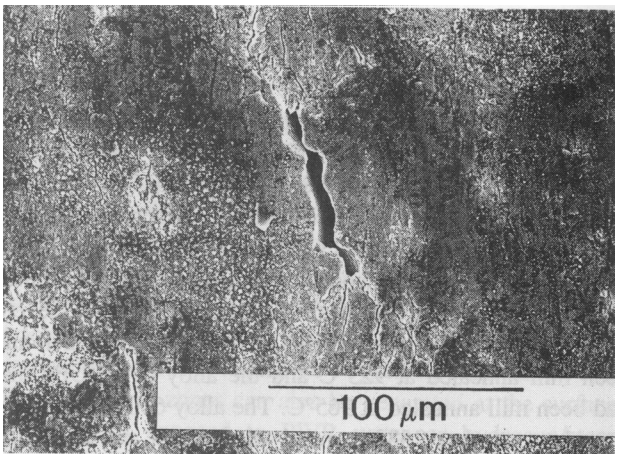

Figure 3-14 Short crack on the RUB specimen I.D. surface produced by flattening at room temperature. The RUB specimen was from Alloy 690 Heat A (the heat did not develop intergranular cracking) and had been exposed to hydrogenated steam at 380°C (716°F) for 13,824 hours.[52]

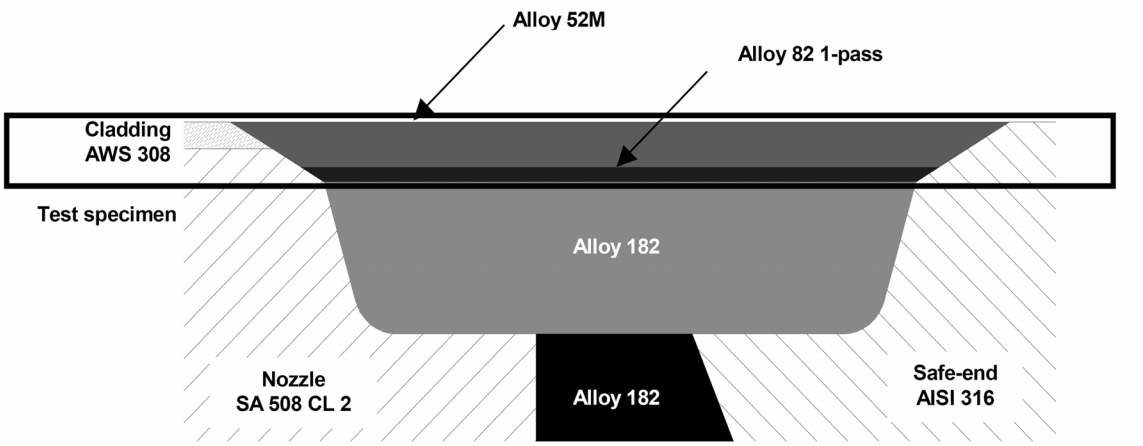

Figure 3-15 Sketch of Alloy 52M Weld Mock-up.[54]

Figure 3-16 Four-Point Bend Specimen Configuration.[54]

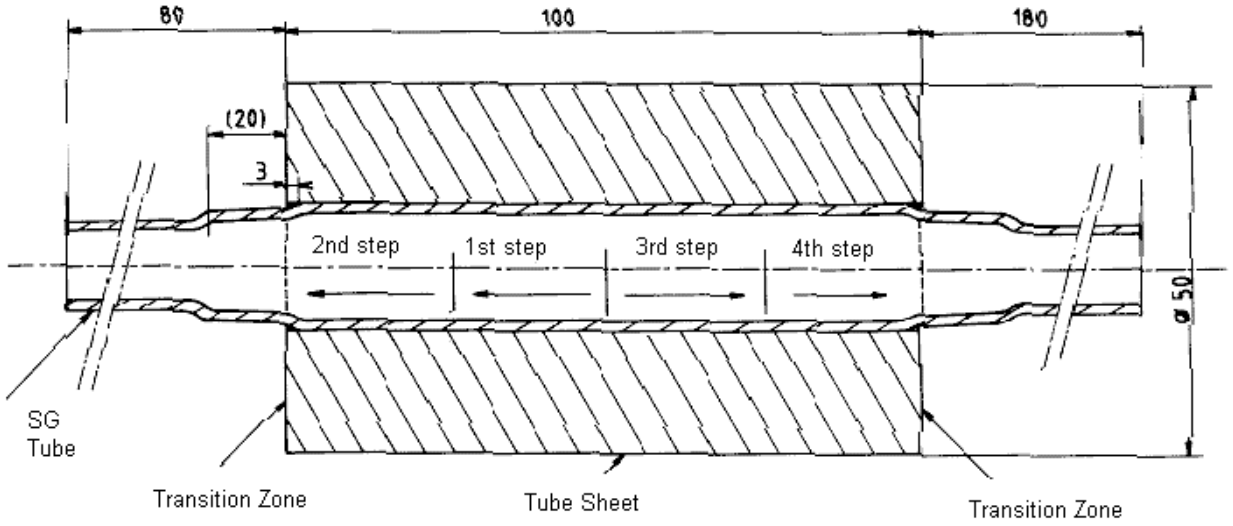

Figure 3-17 SG Tube Mock-Up [App. B]

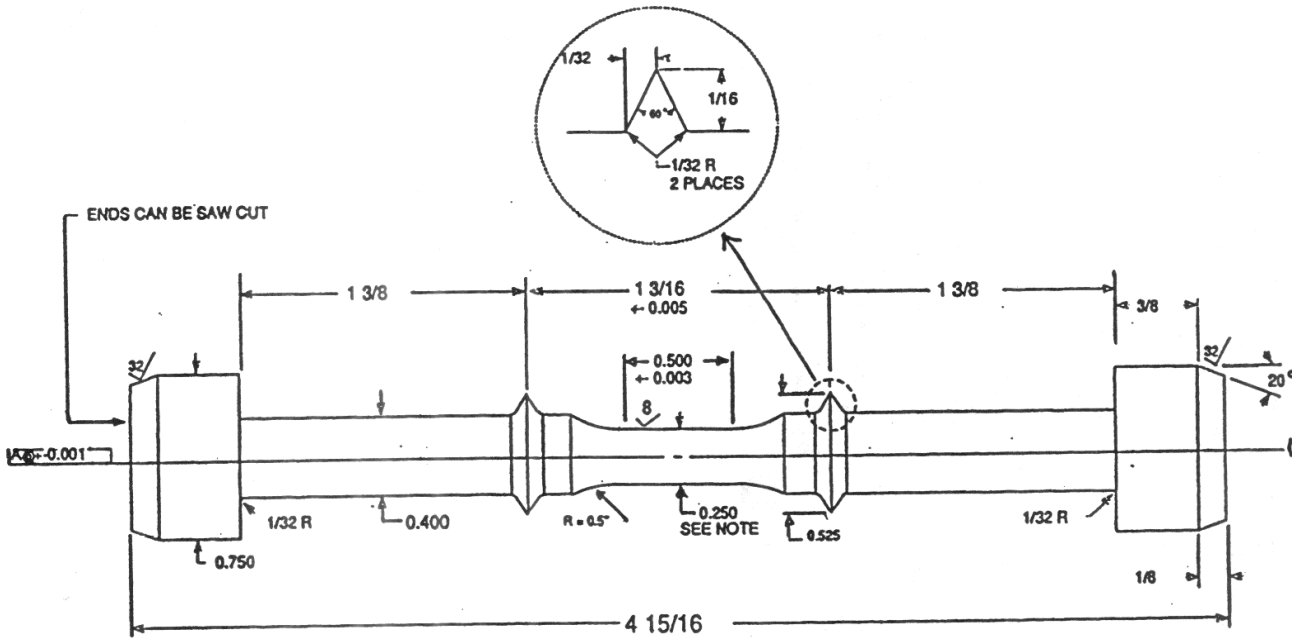

Figure 3-18 SG Low cycle fatigue specimen geometry.[42]

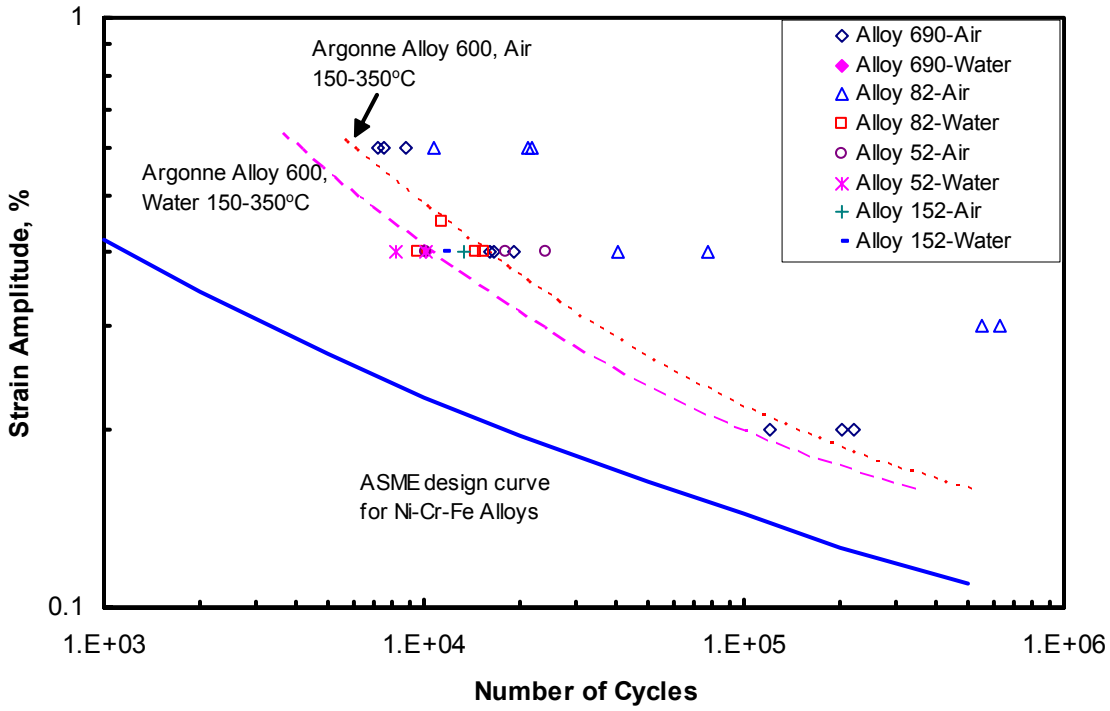

Figure 3-19 Plot of S/N fatigue properties of Alloy 690 and Alloys 52, 152, and 82 weld metals. Test were conducted at 600°F. After Ref. 42.

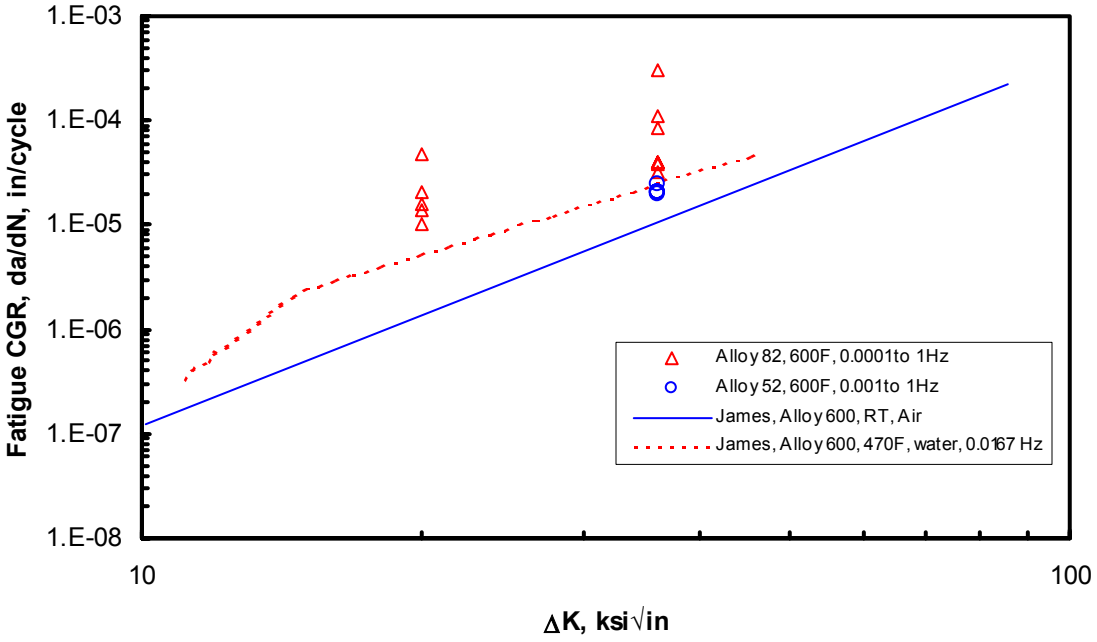

Figure 3-20 Plot of fatigue crack growth properties of Alloys 52 and 82 weld metals. After Ref. 42.

4 DISCUSSION

4.1 Alloy 690/152/52 Test Results

The first published stress corrosion cracking test results on Alloy 690 material in deaerated high temperature water containing 20 ppb or less dissolved O_2 were reported by Sedriks et al. of Inco in 1979.[9] No cracking was produced in any of the Alloy 690MA U-bend specimens fabricated after a maximum exposure of 10,000 hours at 680°F (360°C). Impressed by this test outcome, Sedriks et al. were among the first to suggest that, in high temperature deaerated water, Alloy 690 was effectively "immune" to the stress corrosion cracking that had been observed in all other high nickel alloys, including Alloy 600, tested in this environment. It is noted that a majority of the Alloy 600MA specimens in Sedricks' high temperature deaerated water tests did not develop cracking by the end of the tests, which may be an indication that the testing condition was not aggressive enough or the duration of the tests was not long enough. Airey investigated Alloy 600 PWSCC in pure hydrogenated water and primary water (containing boric acid and lithium).[63] The results showed that SCC initiation time was shorter in pure water than in primary water. Hence, a pure hydrogenated water environment can be considered slightly more aggressive than hydrogenated water containing boric acid and lithium when testing for susceptibility to PWSCC.

Since that time, laboratories in several countries have employed progressively more severe forms of stress corrosion testing under more and more aggressive conditions and to longer test durations in order to assess Alloy 690's resistance to PWSCC. Most of these studies have confirmed that Alloy 690 material has extremely high PWSCC resistance as no cracking was produced in the Alloy 690 specimens at the termination of testing in the vast majority of cases. Section 3.2 has reviewed 15 different studies of Alloy 690 PWSCC in high temperature deaerated water either with or without boric acid and lithium. Approximately 300 U-bend, Double U-bend, and constant load specimens from about 40 heats of Alloy 690 have been tested. The carbon content ranged from 0.001% to 0.065% and the heat treatment included MA, TT, and thermally aged conditions. Only one study included Alloy 52 weld metal and one study included Alloy 152 weld metal. The very few cases where cracking of Alloy 690 and Alloy 52 material were reported and the reasons why they are not representative of in-service PWR conditions are further discussed immediately below.

4.1.1 Single U-Bend Test in Saturated Hydrogen Water with B/Li

In 1987, Nakayama et al. reported results of Alloy 690 single U-bend tests in "saturated" hydrogenated water containing 1000 ppm boron and 2 ppm lithium at 330°C (626°F) for 3000 hours.[40] Slight intergranular cracking was detected in two out of the four Alloy 690 conditions tested. The maximum intergranular crack depth was 70 μm (0.0028") in the Alloy 690TT material with an aging treatment of 24 hours at 500°C (932°F) and 30 μm (0.0012") in the Alloy 690MA material with an aging treatment of 100 hours at 500°C (932°F). The Alloy 690 grain size was not reported, but the 70 μm maximum intergranular crack depth would correspond to

two grains deep for a typical grain size of ASTM No. 6.5. Hence, these cracks were shallow and more comparable to an intergranular attack (IGA) depth than to the much deeper PWSCC cracks routinely seen in Alloy 600 material.

In addition, SEM examinations revealed that the intergranular cracks in the Alloy 690TT specimen (70 μm max. depth) were at the tips of dislocation pile-ups. This indicates that the Alloy 690 intergranular cracking could be caused by mechanical strain from U-bending rather than caused by PWSCC. It is noteworthy that similar mechanically induced surface intergranular cracks have been observed in bent Alloy 690 and Alloy 52 specimens in several other studies. These observations and attributed causes are summarized in Table 4-1 for a side-by-side comparison. It is evident from these reports that Alloy 690 and Alloy 52 can be prone to develop surface defects or intergranular microfissuring induced by plastic straining from bending. Shallow surface modified layers from SG tubing fabrication processes are seemingly responsible for this mechanical cracking propensity. The CEA and EdF studies (see Section 3.2) showed that the plastic strain at the apex of the RUB is typically between 30 to 40%. This level of plastic straining approaches the room temperature ductility limit of Alloy 690. In addition, Alloy 690 has a slight drop in ductility when temperature is increased from room temperature to 600°F (see Figure 2-4). Alloy 690 also has a higher cold work hardening rate as shown in Figure 4-1, which plots the Vickers hardness number as a function of cold reduction percentage. Hence, an Alloy 690 surface is expected to be more sensitive to work hardening during the cold work fabrication steps. Any highly cold worked surface layer is likely to re-crystallize during thermal treatment and is observed to be more prone to developing surface defects compared to Alloy 600. However, the studies listed in Table 4-1 demonstrated that these surface defects or microfissures did not propagate (by PWSCC) by the end of the tests. Hence, it appears that the short IG cracking reported by Nakayama et al. was also due to strain applied during the specimen bending.

In addition to the factors discussed above, the Alloy 690 plate used to fabricate the U-bend specimens tested by Nakayama et al. was made from remelted (in a vacuum induction furnace) Alloy 690 SG tubing. Only the chemical compositions of the Alloy 690 SG tubing were reported. It is unclear whether the remelting might have caused changes in the Alloy 690 chemical composition. Interestingly, these Alloy 690 heats contained a rather high aluminum content of 0.39 or 0.40% (Note, aluminum is not specified in ASME Section II and is often unreported). A. Smith et al. reported that aluminum increases the Alloy 690 propensity to caustic IGA[32, 33] (also see Appendix C, Section C.2.2). Unfortunately, the Alloy 690 microstructure (cracked or not cracked) was not examined to confirm that the thermal treatment had produced intergranular carbide precipitations.

4.1.2 CERT Tests in Hydrogenated Water with or without B/Li

Other than the studies by Nakayama et al., and the CEA and EDF tests using high deformation U-bend or RUB specimens in which only mechanical surface intergranular cracking was detected, reports of intergranular cracking in deaerated water originate from CERT tests at strain rates on the order of 10^{-7} sec.$^{-1}$ or less. CERT tests are very severe tests for evaluating susceptibility of Alloy 600 or Alloy 690 to stress corrosion cracking. The specimens are loaded well past the original yield strength to maintain a continuous (constant) plastic strain rate, and are often continued until the specimens fail by ductile overload, if nothing else. Such continuous

plastic deformation situations are not encountered in nuclear power plants. Angeliu et al. produced intergranular cracking in a 0.002% carbon laboratory heat of Alloy 690 in deaerated water at 360°C (680°F) during CERT tests.[38, 39] Since the same small amount of intergranular cracking (2%) was also produced in argon, the intergranular cracking in the deaerated water should not be considered an indication of Alloy 690 susceptibility to PWSCC.

Other than the study by Angeliu et al, a study by CEA and EdF (Vaillant et al.) also reported Alloy 690 cracking during CERT tests. Vaillant et al. considered the CERT test as a test measuring the stress corrosion crack growth rate rather than crack initiation. Based on Figure 3-10, Vaillant et al. concluded that Alloy 690 material did not necessarily have a lower CGR than Alloy 600 material. Vaillant et al. suggested that the CGR obtained in the CERT tests is mainly dependent on the grain boundary carbide precipitation and the creep rate while the crack initiation time in the RUB tests was mainly a function of Cr contents. It is noted that the most susceptible Alloy 690 heat in this study was a pre-production heat and a heat treatment that gave rise to a very low density of grain boundary carbides.

Compact tension (CT) specimens, wedge opening load (WOL) specimens, double cantilever beam (DCB) specimens, or other forms of precracked specimens per ASTM E 399 or E 813 are commonly used for PWSCC CGR testing of Alloy 600 or Alloy 182 materials.[64, 65] During the CGR test, the specimen is loaded under plane strain condition to a predetermined stress intensity factor which does not increase during the test. On the other hand, the tensile load in CERT tests increases with test time to keep the elongation rate constant. Hence, CERT tests are very different from the typical CGR tests used for Alloy 600 and Alloy 182 materials. In addition, Alloy 690 is known to be susceptible to SCC in deaerated caustic water. The DCB tests conducted by Kawamura et al. showed (see Figure C-4) that, at a stress intensity up to 75 MPa√m, the CGR of Alloy 690TT is approximately 1/100th of Alloy 600MA in deaerated caustic water (see Appendix C, Section C.2). It is obvious from this literature review, that additional test data are needed to support the statement that "Alloy 690 does not necessarily have a lower CGR than Alloy 600 in primary water."

4.1.3 RUB Test in Hydrogenated Steam

In 1997, Sui et al. reported stress corrosion cracking of Alloy 690 specimens in hydrogenated steam at 380°C (716°F).[52, 53] Two RUB specimens from the same heat of Alloy 690 developed cracks between 12,600 and 13,824 hours of exposure at 716°F. Both heats of Alloy 690 had been thermally treated at ~715°C (1319°F) for 15 hours. However, the cracked Alloy 690 Heat B had an unusually (deliberately) low final mill anneal temperature compared to the un-cracked Alloy 690 Heat A (1769°F vs. 1958°F). The average grain size was 25 μm (ASTM No. 7.5) for Heat A and 15 μm (ASTM No. 9.0) or less for Heat B. The small grain size in Heat B is reflected in its higher room temperature yield strength. All the grain boundaries in Heat A had an almost continuous carbide coverage. The carbides were determined to be the $M_{23}C_6$ type rather than M_7C_3 by TEM. In contrast, Heat B was essentially free of intergranular carbides.

The cracked Alloy 690 heat, Heat B, also had a higher aluminum content (0.14%), which tends to result in a finer grain size and therefore a lower density of intergranular carbides. Interestingly, the Alloy 690 heats used by Nakayama et al. also contained a rather high aluminum content. The results

reported by Sui et al. show that Alloy 690 could be susceptible to IGSCC in a hydrogenated steam environment and potentially susceptible to PWSCC if the final mill anneal temperature is too low to produce intergranular carbide precipitation upon subsequent thermal heat treatment, or in the event of re-crystallization after thermal treatment. Because such a low temperature solution anneal heat treatment is prohibited by material specifications for Alloy 690 (or Alloy 600) for use in PWRs and the intergranular carbide precipitation must be verified by optical microscopy and/or SEM, cracking of the type seen by Sui et al. will be prevented. On the other hand, re-crystallization may be a detrimental factor to take into account for the heat affected zones of welds. In any event, the times to failure at 380°C (716°F) reported by Sui et al are such that when extrapolated to normal PWR operating temperatures using an Arrhenius relationship and a standard value of the activation energy for PWSCC the predicted lives (equivalent to 98 EFPYs at 600°F based on the 50 kcal/mole PWSCC activation energy commonly used for Alloy 600, see Table 4-3) would be well in excess of current expectations for plant life extension. Nevertheless, this apparent susceptibility induced by the absence of grain boundary carbides is a potential weakness of Alloy 690 that requires further investigation.

4.2 Weibull and Weibayes Analyses of the Test Results

The results of the laboratory tests reviewed in Section 3.2 are examined to obtain a quantitative or semi-quantitative assessment of Alloy 690's resistance to PWSCC relative to Alloy 600. This is desirable for developing a statistically-based estimation of a hypothetical PWSCC event in Alloy 690 component items that can be used in selecting and justifying an inspection method for Alloy 690 component items.

The two-parameter Weibull distribution of Eq. 4-1 is by far the most widely used distribution for stress corrosion cracking analysis.[66]

$$F(t) = 1 - e^{-\left(\frac{t}{\theta}\right)^{\beta}} \qquad \textbf{(Eq. 4-1)}$$

where: F(t) = the cumulative fraction of cracking by time (t).
θ = the characteristic time (scale parameter) equal to the time to a 63.2% cumulative fraction of cracking.
β = slope or shape parameter
e = 2.71828, the base for natural logarithms.

The significance of β is briefly summarized below:

$\beta < 1$	Implies infant mortality, failure rate decrease with time.
$\beta = 1$	Implies random failure.
$1 < \beta < 4$	Implies early wear out.
$\beta > 4$	Implies old age and rapid wear out. A steeper β means less material variation or tighter quality control. A steeper β means subsequent failures will occur quickly after the first failure.

Weibull analysis has been used to analyze the failures of the Alloy 600 control specimens in the studies reviewed in Section 3.2. If sufficient data were reported or available, a best-fit regression analysis has been performed to determine the Weibull characteristic time (θ) and slope (β).

In addition to Weibull analysis for the Alloy 600 control specimens, a Weibayes analysis (an estimated Weibull) has been used for the Alloy 690 specimens that did not develop cracking by the end of the test period. In the Weibayes method, the slope is assumed to be the same as that from the Alloy 600 analysis. The Alloy 690 specimen characteristic time θ is estimated by Eq. 4-2.[66]

$$\theta = \left[\sum_{i=1}^{N} \frac{t_i^{\beta}}{r} \right]^{1/\beta} \qquad \textbf{(Eq. 4-2)}$$

where: β = the slope or shape parameter from Alloy 600.
t_i = test time of each Alloy 690 specimen tested.
N = total number of Alloy 690 specimens tested.
r = number of Alloy 690 specimens cracked.

As no constant deformation (deflection) or constant load Alloy 690 specimen developed SCC cracks by the end of the test period (except in one study in hydrogenated steam at 380°C (716°F), it is conservatively assumed that the first (i.e., $r = 1$) Alloy 690 specimen failure could occur immediately should the test continue. The confidence level that the true Alloy 690 Weibull line lies to the right of the Weibayes line is 63%. The failure number r can be set to produce any level of confidence desired. For example, Weibest uses 0.693 for r to produce a confidence level of 50%, which is less conservative than the 63% confidence level used by Weibayes.

Figure 4-2 is the Weibull plot of the Alloy 600 RUB test results at 680°F reported by K. Smith et al. The differences in the water chemistry used (beginning-of-fuel-cycle vs. end-of-fuel-cycle) have little impact on the Alloy 600 (one heat) RUB cracking compared to the heat treatment (see Figure 3-3). Hence, the Alloy 600 RUB cracking data in the two primary water environments are combined in Figure 4-2. The Alloy 690 Weibayes characteristic life is calculated based on a total population of 40 RUB specimens from three different heats in either the MA or TT condition since there was no failure of any Alloy 690 RUB specimens. The Alloy 690 Weibayes line in Figure 4-2 assumes a slope of 5.0 (β = 5.0).

Figure 4-3 and Figure 4-4 are the Weibull plots of the Alloy 600 RUB results at 689°F reported by Norring et al. Figure 4-3 plots Alloy 600 RUB results of different heats of SG tubing while Figure 4-4 plots the Alloy 600 RUB results of EPRI special production tubes. Figure 4-4 shows that the Alloy 600MA annealed at 1875°F has a higher PWSCC resistance than the Alloy 600MA annealed at 1700°F. Figure 4-5 compares the influence of the SG tubing diameter on the time to cracking. Even though the RUBs were from the same heats, the 7/8" dia. RUB developed cracking much earlier than the 3/4" dia. RUB. This difference in time to cracking was attributed to different stress levels after the reverse bending of different diameter tubing.[35] However, no stress calculations or measurements were reported. The Alloy 690 Weibayes characteristic life is calculated based on a total population of 67 RUB specimens from three different heats of Alloy 690. These specimens were heat treated in the MA or TT condition with additional variations in heat treatment temperature and duration. None of the 67 Alloy 690 RUB specimens developed cracking after 20,500 to 33,000

hours of exposure. The Alloy 690 Weibayes line in Figure 4-3, Figure 4-4, and Figure 4-5 assumes a slope of 5.0 ($\beta = 5.0$).

Figure 4-6(a) and Figure 4-6(b) are the Weibull plots of Alloy 600MA constant load test (CLT) specimens at 644°F in four primary water chemistries reported by Ogawa et al. Details of the Alloy 600TT CLT specimens tested at 644°F were not reported. The plots in Figure 4-6 show that a slight variation in primary water condition has little effect on the Alloy 600MA cracking behavior. Hence, the Alloy 600MA CLT (644°F) data are combined and re-plotted in Figure 4-7. None of the Alloy 690TT CLT specimens tested at 680°F or of the Alloy 600MA and TT CLT specimens tested at 608°F cracked. The Alloy 690 Weibayes characteristic life is calculated based on a total population of 20 CLT specimens tested in the four variations of primary water chemistry. The Alloy 690 (680°F) and Alloy 600 (608°F) Weibayes lines in Figure 4-7 assume a slope of 5.0 ($\beta = 5.0$).

In addition to the CLT tests, Ogawa conducted RUB tests in the same primary water conditions. Examination of Table 3-33 showed that variation of the primary water did not have a significant impact on the Alloy 600 RUB specimens cracking. Hence, the RUB test data from the four primary water chemistries are combined before applying the Weibull analysis. Figure 4-8 and Figure 4-9 plot the results of the RUB specimens prestrained to 0%, 5%, 10%, 15%, and 20% and tested at 608°F for the Alloy 600MA and the Alloy 600TT, respectively. Figure 4-10 compares the results of 20% prestrained RUB specimens from the Alloy 690TT, the Alloy 600TT, and the Alloy 600MA materials. None of the Alloy 690TT specimens tested at the higher temperature of 680°F developed cracking after 10,000 hours of exposure. The Alloy 690TT Weibayes characteristic life is calculated based on a total population of 40 RUB specimens. The Alloy 690 Weibayes line assumes a slope of 5.0 ($\beta = 5.0$).

The RUB tests in primary water at 680°F reported by Vaillant et al. are evaluated with Weibull analysis. The RUB specimens from different heats of Alloy 600 are separated into the MA and TT conditions The results are plotted in Figure 4-11. None of the Alloy 690TT and Alloy 690MA specimens developed cracking after up to 54,000 hours of exposure. The Alloy 690 Weibayes characteristic life is calculated based on a combined TT and MA population of 4 RUB specimens listed in the report. The Alloy 690 Weibayes line assumes a slope of 5.0 ($\beta = 5.0$).

The results of the SG mockups tested in deaerated, hydrogenated water at 680°F by Framatome ANP, France are plotted in Figure 4-12. None of the Alloy 690TT mockups developed any cracking after 100,000 hours of exposure. The Alloy 690 Weibayes line assumes a slope of 5.0 ($\beta = 5.0$).

The results of the Weibull and Weibayes analyses are used in the next section for estimating the improvement factor (IF_R) of Alloy 690 relative to the Alloy 600 in PWR primary water conditions.

4.3 Improvement Factor by Weibull Analysis

The Weibull parameters of Alloy 600 materials tested with Alloy 690 are listed in Table 4-2. Using the Weibull analysis, the relative improvement factor, IF_R, can be defined by Eq. 4-3.

$$IF_R = \frac{Weibayes\,(r=1)\,\theta, Alloy\,690}{Weibull\,\theta, Alloy\ 600} \qquad \textbf{(Eq. 4-3)}$$

Hence, IF_R is the ratio of the time to a 63.2% cumulative fraction of failure between the Alloy 690 and the Alloy 600 specimens being tested. Transformation of Eq. 4-1 yields Eq. 4-4, which in turn produces Eq. 4-5.

$$t = \theta\left[\frac{1}{1-F(t)}\right]^{\left(\frac{1}{\beta}\right)} \qquad \textbf{(Eq. 4-4)}$$

$$\left.\frac{t_{690}}{t_{600}}\right|_{to\ a\ given\ F(t)} = \frac{\theta_{690}}{\theta_{600}} \qquad \textbf{(Eq. 4-5)}$$

Eq. 4-5 shows that, if the Alloy 690 Weibayes line assumes the same Weibull distribution slope (β) as for the Alloy 600 (either TT or MA condition), the IF_R to any cumulative fraction of cracking would be a constant. However, the slope of Alloy 690, although unknown due to a lack of cracking in the tests, may not vary as much as seen in Alloy 600 materials. Assuming a small Weibull slope value for Alloy 690 can result in a higher Weibayes θ (hence a higher IF_R), making the IF_R less conservative. A review of the Alloy 600 Weibull plots indicates that the slope increases with increasing cracking resistance, i.e., Alloy 600TT tend to have a higher β than Alloy 600MA in the same investigation. However, significant variation exists in PWSCC susceptibility of different heats of Alloy 600. The variation in the Alloy 600 material can be seen in Figure 4-13, which plots the Weibull θ vs. β listed in Table 4-2 except the data in Figure 4-5 which are derived from the data in Figure 4-3 and Figure 4-4. The average β for Alloy 600MA is 4.12 while the average β for Alloy 600TT is 3.28. Hence, the slope for the Alloy 690 Weibayes line arbitrarily set to 5.0 is higher than the average value β for Alloy 600. This introduces additional conservatism in the calculation of the Alloy 690 Weibayes θ. No differentiation is made in this case between Alloy 690 in the MA condition and in the TT condition because neither has cracked in the hydrogenated, deaerated water. Therefore, the improvement factor, IF_R, is redefined as

$$IF_R = \frac{Weibayes\,(r=1, \beta=5.0)\,\theta, Alloy\,690}{Weibull\,\theta, Alloy\ 600} \qquad \textbf{(Eq. 4-6)}$$

The resulting IF_R values are listed in Table 4-2. The Alloy 600 test data shown in Figure 4-7 and Figure 4-10 are normalized per the Arrhenius relationship of Eq. 4-7 to 680°F, the Alloy 690 test temperature in the same study. Overall, the average IF_R of Alloy 690 listed in Table 4-2 is 26.5 relative to Alloy 600MA and 13.3 relative to Alloy 600TT.

$$\frac{t}{t_{ref}} \propto \exp\left[\frac{Q_i}{R}\left(\frac{1}{T}-\frac{1}{T_{ref}}\right)\right] \qquad \textbf{(Eq. 4-7)}$$

where Q_i = 50 kcal/mole.

4.4 Improvement Factor with Minimum Alloy 600 Crack Time

Unfortunately, not all the studies reviewed here had either obtained or reported sufficient data to allow a Weibull or Weibayes analysis. In order to include these data, an alternative way to calculate the improvement factor using Eq. 4-8 can be used:

$$IF_R = \frac{Test\ Time\ of\ Alloy\ 690}{Time\ to\ first\ cracking\ in\ Alloy\ 600} \qquad \textbf{(Eq. 4-8)}$$

Here, the time to first cracking in Alloy 600 refers to the time when the first failure in the Alloy 600 control specimens was observed. The following factors are considered for the IF_R values determined from Eq. 4-8.

1. The PWSCC Alloy 600 resistance has been observed to vary greatly and depend on several factors. Some Alloy 600 TT specimens like the Alloy 690 specimens did not develop any cracking by the end of the test duration. Hence, the calculated IF_R is relative to Alloy 600 materials that are highly susceptible to PWSCC, such as Alloy 600MA with low mill anneal temperature and a high degree of intragranular carbides. The IF_R so calculated would be a more realistic improvement factor, somewhat less conservative than that by Eq. 4-6.

2. The IF_R calculated per Eq. 4-8 is still considered conservative because the actual cracking time of the Alloy 600 specimens was less than the accumulated test time at inspection intervals. Often, the first Alloy 600 specimen cracking was observed at the first scheduled inspection interval. In addition, the actual cracking time of Alloy 690 specimens can be much longer than the test duration, if they ever develop cracking at all.

The resulting IF_R values calculated by Eq. 4-8 are listed in Table 4-3 and Table 4-4. In addition, the equivalent EFPYs at 600°F for each test is also determined per Eq. 4-8. This normalization has no affect on the IF_R per Eq. 4-8 except when the Alloy 600 and Alloy 690 specimens in the same study were tested at different temperatures. The average IF_R of Alloy 690 relative to Alloy 600 in Table 4-3 and Table 4-4 per Eq. 4-8 is 27.1, which is about the same as the 26.5 relative to Alloy 600MA from the Weibull analysis per Eq. 4-6. Figure 4-14 plots the duration of the test for Alloy 690 vs. the IF_R listed in Table 4-3 and Table 4-4. The IF_R is seen to increase with increasing test time, indicating that the IF_R is limited by the test duration.

4.5 Alloy 690/152/52 Material Operating Experience in PWRs

Over the past thirty years, PWSCC of Alloy 600/182/82 material has become an increasingly significant problem in PWRs. As shown in Table 1-1, PWSCC was first detected in Alloy 600 steam generator tubing in 1971. The first report of PWSCC in a pressure boundary penetration was the leak from a pressurizer level nozzle in 1986. Both of these instances occurred after approximately 2 years of service. These initial reports have subsequently been followed by similar occurrences at other PWRs using Alloy 600/182/82 materials for the same component

items. These problems have led to significantly increased inspection efforts, have contributed to the early replacement of many steam generators, have led to long forced outages to repair problems at some units, and have resulted in the expenditure of a significant amount of engineering effort to determine the root cause of the problems, develop inspection and repair methods, and develop strategic plans to manage the problems.

In addition to the initial occurrences of Alloy 600/182/82 PWSCC given in Table 1-1, the following steam generator tubing failures are highlighted:

1. Cracking of Obrigheim steam generator tubes (1971) after approximately 2 years of service.[67] This was the first instance of PWSCC of Alloy 600MA.

2. Cracking of Kori-2 steam generator tubes (1986) after nearly 3 years of service. This was the first occurrence of PWSCC in a steam generator fabricated with Alloy 600TT tubing.[68]

3. Cracking of steam generator mechanical tube plug at North Anna 1 (1989) after just over 3 years of service.[69] This was the first occurrence of PWSCC of Alloy 600TT plugging material.

4. Cracking was identified at Oconee Nuclear Station-1 (1995) after about 8 years of operation.[68] This was the first instance of PWSCC in stress relieved OTSG (Once-Through Steam Generator) tubing.

It seems quite clear that a PWR steam generator is a very demanding material application, involving high temperature, high stress and strain at roll transitions and at tight U-bends, and a primary water environment that facilitates stress corrosion cracking (at a corrosion potential close to the equilibrium potential of the Ni/NiO equilibrium). In addition, the number of SG tubes per PWR varies between 8,000 and 30,000. Hence, steam generator tubing is statistically favored to be the first component item to show PWSCC. Operating experience indicates that a PWSCC-susceptible Alloy 600 material (low temperature mill annealed) cracks in approximately 2 years of operation in this application. Even improved Alloy 600 materials (high temperature mill annealed and thermally treated or high temperature mill annealed and stress relieved) also may be susceptible to cracking in as little as 3 to 8 years of operation.

As shown in Section 3, Alloy 690 material appears to be highly resistant to PWSCC when laboratory tested in conditions where Alloy 600 material tested under the same conditions routinely showed comparatively rapid cracking. Also, as shown in Table 4-5, a number of steam generators manufactured with Alloy 690 tubing material have been in service for significant times without crack indications due to PWSCC. The oldest steam generators with Alloy 690 tubing have been operating for approximately 14 years with no reported signs of PWSCC degradation. There are now 73 PWR units worldwide, with 2-4 steam generators per unit, operating with Alloy 690 steam generator tubing (as of December 2003).

Table 4-6 provides a listing of both replacement and original equipment component items utilizing Alloy 690/152/52 materials. The replacement pressurizer heater sleeves at Calvert

Cliffs-2 have been in operation for about 12 years and visual inspections have not identified any problems to date. In addition, a complete NDE inspection of the Bugey-3 replacement RV head CRDM nozzles was performed in 2002 (after 10 years of service), which did not reveal any defects.[70]

Currently, there has been only one known instance of field repairs with Alloy 152/52 that later showed to be inadequate. In the fall of 2001, three Alloy 600 CRDM nozzles (#51, #62, and #63) on the North Anna Unit 2 reactor vessel head showed evidence of leakage. Subsequent NDE identified crack-like indications in the vicinity of the Alloy 182 butter and Alloy 82 J-groove weld of the three CRDM nozzles. A boat sample was removed from the Alloy 182 butter and Alloy 82 J-groove weld interface region of CRDM nozzle #62. The boat sample showed that cracking was confined to the Alloy 182 butter region. The root cause evaluation concluded that the cracking most likely originated from hot cracking of the Alloy 182 butter during plant construction. PWSCC probably contributed to, but was not believed to be a primary cause of the cracking. The three CRDM nozzles were repaired by an Alloy 52 overlay weld (with at least two layers of Alloy 52) to isolate the original Alloy 182/82 surface from the primary water environment.[71] The overlay of the CRDM J-groove weld at North Anna Unit 2 in 2001 was the first field application of this repair technique to CRDM nozzles. Post repair dye penetrant examination results were acceptable. During North Anna Unit 2's 2002 Fall refueling outage, the three CRDM nozzles repaired in 2001 were re-examined by dye penetrant examinations, which revealed the new indications.

An evaluation concluded that the new indications were attributable to two causes. The first cause was the surface flapping performed prior to the dye penetrant examinations in 2002. The second cause was that the Alloy 52 weld overlay in the 2001 repair did not cover the entire exposed Alloy 182/82 surface. As part of the evaluation, a boat sample was removed from CRDM nozzle #51 and examined in a hot cell. Figure 4-15 shows a sketch of the radial location of the boat sample relative to the J-groove weld, butter, and stainless steel cladding. The boat sample's long axis was tangential to the circular Alloy 52 weld overlay. Figure 4-15 also shows the weld metals determined by EDS on the as-received surface. Examination of the boat sample revealed cracking (also termed fissuring) associated exclusively with the interface between the weld beads, where the underlying Alloy 182/82 weld metal was susceptible to reheat cracking as a result of excessive dilution (>30%). It was found that the reheat cracking in the Alloy 182/82 propagated into the thin layer of Alloy 52 at the edge of the repair weld bead. However, no hot cracking was observed in the Alloy 52 weld overlay on top of the Type 308 stainless steel cladding, where the Alloy 52 dilution was limited. It was concluded that none of the cracking in the boat sample was due to environmental conditions and the embedded flaw repair method is acceptable if the entire J-groove weld and buttering is covered by the Alloy 52 weld overlay.[72] Therefore, it is concluded that the indications found in or near the Alloy 52 weld overlay to the CRDM nozzle J-groove welds at North Anna Unit 2 were not caused by PWSCC, and hence are not an indication of Alloy 52 susceptibility to PWSCC.

Obviously a number of additional improvements to fabrication practice have also been made to reduce the likelihood of initiating PWSCC with Alloy 690/152/52 materials. These include optimizing component item construction practices, optimizing material melting and manufacturing practices, and reducing residual stresses. However, the excellent operating

experience to date with Alloy 690/152/52 materials provides reasonable assurance that these alloys are very highly resistant to PWSCC.

Table 4-1 Summary of Surface IG Cracking in Alloy 690 and Alloy 52 Specimens

Ref.	Matl.	Description of Surface IG Cracks and Defects	Attributed Cause
Miglin, [88] 1986	Alloy 690MA&TT SG Tubing	Longitudinal shallow and blunt defects were found on the I.D. surface of the Alloy 690 RUB apex. These defects were not typical of IGSCC. Metallographic examinations showed that some of these defects appeared to be like mechanical grooves while others appeared to be separation along the grain boundaries. No evidence of further IGSCC cracking emanating from the base of these defects were found. SEM examinations of archive Alloy 690 RUB specimens found similar longitudinal defects, but they were shorter in length than those detected after the AVT autoclave exposure (0.1 to 0.35 mm long in archive Alloy 690 RUB vs. ~1.0 mm in Alloy 690 RUB after the AVT exposure). The less strained leg portions of the RUB specimens were free from these defects.	The growth in length observed was due to an opening process of closed or partially closed defects. During the high temperature exposure, the surface oxide growth (in the defects) would enhance an opening process by a wedging effect to give an appearance of longitudinal growth.
Sui, [52] 1997	Alloy 690TT SG Tubing	Short IG cracks (see Figure 3-14, depth not reported) on the RUB specimen I.D. surface produced by flattening at room temperature. The RUB specimen had been exposed to hydrogenated steam at 380°C (716°F) for 13,824 hours.	Embrittlement of grain boundaries near the surface from the exposure.
Vaillant, [49] 1999	Alloy 690TT SG Tubing	Shallow cracks (10 µm or 0.0004" deep) appeared at the apex of the Alloy 690 RUB specimens after bending, but before immersion inside the autoclave. So the stress measured in the Alloy 690 RUB specimen apex surface was not well-defined. However, the stress level measured after removing the 10 µm deep crack was the same as for the Alloy 600 RUB specimens. Hence, the stress at the tip of the short crack caused by bending is at least as high as the apex surface stress of the Alloy 600 RUB specimens. No crack growth observed in the Alloy 690 RUB specimens during the testing.	Cracking was due to bending.
Framatome, France 2003 [App. B]	Alloy 690 TT, SG Tubing	IG cracks on the inner tube surface in the transition zones of the kiss rolling (1.5 mm and their width 2 µm, see Appendix B for details). Examination of the flattened half tube revealed the presence of many microcracks, some of the opened microcracks corresponded to those which were also observed before flattening but numerous others were new ones opened or created during the mechanical flattening operation. This type of flaw was also observed on parts of the tube which were not rolled, that is remote from the rolled zone. The crack depth was always limited to the thickness of the perturbed surface layer on the internal surface of the tube (about 10 µm thick in this case). These microcracks were intergranular but did not propagate in the tube during exposure to hydrogenated water at 360°C during 60,000 hours exposure.	Strain induced by rolling and are limited to the hard perturbed surface layer already present on the inside surface of the tube in the as-received condition.
Jacko [54]	Alloy 52M	After 1343 hours, short (0.16 and 0.20-mm in length) indications were observed on the surface of the two high-strain Alloy 52M four-point bend specimens. These indications did not change in subsequent exposures.	Metallographic cross-sectioning indicated these to be shallow hot-microfissures that were present from the weld preparation, but were not clearly identified in the earlier examinations.

Table 4-2 Weibull Analysis for Alloy 600 Tested With Alloy 690

Figure	Matl.	Heat	Test	Environ.	Temp (°F)	Weibull, θ (hour)	Weibull slope, β [a]	IF_R [b]
Figure 4-2	690MA&TT	Pre-series 3 Heats	RUB	Deaerated water + B + Li	680	30,950	5.00	N/A
Figure 4-2	600MA	No info	RUB	Deaerated water + B + Li	680	8,112	1.96	3.8
Figure 4-2	600TT	No info	RUB	Deaerated water + B + Li	680	14,539	5.08	2.1
Figure 4-3 Figure 4-4 Figure 4-5	690MA&TT	Many heats	RUB	Deaerated water	689	59,748	5.00	N/A
Figure 4-3	600	PWR Ringhals 2, 7/8" dia.	RUB	Deaerated water	689	910	1.74	65.7
Figure 4-3	600MA	Alloy 600MA, 7/8" dia.	RUB	Deaerated water	689	1,440	3.91	41.5
Figure 4-3	600	PWR Ringhals 4, ¾" dia.	RUB	Deaerated water	689	4,590	2.47	13.0
Figure 4-3	600	PWR Ringhals 3, ¾" dia.	RUB	Deaerated water	689	5,620	6.05	10.6
Figure 4-3	600TT	Alloy 600TT, ¾" dia	RUB	Deaerated water	689	8,060	5.52	7.4
Figure 4-4	600MA	EPRI Provided B&WTP, 1700°F	RUB	Deaerated water	689	740	4.53	80.7
Figure 4-4	600MA	EPRI Provided Huntington, 1700°F	RUB	Deaerated water	689	2,480	10.43	24.1
Figure 4-4	600MA	EPRI Provided Sandvik, 1700°F	RUB	Deaerated water	689	3,490	5.77	17.1
Figure 4-4	600MA	EPRI Provided B&WTP, 1875°F	RUB	Deaerated water	689	10,260	5.48	5.8
Figure 4-4	600MA	EPRI Provided Sandvik,1875°F	RUB	Deaerated water	689	10,990	5.27	5.4
Figure 4-5	600	7/8" dia., Ringhals 2, NX 1991, NX 2650	RUB	Deaerated water	689	1,118	1.91	53.4
Figure 4-5	600	3/4" dia. Ringhals 3 and 4	RUB	Deaerated water	689	5,397	3.05	11.1
Figure 4-7	690MA&TT	One heat	CLT	Deaerated water + B + Li	680	18,206	5.00	N/A
Figure 4-7	600MA	One heat	CLT	Deaerated water + B + Li	644	5,358	5.91	--
					680	1464 [c]	5.91	12.4
Figure 4-10	690TT	One heat	RUB 20% prestrain	Deaerated water + B + Li	680	20,913	5.00	N/A
Figure 4-10	600MA	One heat	RUB 20% prestrain	Deaerated water + B + Li	608	6,051	2.10	--
					680	414 [c]	2.10	51.2
Figure 4-10	600TT	One heat	RUB 20% prestrain	Deaerated water + B + Li	608	9,530	3.64	--
					680	652	3.64	32.2

Figure 4-11	690TT	Four heats	RUB	Deaerated water + B + Li	680	54,284	5.00	N/A
Figure 4-11	600MA	Three heats	RUB	Deaerated water + B + Li	680	1,776	1.04	30.6
Figure 4-11	600TT	Four heats	RUB	Deaerated water + B + Li	680	3,945	1.85	13.8
Figure 4-12	690TT	One heat	SG Mock-up	Deaerated water	680	174,110	5.00	N/A
Figure 4-12	690MA	WD281	SG Mock-up	Deaerated water	680	8,954	0.95	19.4
Figure 4-12	690TT	WD281	SG Mock-up	Deaerated water	680	11,199	1.28	15.5
Figure 4-12	690TT	NX3335	SG Mock-up	Deaerated water	680	20,231	2.29	8.6

(a) θ is time to Weibull 63.2% cumulative failure for Alloy 600 and the equivalent Weibayes for Alloy 690.
(b) IF_R per Eq. 4-6.
(c) The equivalent time at 680°F per Eq. 4-7 based a PWSCC crack initiation time of 50 kcal/mole.

Table 4-3 Summary of Alloy 690 Primary Water Stress Corrosion Test Data

Ref.	Test	Test Environ.	Test Temp (°F)	Alloy 690 Heat Number	Alloy 690 Heat Cond.	Total Speci No.[a]	Test Time at test temp. (hour)	Eq. Test Time at 600°F [b] (year)	Time to First Alloy 600 failure (hour)	Improve. Factor (IF_R)
Sedricks [9]	Double U-Bend	Deaerated water	600	Y24A7L	MA, TT, MA+CW, MA+Weld	52	8064	0.9	3024	2.7
	Double U-Bend	Deaerated water	680	NX4458H NX4460H	MA, TT	8	8064	23.2	No 600 control	N/A
K. Smith [11]	RUB	Deaerated water + B + Li	680	Three pre-series, Heats 1-3	MA, TT	20	13000	29.9	1500	6.5
						20	16000	36.8	2000	6.4
Yonezawa [17]	RUB	Deaerated water + B + Li	680	One Alloy 690 heat	MA	3	6600	15.2	340	19.4
					TT	2	12000	27.6		35.3
	CLT				TT	5	7000	16.1	1144	6.1
A. Smith [32, 33]	C-Ring	Deaerated water	644	Two industrial heats A, E	TT	2	1500	0.9	No 600 control	N/A
Norring [35, 36, 37]	RUB	Deaerated water	689	F	MA	6	33000	103.6	800	41.3
				H, G, A, B, D, C, I	MA, TT	47	25000	78.5		31.3
				PP	TT	6	23000	72.2		28.8
				Y, Z	MA	8	20500	64.3		25.6
Ogawa [43]	RUB	Deaerated water + B + Li	680	One Alloy 690 heat	TT	40	10000	23.0	3000	3.3
	CLT					20	10000	23.0	1142[c]	8.8
Angell [44]	RUB	Deaerated water + B + Li with or without Zn	662	752246	TT	20	7500	9.1	5500	1.4
Vaillant [49]	RUB	Deaerated water + B + Li	680	9.092Exp 9.592Exp 9.799Ind 9G4	TT, MA	4	54000	124.1	500	108
Framatome, France [App. B]	SG Mockup	Deaerated water	680	WE094, Pre-series	TT	16	100000	229.8	800	125

(a) Total number of specimens of similar heat treatment and test condition and duration.
(b) The equivalent test time at 600°F for Alloy 690 is calculated based a PWSCC crack initiation time of 50 kcal/mole (Eq 4-7).
(c) 1142 hours is the equivalent of the 4179 hours failure time at 644 °F for the Alloy 600 control CLT specimens based on Eq. 4-7. Only two of four Alloy 600 MA series results were reported. Hence, the time to the first Alloy 600 failure could be less than 4179 hours.

Table 4-4 Summary of Alloy 690 Hydrogenated and Doped Hydrogenated Steam Stress Corrosion Test Data

Test Ref.	Test	Test Environ.	Test Temp (°F)	Alloy 690 Heat Number	Alloy 690 Heat Cond.	Total Speci No.[a]	Test Time at test temp. (hour)	Eq. Test Time at 600°F [b] (year)	Time to First Alloy 600 failure (hour)	Improve. Factor (IF)
Sui [52]	RUB	H_2 Steam	716	690 (A)	TT,	1	13824	107.4	552	25.0
				690 (B)	TT	1	12600 [c]	97.9		22.8
					TT+aged	1	12600 [c]	97.9		22.8
Jacko [54]	4-point Bend 1% strain	H_2 Steam + 30ppm for each Cl^-, F^- ,SO_4^{-2}	752	Alloy 52M Weld, Y9570	Weld	2	2051	50.1	214 [d]	9.6
	4-point Bend 0.3% strain					2	2051	50.1	450 [d]	4.6
Framatome, Germany [App. A]	RUB	H_2 Steam	752	754380	TT	3	9720	237.4	336	28.9
	RUB surface scored					3	9720	237.4	336	28.9

(a) Total number of specimens of similar heat treatment and test condition and duration.
(b) The equivalent test time at 600°F for Alloy 690 is calculated based a PWSCC crack initiation time of 50 kcal/mole (Eq. 4).
(c) Two of the three Alloy 690 specimens in Sui's investigation cracked after 13824 hours of testing. To be conservative, it is assumed here that these two Alloy 690 specimens developed crack soon after the previous examination made after accumulating 12600 hours. None of the other Alloy 690 specimens in this table failed during the test duration.
(d) The Alloy 52M is compared with Alloy 182.

Table 4-5 List of Operating Steam Generators Manufactured with Alloy 690 Tubing [68]

(As of December 2003)

Installation Date	PWR
1989	D.C. Cook-2, Indian Point-3, Ringhals-2
1990	Dampierre-1
1991	Ohi-3
1992	Penly-2
1993	Millstone-2, North Anna-1, Beznau-1, Ohi-4
1994	Mihama-2, Takahama-2, Genkai-1, V.C. Summer, Gravelines-1, Daya Bay-1, Daya Bay-2, Golfech-2, Genkai-3, Ikata-3
1995	Ohi-1, Tihange-1, North Anna-2, Ringhals-3, Dampierre-3, St. Laurent-B1, Sizewell-B
1996	Mihama-1, Takahama-1, Doel-4, Catawba-1, Ginna, Gravelines-2
1997	McGuire-1, McGuire-2, Point Beach-2, Mihama-3, Ohi-2, Tricastin-2, Genkai-4
1998	Byron-1, St. Lucie-1, Tihange-3, Braidwood-1, Kori-1, Ikata-1, Tricastin-1
1999	Beznau-2
2000	Farley-1, D.C. Cook-1, Krsko, South Texas Project-1, Arkansas Nuclear One-2, Chooz-B1, Civaux-1, Civaux-2, Gravelines-4
2001	Genkai-2, Ikata-2, Kewaunee, Shearon Harris, Farley-2, Tihange-2
2002	Tricastin-3, Fessenheim-1, Chooz-B2, Calvert Cliffs-1, South Texas Project-2
2003	Calvert Cliffs-2, Palo Verde-2, Sequoyah-1, Oconee-1, St.-Laurent Des Eaux B

Table 4-6 List of Alloy 690/152/52 Reactor Coolant System (Excluding Steam Generators) Original Equipment or Replacement Component Items and Welds

As of December 2003 [(a)]

Component Item	In-Service Date	PWR	Material
Pressurizer Heater Sleeves	1990	Calvert Cliffs-2	Alloy 690 Tubing
	2003	Palo Verde-2	Alloy 690 Tubing and Alloy 52 Weld
Pressurizer Instrument Nozzles	1990	Calvert Cliffs-2	Alloy 690 Tubing
	1992	Palo Verde-1,San Onofre-3, San Onofre-2, Palo Verde-1	
	1993	St. Lucie-2, Palo Verde-2	
	1994	Palo Verde-3, St. Lucie-2	Alloy 690 Tubing and Alloy 52 Weld
	1995	San Onofre-3, St. Lucie-1	
	1997	San Onofre-2, San Onofre-3	
	1998	Calvert Cliffs-2, San Onofre-3	
	1999	San Onofre-3	
	2001	Waterford-3	
RV Head CRDM Nozzles/Welds [(b)]	1992	Bugey-3	Alloy 690 Tubing and Alloy 152/52 Weld
	1994	Bugey-5, Blaiyais-1, Gravelines-4, Bugey-2	
	1995	Blayais-2, St. Alban-1, Flamanville-1, Gravelines-3, Blaiyais-3, Tricastin-1	
	1996	Tricastin-4, Paluel-4, St. Laurent-B2, Blaiyais-4, Dampierre-1, Fessenheim-1, St. Alban-2	

Component Item	In-Service Date	PWR	Material
	1997	Bugey-4, Dampierre-2, Dampierre-4, Belleville-2, Cruas-4, Gravelines-5	
	1998	Flamanville-2, Dampierre-3, Paluel-3, Cattenom-2, Fessenheim-2, Cruas-2	
	1999	Chooz-B1, Chooz-B2	
	2000	Civaux-1, Civaux-2	
	2002	North Anna-2	
	2003	North Anna-1, Surry-1, Oconee-1, Oconee-3, Ginna, Three Mile Island-1, Crystal River-3, Surry-2	
Hot Leg Piping Nozzles	1993	San Onofre-2, Palo Verde-2	Alloy 690 Tubing
	1995	San Onofre-3, St. Lucie-1	Alloy 690 Tubing and Alloy 52 Weld
	1997	San Onofre-2, San Onofre-3	
	2000	ANO-1	
	2001	Waterford-3	
	2002	Palo Verde-1, Palo Verde-3	
	2003	St. Lucie-2, Davis-Besse	
Cold Leg Piping Nozzles	1997	San Onofre-2, San Onofre-3	Alloy 690 Tubing and Alloy 52 Weld
RV Nozzle Butt Welds	2000	V.C. Summer	Alloy 690 Forging and Alloy 52 Weld
Pressurizer Manway Diaphragm Plate Weld	2002	Catawba-1	Alloy 152/52 Weld
Pressurizer Surge Nozzle Weld	2003	TMI-1	Alloy 52 Weld Overlay (O.D. of Pipe)

Component Item	In-Service Date	PWR	Material
RV Lower Head BMI Nozzles	2000	Civaux-1, Civaux-2	Alloy 690 Tubing and Alloy 152/52 Weld
	2003	South Texas-1	Alloy 690 Tubing and Alloy 52 Weld

(a) Table entries are based on the information currently available. Additional replacements may exist, which are not included in this table.
(b) This list represents complete RV closure head replacements. Numerous CRDM nozzle repairs on various existing RV closure heads are also in service at this time.

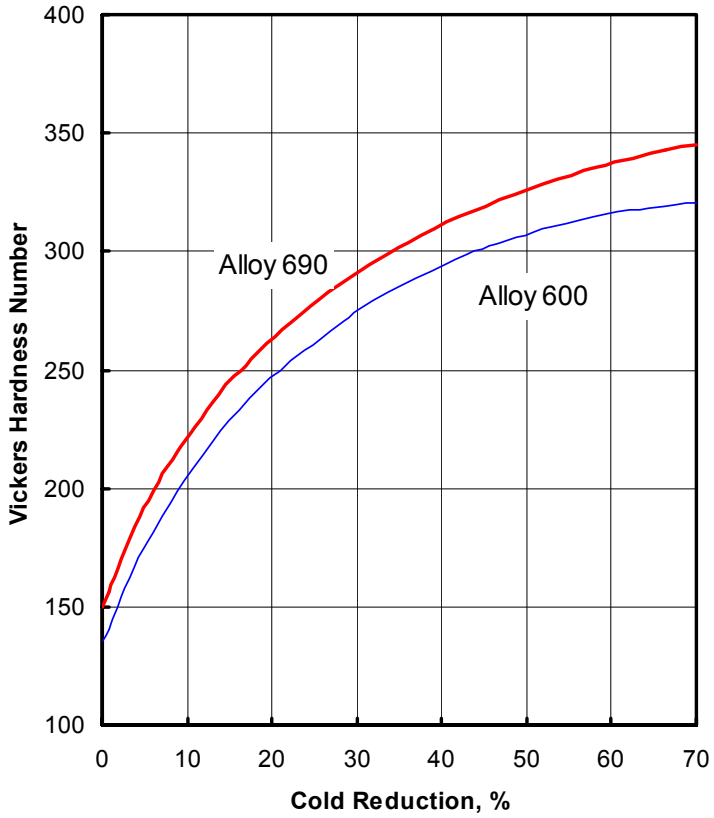

Figure 4-1 Vickers hardness number as a function of cold reduction %. Alloy 690 has a higher work-hardening rate than Alloy 600. After Ref. 6.

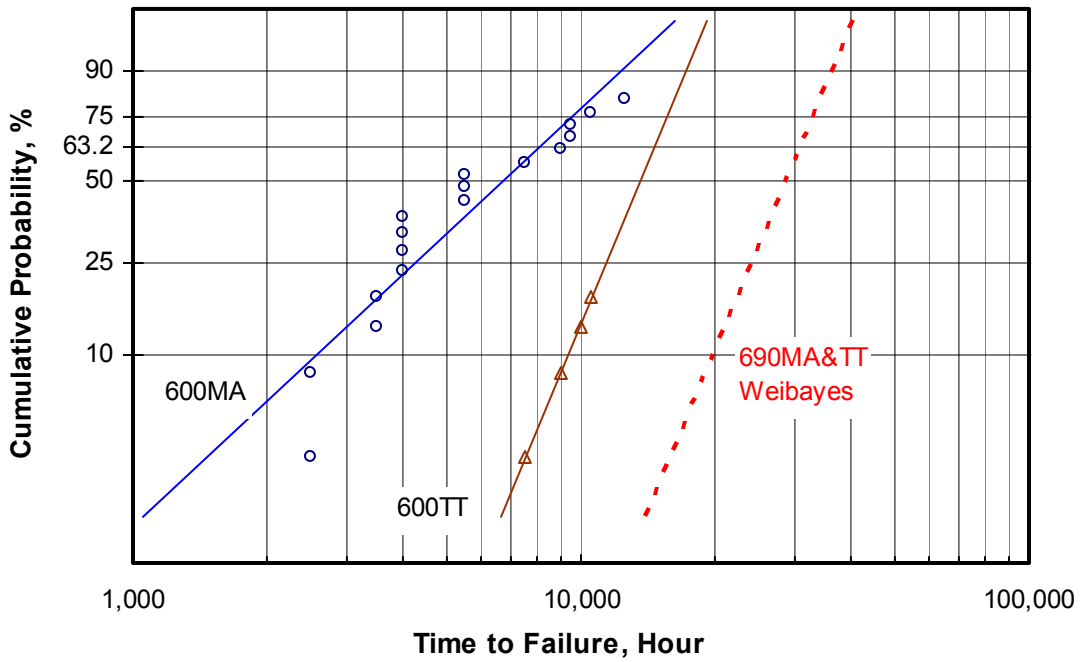

Figure 4-2 Weibull plot of Alloy 600 RUB results in primary water at 680°F reported by K. Smith et al. (shown in Figure 3-3). The test data in the beginning-fuel-cycle and the end-fuel-cycle water have been combined. The Alloy 690 (three heats) Weibayes line assumes β = 5.0.

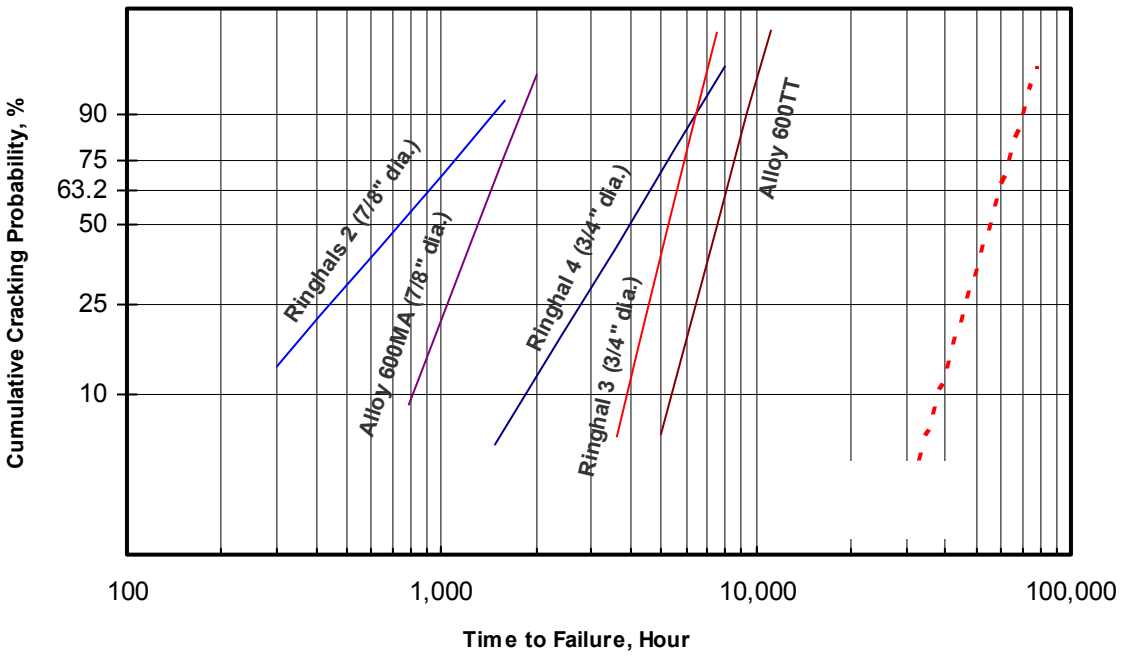

Figure 4-3 Weibull plot of different heats of Alloy 600 RUB results in deaerated water at 689°F reported by Norring et al. The Alloy 690 (many heats) Weibayes line assumes β = 5.0.

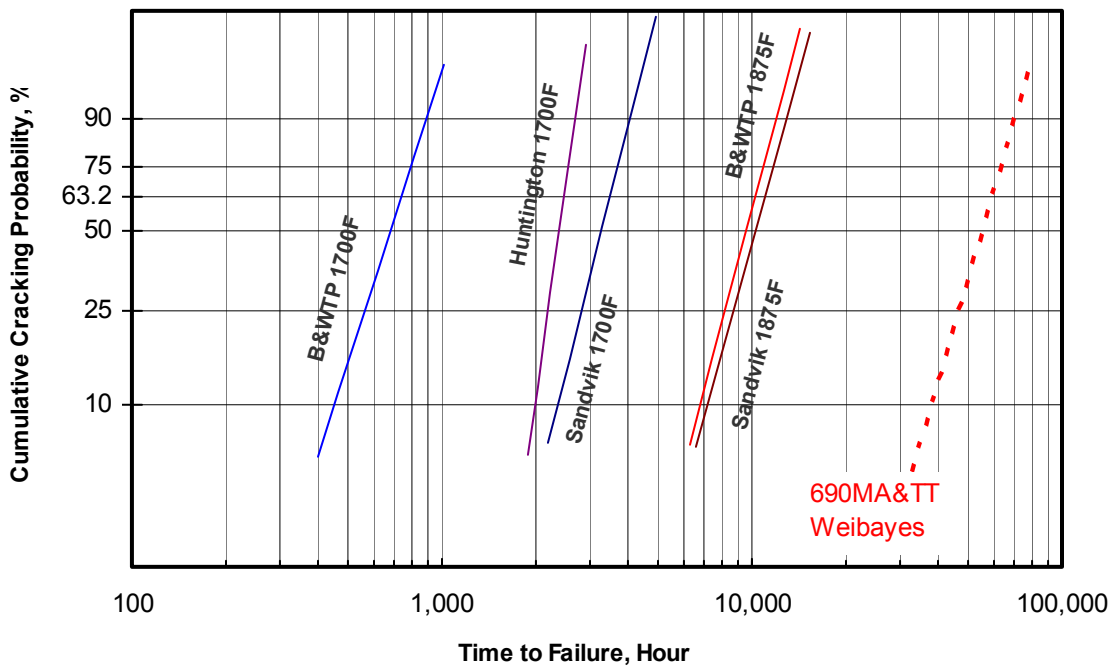

Figure 4-4 Weibull plot of different EPRI special production heats of Alloy 600 RUB results in deaerated water at 689°F reported by Norring et al. The Alloy 690 (many heats) Weibayes line assumes β = 5.0.

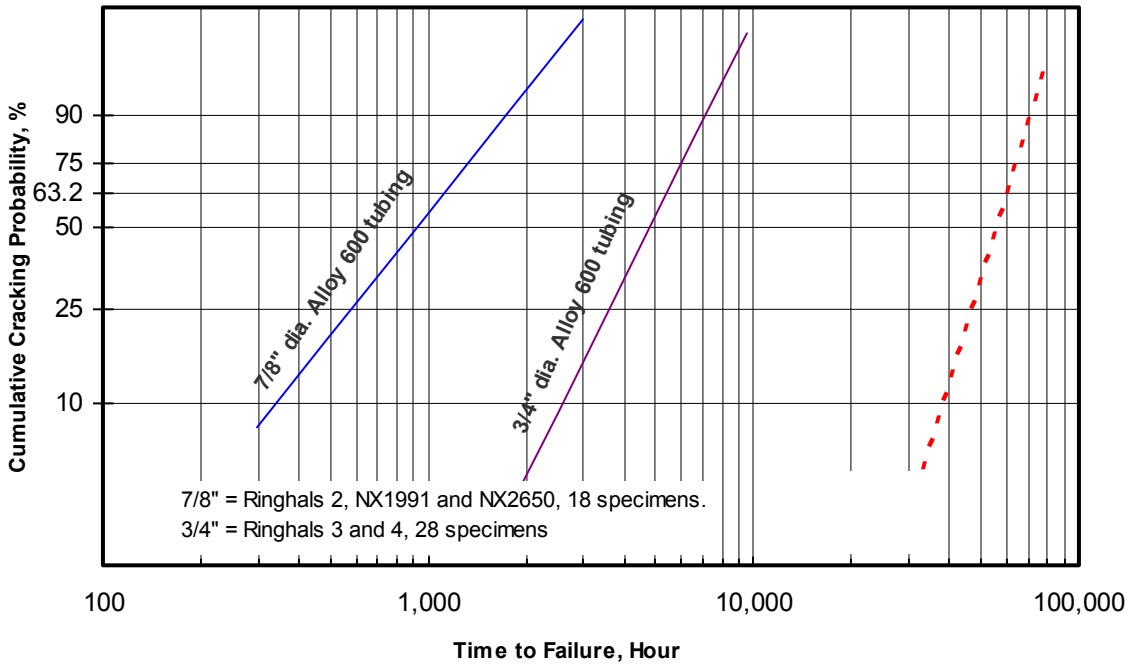

Figure 4-5 Weibull comparison between 7/8” dia. and 3/4" dia. Alloy 600 RUB results in deaerated water at 689°F reported by Norring et al. The Alloy 690 (many heats) Weibayes line assumes β = 5.0.

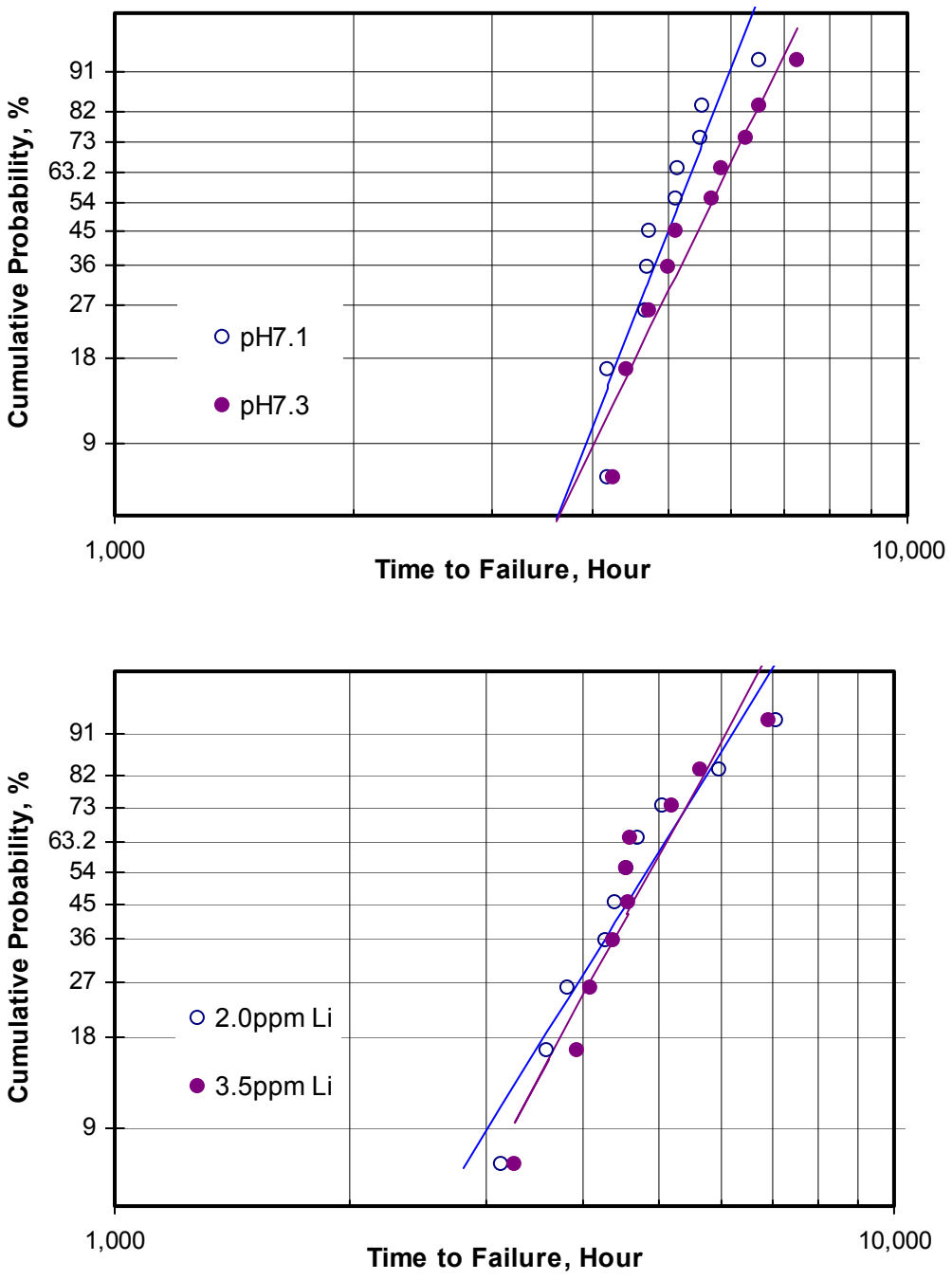

Figure 4-6 Weibull plots of Alloy 600MA (one heat) during constant load test (CLT) at 85.3 ksi, 644°F reported by Ogawa et al. (a) Results in the optimum (pH=7.1) and reference pH (pH=7.3) primary water chemistry. (b) Results in the candidate (2.0 ppm Li) and reference primary water chemistry (3.5 ppm Li). The Alloy 600MA CLT specimens showed similar cracking behavior in the four variations of primary water chemistry.

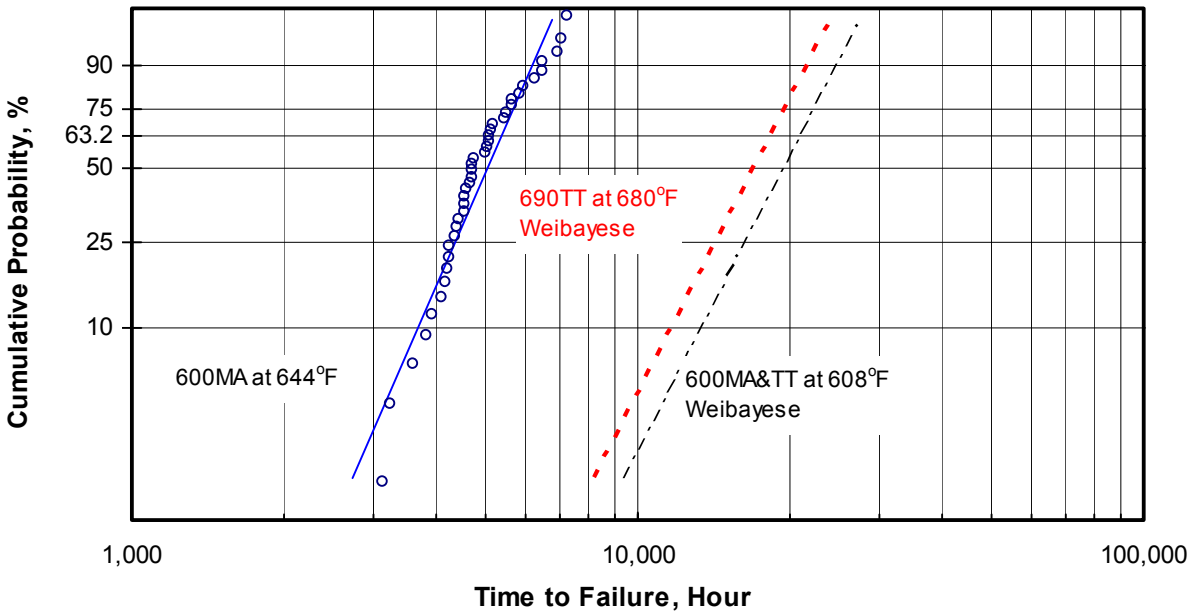

Figure 4-7 Weibull plots of Alloy 600MA (one heat) CLT results at 85.3 ksi, 644°F in primary water reported by Ogawa et al. No failure was observed in all Alloy 600MA&TT CLT specimens tested at 608°F and in the Alloy 690TT (one heat) CLT specimens tested at 680°F. The Weibayes lines for the Alloy 690TT and Alloy 600MA&TT assume β = 5.0.

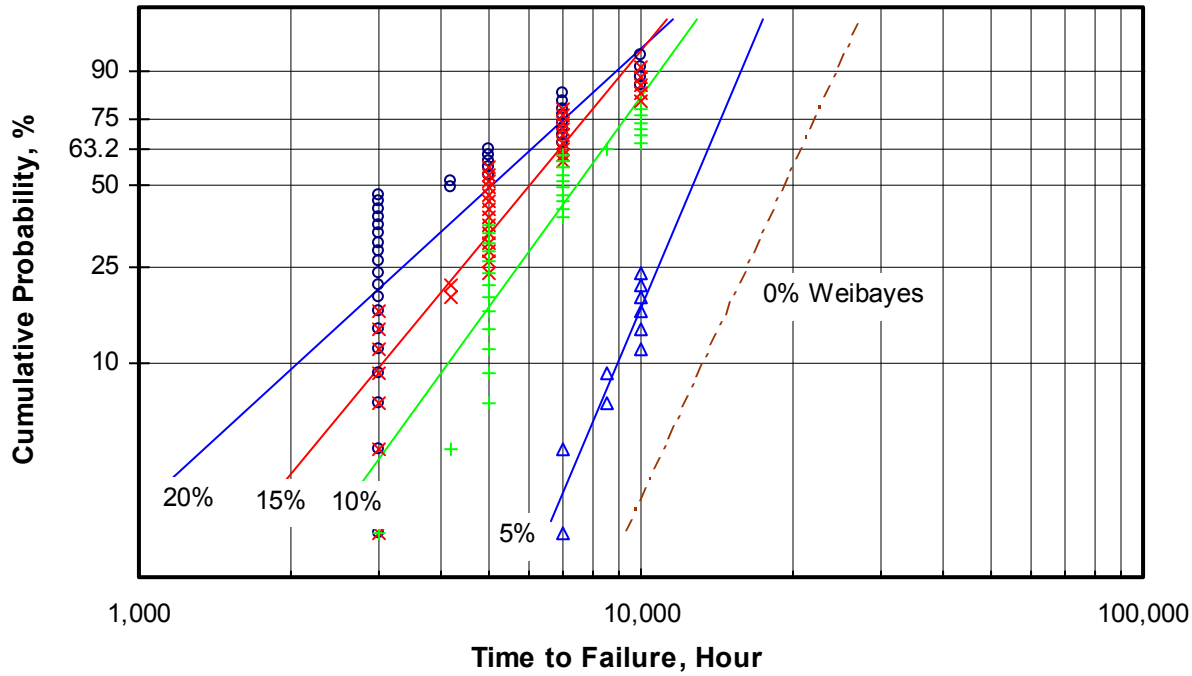

Figure 4-8 Weibull plot of Alloy 600MA (one heat) RUB results at 608 °F in primary water reported by Ogawa et al. The RUB specimens were prestrained to different levels. The Weibayes line for the 0% prestrain (no failure) assumes β = 5.0.

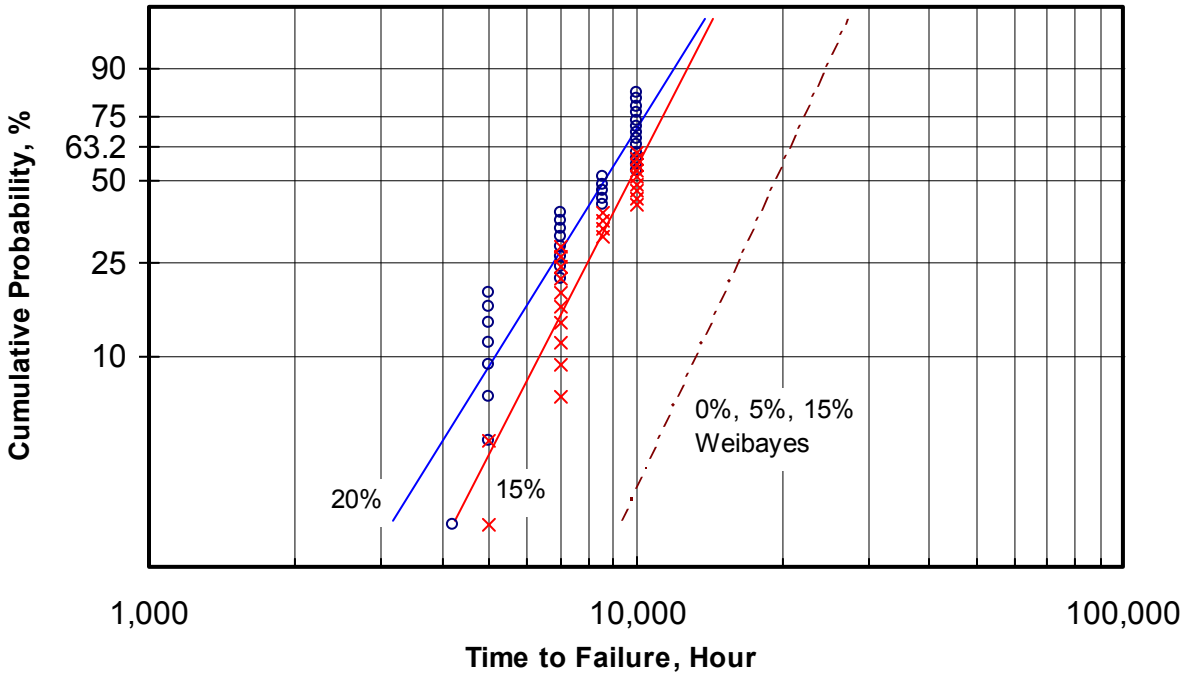

Figure 4-9 Weibull plot of Alloy 600TT (one heat) RUB results at 608 °F in primary water reported by Ogawa et al. The RUB specimens were prestrained to different levels. The Weibayes line for the 0%, 5%, and 15% prestrain (no failure) assume β = 5.0.

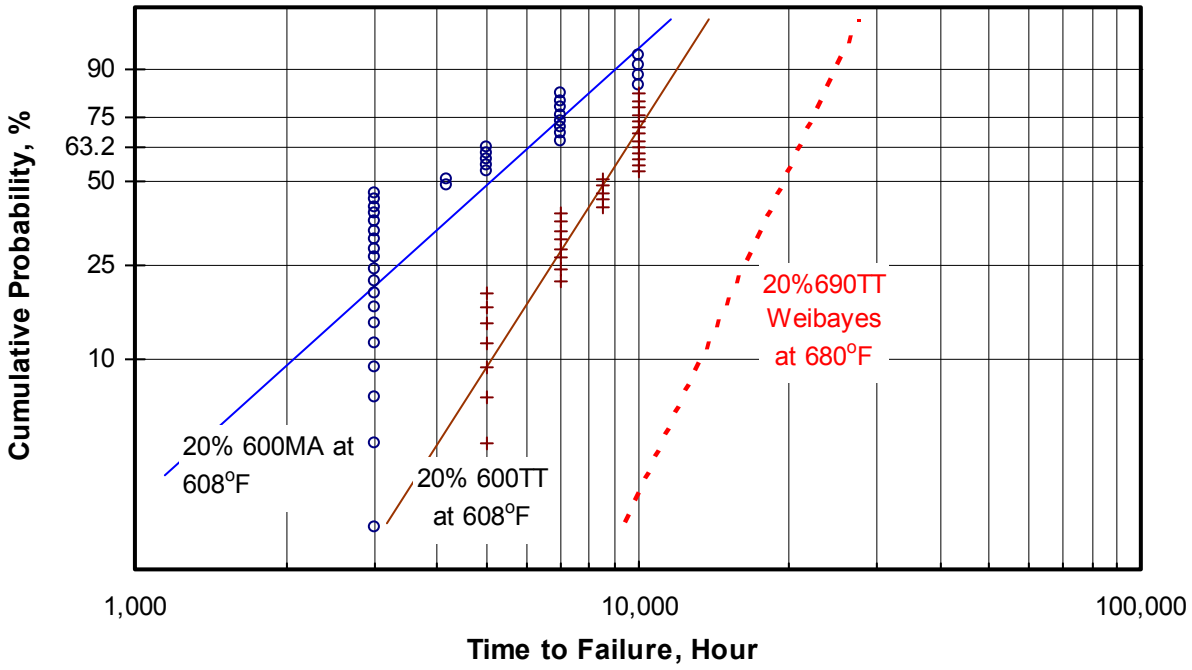

Figure 4-10 Comparison of the 20% prestrained RUB from Alloy 600MA&TT (tested at 608°F) and from Alloy 690TT (tested at 680°F) in primary water reported by Ogawa et al. The Alloy 690TT Weibayes line for the assume β = 5.0.

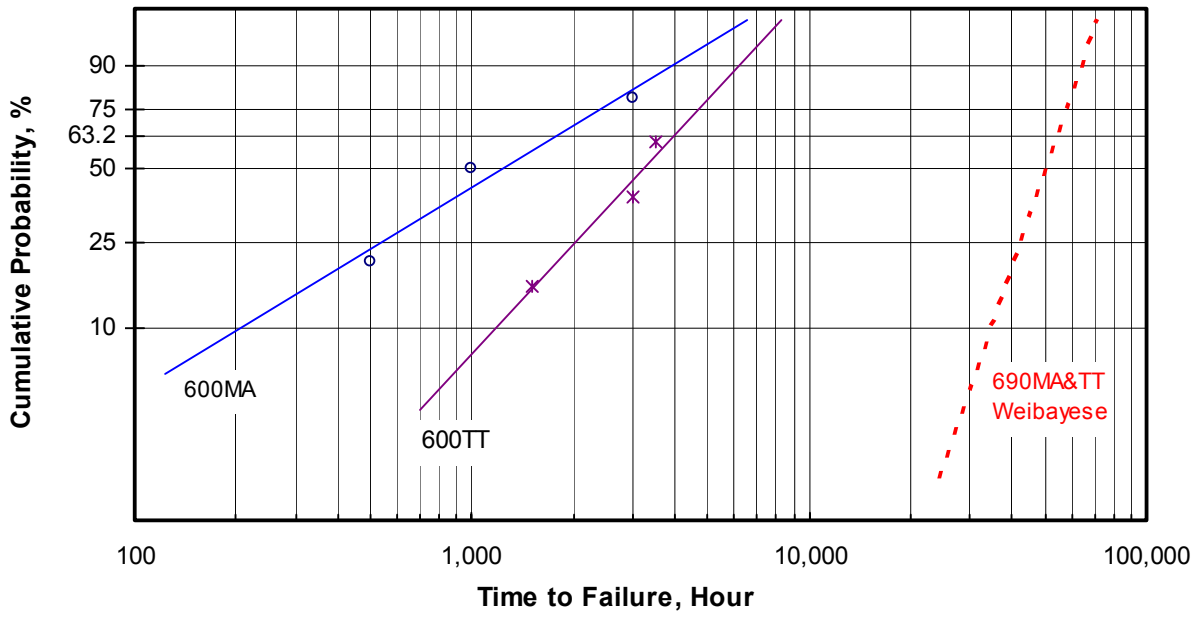

Figure 4-11 Weibull plot of RUB results at 680°F in primary water reported by Vaillant et al. The Alloy 600 RUB specimens were from four different heats in the MA and TT conditions. The Alloy 690 RUB specimens, from four different heats in the TT and MA conditions, experienced no failure after up to 54,000 hours of exposure. The Alloy 690 Weibayes line assumes β = 5.0.

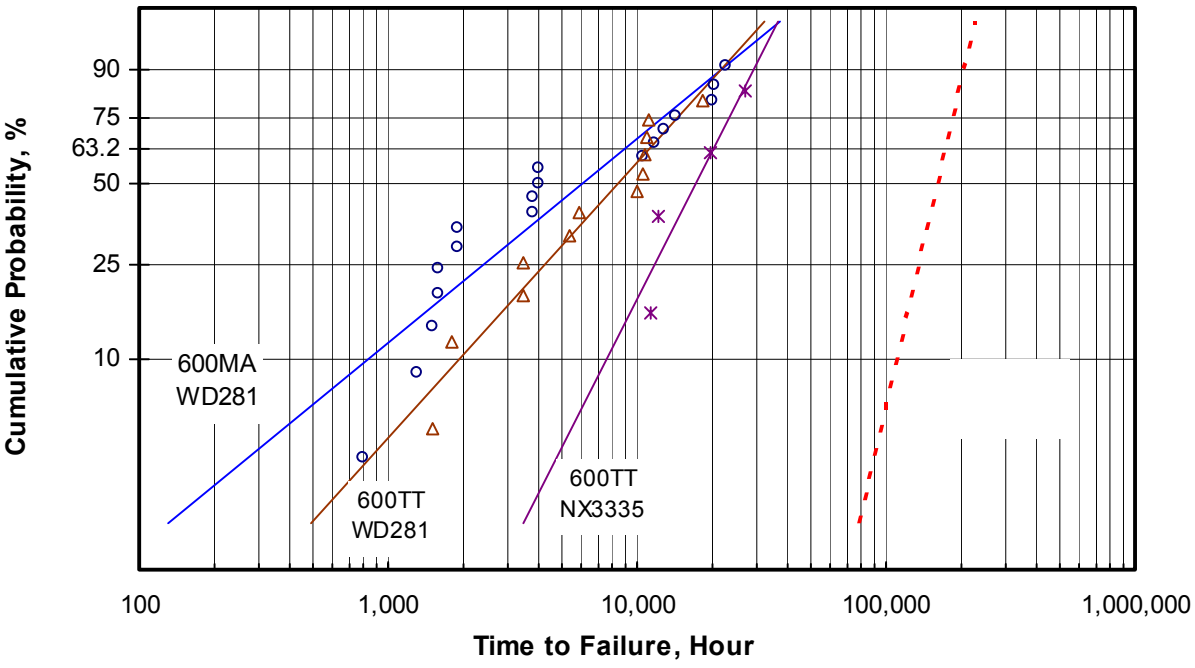

Figure 4-12 Weibull plot of SG mockups tested in deaerated water at 680°F by Framatome ANP, France. Alloy 690TT SG mockups experienced no failure after 100,000 hours of exposure. The Alloy 690 Weibayes line assumes β = 5.0.

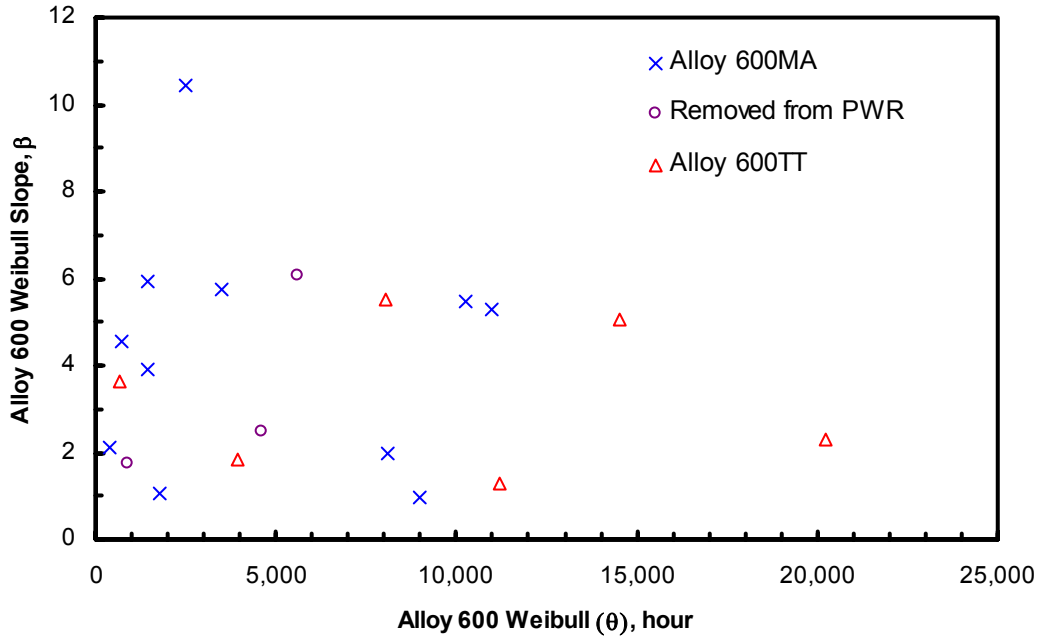

Figure 4-13 Weibull θ and β for Alloy 600 listed in Table 4-2.

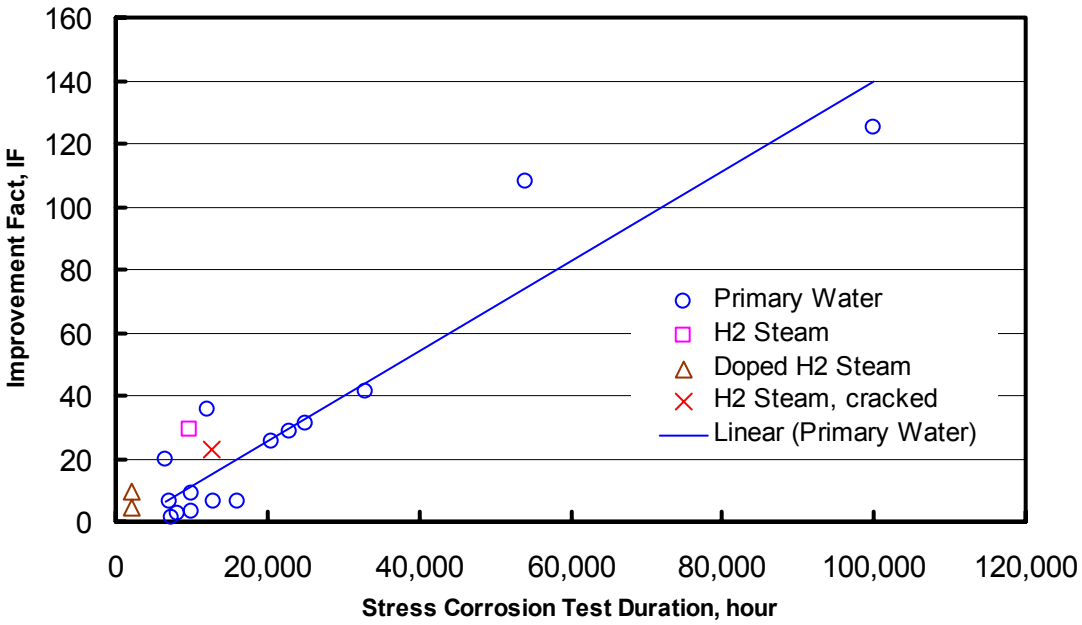

Figure 4-14 Improvement factors listed in Table 4-3 and Table 4-4 per Eq. 4-8.

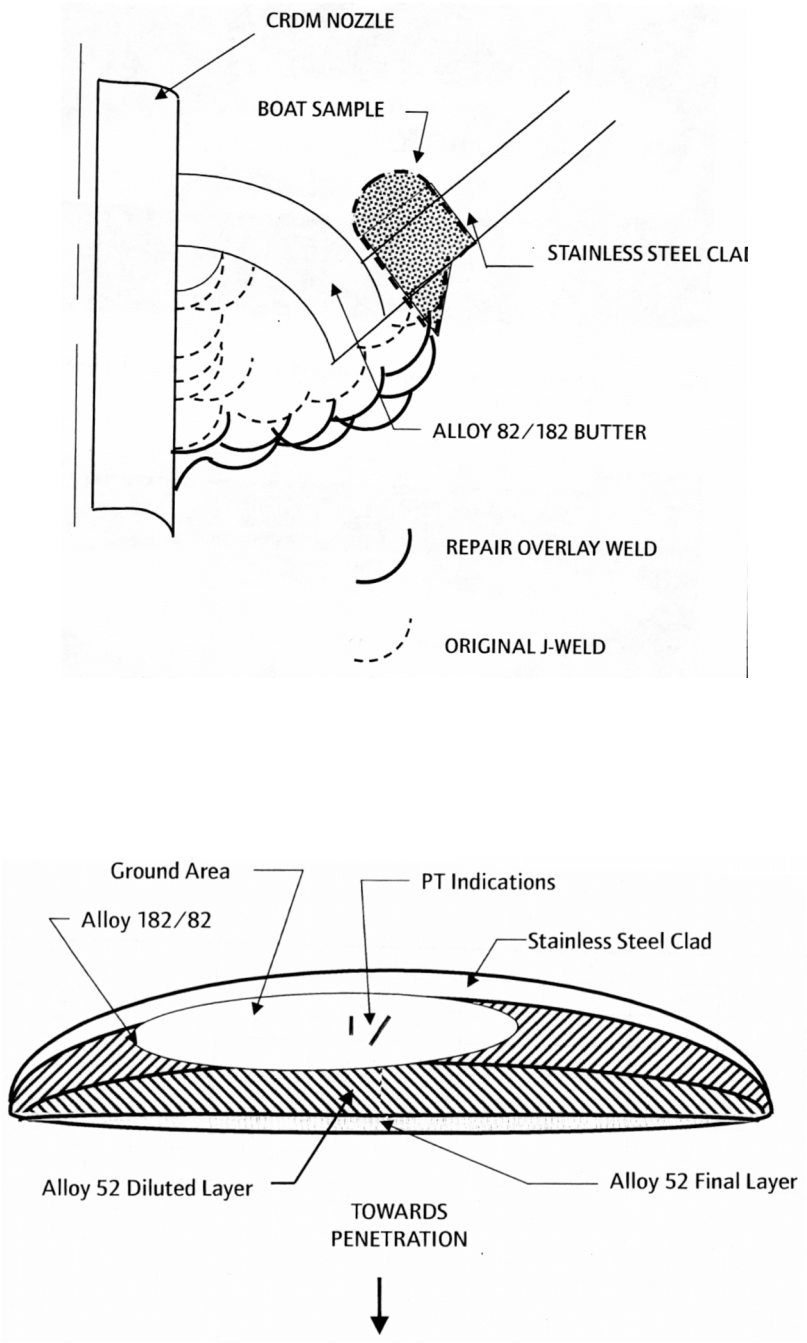

Figure 4-15 Boat Sample Removed from North Anna Unit 2, CRDM Nozzle #51 in 2002. Above, a sketch of the boat removal location with respect to the Alloy 52 weld overlay repair made in 2001. Below, a sketch of the wetted surface (plan view) with the weld materials determined by EDS analysis.[72]

5 SUMMARY AND CONCLUSIONS

Over the last thirty years, PWSCC has been observed in numerous Alloy 600 component items and associated welds. The occurrence of PWSCC has been responsible for significant downtime and replacement power costs. Notable examples of equipment failures in the U.S. include extended outages and emergency repairs or replacements at Calvert Cliffs, V.C. Summer, Oconee Nuclear Station, Davis-Besse, and North Anna. Repairs and replacements have generally utilized wrought Alloy 690 material and its compatible weld metals (Alloy 152 and Alloy 52), which have been shown to be very highly resistant to PWSCC in laboratory experiments and free from cracking in operating reactors over periods already up to nearly 15 years.

Since many cases of PWSCC in Alloy 600 have occurred after very long incubation periods, even if there have often been short term premature failures, it is nevertheless prudent for the PWR industry to question, test and quantify the longevity of wrought Alloy 690 material and its weld metals (Alloys 52 and 152) with respect to aging degradation by corrosion in primary water environments. Such an assessment has obvious implications for the anticipated service life of Alloy 690 replacement component items, e.g., RV closure head CRDM/CEDM nozzles, and the specification of appropriate inspection regimes. To this end, the present report evaluates available field and laboratory data on potential Alloy 690/152/52 corrosion degradation, particularly PWSCC, and provides a technical basis for development of future inspection requirements for thick-walled component items made of these alloys. Developing a coherent approach for the use and inspection of Alloy 690/152/52 materials should provide a significant benefit in the regulatory arena.

5.1 Summary of Laboratory and Field Data

Most laboratory testing has been performed with wrought Alloy 690 materials, with very few tests having been identified for Alloy 52 or Alloy 152 weld materials. Numerous investigations have been performed under a variety of environmental conditions relevant to the PWR primary circuit:

1. High temperature de-oxygenated (deaerated) and hydrogenated water
2. Simulated PWR primary water
3. Hydrogenated steam
4. Hydrogenated steam doped with chloride, fluoride, and sulfate anions
5. Additions of injurious impurities or of potentially mitigating substances such as zinc

The various test conditions cited in this report, including those for the previously unreported, long-term studies described in Appendices A and B, cover temperatures up to 680°F (360°C) water, dissolved oxygen levels < 20 ppb, tests in doped and undoped 752°F (400°C) steam,

lithium concentrations up to 3.5 ppm, boron concentrations up to 1800 ppm, hydrogen concentrations up to 100 cc/kg H_2O, and additions of chlorides and zinc.

A number of tests have also been performed to determine the general corrosion rate and metal release rate for Alloy 690 material in primary water. All studies agree that the general corrosion rate and metal release rate of nickel-base alloys decrease with an increasing chromium concentration in the alloy. The general corrosion rate and metal release rate of Alloy 690 material has been shown to be 2 to 4 times lower than Alloy 600 material.

Accelerated stress corrosion testing has been performed on double U-bend (simulating crevice conditions), reverse U-bend (RUB), constant load test (CLT), four-point bend, and steam generator tubing mock-up specimens. The results of these accelerated stress corrosion tests have shown Alloy 690 and its weld metals to be extraordinarily resistant to cracking. In high temperature deaerated, hydrogenated water, no Alloy 690 material specimen at constant load or deformation has exhibited stress corrosion cracking at testing times up to 100,000 hours at a temperature of 680°F (360°C). In this timeframe, most Alloy 600 MA and TT control specimens had developed cracking, often after relatively short periods. A test duration of 100,000 hours at 680°F is equivalent to approximately 230 years at 600°F, assuming the same activation energy of 50 kcal/mole for PWSCC crack initiation in Alloy 690. This means that Alloy 690 material is not expected to develop PWSCC during any feasible operating lifetime of PWRs.

No cracking of Alloy 690 and its weld metals has been observed under most other test conditions pertinent to primary water, or even under some non-primary water conditions, e.g. oxygenated conditions (up to 16 ppm) and creviced conditions. This includes material with carbon contents ranging from 0.001% to 0.065%, in the mill annealed or thermally treated condition, with and without surface cold work, including material that exhibited surface microcracks before testing.

Two approaches have been used to provide a quantitative estimate of the improvement for Alloy 690 relative to Alloy 600 materials. The first method estimates the relative improvement factor, IF_R, based on a Weibull/Weibayes analysis. Using this method, the average IF_R of Alloy 690 material is 26.5 relative to Alloy 600MA material and 13.3 relative to Alloy 600TT material. Since not all the studies either obtained or reported sufficient test data to allow a Weibull type analysis, a second, simpler method was also used, based on the ratio of the total Alloy 690 material test time (without cracking being observed) over the time to the first Alloy 600 material failure. Using this approach, the average IF_R of Alloy 690 relative to Alloy 600 is 27.1, i.e., about the same as the factor obtained for Alloy 600MA material by the first method. In addition, the IF_R is clearly seen to be limited by the maximum test duration for the Alloy 690 specimens, rather than actual PWSCC failures in this material.

Hence, the relative improvement factor for Alloy 690 can be conservatively estimated to be at least 26 relative to Alloy 600MA and 13 relative to Alloy 600TT material, based on the accelerated testing performed to date in high temperature deaerated water. Furthermore, it is anticipated that these factors will increase in the future as Alloy 690 material test data to longer test durations become available and are confirmed by the future in-service inspection results.

Alloy 690 and its weld metals have been utilized in a number of PWR replacement component items, such as steam generator tubing, pressurizer heater sleeves, and RV closure head

CRDM/CEDM nozzles. Alloy 690 steam generator tubing has been in service for approximately 14 calendar years (i.e., since 1989), pressurizer heater sleeves have been in service for over 12 calendar years (i.e., since 1990), and CRDM nozzles have been in service for over 10 calendar years (i.e., since 1992). Alloy 52 weld material initially was used for a pressurizer nozzle replacement application in 1992 and has been in service now for over 10 years. No stress corrosion degradation of the Alloy 690 materials has been observed in any replacement application to date.

Nevertheless, some tests have shown that cracking of Alloy 690 materials is possible, either under certain extreme testing conditions that are not found in PWRs, or with experimental, pre-production materials (often with atypical heat treatments and chemical compositions). For example, in a deaerated and hydrogenated high temperature water environment, intergranular cracking has been observed during CERT experiments at a strain rate on the order of 10^{-7} sec.$^{-1}$ or less. CERT is a very severe laboratory technique for evaluating susceptibility to stress corrosion cracking. The specimens are loaded well past the yield point to produce continuous, slow plastic deformation and eventually fail by ductile overload. Such mechanical loading is not directly relevant to component operating conditions in nuclear power plants.

Two isolated studies have reported some minor amounts of apparent stress corrosion cracking on highly strained specimens under static loading in simulated PWR water or hydrogenated steam. (It is noted that minor cracking observed in CERT specimens is excluded based on the discussion in Section 4.1.2) In 1987, Nakayama et al.[40] reported slight intergranular cracking in Alloy 690 single U-bends tested in hydrogen saturated water containing 1000 ppm boron and 2 ppm lithium at 330°C (626°F) for 3000 hours. However, this shallow intergranular cracking was atypical of PWSCC, and probably more consistent with microfissuring from mechanical straining. Hence, these results should not be considered a real indication of Alloy 690 PWSCC susceptibility.

In 1997, Sui et al. reported stress corrosion cracking of two Alloy 690 specimens after long exposure times (13,824 h) in hydrogenated steam at 380°C (716°F).[52, 53] However, the cracked Alloy 690 Heat B had an intentionally unusual microstructure with very few intergranular carbides compared to an un-cracked Alloy 690 Heat A with normal intergranular carbide coverage. These results suggest that Alloy 690 could be made susceptible to SCC in a hydrogenated steam environment (and therefore potentially susceptible to PWSCC) with out-of-specification thermo-mechanical processing. Since such processing is prohibited by Alloy 690 material ordering specifications, and intergranular carbide precipitation must be verified by optical and/or SEM microscopy, cracking as seen by Sui et al. should not occur for Alloy 690 material as used in PWRs. The work nevertheless exposes a potential weakness if, for some reason, the material is recrystallized without taking the carbides back into solution (as could conceivably happen, e.g., in a weld heat affected zone). Although such effects require further investigation, it is noted that extrapolation of the above failure times observed in steam at 380°C to normal PWR operating temperatures, using the normal Arrhenius activation energy approach, would still predict comfortable margins against failure over foreseeable PWR plant lifetimes, even for Alloy 690 with non-standard carbide morphology.

Although it is not the purpose of this report to assess the secondary-side corrosion behavior of Alloy 690, Appendix C reviews the main points of the extensive work that has been carried out in connection with replacement SG tubing in relevant environments. In summary, even though it

cannot be considered immune to IGA/SCC, Alloy 690TT material has nevertheless demonstrated far superior IGA/SCC resistance compared to Alloy 600MA or Alloy 600TT materials under most conditions pertinent to faulted secondary water. Lead-doped caustic water is an exception here. Furthermore, Alloy 690 appears to be just as resistant to IGSCC in all volatile treatment (AVT) water as it is to PWSCC in primary water.

5.2 Gaps in the Test Data

This literature review has also identified some apparent information gaps in the study of the corrosion behavior of Alloy 690 and its weld metals for PWR service:

1. Alloy 52 and 152 weld metals

Only one investigation each has been reported concerning PWSCC testing of Alloy 152 and Alloy 52M weld metals. In 2003, two Alloy 600 bottom mounted instrumentation (BMI) nozzles (#1 and #46) at South Texas Project (STP) Unit 1 were identified to have leaked primary water. Laboratory examinations of a boat sample removed from BMI nozzle #1 revealed intergranular cracking consistent with PWSCC in the Alloy 600 nozzle portion of the boat sample. According to Ref 73, STP attributed the cracking to be most likely initiated by lack-of-fusion defects or other types of fabrication defects in the Alloy 182 J-groove weld. Although Alloy 690/152/52 was not involved in the cracked BMI nozzles at STP Unit 1, the STP BMI incident has heightened industry awareness to the possibility of PWSCC initiation due to Alloy 152/52 weld defects, and the potential to propagate flaws in the Alloy 152/52 weld metal and into the Alloy 690 base metal. As mentioned in Section 2.1 of the present report, modified versions of Alloy 152/52 with improved weldability are currently being developed. Clearly, additional studies need to be performed on these materials, in particular using the latest composition of Alloy 152/52 weld metal. In addition, the Alloy 152/52 weld studies need to examine weld metal dilution, mainly the lowering of chromium content near the weld interface with carbon steel and stainless steel base metal, and its impact on PWSCC resistance.

2. Effects of product form (plate, tube, rolled bar, forged bar, and extruded bar)

Nearly all testing has been performed with specimens obtained from steam generator tubing. Only one investigation has been performed with an Alloy 690 plate, one with a laboratory heat cast and rolled into bar, and one with a forged Alloy 690 material. Further consideration of product form is desirable, especially in conjunction with the following item 3.

3. Subtle changes in chemical composition and thermo-mechanical processing effects on surface finish.

The studies by Angeliu and Vaillant identify the need for further investigation into the possible effect of subtle changes in the chemical composition of Alloy 690 material (e.g., low Fe and high C and Al). Processing effects which could lead to intergranular micro-fissuring at Alloy 690 surfaces also need to be better understood and avoided, although the existing data do not suggest that this would result in susceptibility to PWSCC.

4. Crack growth rates of base metal, HAZ, and weld metals

Given the welcome difficulties in initiating cracking of Alloy 690 and its weld metals, no plausible estimates of crack growth rates are available at this time. Consideration of advanced testing techniques may be required to permit quantification of realistic factors of improvement in crack growth rate for these highly PWSCC resistant materials. This consideration would be pertinent, e.g., to repaired Alloy 600 component items where cracks may initiate in residual Alloy 600 or 182 material and grow towards Alloy 690 or its compatible weld metals. Some recent test results also indicate that the crack growth rate in HAZs of Alloy 600 TT material may be up to 30 times faster than in the thermally treated base material.[74] Further studies should be conducted to evaluate the effect, if any, of such modified microstructures on Alloy 690 TT materials.

5. Pitting and crevice corrosion

Some testing of Alloy 690 has been performed with double U-bend specimens to simulate crevice conditions and minimal testing has also been performed to evaluate pitting. Both of these forms of corrosion need to be further investigated with regard to faulted secondary-side environments, but are not an issue in PWR primary water.

6. Corrosion fatigue

Only one study appears to have been performed on Alloy 690 and its weld metals concerning the combined effects of exposure to primary water and fatigue. The results suggest that models developed for Alloy 600 may also be applicable here, but additional work would be appropriate.

7. LTCP (low temperature crack propagation)

Although it is not the subject of this report, a brief synopsis of the available information has been provided. Additional efforts may be needed to confirm its lack of relevance for Alloys 690/152/52 in PWR primary water, even though the available operating experience does not suggest that a practical problem exists.

5.3 Conclusions

1. Some 300 U-bend, Double U-bend, and constant load specimens from about 40 heats of Alloy 690 have been tested typically in primary water, deaerated water, or hydrogenated steam. The carbon content ranged from 0.001% to 0.065% and the heat treatment included MA, TT, and thermally aged conditions. The vast majority of the Alloy 690 specimens in both MA and TT conditions did not develop cracking after exposure times as long as 100,000 hours. In the same studies, most of the Alloy 600 specimens in both

MA and TT conditions developed PWSCC, often after relatively brief periods. These laboratory test results demonstrate that Alloy 690 is very highly resistant to PWSCC.

2. Cracking of Alloy 690 was observed only in two of the above studies. In one case, two Alloy 690 RUB specimens from a single Alloy 690 heat, which was deliberately solution annealed at unusually low temperature to prevent grain boundary carbide precipitation, developed intergranular cracking after at least 12,600 hours in hydrogenated steam at 380°C (716°F). Such cracking should not occur for properly heat treated Alloy 690 in PWRs. Furthermore, extrapolation to normal PWR operating temperatures would predict comfortable margins against failure within foreseeable PWR plant lifetimes, even for Alloy 690 with non-standard carbide morphology. In the second study, very shallow intergranular cracks were observed in Alloy 690 single U-bend specimens exposed to hydrogen-saturated water containing 1000 ppm boron and 2 ppm lithium at 330°C (626°F) for 3000 hours. However, this cracking was atypical of PWSCC, and probably more consistent with microfissuring from mechanical straining, as reported in several other Alloy 690 studies. Hence, this result should not be considered a real indication of Alloy 690 PWSCC susceptibility.

3. Based on the duration of the laboratory test, two methods have been used to provide a quantitative estimate of IF_R, the improvement factor for Alloy 690 relative to Alloy 600. The first method, based on a Weibull analysis, provides an average IF_R of 26.5 relative to Alloy 600MA material and 13.3 relative to Alloy 600TT material. The second method, based on the ratio of the Alloy 690 material test time over the time to the first Alloy 600 material failure, provides an average IF_R of 27.1. The IF_R is seen to increase with increasing test time, indicating that the IF_R is limited by the test duration. Hence, the average IF_R values listed are very conservative estimates (or underestimates) of the actual improvement of Alloy 690 relative to Alloy 600.

4. In a hydrogenated high temperature water environment, minor intergranular cracking has been observed during CERT experiments at a strain rate on the order of 10^{-7} sec.$^{-1}$ or less, particularly for experimental heats of Alloy 690. However, CERT is a very severe laboratory technique for evaluating susceptibility to SCC, involving mechanical loading that is not directly relevant to component operating conditions in nuclear power plants.

5. These laboratory test results have been confirmed by the excellent field experience with Alloy 690 for up to fourteen years, and with Alloys 52 and 152 for up to twelve years. Worldwide, numerous PWR units now operate with steam generators having Alloy 690 tubing and many other component items containing Alloys 690 and its weld metals, most notably replacement penetration nozzles in pressurizers and RPV heads, have been in operation since the early 1990s. To date, there have been no indications of PWSCC in any of the Alloy 690 component items in service.

6. Many corrosion studies of Alloy 690 conducted in environments pertinent to (faulted) PWR secondary water have also been reviewed in order to provide a comprehensive comparison with Alloy 600. Even though it cannot be considered immune to IGA/SCC, Alloy 690TT material has nevertheless demonstrated far superior IGA/SCC resistance

compared to Alloy 600MA or Alloy 600TT materials under most conditions and appears to be just as resistant to IGSCC in AVT water as it is to PWSCC in primary water.

In summary, it is concluded that wrought Alloy 690 and its weld metals (Alloys 52 and 152) are acceptable and highly corrosion-resistant replacement materials for Alloy 600 and its weld metals in PWRs, although limited, further testing is needed to examine some specific knowledge gaps that have been identified. Wherever possible, the existing laboratory test data have been evaluated to estimate the improvement factor of Alloy 690 relative to Alloy 600. Average improvement factors of at least 26 relative to Alloy 600MA material and 13 relative to Alloy 600TT material can be derived, but these numbers are clearly conservative, due to an absence of PWSCC in most Alloy 690 specimens within the test duration.

In addition, Alloy 690 service experience in PWRs has been reviewed to augment the laboratory findings. Based on both laboratory and field data, it is concluded that Alloy 690 and its weld metals Alloys 52 and 152 are very unlikely to develop PWSCC during extended PWR plant lifetimes (60^{+} years). Hence, the PWSCC inspection regimes developed in recent years for thick-walled component items made of Alloys 600, 182, and 82 would be unnecessarily stringent if applied in exactly the same way to comparable component item locations involving Alloy 690 and its weld metals. A separate inspection program, commensurate with the magnitude of improvement in PWSCC resistance already demonstrated, should be developed. It is anticipated that this could be further refined as additional laboratory results and field inspection data become available.

A EFFECTS OF SURFACE DEFECTS ON THE PWSCC BEHAVIOR OF 690TT AND 600MA – A FRAMATOME ANP (GERMANY) REPORT

A.1 Introduction

Alloy 600 and its weld metals 182 and 82 are considered to be immune to chloride-induced stress corrosion cracking (SCC) and were chosen as an alternative material for key component items such as steam generator (SG) tubes by most nuclear power plant suppliers in the sixties. However, as observed by Coriou[75, 76, 77] and co-workers the nickel base Alloy 600 is not immune to high temperature pure water cracking (see Figure A-1). According to Shah[78] primary water stress corrosion cracking (PWSCC) is a thermally activated, intergranular cracking mechanism that generally follows the principles of "regular" SCC, since it only occurs if the following three conditions are simultaneously fulfilled and maintained: susceptible material condition, corrosive environment and the presence of tensile stresses (see Figure A-2).

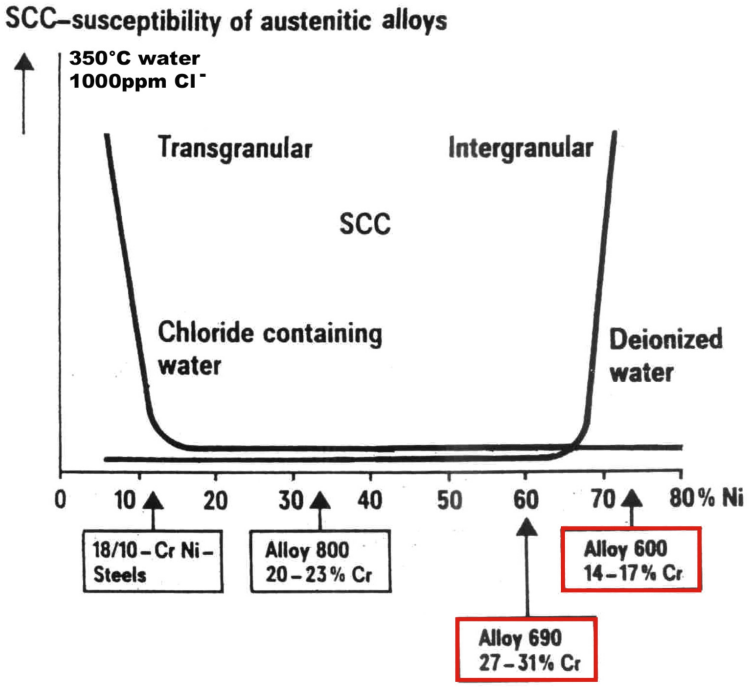

Figure A-1 Schematic diagram showing the influence of nickel content on the cracking behavior of different alloys when stressed slightly above yield strength in 350°C water (demineralized or 1000 ppm Cl–); according to Coriou [75]

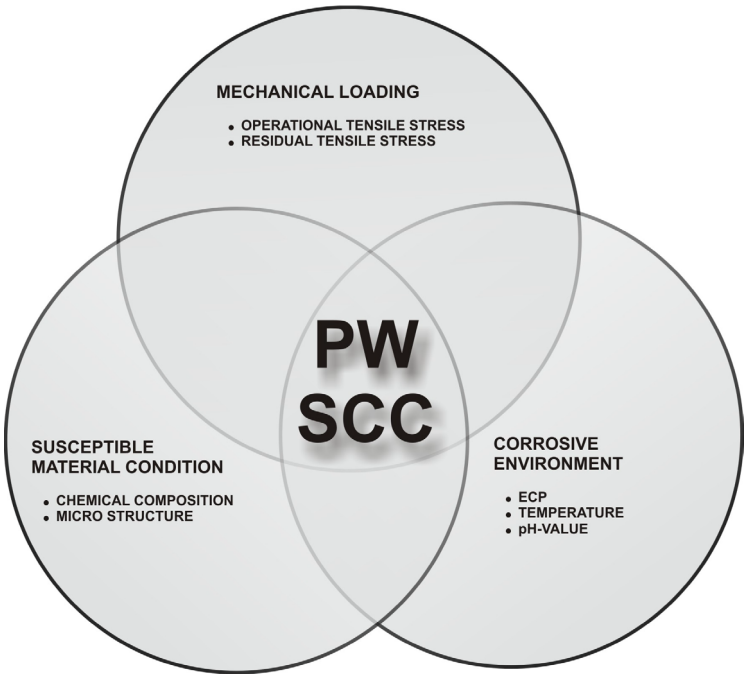

Figure A-2 Schematic The PWSCC system and the necessary conditions for cracking to occur.

According to [79] this type of environmentally-assisted cracking was experienced in the field preferentially in SG tubes manufactured from Alloy 600 being in a low temperature mill annealed condition (LTMA). This condition is characterized by high yield strength and discontinuous intergranular and intragranular carbide precipitation. High temperature mill annealed (HTMA) or thermal treated (TT) Alloy 600 exhibits an increased resistance to PWSCC. The most decisive factors affecting PWSCC of Alloy 600 SG tubes were found to be:[79]

- Material properties (annealing temperature, mechanical properties, grain size, microstructure)
- Residual tensile stresses originating from cold work
- Coolant temperature
- Water chemistry (hydrogen content and possible lithium concentration, pH-value)

Despite extensive research carried out since the sixties, the primary reason leading to PWSCC is not fully understood. However, in the recent past several theoretical models describing PWSCC of Alloy 600 have been developed and proposed. The explicit discussion of these models would exceed the scope of this investigation. However, for completeness some of the theoretical approaches are listed below. Therefore, PWSCC may be caused by one or more of the following:

- a hydrogen induced cracking mechanism [80, 81]

- an anodic dissolution at crack tips [82]
- a thermally activated dislocation creep mechanism [83]
- an internal oxidation model [84]

The widespread occurrence of PWSCC in PWR component items manufactured from Alloy 600 and recently also in Alloy 182/82 has led to its replacement with Alloy 690 and its corresponding weld metals 152/52.

However, safety authorities are reluctant to relax stringent inspection regimes that are based on Alloy 600 degradation of key component items such as RPV Head Penetrations. There is strong economic incentive to quantify the margin of improvement resulting from the application of Alloy 690/152/52 versus Alloy 600/182/82. In addition to the technical basis document summarizing the current state of knowledge and operating experience with Alloy 690 this report describes one particular testing technique allowing a quantification of the improved PWSCC resistance of Alloy 690 in comparison to Alloy 600.

A.2 Objective

The primary objective of this experiment was to evaluate the corrosion behavior of mechanically marked/scored Alloy 600MA and Alloy 690TT SG tubing under primary water conditions. Also the quantification of the margin of improvement provided by Alloy 690TT was part of this investigation.

The experiments were performed in the context of actual indications found during manufacture of replacement SGs. Inspection with eddy current techniques showed indications in some of the SG tubing material at the roll-in zone in the tubesheet. The indications, in the form of internal surface defects, most likely originated from a malfunctioning roller/roller cage during manufacturing when SG tubes are rolled into the tubesheet and/or a special tool for pulling the polymer device used for plugging tubes.

The defects appeared as longitudinal and circumferential scratches/scores with a maximum depth of 80% of the nominal tube's wall thickness. Applicable procedures required the tube to be plugged if scores were identified at a depth greater than 40% of the nominal wall thickness. Thus, this particular experiment was focused on the corrosion behavior of tubes with surface marks between 20% and 40% of the nominal wall thickness and whether such tubes could go into service with a satisfactory performance under primary water conditions. The experiments included the following tasks:

- Comparative hot steam testing using Reverse U-bend Specimens (RUB);
- Metallography at selected locations removed from one RUB specimen of each material;
- Vickers microhardness measurements
- Photographic documentation

A.3 Experimental Procedure

A.3.1 Test Materials

A.3.1.1 Alloy 600MA – Mill Annealed

A custom mill anneal by Sandvik at a relatively low temperature ranging from 850°C to 900°C resulted in a more susceptible material condition. This approach was chosen in order to utilize this particular heat as a susceptible reference material for numerous exposure tests.

A.3.1.2 Alloy 690TT – Thermally Treated

This material condition comprised mill annealing at a nominal temperature of 1080°C and a subsequent thermal treatment at 715°C. This was performed in order to achieve the desired, more corrosion resistant microstructure with a semi-continuous network of grain-boundary carbide precipitates.

Table A-1 and Table A-2 below summarize the chemical composition and mechanical properties of the corresponding materials.

Table A-1 Chemical composition of Alloy 600MA and Alloy 690TT

CHEMICAL COMPOSITION (wt.%)														
Element	**C**	**Si**	**Mn**	**P**	**S**	**Cr**	**Ni**	**Mo**	**Ti**	**Cu**	**Co**	**Al**	**N**	**Fe**
Alloy 690TT heat 754380	0.019	0.35	0.32	0.008	0.001	29.95	59.40	0.01	0.30	0.010	0.012	0.025	0.025	9.45
Alloy 600MA heat 752677	0.027	0.29	0.80	0.008	0.003	16.55	72.7	N/A	0.29	0.010	0.011	0.14	N/A	9.19

Table A-2 Mechanical properties and SG tube dimensions of Alloy 600MA and Alloy 690TT

MECHANICAL PROPERTIES/DIMENSIONS					
	0.2% Yield Strength	**Tensile Strength**	**Elongation (2")**	**outer diameter**	**wall thickness**
Alloy 690TT heat 754380	349 MPa (51 ksi)	746 MPa (108 ksi)	44 %	19.05 mm (0.75")	1.09 mm (0.043")
Alloy 600MA heat 752677	399 MPa (58 ksi)	715 MPa (104 ksi)	42 %	22.23 mm (0.875")	1.27 mm (0.05")

Note: The above data shown in Table A-1 and Table A-2 originates from Sandvik mill certificates L93013 and L87001 for Alloy 690TT and Alloy 600MA, respectively.

A.3.2 Hot Steam Testing

Hot steam testing represents an accelerated laboratory test[85] utilized for drastically reducing crack incubation times of nickel-base alloys such as Alloy 600MA. Incubation times of typically several years observed in the field are reduced down to several days. The high cracking susceptibility during this particular test is primarily attributed to:

- Specimen exposure to a temperature of 400°C (752°F)
- Specimen exposure to suitable steam conditions with
  hydrogen partial pressure of 1.1 bar (16 psi)
  and total pressure of 200 bar (2900 psi)
- Utilization of highly cold worked RUB specimens (with and without surface marks)

A.3.3 Test Specimens

For this comparative hot steam test of SG materials, split tube RUBs were used. RUBs are prepared from longitudinally split SG tube sections that are bent around a mandrel in a manner exposing the internal tube surface outward. For ensuring a representative and reproducible stress condition, a special bending procedure was established using a custom-built bending device as shown in Figure A-3. To maintain a defined stress state during testing, the RUB legs are held in place by socket head cap screws of the same material that are bolted to a machined metal bar. A typical example of one RUB specimen and an overview of all tested samples is shown in Figure A-4and Figure A-5.

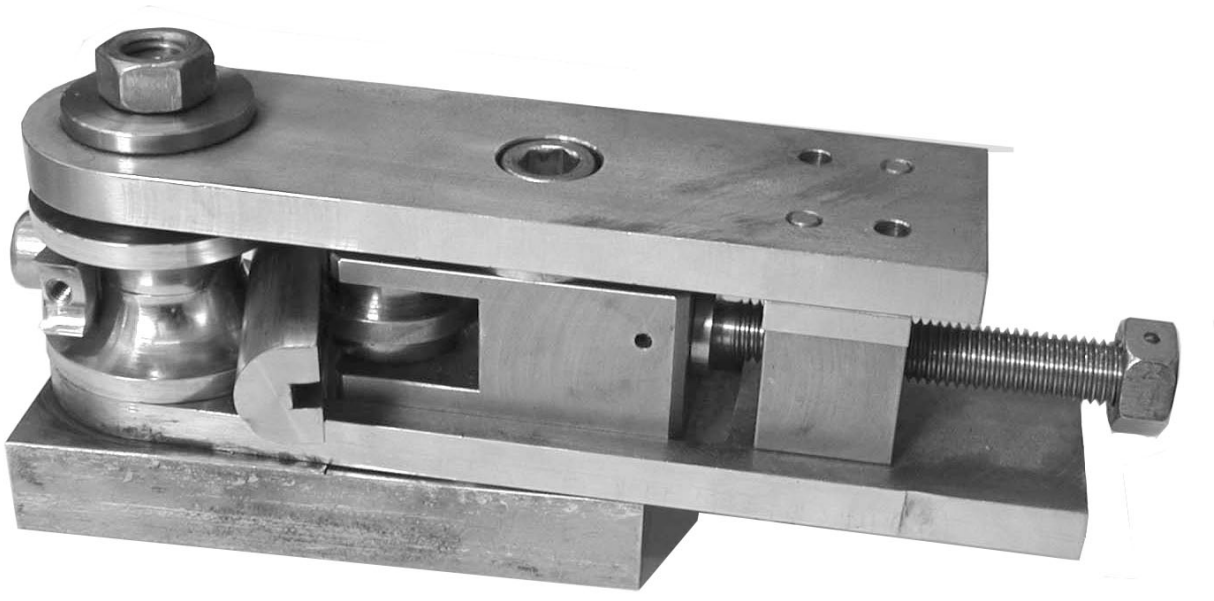

Figure A-3 Bending device used for RUB manufacturing

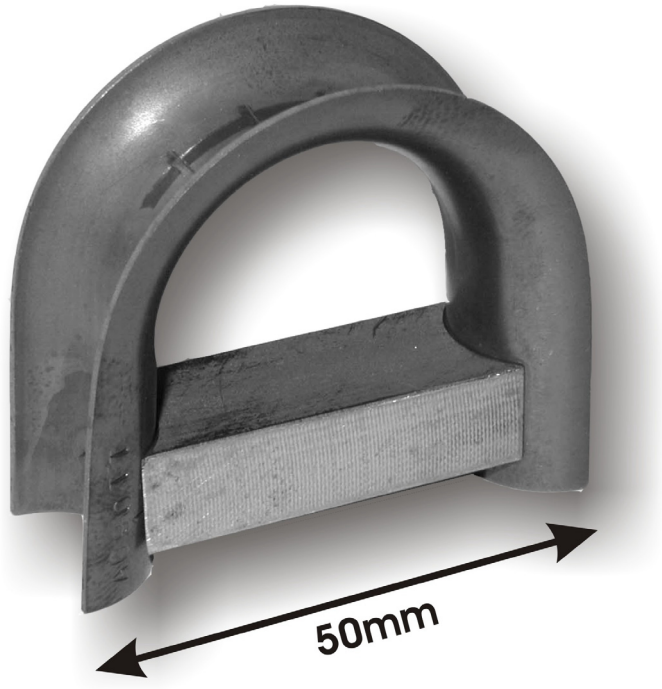

Figure A-4 Typical RUB specimen manufactured by bending a split SG tube.

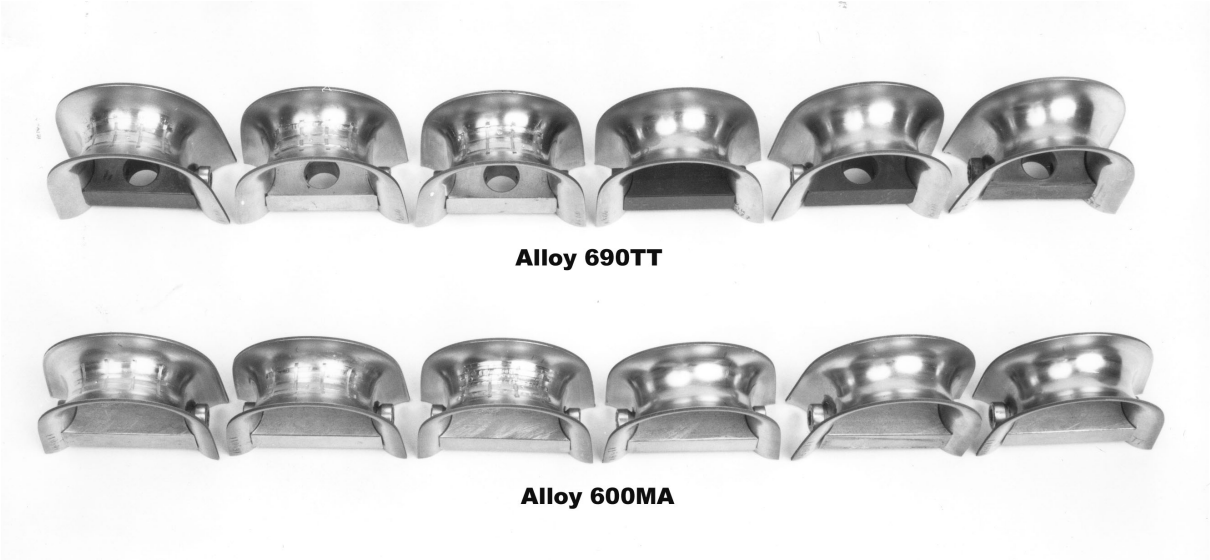

Figure A-5 View of total number of test specimens

To simulate a malfunctioning rolling tool, 50% of the RUBs (three specimens per material) were deliberately scored with actual tools used during manufacturing. These surface marks were introduced into the internal surfaces of split tube sections prior to bending. The scores were shaped in the form of longitudinal and circumferential grooves with a width of approximately 1 mm (0.04") and a depth ranging from 20% to a maximum of 40% of the tube's wall thickness as shown in Figure A-6. The scoring process and the actual depth of grooves were controlled with surface profilometry. However, due to the hardware set-up of

the surface profilometer, only readings of circumferential grooves were performed. A typical example of a profilometry printout obtained from a 690TT RUB specimen is displayed in Figure A-7.

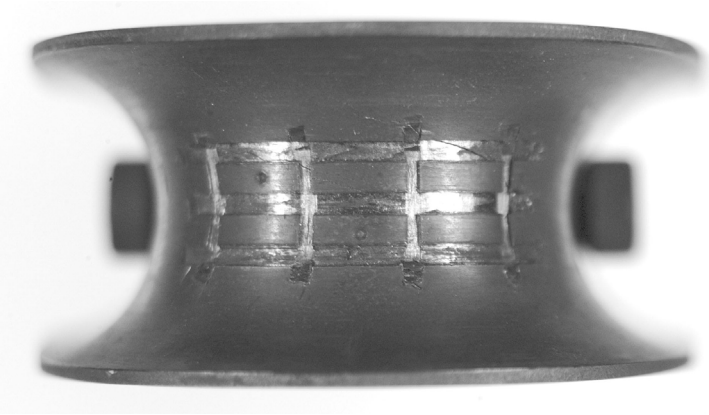

Figure A-6 Top view of scored RUB specimen showing the nature and orientation of grooves

Figure A-7 Typical printout obtained during surface profilometry. The groove depth of this particular sample is approximately 280 µm, which corresponds to 26% of the nominal wall thickness.

A.4 Results

A.4.1 Visual Inspection of RUB Specimens

The total duration of this hot steam test was 405 days with inspection intervals after 14, 30 and 60 days. The inspections were performed visually using a stereomicroscope at magnifications ranging from 25X to 40X. It should be noted that the level of detection for crack indications using a stereomicroscope at the above mentioned magnifications is approximately 150µm (0.006").

The first inspection after 14 days revealed that all scored and non-scored Alloy 600MA RUBs had developed cracking. The cracking exhibited a multi-directional nature and occurred predominantly in an area associated with the apex of the RUB specimens. A typical example of crack indications

in a scored and non-scored RUB specimen is displayed in Figure A-8 and Figure A-9. After cracking was observed in Alloy 600MA RUBs, the specimens were removed and testing was resumed with Alloy 690TT specimens only.

All of the Alloy 690TT RUB specimens did not reveal any crack indications, even after a total exposure time of 405 days. Table A-3 below summarizes the results obtained during the hot steam test for both materials in the scored and non-scored condition, respectively:

Table A-3 Results of hot steam test with RUB specimens

PWSCC Behavior of Alloy 600MA and Alloy 690TT						
Material	**scored surface**	**total No. of specimens**	**cracked RUBs after 14 days**	**cracked RUBs after 30 days**	**cracked RUBs after 60 days**	**cracked RUBs after 405 days**
690TT	yes	3	0/3	0/3	0/3	0/3
	no	3	0/3	0/3	0/3	0/3
600MA	yes	3	**3/3**	-	-	-
	no	3	**3/3**	-	-	-

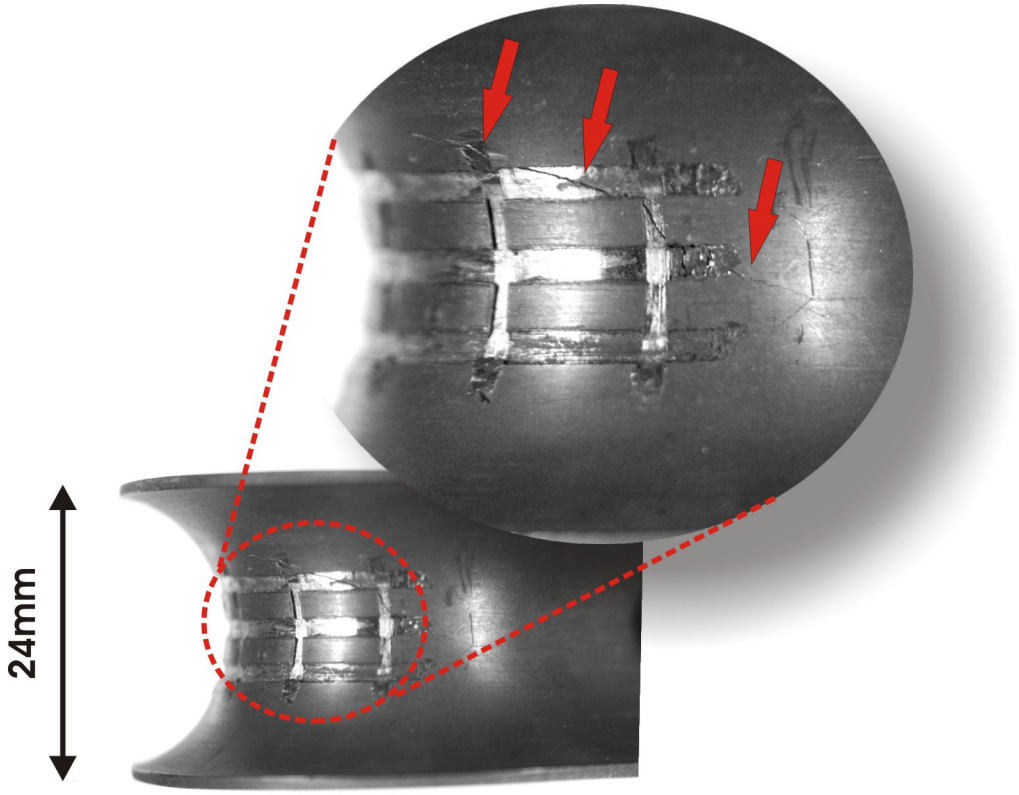

Figure A-8 Typical appearance of cracking observed in the scored Alloy 600MA specimens as indicated by the red arrows

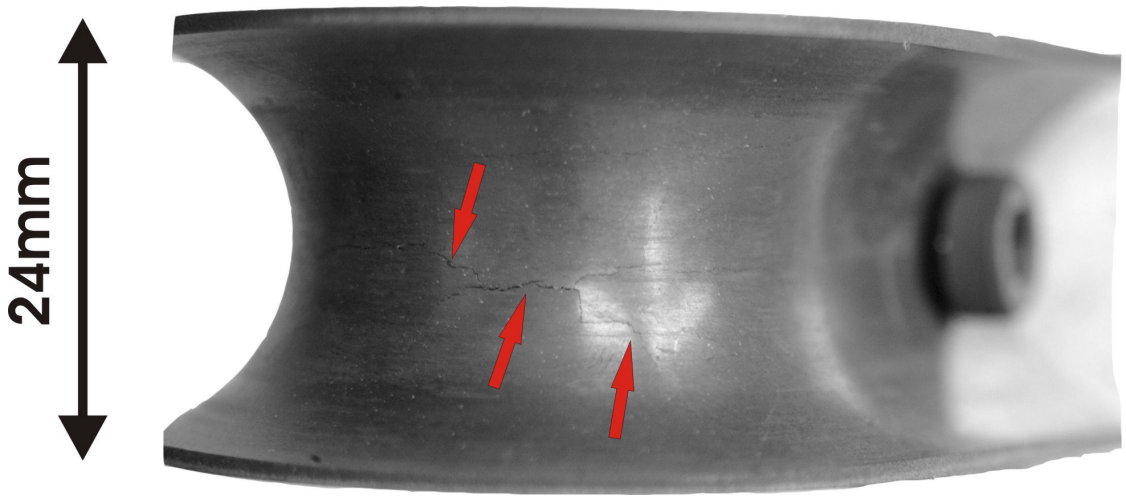

Figure A-9 Typical appearance of cracking observed in the non-scored Alloy 600MA specimens as indicated by the red arrows.

A.4.2 Metallography/Microhardness Measurements

Metallographic examination of a scored and non-scored specimen of each material was conducted. The samples were mounted into bakelite and polished to a 1µm surface finish. After etching (approximate etchant composition: 25% Ethanol, <5% HNO3, 16% HCl) the microstructure was evaluated at high magnifications with a metallograph. Also Vickers microhardness measurements (100g load – HV0.1) were conducted at selected locations.

A.4.2.1 Alloy 600MA

The microstructural examination of this material disclosed semi-continuous to a discontinuous grain boundary precipitates as a result of the final mill anneal at temperatures between 850°C and 900°C. The grain size was determined according to ASTM E 112 and was found to be 8.5 (see Figure A-10 to Figure A-13).

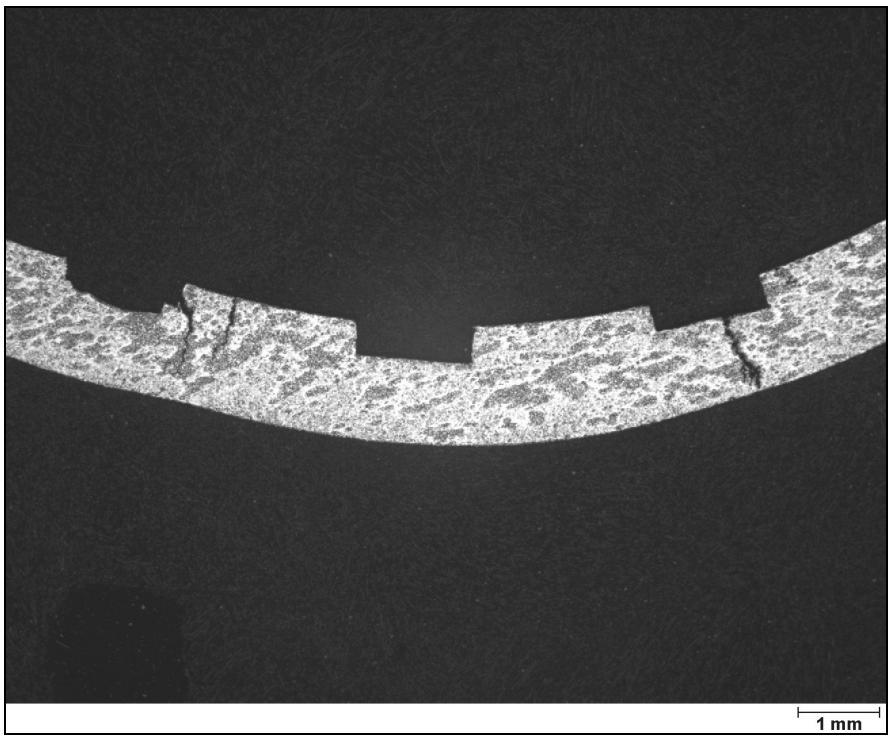

Figure A-10 Typical view of scored Alloy 600MA metallographic specimen exhibiting numerous cracks, some of which had developed into through-wall defects.

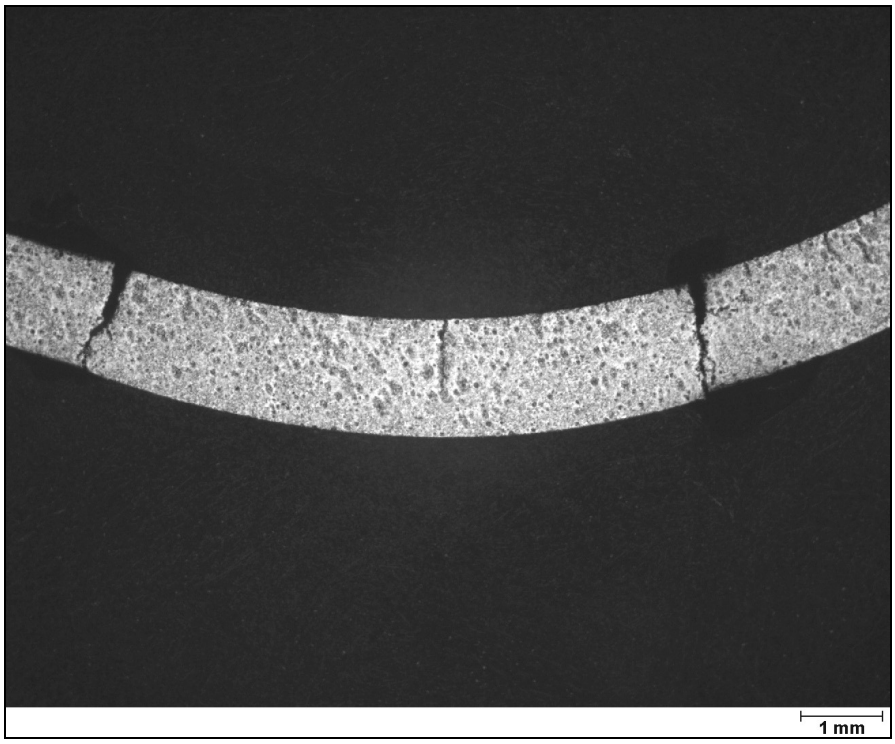

Figure A-11 Typical view of non-scored Alloy 600MA metallographic specimen exhibiting numerous cracks, some of which had developed into through-wall defects.

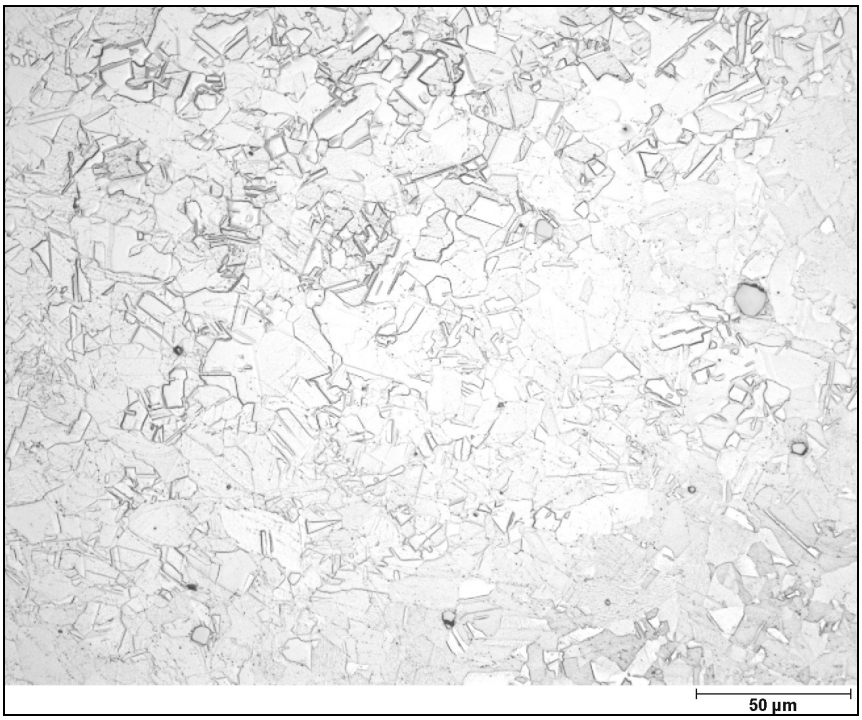

Figure A-12 General microstructure found in Alloy 600MA specimens displaying a typical austenitic appearance. The grain size according ASTM E 112 was determined to be 8.5.

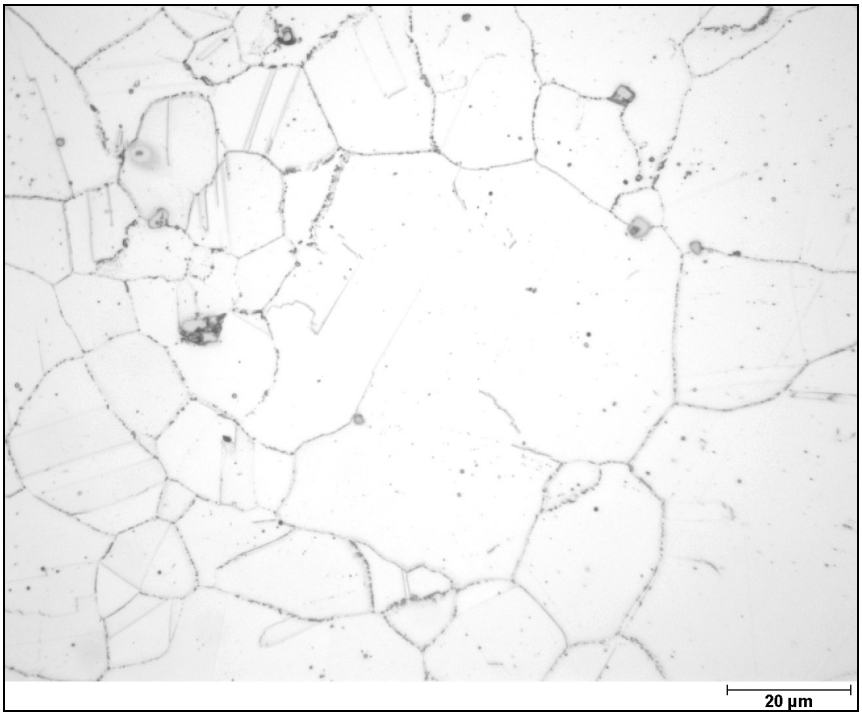

Figure A-13 Close up of Figure A-12 showing intragranular carbides and semi-continuous to discontinuous grain boundary carbide precipitates as a result of custom mill annealing at temperatures between 850°C and 900°C

Alloy 600MA specimens exhibited PWSCC on numerous locations, which appeared absolutely independent from the presence of surface marks/scores. The crack progression occurred in an intergranular manner normal to the tube surfaces. Some locations exhibited through-wall defects. Typical examples of cracking found in the Alloy 600MA specimens are shown in Figure A-14 to Figure A-16.

Vickers microhardness readings ranged from 290HV to 307HV for the bulk microstructure. Immediately adjacent to the mechanically-induced scores the microstructure yielded hardness ranging from 337HV to 345HV

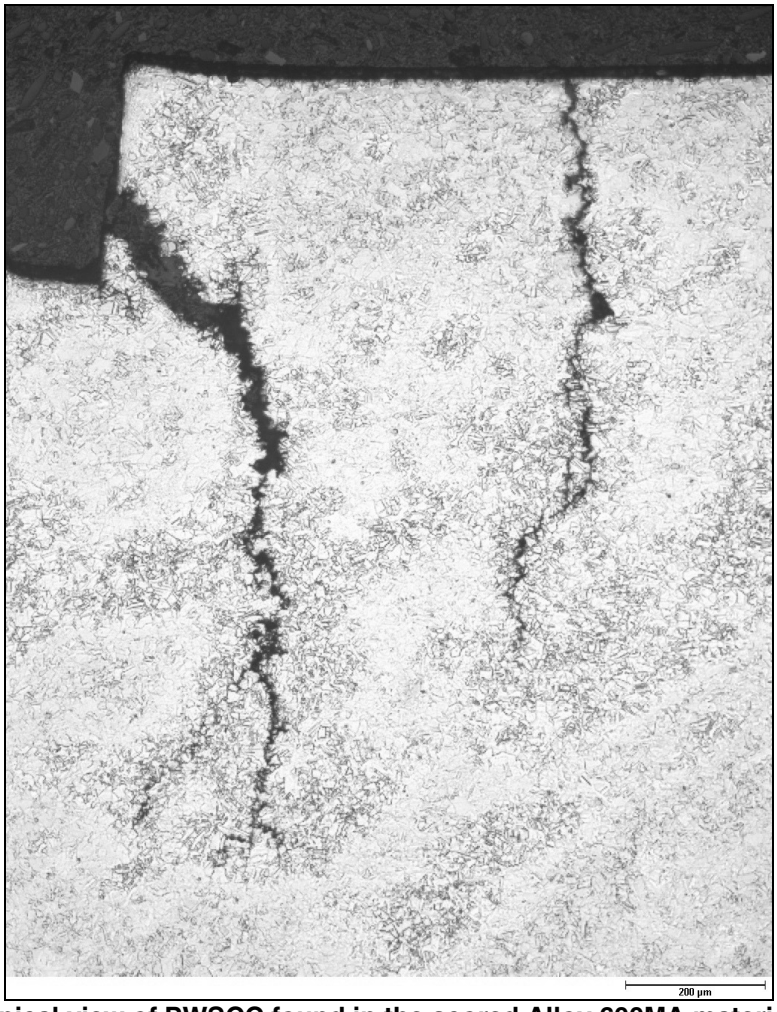

Figure A-14 Typical view of PWSCC found in the scored Alloy 600MA material; cracking initiated on the highly cold worked external specimen surface (formerly the internal SG tube surface); the crack propagation occurred in an intergranular manner.

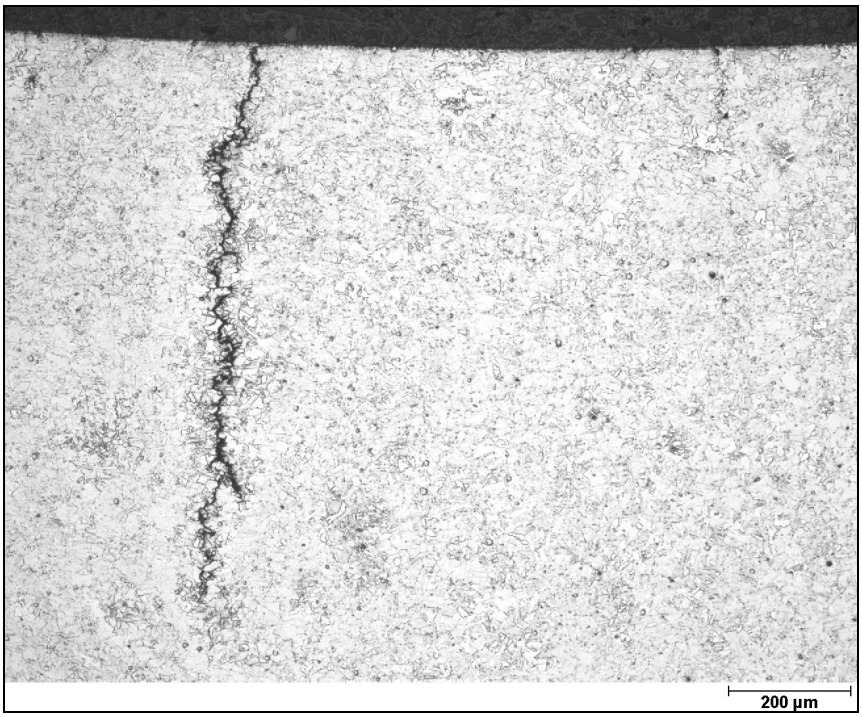

Figure A-15 Typical view of PWSCC found in the non-scored Alloy 600MA specimens also displaying an intergranular crack progression mode.

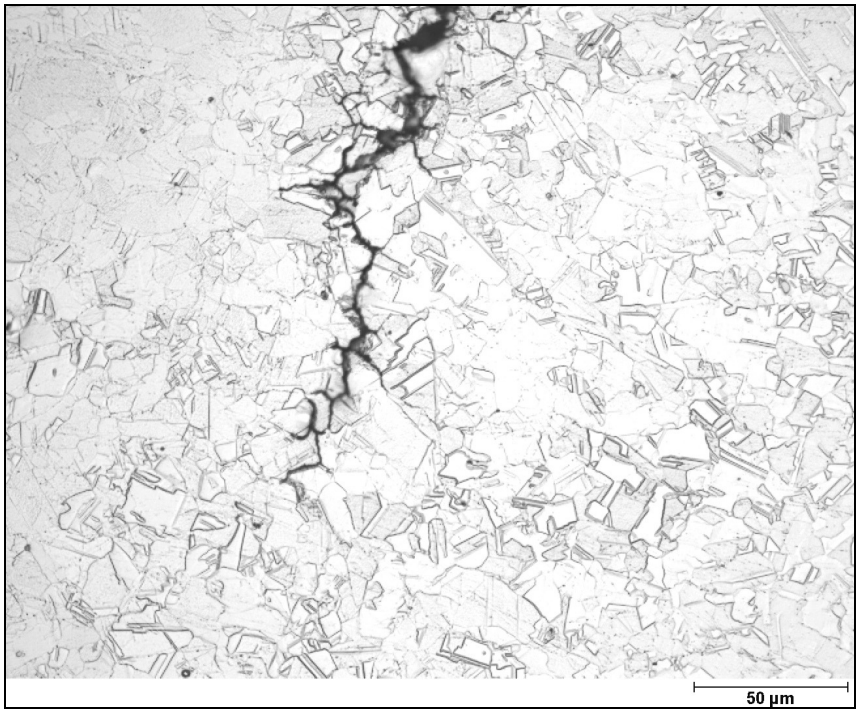

Figure A-16 Close-up of typical crack tip found in Alloy 600MA; the crack progression clearly occurred in an intergranular manner.

A.4.2.2 Alloy 690TT

The microstructure of this material appeared sound and did not show any anomalies. As expected, the matrix disclosed a semi-continuous to a continuous network of grain boundary precipitates as a result of mill annealing and the subsequent thermal treatment. The grain size was determined according to ASTM E 112 and showed relatively large variations since it ranged between 5 and 7. No crack indications were found in this material confirming the findings from visual inspection (see Figure A-17 to Figure A-21).

With a microhardness range from 260HV to 278HV for the bulk microstructure, Alloy 690TT disclosed numbers approximately 30 points lower if compared with Alloy 600MA. Locations immediately adjacent to the scores yielded numbers ranging from 327HV to 335HV, which is approximately 10 points lower if compared to Alloy 600MA.

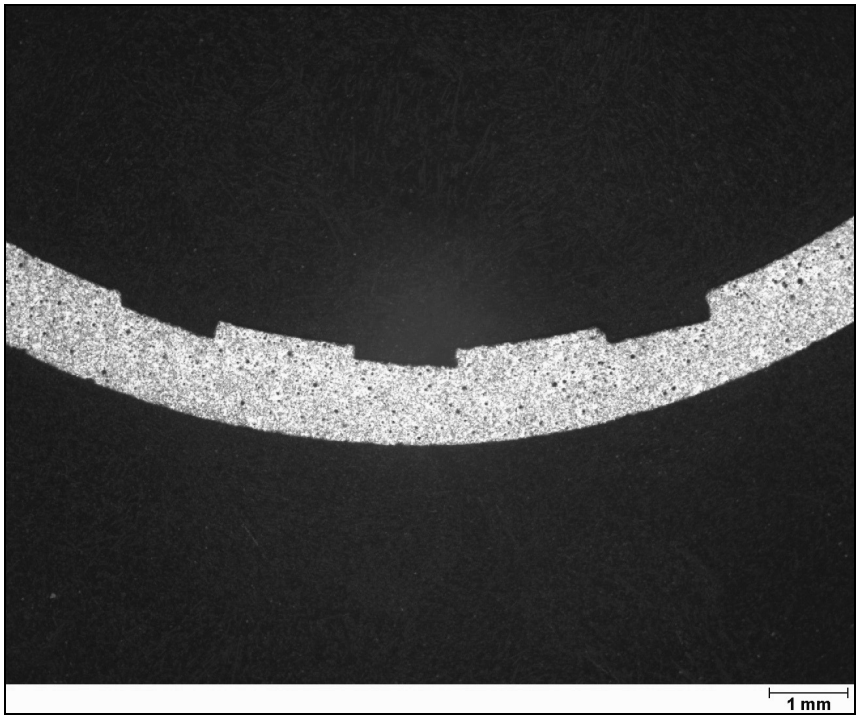

Figure A-17 Typical view of scored Alloy 690TT metallographic specimen exhibiting no PWSCC.

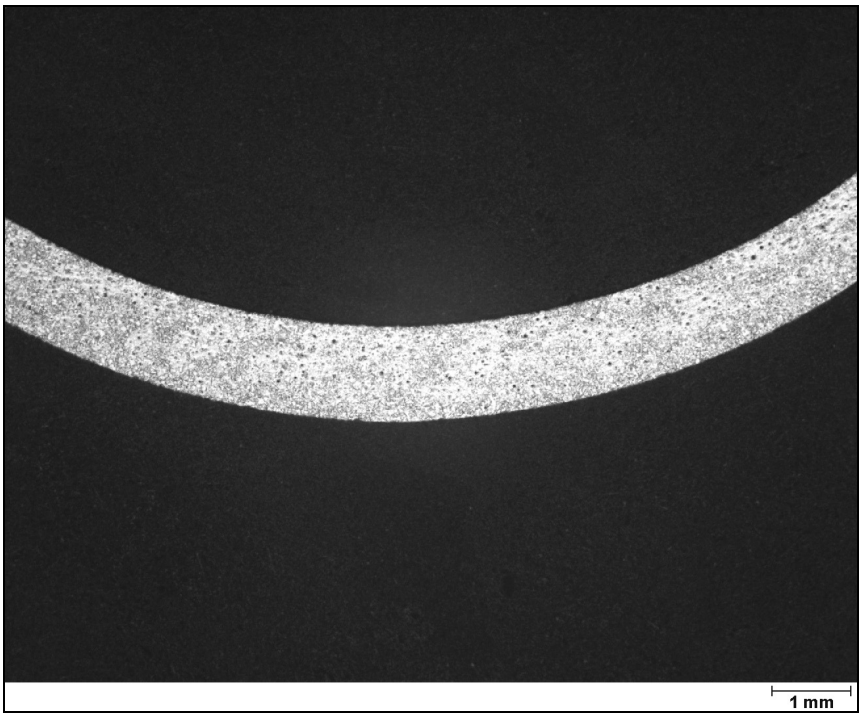

Figure A-18 Typical view of non-scored Alloy 690TT metallographic specimen exhibiting no PWSCC.

Figure A-19 General microstructure of Alloy 690TT displaying some intragranular carbides and a semi-continuous to continuous network of grain boundary carbide precipitates as a result of the thermal treatment. The grain size for this material ranged between 5 and 7.

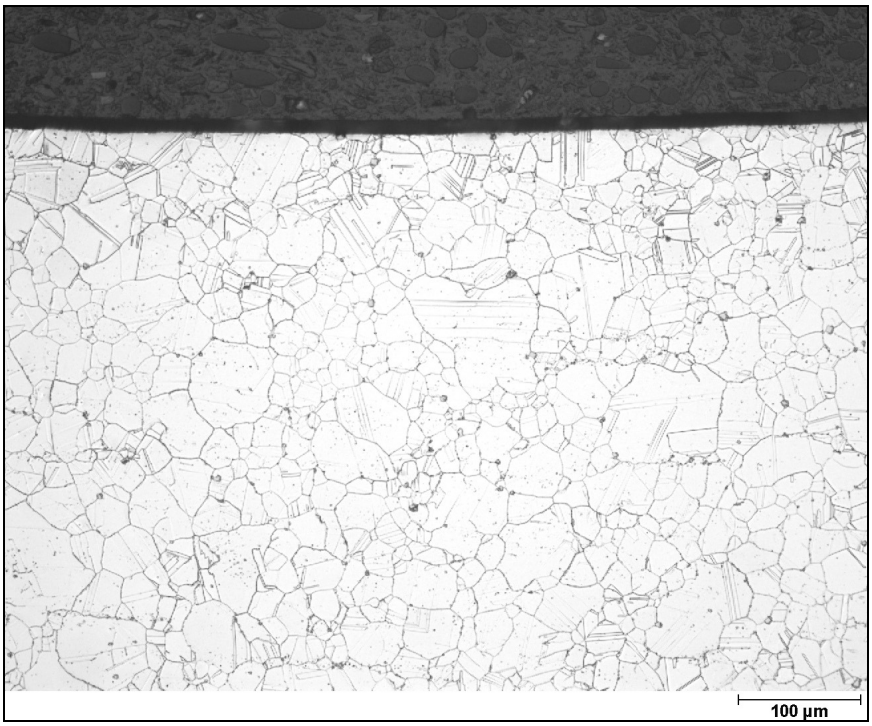

Figure A-20 Non-scored Alloy 690TT specimen showing no PWSCC.

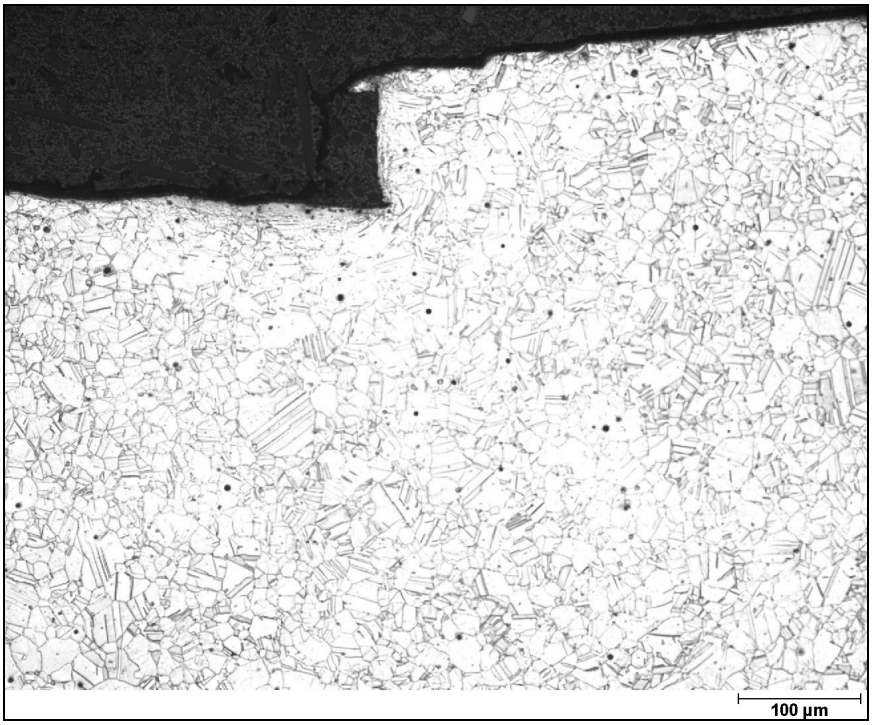

Figure A-21 Scored Alloy 690TT specimen showing no PWSCC.

A.5 Conclusions

A.5.1 Improvement Factor

One objective of this evaluation was to present the results in terms of an "improvement factor" or IFR of Alloy 690TT relative to Alloy 600MA. In this particular study the improvement factor was to be generated as follows:

$$IF_R = \frac{\text{time to crack in } 690\text{TT}}{\text{time to crack in } 600\text{MA}}$$

Since no crack initiation for Alloy 690TT was observed within the total test duration of 405 days, the improvement factor as stipulated above could not be established. However, for this particular investigation a modified improvement factor was found:

$$IF_{R\,\text{mod.}} = \frac{\text{max. exposure time } 690\text{TT}}{\text{time to crack in } 600\text{MA}} = \frac{405\ d}{14\ d} \approx 30$$

A.5.2 Quantification of Experimental Data/Margin of Improvement

The hot steam test using RUB specimens proved to be a suitable test to compare the two materials. It allowed a distinct differentiation between Alloy 600MA and Alloy 690TT with respect to their PWSCC behavior. Unlike initial concerns, the high degree of cold work and the corresponding residual stresses inherent to this type of test with RUB specimens did not diminish the benefit provided by Alloy 690TT.

RUBs manufactured from Alloy 600MA exhibited PWSCC after an exposure time of only 14 days (the actual crack initiation might have occurred even earlier, but the first inspection interval was stipulated after 14 days). These findings in Alloy 600MA were independent from the presence of surface marks/scores since they were observed at the same level of severity in scored and non-scored samples. The crack formation occurred predominantly at the RUB's apex corresponding to a highly cold worked area.

In contrast, Alloy 690TT showed no cracking in all of the specimens, even after a total exposure time of 405 days. Both, the scored and the non-scored specimens remained unaffected. Findings gained during this experiment correspond with results presented by Gimond [86]. There, non-scored 690TT RUBs were exposed to very similar conditions (400°C; 1 bar H_2 partial pressure) and did not show any indications of PWSCC after a total exposure time of 6000h (250 days).

A.5.3 Comparability of Experimental Data to In-Service Conditions

The time necessary to initiate cracking in Alloy 600MA RUBs can be reduced down to several days under laboratory conditions by means of hot steam techniques (i.e. temperature, defined hydrogen pressure).

PWSCC in Alloy 600MA tubing was observed in row 1 U-bends of actual SGs after approximately one year of plant operation. According to [87], the configuration of a RUB specimen is comparable to a row 1 U-bend tube. However, the tighter bend radius and the split-tube configuration of the RUB specimens accelerate the time necessary to initiate cracking by a factor of 2 to 3, if compared to an actual row 1 U-bend. Thus, the time necessary to initiate cracking in an actual row 1 U-bend under hot steam test conditions is 14 to 21 days. Based on the geometry of a row 1 U-bend, the conclusion can be drawn that one year of plant operation corresponds to approximately 20 days under hot steam test conditions. With respect to this last statement, an exposure to hot steam under laboratory conditions for 405 days without cracking corresponds to approximately 20 years of plant operation for a row 1 U-bend.

B TESTS ON MOCK-UPS REPRESENTATIVE OF ROLLING ZONES OF STEAM GENERATOR TUBES IN HIGH TEMPERATURE, HYDROGENATED, PURE WATER AT 360°C – A FRAMATOME ANP (FRANCE) REPORT

B.1 Introduction

The widespread occurrence of Primary Water Stress Corrosion Cracking (PWSCC) of Alloy 600 in PWRs has led manufacturers to propose its replacement for many key component items such as steam generator (SG) tubes and reactor vessel (RV) upper head penetration nozzles by Alloy 690. Despite the excellent operating experience to date with Alloy 690 (up to 15 years in the case of the replacement of SG tube bundles and up to 10 years for replacement RV upper heads), safety authorities worldwide have been reluctant to relax stringent inspection regimes imposed to manage the degradation of Alloy 600 in PWR primary water service. Consequently, there is a strong economic incentive to develop and quantify the margin of improvement resulting from the use of alloy 690 replacement materials with the immediate aim of relaxing the number and extent of costly non-destructive examinations.

The present report deals with the results of a long term study of the resistance to PWSCC of mock-ups representative of the roll transitions of SG tubes close to the tubesheet, comparing the performance of Alloys 690 and 600. Mock-ups were manufactured using three tube materials; Alloy 600 MA, Alloy 600 TT and Alloy 690 TT. The Alloy 600 tubes were standard products used for SG manufacture. The Alloy 690 TT tubes are a pre-series lot from a tube mill later used for production runs. The pre-series lot of Alloy 690 TT (WE092) was considered to be potentially more sensitive to PWSCC than the standard tubes produced thereafter based on standard comparative laboratory tests such as the slow strain rate test (SSRT). The tests reported here were performed during a 15 year period; the destructive examinations of the mockups were completed during 2002.

B.2 Experimental

B.2.1 Materials

Four heats of SG tubing were used in this program:

Alloy 600 tubes:

WD281 MA: ¾" diameter tubes manufactured by Vallourec (now Valinox) SA from ingots made by Imphy SA

WD281 TT: ¾" diameter tubes manufactured by Vallourec (now Valinox) SA from ingots made by Imphy SA. These tubes were thermally treated.

NX3335 MA: 7/8" diameter tubes manufactured by Huntington Alloys (now Special Metals).

These tubes were typical of manufacturing practice ~16 years ago with a mill annealing temperature at 980°C and the thermal treatment was 700°C for 15 hours.

Alloy 690 tubes:

WE094 TT: ¾" diameter tubes manufactured in a pre-production run by Imphy SA. Again, the tubes were typical of manufacturing practice about 16 years ago. The origin and thermal history of this particular heat has been extensively discussed in Section 3.2.2.7. The tubes were mill annealed at 980°C and thermally treated at 700°C and then mill annealed again as follows:1040°C / 3 min then 700°C / 5 hours in order to ensure the mechanical properties were within specification. As a consequence, the grain size was unusually small and the carbides were mainly intragranular rather than intergranular as described in Section 3.2.2.7.

Table B-1 shows the chemical composition of the different heats of material used in this study while Table B-2 gives the mechanical properties.

The grain size of the Alloy 690 at mid-thickness was aproximately10 µm (ASTM #10) but a perturbed layer was detected on the inner surface of the tube. This layer was characterized by a finer grain size of about 2µm (ASTM #15), the presence of dense carbide precipitates and a higher hardness. Figure B-1 shows, as an example, a view of the microstructure at mid thickness, and in Figure B-2 a typical view of the inside perturbed layer. Figure B-3 shows measurements of the hardness across the tube thickness revealing the increased hardness near the inner surface over about 100 microns in depth. This structure was typical of the pre-series heats, which were the only ones available when the mock-ups were manufactured. Since then, Alloy 690 TT tubes used in steam generators have been given much more rigorous quality control and the inner surfaces are free of such perturbed layers.

Table B-1 Chemical composition of the tested materials

Element	RCCM M4101 Specification Alloy 600	WD281	NX3335	RCCM M4105 Specification Alloy 690	WE094
C	0.010 / 0.050	0.035	0.03	0.010/0.030	0.027
Si	< 0.50	0.33	0.16	< 0.50	0.28
S	< 0.015	0.001	< 0.005	< 0.010	0.002
P	< 0.025	0.010	0.010	< 0.010	0.005
Mn	< 1	0.81	0.14	< 0.50	0.23
Ni	> 72.00	73.40	75.11	> 58.00	61.29
Cr	14.00 / 17.00	16.03	15.76	28.00 / 31.00	28.99
Cu	< 0.50	0.01	0.11	< 0.50	0.01
Co	< 0.10	0.013	0.036	< 0.035	0.01
Ti	< 0.50	0.21	0.10	< 0.50	0.25
Al	< 0.50	0.25	0.081	< 0.50	0.17
Fe	6.00 / 10.00	8.89	8.45	8.00 / 11.00	8.75
N	-	0.0158	-	< 0.05	-

Table B-2 Mechanical properties of the tested materials

Parameter		WD281 MA	NX3335	WE094
Yield strength (MPa)	**20 °C**	339	329	419
	343°C	262	266	358
Ultimate strength (MPa)	**20°C**	723	721	825
	343°C	675	623	723
Elongation (%)	**20°C**	41.7	41.3	37
	343°C	39.1	36.1	36

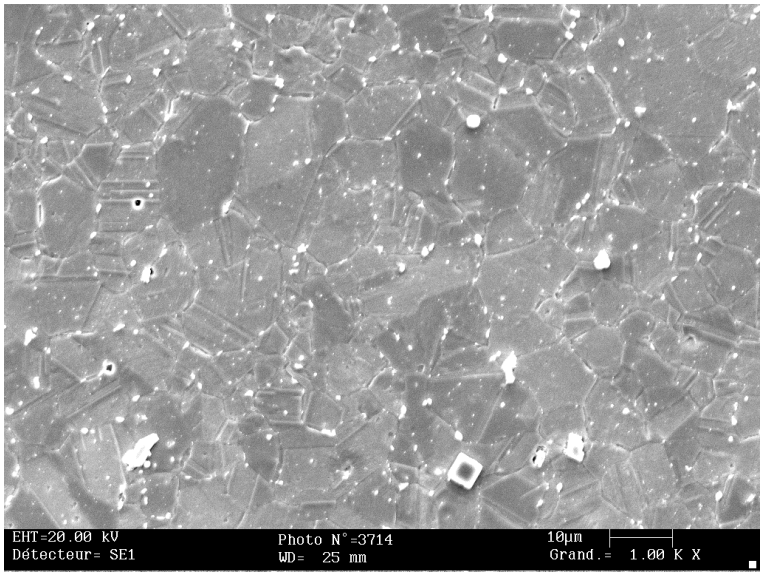

Figure B-1 Structure of the Alloy 690 TT WE 094 tube at mid thickness.

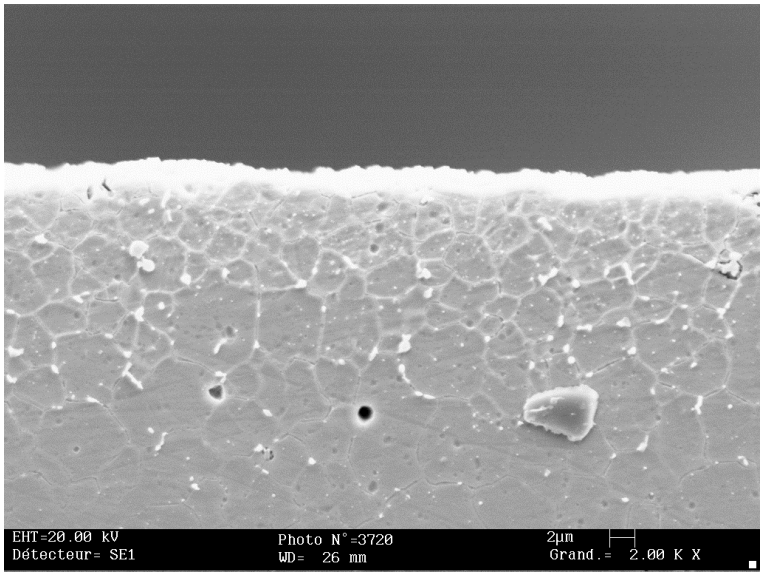

Figure B-2 Structure of the Alloy 690 TT WE 094 tube at the inner surface.

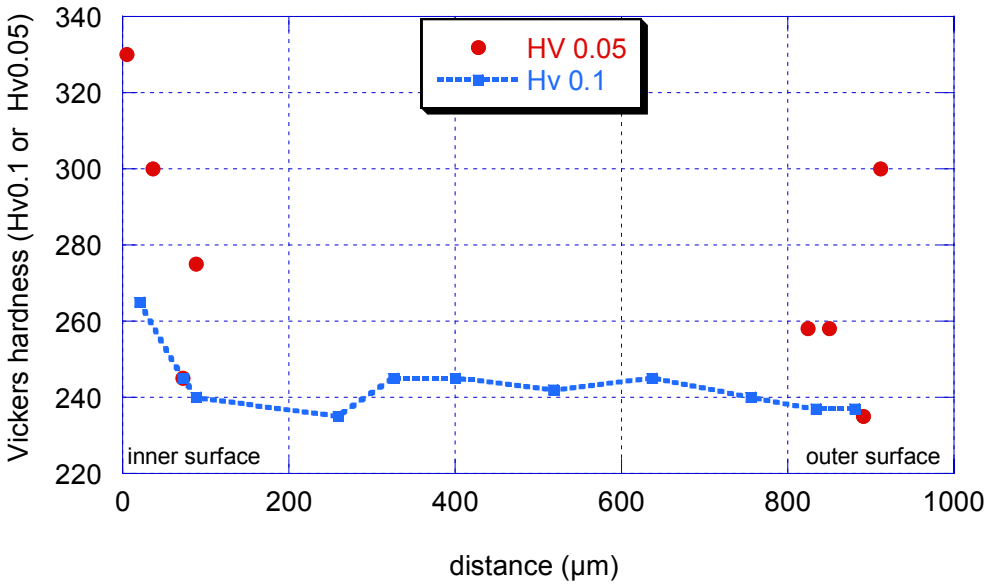

Figure B-3 Hardness across the Alloy 690 TT WE 094 tube wall thickness.

B.2.2 Mock-up manufacture

The mock-ups were manufactured by Framatome-ANP at the factory located in Chalon sur Saône using the same tools and procedures as those used for PWR steam generators. Each mock-up consisted of a SG tube section and a thick carbon-steel cylinder representing the top side of the tubesheet. The tube section was expanded into holes drilled in the carbon steel cylinder representing the tubesheet using a mechanical rolling tool. Four rolling steps were needed inside each carbon steel cylinder. A kiss-rolling step was then carried out on each side of the carbon steel cylinder. Thus, two roll transition zones were available on each mock-up, as represented in Figure B-4, which shows a cross section view of the standard mock-up design. In addition, between the two roll transition zones, several nonconformities such as a lack of overlap between two rolling steps or a skipped roll step were introduced in some cases. Such fabrication nonconformities were known to be extremely detrimental for primary water side cracking of tubes in the case of steam generators with Alloy 600 tube bundles; see Section B-4.

Kiss rolling, illustrated in Figure B-4, is the process by which of a double step is introduced between the diameter of the free span of an SG tube and the expanded tube diameter in the tube sheet. During the roll expansion of many thousands of tubes, it is possible to miss a step in the roll expansion in the tube sheet, which is known as a "skip roll". If the expanded roll diameter of the tube in the tube sheet projects above -4 mm with respect to the tube sheet upper surface, this is known as an "over-roll".

All the mock-ups were characterized by profilometry using eddy current or ultrasonic techniques.

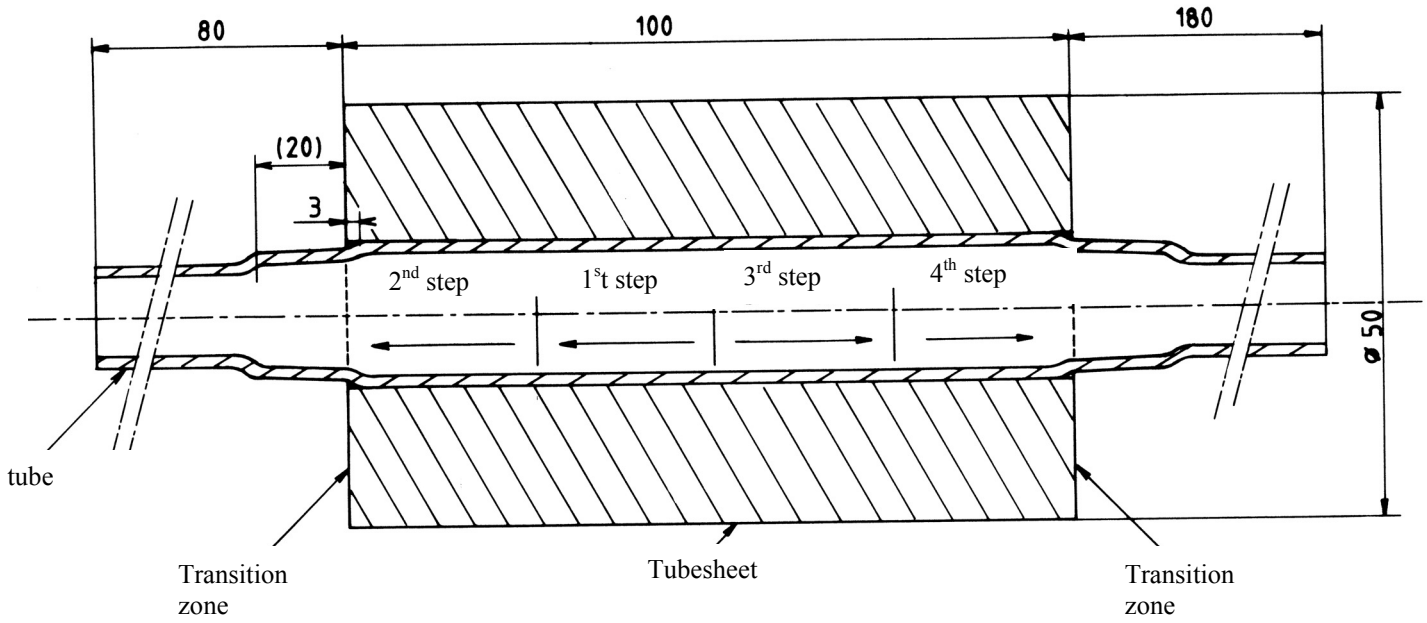

Figure B-4 Sketch of a standard mock-up (dimensions in mm).

The total number of roll transition zones manufactured from Alloy 690 TT was 16 whereas 40 were manufactured from the Alloy 600 heats. The mock-ups (each comprising two roll transition zones) were identified with a number between 1 and 21 for the Alloy 600 mock-ups and between 501 and 508 for Alloy 690 TT mock-ups. A letter (H or B, corresponding to the upper or lower orientation in the furnace, respectively) was also added to the identification number for each transition zone.

An Alloy 600 plug was manual metal arc welded into each end of the mock-ups in order to form a capsule. During this operation, the tube was cooled in order to maintain the residual stresses in the roll transition zones introduced by the roll expansion. Each mock-up (capsule) was equipped with small stainless steel tubing to allow the test environment to be introduced, a high pressure valve, a manometer and an external thermocouple inserted in the carbon steel sheet as shown in Figure B-5.

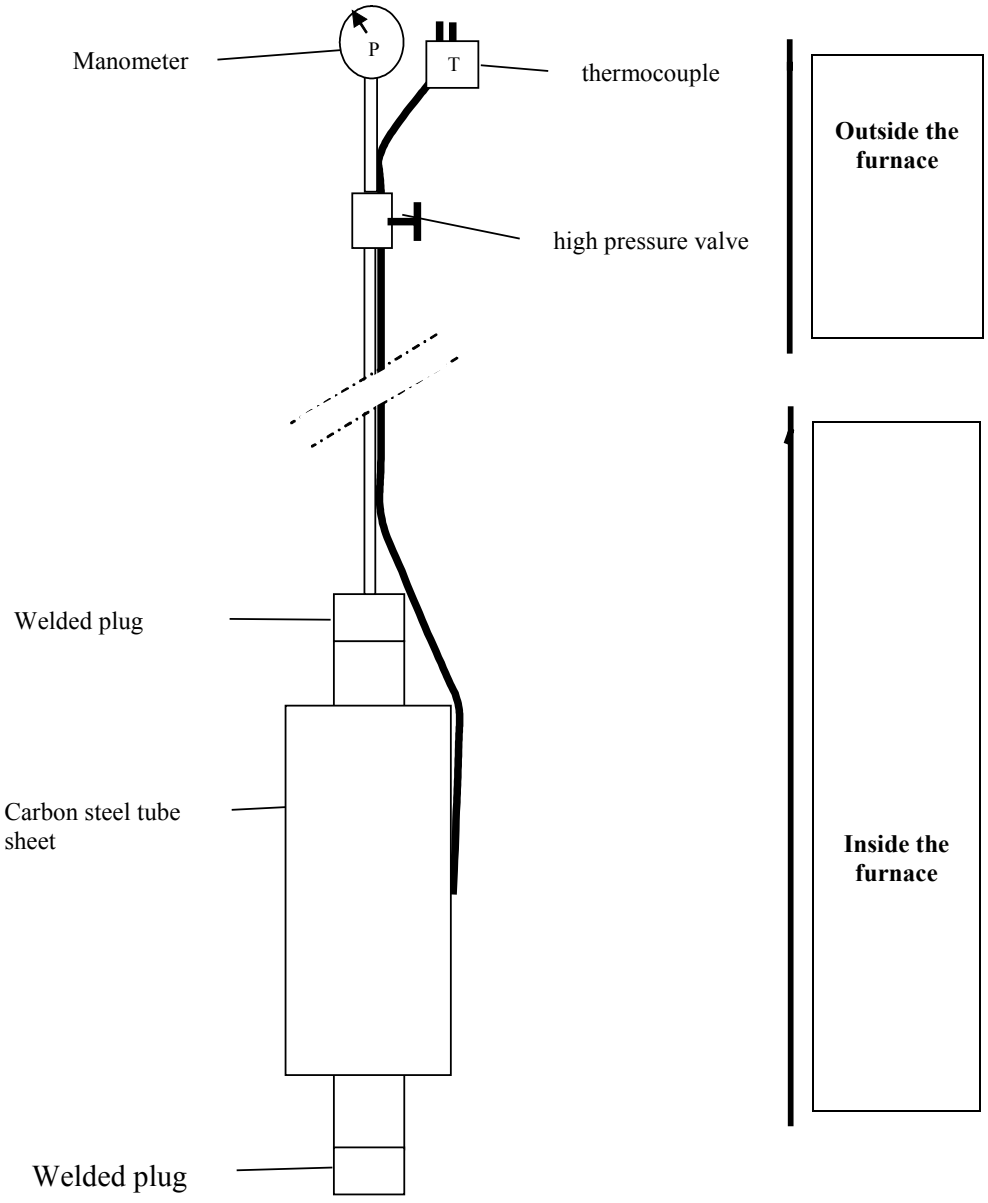

Figure B-5 Schematic representation of the mock-ups for long-term exposure tests.

B.2.3 Test procedure

A specific test procedure was defined for the preparation of the long-term exposure tests including intermediate interruptions for capsule inspection and renewal of the test environment.

The test environment was high purity deaerated water with a hydrogen overpressure. This environment was chosen to facilitate good control of the test environmental parameters and also knowing that hydrogenated pure water is slightly more aggressive from the stress corrosion viewpoint than PWR primary water that also contains lithium hydroxide and boric acid in varying concentrations throughout any given fuel cycle. The single parameter used to monitor

the quality of the aqueous environment was a measure of conductivity because the total volume of the capsules was too small for repeated sampling for chemical analyses.

The mock-ups were introduced into a furnace whose temperature was subsequently controlled at 360°C. Before heating, the mock-ups were carefully washed with demineralized and deaerated water at room temperature (RT) until the conductivity was lower than 1 µS/cm and then subsequently at 200 and 290°C until the conductivity of the effluent washing water was lower than 2 µS/cm.

The test procedure at the beginning of each exposure period comprised the following steps:

- Filling the mock-up/capsule; Evacuation of the air and introduction of a specified volume (35 cm^3) of high purity demineralized water (conductivity < 0.5 µS/cm). Removal of the residual atmosphere with a vacuum pump during 1 hour in order to deaerate the aqueous environment.
- Verification of leak-tightness: Introduce argon at a pressure of 170 bars. Monitor the total pressure during 48 hours; a decrease of pressure less than 20 bar was acceptable.
- Conditioning: Reduce the argon pressure to 10 bars and inject hydrogen up to a total pressure of 35 bars.
- Heating up: Place the mock-up in the furnace and heat to 360°C.

B.2.4 Monitoring the mock-up's during exposure tests

During the exposure period at 360°C, the total pressure of each mock-up/capsule was between 190 and 210 bars. The temperature control assured a temperature of 360°C± 3°C for each individual mock-up. During the exposure period, the total pressure and the temperature of each mock-up was monitored twice a day. Every 4 to 6 weeks, each mock-up was cooled to RT and the overpressure was adjusted to 35 bars by hydrogen injection.

If the total pressure of any mock-up decreased for any reason, it was cooled to RT outside the furnace and the internal pressure of the mock-up concerned was then increased to 180 bar with argon. Leakage of any gas was revealed and localized by bubbling in a water container. If the leak was located in the roll expanded zone, a destructive examination was carried out. For leaks located in the transition zones (H or B), the mock-up was machined in such a way as to isolate the cracked zone and to allow the other part to be sealed and pressurized as a single-zone mock-up for a further exposure period. If the leak was located in the tubesheet (at a transition zone of a skipped roll step or between two roll steps without overlap, for example) the mock-up was destructively examined in its entirety. Cracks were located by ultrasonic testing (UT) or Eddy Current testing (ET) inspection and were then characterized by liquid dye-penetrant testing (PT) and by optical binocular examination of flattened half-tubes. Subsequently, any cracks were examined by Scanning Electron Microscopy (SEM).

B.3 Alloy 690 TT Mock-Up Results

B.3.1 Test Results

Table B-3 gives fabrication details of all the tested mock-ups (with two rolling transition zones on each mockup).

Table B-3 Characteristics of the Alloy 690 TT mock-ups.

Mock-up	Rolling		Kiss-roll expansion Ø (mm)	Skip-roll
	Tube /tubesheet gap (mm)	Over-roll (mm)		
501 H	0.4	-1.5	0.15	No
501 B	0.4	-1.5	0.30	
502 H	0.4	+1.5	0.15	No
502 B	0.4	+1.5	0.30	
503 H	0.4	+ 20	0.15	No
503 B	0.4	+ 20	0.30	
504 H	0.4	- 1.5	0.15	Yes
504 B	0.4	+ 20	0.30	
505 H	0.95	-1.5	0.15	No
505 B	0.95	-1.5	0.30	
506 H	0.95	+1.5	0.15	No
506 B	0.95	+1.5	0.30	
507 H	0.95	+ 20	0.15	No
507 B	0.95	+ 20	0.30	
508 H	0.95	- 1.5	0.15	Yes
508 B	0.95	+ 20	0.30	

The rolling conditions can be summarized as follows:

3 zones with standard specification rolling and kiss-rolling, nominal tube/ tubesheet gap (0.4 mm), nominal over-roll (between – 1.5 and + 1.5 mm), no non conformity in tubesheet

8 zones with high tube/tubesheet gap (0.95 mm),

8 zones with excessive kiss-roll expansion (0.30 mm),

6 zones with excessive over-roll (about 20 mm),

2 mock-ups with a skip-roll.

Throughout the exposure period at 360°C the conductivity of the aqueous environment was less than 1 µS/cm. After, the first and the sixth test periods of about 10,000 hours, the water from several mock-ups was sampled and analyzed. The results are given in Table B-4.

Table B-4 Chemical analysis of the aqueous environment in the mock-ups after the 1st and 6th test period of 10,000 hours

Mock-up	501+503+504+507		502+505+506+508	
	1st period	6th period	1st period	6th period
Cl^- (mg/kg)	0.7	0.46	0.4	0.57
F^- (mg/kg)	0.08	0.56	0.25	0.05
Na^+ (mg/kg)	0.19	0.43	0.14	0.10
SiO_2 (mg/kg)	0.71	4.3	0.43	4.8

During the first 17,000 hours of the exposure period, no hydrogen was injected in the mock-ups. Subsequently, an overpressure of hydrogen of 15 bar was added at the beginning of each test period and was renewed every 2 months when half of the over-pressure was lost by diffusion.

Testing of the Alloy 690 TT mock-ups lasted 100,000 hours at 360°C (10 periods of 10,000 hours) and an internal total pressure between 210 and 230 bar was maintained. No leak occurred during this entire test duration on any mock-up. One mockup, 506, was extracted for destructive examination after 60,000 hours of test.

B.3.2 Mock-up examinations

B.3.2.1 Examination of mock-up 506 after 60,000 hours exposure

Liquid dye-penetrant test

A liquid dye-penetrant test was performed after splitting the mock-up longitudinally into two half tubes. One was preserved and the other was flattened with the aim of opening up any existing flaws. Figure B-6 shows the two half tubes. No indication of any kind was observed on the two half tubes. However, a pink coloration was observed on the flattened tube and was probably due to small flaws that are homogeneously dispersed on the perturbed inner surface of the tube, as revealed by later more detailed examinations.

Figure B-6 Liquid penetrant test on mock-up 506. View of the two half tubes after splitting the mock-up longitudinally (the right hand half is flattened, the other is not flattened).

SEM surface observations

The internal surface of the two half tubes was examined by SEM. Special attention was paid to detecting possible small flaws in the different roll transition zones.

On the non-flattened half tube, some tiny cracks were observed on the inner tube surface in the transition zones of the kiss rolling. Their length was about 1.5 mm and their width 2 µm. Figure B-7, Figure B-8, and Figure B-9 show examples of such microcracks at the limit of the rolling zone on each side of the roll transition (506B and 506H).

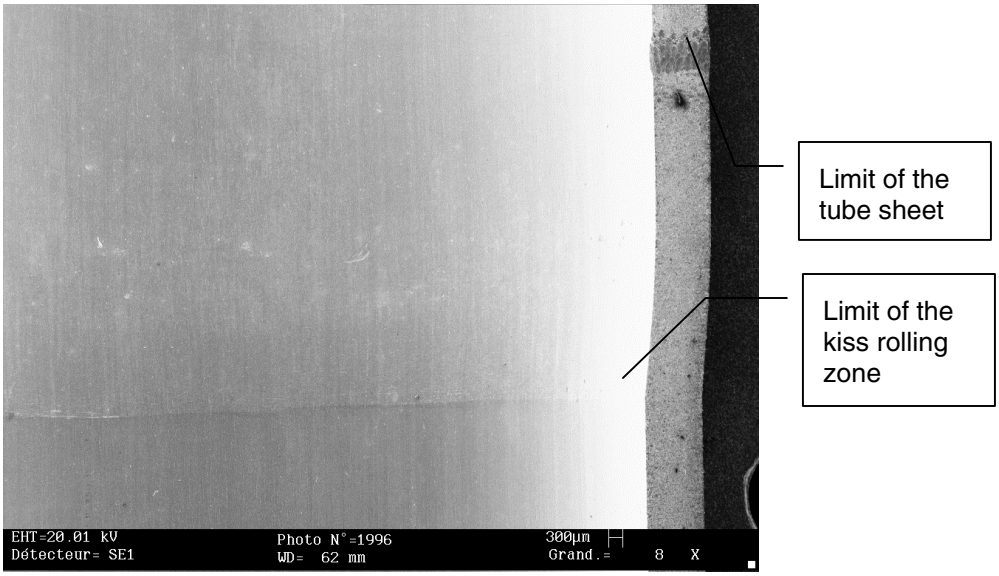

Figure B-7 Macrograph of the non-flattened half tube at the limit of the rolling zone 506B.

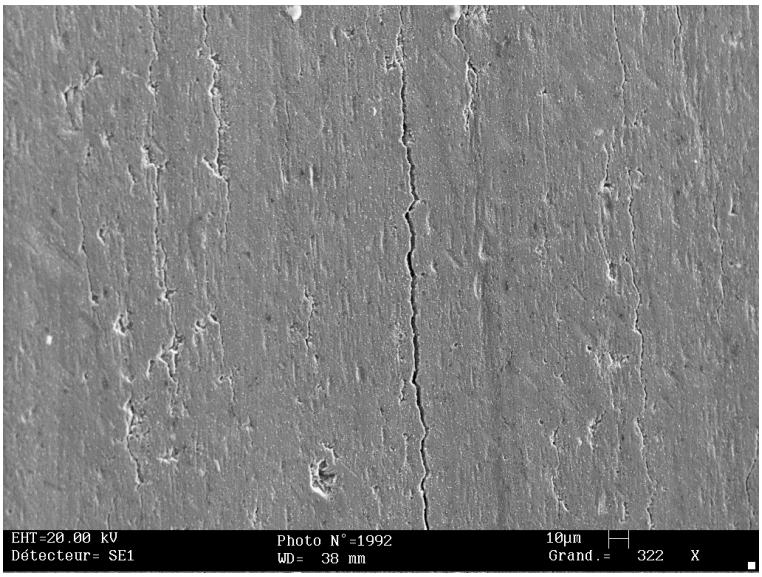

Figure B-8 SEM view of the inner surface of the non-flattened half tube at the limit of the rolling zone 506B.

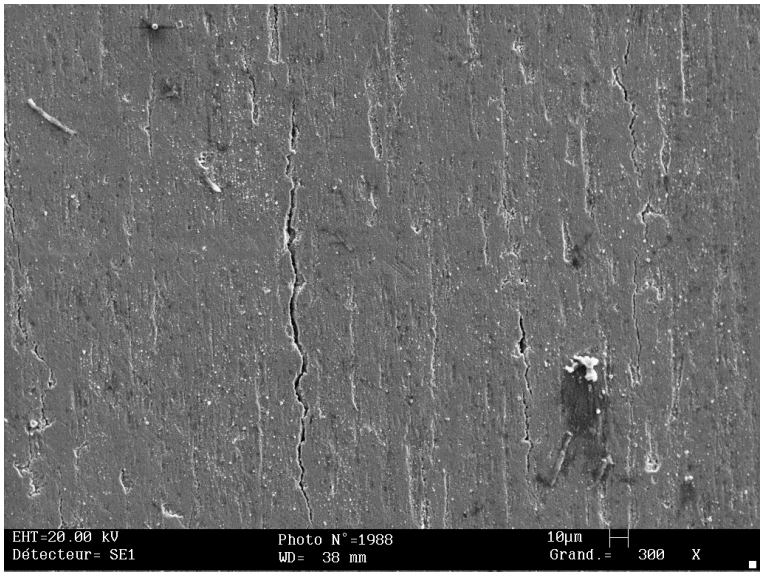

Figure B-9 SEM view of the inner surface of the non flattened half tube at the rolling zone limit 506H.

Examination of the flattened half tube revealed the presence of many microcracks. Figure B-10 and Figure B-11 show views of the limiting edges of the kiss rolling of 506B: some of the opened microcracks corresponded to those that were also observed before flattening but numerous others were new ones opened or created during the mechanical flattening operation. This type of flaw was also observed on parts of the tube which were not rolled, which is remote from the rolled zone.

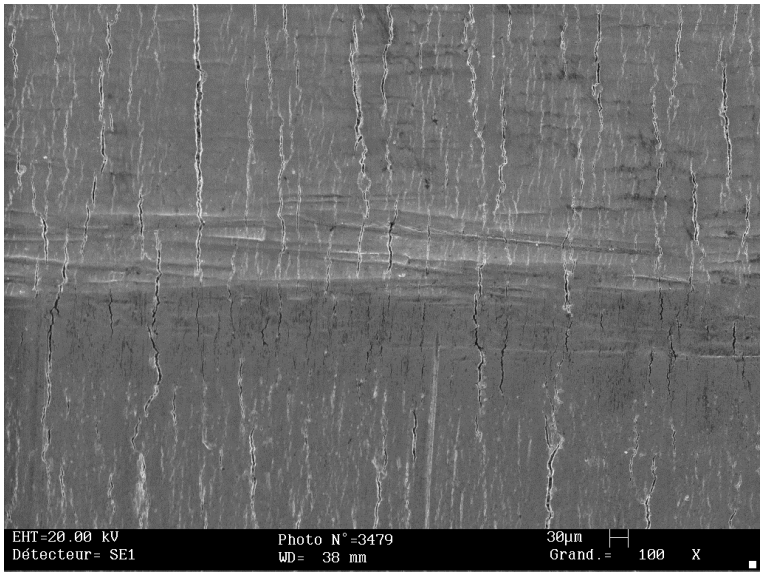

Figure B-10 Limit of the kiss rolling zone of the flattened half tube 506B (Maximum length of the microcracks: 1.5 mm).

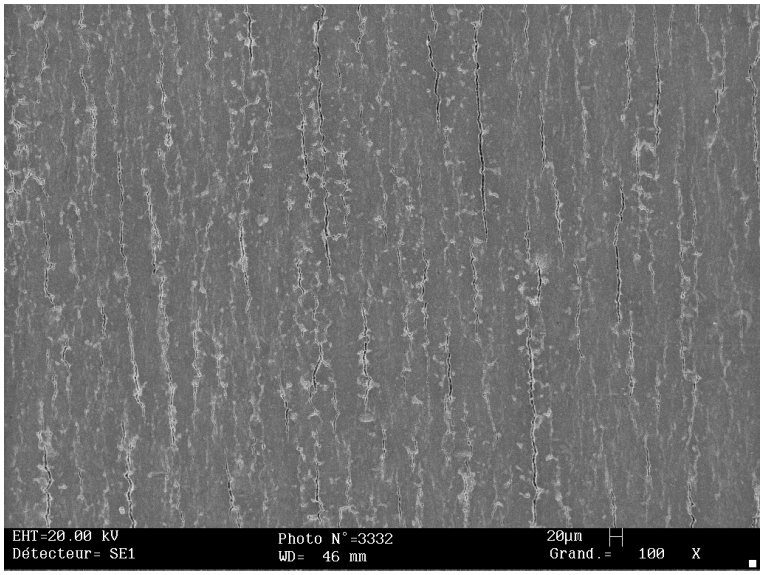

Figure B-11 Limit of the rolling zone of the flattened half tube 506B (Maximum length of the microcracks: 0.5 mm).

SEM metallographic examination

The microcracks were fully characterized by metallographic examination. They were intergranular and their length was always limited to the thickness of the perturbed surface layer on the internal surface of the tube (about 10 µm thick in this case). Figure B-12 and Figure B-13 show examples of such flaws observed at the limit of the kiss rolling zone of 506B.

For comparison, Figure B-14 and Figure B-15show typical microcracks observed in a sample taken away from the rolled zone of the flattened half tube. These cracks were also observed to be limited to the perturbed surface layer.

The conclusions of these examinations were:

The wide microcracks were due to the strain induced by rolling and were limited to the hard perturbed surface layer already present on the inside surface of the tube in the as-received condition.

These microcracks were intergranular but did not propagate in the tube during exposure to hydrogenated water at 360°C during 60,000 hours exposure.

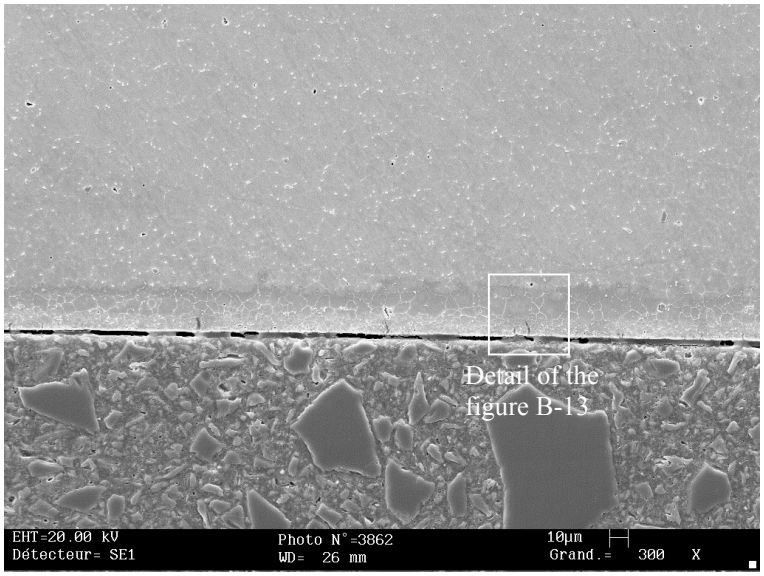

Figure B-12 SEM view of a etched circumferential cross section at the limit of rolling zone 506B.

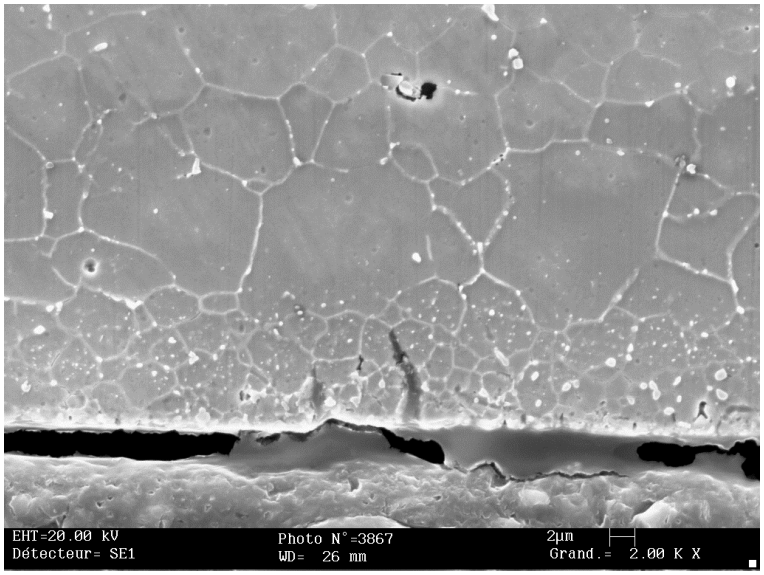

Figure B-13 SEM view of a etched circumferential cross section of the limit of rolling zone 506B. Detailed view.

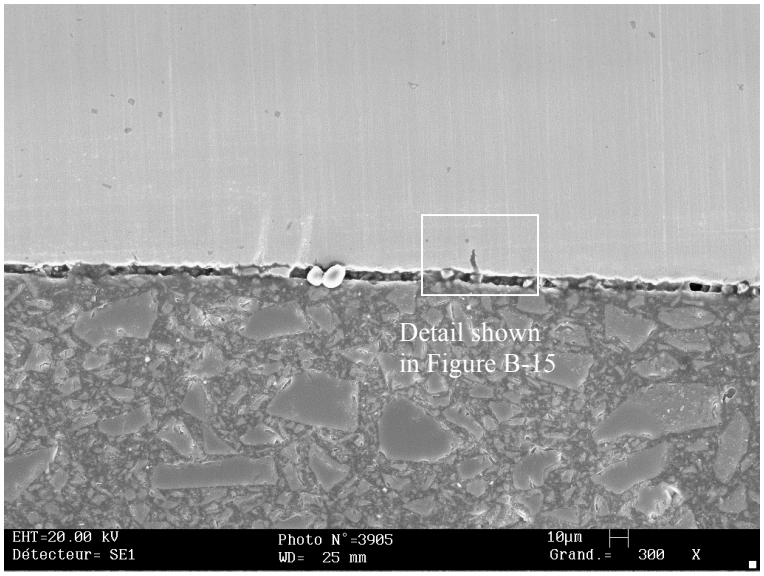

Figure B-14 SEM view of a circumferential cross section of the tube outside the rolling zone (unetched surface).

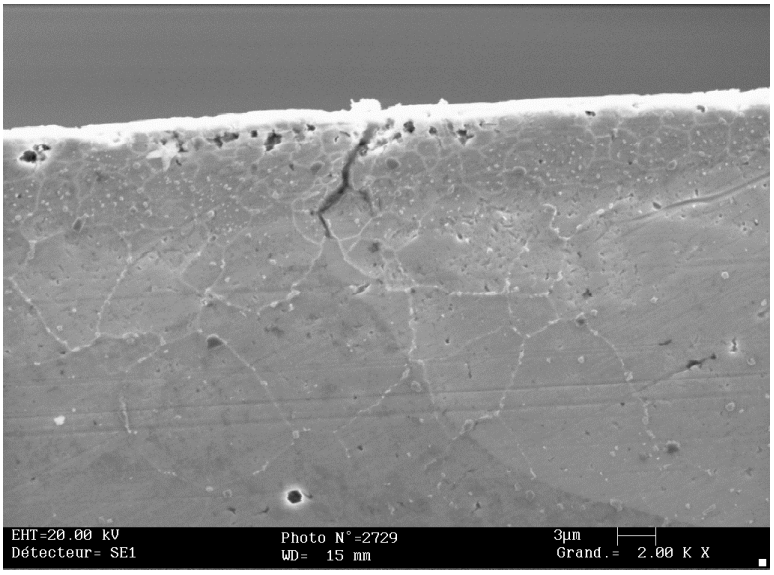

Figure B-15 SEM view of a circumferential cross section of the tube remote from the rolling zone. Detailed view.

Study of the evolution of the metallurgical structure

The possibility that the microstructure evolved during the exposure test at 360°C was examined. A test for IGA susceptibility according to the ASTM A 262 Practice C standard was used. Several coupons were taken from an area remote from the rolled part of the tube of mock-up 506 and from a reference tube of the same heat. Following ASTM A 262 Practice C, they were tested in boiling 25% nitric acid solution for 48 hours and mass losses were measured. The results are presented in Table B-5.

Table B-5 Mass loss results after the IGA susceptibility test following ASTM A 262 Practice C on Alloy 690 TT tubes

Material	Mass loss ($mg/dm^2/day$)
Reference tube. As received	8.75
Reference tube. As received	9.4
Reference tube. Polished	1.83
Mock-up 506 tube	37.9
Mock-up 506 tube	39.7
Mock-up 506 polished tube	1.37

The surfaces of the tube coupons were compared, as shown in Figure B-16 and Figure B-17 for the as-received coupons (# 1 and 4) after the nitric acid test. Extensive intergranular attack was observed on the two samples.

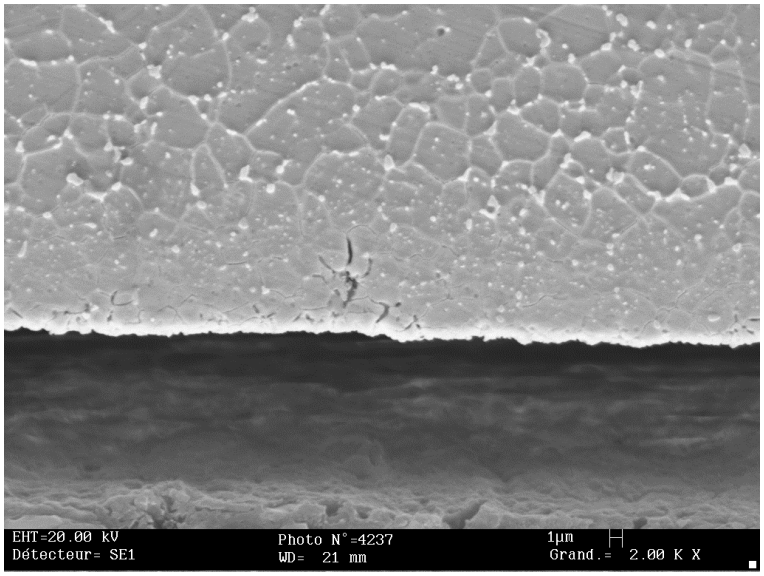

Figure B-16 Reference tube of heat WE094. SEM view of an etched cross section after IGA susceptibility test.

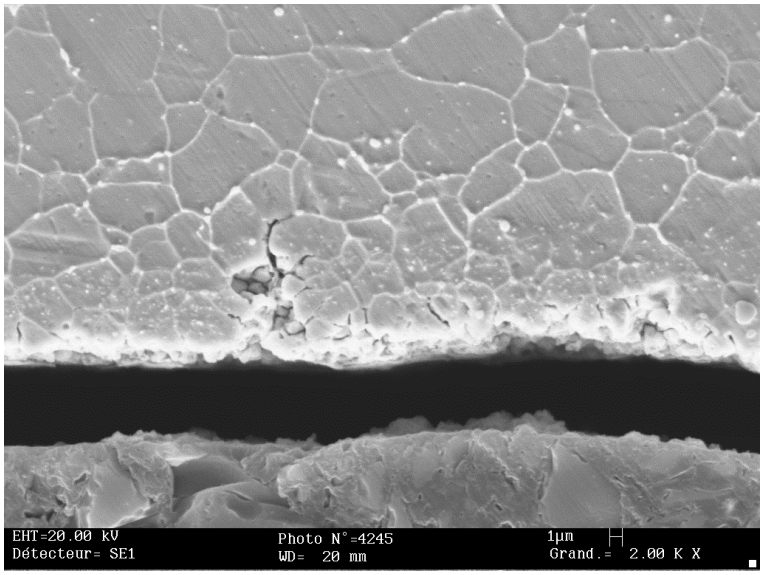

Figure B-17 SEM view of an etched cross section of unstrained tube from mockup 506 after IGA susceptibility test.

The IGA was limited to the thickness of the perturbed surface layer and the mass losses of the polished coupons showed clearly that only the surfaces were sensitized. The mass loss was higher for the coupons of the tube tested for 60,000 hours at 360°C. Therefore, it seemed that long-term aging at 360°C had slightly increased the sensitization of the surface layer of the material.

B.3.2.2 Examination of mock-ups 502 and 508 after 100,000 hours exposure

The characteristics of these two mock-ups are described in the Table B-6.

Table B-6 Characteristics of mock-ups #502 and #508

Mock-up	Rolling		Kiss rolling expansion Ø (mm)	Skip-roll
	Tube /tubesheet gap (mm)	Over-roll (mm)		
502 H	0.4	+1.5	0.15	No
502 B	0.4	+1.5	0.30	
508 H	0.95	- 1.5	0.15	Yes
508 B	0.95	+ 20	0.30	

Mock-up 502 was manufactured with no fabrication anomaly whereas mock-up #508 had two major non-conformities: a high tube/tubesheet gap and a skip roll. These anomalies were found to be very detrimental for stress corrosion resistance in the case of the Alloy 600 mock-ups (see Section B-4).

These two mock-ups were tested during 100,000 hours at 360°C and were examined to look for possible evolution of cracks or metallurgical structure after long-term exposure, in comparison to the mock-up #506 tested for 60,000 hours.

Liquid penetrant test

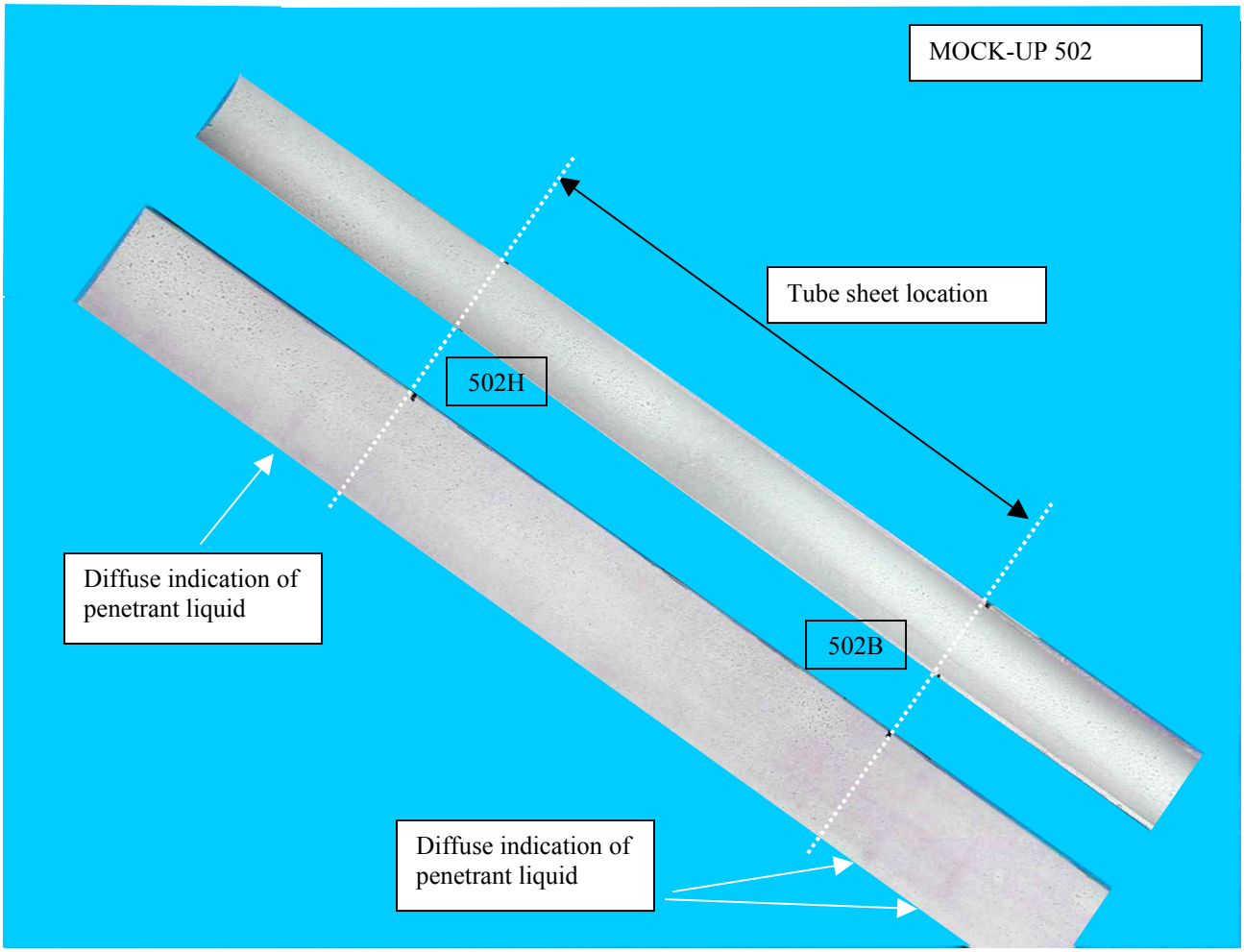

Figure B-18 Liquid penetrant test on mock-up #502. View of the two half tubes, (one is flattened, the other is not flattened).

After the liquid penetrant test, diffuse indications appeared in the transition zone of the rolling and kiss rolling zone on each mock-up, as observed previously. Figure B-18 shows these features for mock-up #502. Some diffuse indications were visible on the flattened half tube and, to a lesser extent, on the other non-flattened half tube. However, no clear indications of flaws or cracks were detected on them.

SEM surface examination

In the same way as for mock-up #506, the internal surfaces of the two mock-ups #502 and #508 exposed for 100,000 hours were examined using SEM. The general appearance of the unstrained tube is presented in Figure B-19. Two types of flaw were identified: some small cavities (diameter: 40 to 50 µm), corresponding to scale particles and small holes (diameter of 2 to 5 µm) corresponding to locations of drop out of other inclusions.

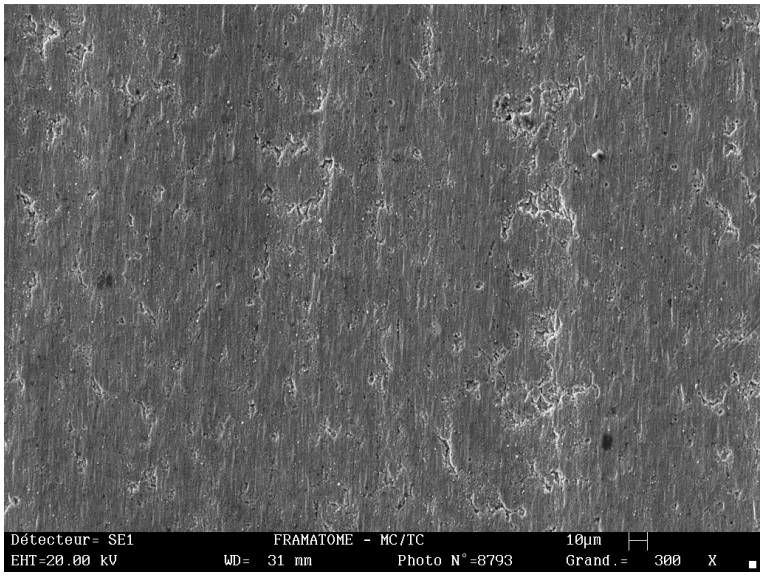

Figure B-19 SEM view of the inner surface of the tube in an unrolled zone. (Non flattened half tube).

After flattening, some microcracks were again observed (see Figure A-20), of which some were related to loss of scale particles.

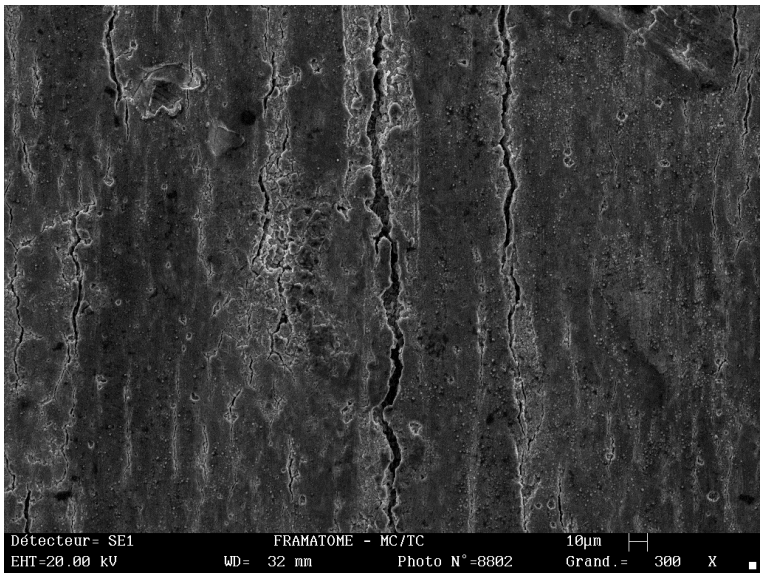

Figure B-20 SEM view of the inner surface of the tube in an unrolled zone. (Flattened half tube).

In the rolling transition zones, some fine cracks were also observed as before on the non-flattened tube (Figure B-21) but many more were detected on the corresponding flattened half tube (Figure B-22).

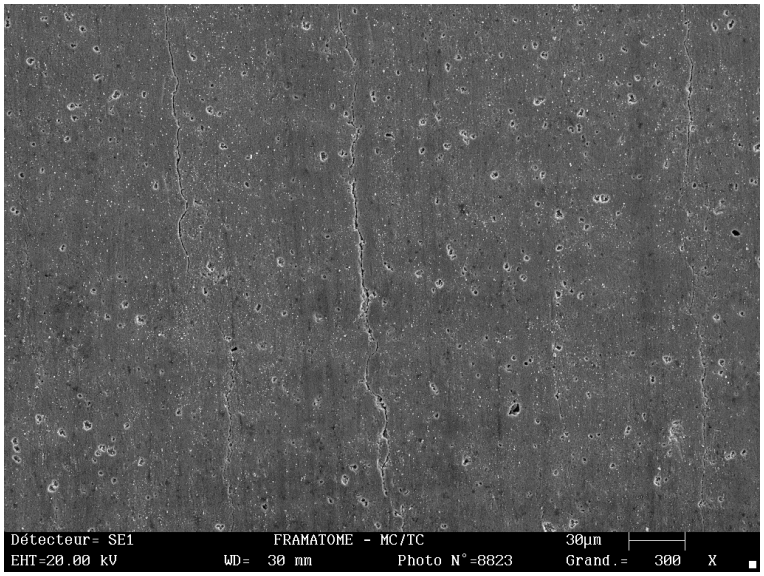

Figure B-21 Mock-up #508B. SEM view of the inner surface of the non-flattened half tube at the limit of the rolling zone.

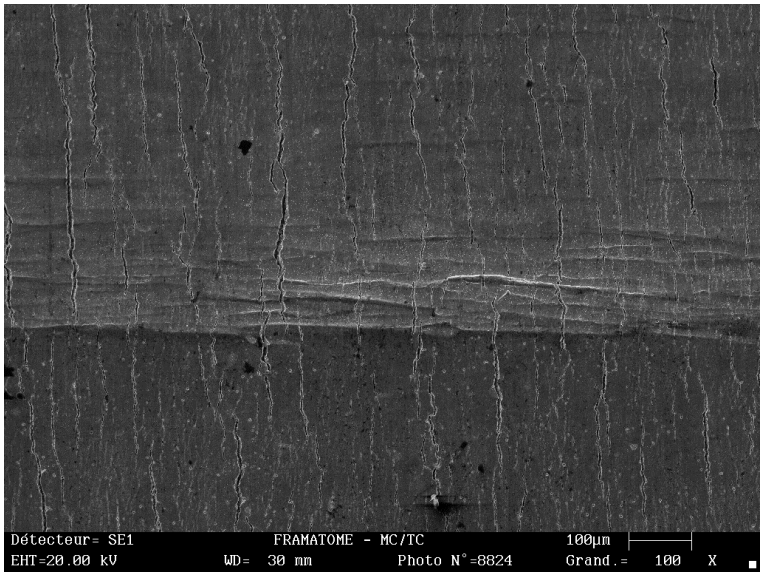

Figure B-22 Mock-up #508B. SEM view of the inner surface of the flattened half tube at the limit of the rolling zone.

On a metallographic cross section, the cracks appear blunt at the tip and were limited to the perturbed surface layer (Figure B-23 and Figure B-24).

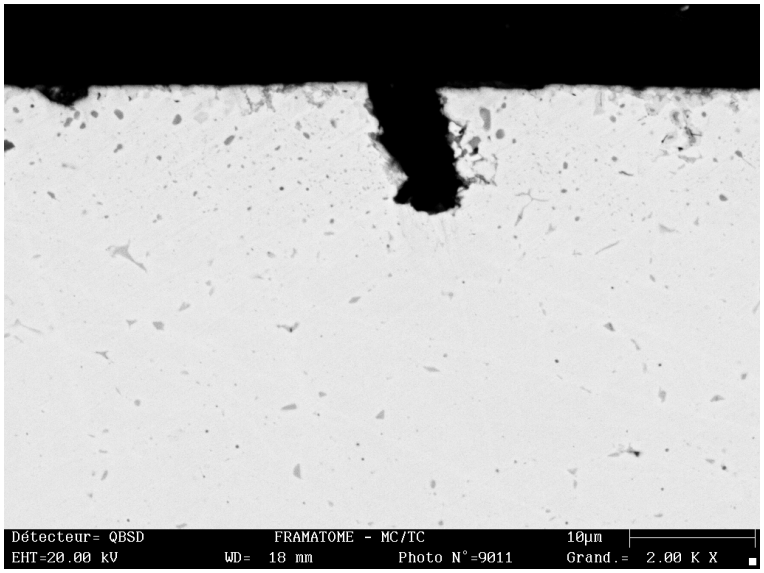

Figure B-23 Mock-up #508B. SEM view of the non etched circumferential cross section through the rolling limit zone.

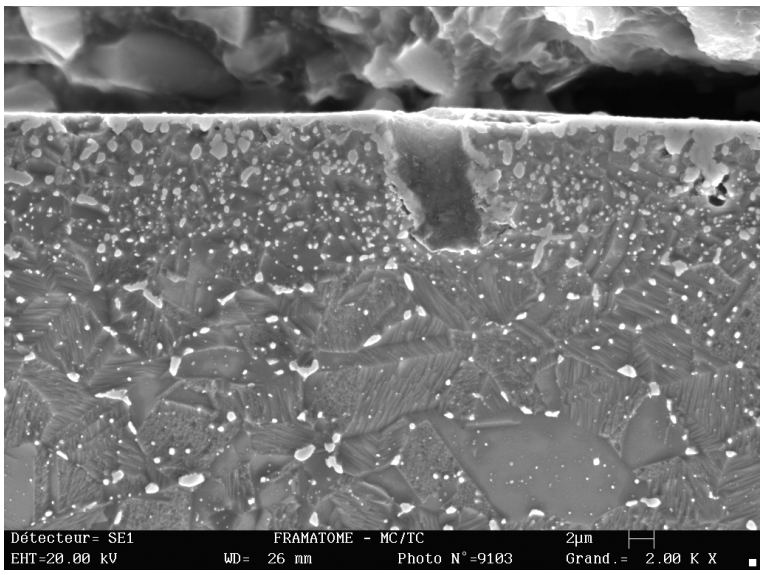

Figure B-24 Mock-up #508B. SEM view of the etched circumferential cross section at the limit of the rolling zone

B.3.3 Conclusions

The main conclusions of the examinations of the mock-ups manufactured with Alloy 690 TT tubing, tested in 360°C hydrogenated water are:

- 16 roll transition zones were tested and did not show any leakage after up to 100,000 hours of test;

- Different roll transition manufacturing anomalies were tested: large tube / tubesheet gaps, skip rolls, large over rolls, large kiss rolling. None of these had any detrimental effect on the stress corrosion cracking resistance under the test conditions used;

- No stress corrosion cracks were found to initiate during the tests despite the presence of manufacturing anomalies known to be detrimental in the case of Alloy 600 tubing;

- The bulk Alloy 690 TT material was not sensitized by the aging at 360°C during 100,000 hours, but a perturbed surface layer between 10 and 100 μm thick was shown to be slightly sensitized before testing and became significantly more sensitized after the long-term aging at 360°C;

- The Alloy 690 TT material used for the mock-ups came from a pre-production heat which exhibited an inner perturbed layer (fine grain size, dense carbide precipitation, higher hardness). This perturbed material exhibited reduced ductility on the inner tube surface and was susceptible to intergranular microcracking when strained. This microcracking was limited to the thickness of the perturbed surface layer and they did not propagate in hydrogenated water at 360°C during 100,000 hours.

B.4 Alloy 600 TT Mock-Up Results

B.4.1 Test Results

Table B-7 gives the as-manufactured characteristics of all the mock-ups that were tested.

The rolling conditions examined can be summarized as follows:

7 zones with standard specification rolling and kiss-rolling, nominal tube / tubesheet gap (0.4 mm), nominal over-roll (between – 1.5 and + 1.5 mm), no in-tubesheet non-conformity.

33 roll transition zones out of specification of which:

21 zones with high over-roll (up to 26 mm),

4 roll transitions without kiss rolling,

21 zones with high kiss rolling expansion (0.30 mm),

4 mock-ups with a skip-roll in the tubesheet,

18 zones with a high tube / tubesheet gap (0.95 mm),

2 mock-ups with lack of roll overlap in the tubesheet.

Table B-7 Characteristics of the tested mock-ups

Mock-up	Heat	Thermal Treatment	Tube to tubesheet gap (mm)	Rolling area	Over-roll (mm)	Kiss-roll expansion (mm)	In-tubesheet non conformity
1	WD 281	MA	0.4	1H	-1.5	0	
				1B	3	0	
2	WD 281	MA	0.4	2B	+6	0	
				2B	+20	0	
3	WD 281	TT	0.4	3H	-1.5	0.15	
				3B	+20	0.15	
4	NX3335	MA	0.4	4H	+1.5	0.30	
				4B	+20	0.30	
5	WD281	MA	0.4	5H	- 1.5	0.15	Skip roll
				5B	+ 20	0.15	
6	WD 281	MA	0.4	6H	- 1.5	0.15	Skip roll
				6B	+20	0.30	
7	WD 281	TT	0.4	7H	- 1.5	0.15	Skip roll
				7B	+20	0.30	
8	WD 281	MA	0.4	8H	-1.5	0.15	
				8B	+ 20	0.30	
9	NX3335	MA	0.95	9H	+ 20	0.30	
				9B	+ 20	0.30	
10	WD 281	TT	0.4	10H	- 1.5	0.30	
				10B	+ 1.5	0.30	
11	WD 281	TT	0.4	11H	+20	0.30	
				11B	+ 20	0.30	
12	WD 281	MA	0.4	12H	+1.5	0.30	
				12B	+ 20	0.30	
14	WD 281	MA	0.95	14H	- 1.5	0.15	
				14B	+ 1.5	0.15	
15	WD 281	MA	0.95	15H	+ 20	0.15	
				15B	+ 20	0.15	
16	WD 281	TT	0.95	16H	- 1.5	0.15	Lack of overlap
				16B	+ 1.5	0.15	
	WD 281	TT	0.95	17H	+ 20	0.15	

17	WD 281	TT	0.95	17H	+ 20	0.15	
18	WD 281	MA	0.95	18H	+ 20	0.30	
				18B	+ 20	0.30	
19	WD 281	MA	0.95	19H	- 1.5	0.30	Lack of overlap
				19B	+ 1.5	0.30	
20	WD 281	TT	0.95	20H	- 1.5	0.30	
				20B	+ 1.5	0.30	
				21H	+ 1.5	0.30	
				21B	+20	0.30	

The profilometry of each mock-up was verified by ET or UT inspection techniques. All specific as-manufactured characteristics of each mock-up were thus identified and recorded. For example, in Figure B-25 and Figure B-26, a part of the mock-up 21H (by ET), with a skip roll inside the tubesheet and a part of the mock-up 3H (by UT), with a normal kiss-roll transition are identified. For mock-up 3H, the determination of the profile at different angular coordinates shows clearly that the kiss-rolling process was not homogeneous on the whole circumference of the tube.

As described earlier, the test environment was pure, hydrogenated, demineralized water with an initial conductivity of less than 1 µS/cm. After, a test period of about 10,000 hours, the water environment from several mock-ups was sampled and analyzed. The results are given in Table B-8.

Table B-8 Chemical analyses of the water environment from several mock-ups after a test period of 10,000 hours

Mock-up	**# 1**	**#8**	**# 10**	**# 12**
Cl^- (mg/kg)	0.7	0.9	0.4	0.5
F^- (mg/kg)	0.4	0.4	0.9	0.8
Na^+ (mg/kg)	0.2	0.15	0.15	0.15
SiO_2 (mg/kg)	5.3	9.2	7.1	7.2
Cond. (µS / cm)	4.54	5.55	6.25	8.33

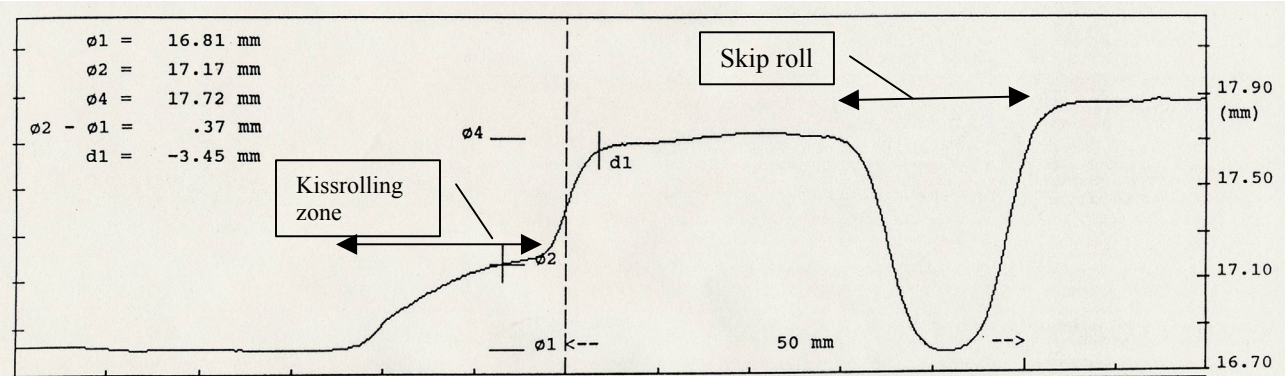

Figure B-25 Profilometry of mock-up 21H determined by an eddy current technique.

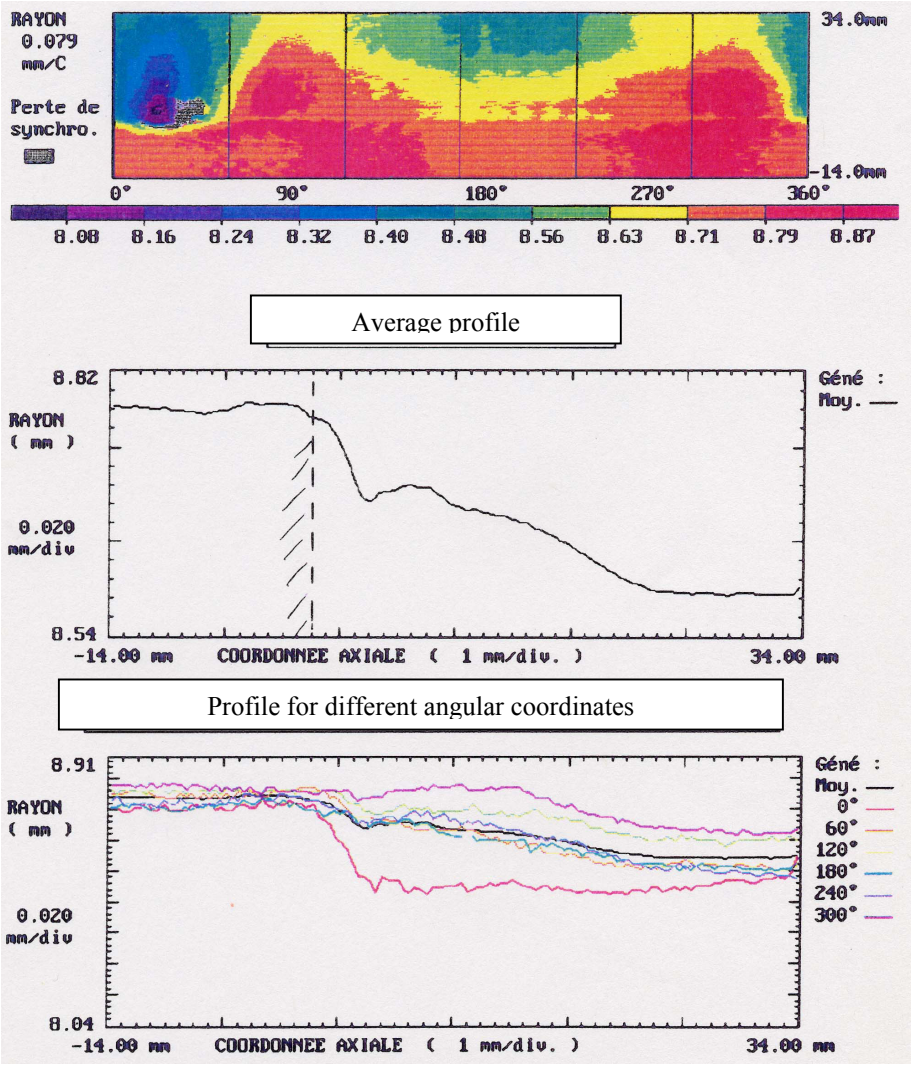

Figure B-26 Profilometry of mock-up.

Table B-9 and Table B-10 give the principal characteristics and test durations for all the Alloy 600 mock-ups. The column marked "result" in these tables gives the locations (see footnote to Table B-10) of the observed through-wall cracks leading to loss of pressure in the capsules.

Table B-9 Results for all mock-ups fabricated from Alloy 600 heat WD281

Mock-up	Heat treatment	T/TS Gap (mm)	Kiss rolling (mm)	Skip roll	Intended Over-roll (mm)	Measured Over-roll (mm)	Duration (h)	Result
1B	MA	0.4	0	no	+3	+10	14 400	RTZ
1H					- 1.5	0	20 250	RTZ
2B	MA	0.4	0	no	-	-	-	-
2H					+ 6	+ 6	22 800	RTZ

3B	TT	0.4	0.15	no	+ 20	-	10 000	RTZ
3H					- 1.5	+1	18 400	RTZ
5B	MA	0.4	0.15	yes	+20	+8	1 500	SR
5H					-1.5	4	10 600	RTZ
6B	MA	0.4	0.15	yes	-1.5	0	1 900	SR
6H			0.30		+20	+23		
7B	TT	0.4	0.30	yes	+20	+26	11 100	OZ
7H					-1.5	+3	11 000	SR
8B	MA	0.4	0.30	no	+20	+23	11 750	RTZ
8H					-1.5	+2	12 850	RTZ
10B	TT	0.4	0.30	no	+1.5	-	34 000	No leak
10H					-1.5	-		
11B	TT	0.4	0.30	no	+20	+22	10 750	RTZ
11H					+20		10 500	RTZ
12B	MA	0.4	0.30	no	+20	+24	20 000	RTZ
12H					+1.5	-	30 000	No leak
14B	MA	0.95	0.15	no	+1.5	+1.5	1 300	RTZ
14H					-1.5	+2	800	RTZ
15B	MA	0.95	0.15	no	+20	+23	3 800	RTZ
15H					+20	+23	4 050	RTZ
16B	TT	0.95	0.15	no	+1.5	+7	3 500	OZ
16H					-1.5	+2		
17B	TT	0.95	0.15	no	+20		5 400	RTZ
17H					+20	+23	5 900	RTZ
18B	MA	0.95	0.30	no	+20	+23	4 000	No leak
18H					+20	+23		RTZ
19B	MA	0.95	0.30	no	-1.5	+1	1 600	OZ
19H					+1.5	+6		
20B	TT	0.95	0.30	no	+1.5		1 800	RTZ
20H					-1.5	+2	1 500	RTZ
21B	MA	0.95	0.30	yes	+20	+25	3 800	RTZ
21H					+1.5	+2		No leak

RTZ : cracked in roll transition zone - SR : cracked in skip roll - OZ : cracked in overlap zone

Table B-10 Results for all mock-ups fabricated from Alloy 600 heat NX3335

Mock-up	T/TS Gap (mm)	Kiss rolling (mm)	Skip roll	Intended Over-roll (mm)	Duration (h)	Result
4B	0.4	0.30	No	+20	19 600	RTZ
4H				+1.5	27 000	RTZ
9B	0.95	0.30	No	+20	11 300	RTZ
9H				+20	12 150	RTZ

RTZ : cracked in roll transition zone

B.4.2 Mock-up examinations

As previously explained, most of the leaking mock-ups were examined by ET or UT non-destructive techniques, and then by PT and optical microscopy in order to determine the cause of cracking (inevitably stress corrosion cracking initiated inside the tube). Several mock-ups that were not destructively examined were retained for use in another program.

The location and length of the cracks detected by non-destructive testing (NDT) were compared with the results of the destructive examinations and a very good correlation was obtained. All detected defects were correlated with actual cracks. However, several cracks were not detected by NDT when their length was shorter than 2 mm.

As an example, Figure B-27 and Figure B-28 show the results obtained for mock-up 17H using the EC technique. The profile was determined with an axial probe and the cracks shape with a rotating probe. Figure B-29 shows photographs of the corresponding half-tubes after liquid dye penetrant testing of mock-up 17H while Figure B-30 shows macro-photographs of two of the detected cracks.

The main observations were:

All the cracks were axial

All the cracks were located in the roll transition zones, i.e., the roll transition zone at the edge of the tubesheet (RTZ), or the two transition zones of the skip rolls (SR), or the transition zone due to lack of overlap between two rolling steps (OZ).

The lengths of the through-wall cracks were between 1 and 9 mm. The longest cracks were located within the tubesheet, (OZ or SR).

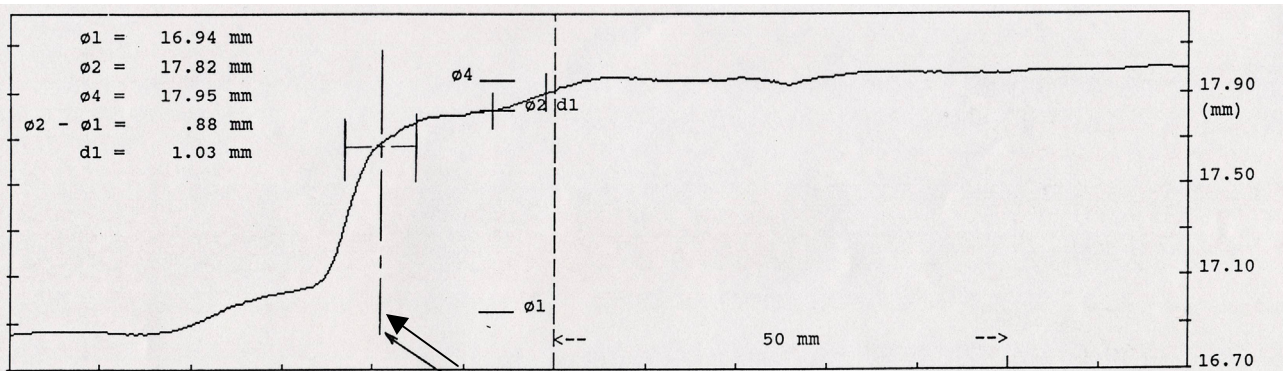

Location of the indication
(see in Fig B-8)

Figure B-27 Profilometry of mock-up 17-H showing the location of the cracks detected by the EC technique.

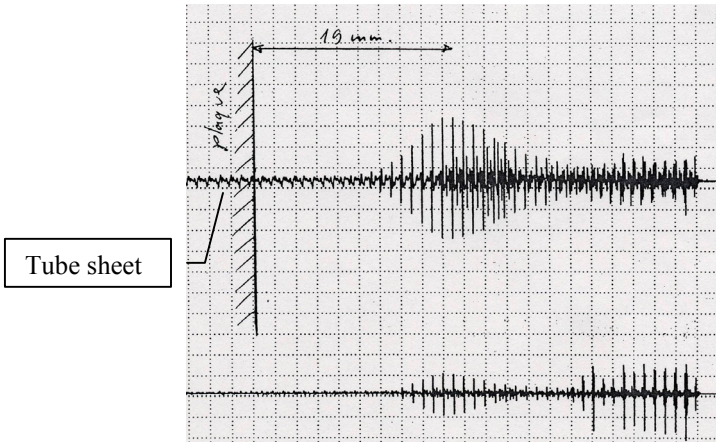

Figure B-28 Detection and location of cracks on mock-up 17H found at the limit of the kiss roll by an EC technique.

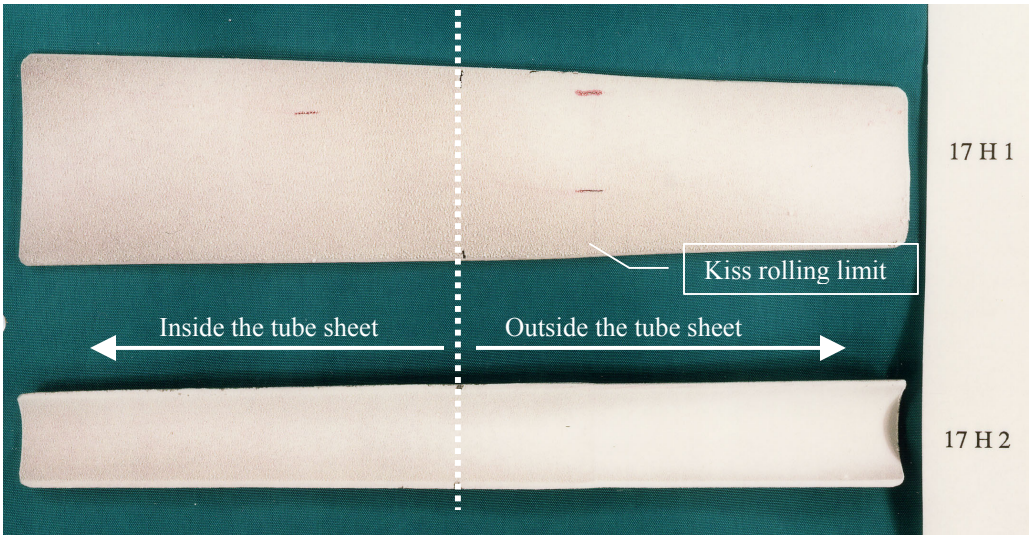

Figure B-29 Liquid dye penetrant test on mock-up 17H. View of the two half tubes after test showing the detected cracks.

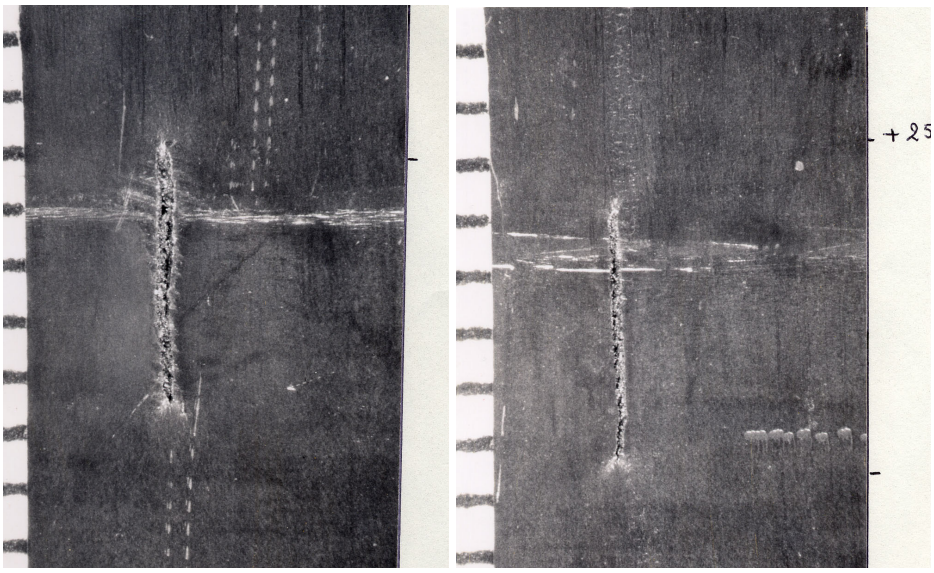

Figure B-30 Macrograph of two cracks after flattening the half tubes of mock-up 17H.

Several metallographic examinations were performed to characterize the cracking. Figure B-31 gives a typical view of such cracks. They were intergranular, often with several branched secondary cracks. In the particular case shown in Figure B-31, the half tube was flattened before examination; thus the cracks were opened with considerable plastic strain located at the crack tip. No intergranular attack was detected on the internal surfaces of the tubes outside the rolling zones.

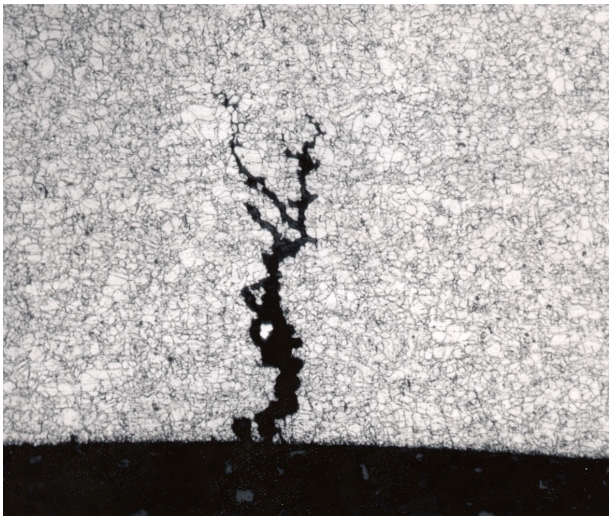

Figure B-31 Metallographic cross section of cracks in mock-up 17H.

Table B-11 summarizes the NDT and optical microscopy results for the cracked mock-ups.

Table B-11 Main results obtained by NDT and optical metallographic examination

Mock-up	Characteristics of the mock-up	Through-wall crack		Detected cracks on half tube	
		Location	Inside length (mm)	Number	Location
1H	Gap 0.4mm	RTZ	3	4	RTZ
1B	Gap 0.4mm	RTZ	5	3	RTZ
2H	Gap 0.4mm	RTZ	5	5	RTZ
3H	Gap 0.4mm	RTZ	3	4	RTZ
5H	Gap 0.4mm – KR – SR	RTZ	6	2	RTZ
5B	Gap 0.4mm – KR – SR	SR	9	8, 6	SR, RTZ
6H	Gap 0.4mm – KR – SR	SR	9	8	SR
7H	Gap 0.4mm – KR – SR	SR	-	-	SR
7B	Gap 0.4mm – KR – SR	RTZ	8	1	RTZ

	SR				
8H	Gap 0.4mm – KR	RTZ	6	2	RTZ
8B	Gap 0.4mm – KR	RTZ	7	5	RTZ
9H	Gap 0.95mm – KR	RTZ	6	3	RTZ
9B	Gap 0.95mm – KR	RTZ	1	3	RTZ
11H	Gap 0.4mm – KR	RTZ	7	5	RTZ
11B	Gap 0.4mm – KR	RTZ	6	4	RTZ
12B	Gap 0.4mm – KR	RTZ	6	2	RTZ
14H	Gap 0.95mm – KR	RTZ	6	2	RTZ
14B	Gap 0.95mm – KR	RTZ	6	6	RTZ, OZ
15H	Gap 0.95mm – KR	RTZ	5	6	OZ
15B	Gap 0.95mm – KR	RTZ	5	4	RTZ
16H	Gap 0.95mm – KR	RTZ	3	1	RTZ, OZ
16B	Gap 0.95mm – KR	RTZ	3	4, 4	RTZ, OZ
17H	Gap 0.95mm – KR	RTZ	5	2, 1	RTZ, OZ
17B	Gap 0.95mm – KR	RTZ	8	6	RTZ, OZ
18H	Gap 0.95mm – KR	RTZ	4	1	RTZ
19B	Gap 0.95mm – KR	OZ	4	4, 4	RTZ, OZ
20H	Gap 0.95mm – KR	RTZ	5	3	RTZ
20B	Gap 0.95mm – KR	RTZ	6	9	RTZ
21B	Gap 0.95mm – KR-SR	RTZ	5	1	RTZ, SR

KR: kiss roll transition zone - RTZ : cracked in roll transition zone - SR : cracked in skip roll - OZ : cracked in overlap zone

B.4.3 Analysis of results

Among the 40 roll transition zones tested in Alloy 600, six were stopped without any through wall crack (leak) occurring. Those mock-ups were:

21H and 18B that were stopped after about 4,000 hours because of cracking of the adjacent roll transition zone in the mock-up and could not be tested anymore. However, mock-ups 2B, 12H, 10B and 10H survived more than 30,000 hours of testing without leaking.

B.4.3.1 Tube / tubesheet gap and heat treatment influence

A statistical analysis of the results was carried to evaluate the failure time as a function of the as-manufactured characteristics: initial tube / tubesheet gap size and material heat treatment (mill annealed or thermally treated). Table B-12 summarizes the results of this analysis using initially only results corresponding to cracks / leaks in the roll transition zone.

Table B-12 Results of statistical analysis of the influence of tube/tubesheet gap and heat treatment of Alloy 600 tubes on failure time

Tube/tubesheet gap (mm)	MA	TT
0.95	Mean = 3 427 h. σ = 1 770 h.	Mean = 3 620 h. σ = 2 072 h.
0.4	Mean = 16 092 h. σ = 4 829 h.	Mean = 12 412 h. σ = 4 004 h.

The analysis of variance shows, within 95% confidence limits, that for a tube / tubesheet gap of 0.95 or 0.4 mm there is no noticeable influence of heat treatment on the time to failure. For either heat treatment condition, there was a larger influence of the tube / tubesheet gap size on the time to leakage.

The influence of tube heat treatment was analyzed more accurately by taking into account some results where cracks were not observed in the rolling transition zone due to cracking having previously occurred in the adjacent zone. These results are presented in the Table B-13 and Table B-14.

Table B-13 Influence of the heat treatment for mock-ups with a large tube / tubesheet gap

Mock-up	Gap (mm)	Kiss rolling expansion (mm)	Skip roll	Over-roll (mm)	Time to leak (h)		Location of the crack
14H	0.95	0.15	No	+2	MA	800	RTZ
16H	0.95	0.15	No		TT	3500	ROL
14B	0.95	0.15	No	+1.5	MA	1300	RTZ
16B	0.95	0.15	No	+7	TT	3500	ROL
15B	0.95	0.15	No	+23	MA	3800	RTZ
15H	0.95	0.15	No	23	MA	4050	RTZ
17B	0.95	0.15	No	?	TT	5400	RTZ
17H	0.95	0.15	No	+23	TT	5900	RTZ
19H	0.95	0.30	No	+1	MA	1600	ROL
20H	0.95	0.30	No	+2	TT	1500	RTZ
19B	0.95	0.30	No	+6	MA	1600	ROL
20B	0.95	0.30	No	?	TT	1800	RTZ
18H	0.95	0.30	No	+23	MA	4000	RTZ
21B	0.95	0.30	YES	+25	MA	3800	RTZ

Table B-14 Influence of the heat treatment for mock-ups with the nominal specification tube/tubesheet gap.

Mock-up	Gap (mm)	Kiss rolling expansion (mm)	Skip roll	Over-roll (mm)	Time to leak (h)		Location of the crack
5H	0.4	0.15	No	+4	MA	10 600	RTZ
8H	0.4	0.15	No	+2	MA	12 850	RTZ
3H	0.4	0.15	No	+1	TT	18 400	RTZ
3B	0.4	0.15	No	(+20)	TT	10 000	RTZ
5B	0.4	0.15	YES	+8	MA	1500	SR
6H	0.4	0.15	YES	0	MA	1900	SR
7H	0.4	0.15	YES	+3	TT	11 000	SR
8B	0.4	0.30	No	+23	MA	11 750	RTZ
12B	0.4	0.30	No	+24	MA	20 000	RTZ
11H	0.4	0.30	No	(+20)	TT	10 500	RTZ
11B	0.4	0.30	No	+22	TT	10 750	RTZ
7B	0.4	0.30	No	+26	TT	11 100	ROL
6B	0.4	0.30	YES	+23	MA	1 900	SR
7B	0.4	0.30	YES	+26	TT	11 000	SR

In the case of the large tube / tubesheet gap, the thermally treated tubes showed statistically significant higher times to leakage compared to other configurations with large stresses (short times to leakage) such as roll transition zone cracks with high gaps, or SR cracks with small tube / tubesheet gap configuration. On the other hand, the times to leakage, for TT tube or MA tube belong statistically to the same population in the case of moderate stresses (long times to leakage) such as roll transition zone cracks with small tube / tubes sheet gaps and kiss rolling. Thus, thermally treated tubes seemed to have better resistance to PWSCC in the case of severe non conformities such as a large tube / tubesheet gaps but in case of roll transition parameters typical of the specification for steam generator manufacture, no effect of thermal treatment was observed.

B.4.3.2 Influence of skip roll

Four mock-ups were manufactured with skip rolls: 5, 6, 7 and 21.

Table B-15 shows the data used to examine the influence of a skip roll on failure time.

Table B-15 Data used to examine the influence of skip roll

Mock-up	Heat treatment	T/TS gap (mm)	Over-roll (mm)	Kiss roll expansion (mm)	Skip roll	Time to leak (h) and location
5B	MA	0.4	+20	0.15	YES	1500 SR
3B	MA	0.4	+20	0.15	NO	10 000 RTZ
6H	MA	0.4	-1.5	0.15	YES	1900 SR
5H	MA	0.4	-1.5	0.15	NO	10 600 RTZ
8H	MA	0.4	-1.5	0.15	NO	12 850 RTZ
7H	TT	0.4	-1.5	0.15	YES	11 000 SR
3H	TT	0.4	-1.5	0.15	NO	18 400 RTZ
21B	MA	0.95	+20	0.30	YES	3 800 RTZ
18H	MA	0.95	+20	0.30	NO	4 000 RTZ

For a nominal tube / tubesheet gap of 0.4 mm, a skip roll gave rise to very rapid cracking (between 1,500 and 1,900 hours) in comparison with the normal roll transition zone that survived > 10,000 hours).

For a large tube / tubesheet gap of 0.95 mm, the presence of a skip roll did not seem to induce cracking earlier than was typical of the roll transition. However, just one mock-up was tested in this configuration combining a large tube / tubesheet gap and a skip roll.

B.4.3.3 Influence of kiss rolling

Table B-16 shows the results that were compared to examine the influence of kiss rolling.

Table B-16 Analysis of the influence of kiss rolling

Heat treatment	T/TS gap (mm)	Over-roll (mm)	Kiss roll expansion (mm)	Skip roll	Time to leak (h) and location
MA	0.4	-1.5	NO	0.15	10 600 RTZ
MA	0.4	-1.5	NO	0.15	12 850 RTZ
MA	0.4	+20	NO	0.30	11 750 RTZ
MA	0.4	+20	NO	0.30	20 000 RTZ
MA	0.4	+3	NO	0	14 400 RTZ
MA	0.4	-1.5	NO	0	20 250 RTZ
MA	0.4	+6	NO	0	22 800 RTZ

By inspection, the time to leakage in the roll transition zone seemed to be longer without a kiss roll than with one in the case of a nominal tube / tubesheet gap. However, if the variance of these samples is analyzed, this hypothesis cannot be sustained with 95% confidence. Thus kiss rolling did not statistically improve or degrade significantly the resistance of the rolling zone to stress corrosion cracking on the primary side (internal surface of the tube).

B.4.3.4 Influence of Alloy 600 heat

Table B-17 shows a comparison of mock-ups manufactured with similar characteristics from two heats of Alloy 600 including heat NX3335, which was known to have low susceptibility to PWSCC.

Table B-17 Influence of Alloy 600 heat

Heat	Mock up	T/TS gap (mm)	Over-roll (mm)	Time to leak (h)
NX3335 MA	4H	0.4	+1.5	19 600
	4B	0.4	+20	27 000
WD281 MA	5H	0.4	+1.5	10 600
	8B	0.4	+20	11 750
NX3335 MA	9H	0.95	+20	12 150
	9B	0.95	+20	11 300
WD281 MA	15H	0.95	+20	4 050
	15B	0.95	+20	3 800

The less susceptible heat clearly gives longer times to leakage under the same test conditions. However, this observation is difficult to support statistically since it depends on a one-to-one comparison of mock-ups. Nevertheless, it demonstrates the large influence of tube heat on the PWSCC phenomenon.

B.4.4 Conclusions

The main results of this part of the study on Alloy 600 mock-ups were:

40 roll transitions zones were exposed to hydrogenated, pure water at 360°C of which 6 did not crack after the tests lasting up to 30,000 hours. All the others cracked after exposure times between 800 and 22,800 hours.

All the cracks were axial, intergranular and were always located in a transition zone characterized by a change in tube diameter due to rolling.

Cracking was ascribed to IGSCC in pure hydrogenated water, which is indistinguishable from that which occurs in PWR primary water except for a small increase in the kinetics of the degradation process.

The most detrimental parameters were: a skip-roll and an over-size tube /tubesheet gap.

The kiss-roll transition did not seem to have a statistically demonstrable beneficial or detrimental effect independent of the value of the tube expansion.

Thermally treated tubes seemed to have better resistance to PWSCC in the case of severe non conformities such as a large tube / tubesheet gaps but in case of roll transition parameters typical of the specification for steam generator manufacture, no effect was observed.

A marked heat-to-heat effect on PWSCC was observed, as is characteristic of field behavior, independent of roll transition fabrication characteristics.

B.5 Conclusions

The aim of the present program was a comparative study of the resistance of Alloy 690 TT and Alloy 600MA and TT to PWSCC using mock-ups representative of the tube expansion zones in the tubesheet of recirculating PWR steam generators.

Several different types of manufacturing anomalies were reproduced in the mock-ups:

- Over-size tube / tubesheet gaps
- Over-rolling
- Skip rolls in the tubesheet
- Excessive kiss-rolling

The mock-ups were tested in the form of heated capsules containing deaerated, hydrogenated and demineralized water at 360°C.

The first leaks due to through-wall cracking appeared on the Alloy 600 MA mock-ups after exposure times as short as 800 hours. Alloy 600TT tubes seemed to have better resistance to PWSCC in the case of severe nonconformities such as over-sized tube / tubesheet gaps. With normal roll transition parameters, no effect of the thermal treatment was observed. Nevertheless, there was a marked heat-to-heat effect on PWSCC (as is characteristic of field behavior) independent of roll transition fabrication characteristics.

Almost all the Alloy 600 mock-ups cracked. Of the 40 different roll transition zones that were tested, two were withdrawn without any leakage after short exposure times and four zones survived 30,000 hours (the maximum exposure time of the Alloy 600 mock-ups) without any leakage occurring. All the other roll transition zones cracked. The average time to leakage of the Alloy 600 mock-ups was 8,350 hours with a standard deviation equal to 6,600 hours. The most susceptible zones were roll transition zones with over-size tube / tubesheet gaps and / or with skip rolls inside the tubesheet (independent of the tube / tubesheet gap if skip rolls were present).

Eight mock-ups were manufactured with Alloy 690 TT tubing and tested in the same conditions as the Alloy 600 mock-ups. None of the Alloy 690 TT mock-ups cracked even after exposure times extending up to 100,000 hours. Non-destructive and destructive examinations showed that no stress corrosion crack initiation or propagation had occurred, despite the simulated manufacturing anomalies that had such severe detrimental effects on PWSCC resistance of similar Alloy 600 mock-ups.

Since leak events occurred in Alloy 600 mock-ups before 20,000 hours with 95% confidence (average value plus two standard deviations) and given that no failure occurred in the comparable Alloy 690 TT mock-ups after 100,000 hours, the beneficial effect of using Alloy 690 TT instead of Alloy 600 was greater than a factor of 5.

Metallurgical examinations of the Alloy 690 TT mock-ups confirmed that even when some mechanically-induced intergranular cracks were initiated by severe straining of a hard perturbed internal surface layer, such cracks did not propagate in hydrogenated water at 360°C after exposure times up to 100,000 hours.

In conclusion, no initiation of stress corrosion cracks was observed and mechanically-induced intergranular cracks created by severe straining of a perturbed surface layer did not propagate in Alloy 690 TT material. These tests demonstrated that the change from Alloy 600 to Alloy 690 TT gives an improvement factor greater than 5 for PWSCC initiation.

C ALLOY 690 CORROSION IN SECONDARY WATER

The laboratory data and field experiences reviewed in the proceeding sections are related to corrosion degradations of Alloys 690, 152, and 52 in PWR primary water. In addition to corrosion concerns in primary water, an equally amount of research efforts have been directed toward Alloy 690 SG tubing corrosion degradations pertinent to PWR secondary water environment (the secondary side of steam generators). Even though the secondary water corrosion is not the focus of the present review, many studies of Alloy 690 conducted in environments pertinent to PWR secondary water have been reviewed in this section in order to provide a comprehensive comparison of Alloy 690 and Alloy 600 under various environmental conditions encountered in PWRs. By examining the secondary water conditions and the thermal mechanical processing parameters that promote stress corrosion cracking or intergranular attack in Alloy 690, some insights may be obtained as to Alloy 690 corrosion resistance in primary water. Furthermore, the types of corrosion specimens used in secondary water are the very same ones used in primary water. A couple of studies listed below are referenced in the proceeding sections to compare with similar observations made in a few primary water studies.

C.1 AVT Water Environment

Miglin et al. performed stress corrosion cracking tests of Alloys 600 and 690 in all-volatile treated (AVT) water.[88] Five types of stress corrosion cracking test specimens were used including RUB (also called split-tube U-Bend), Single U-Bend, Double U-Bend, Ring-Tensile, and C-Ring. Identical specimens were fabricated from Alloy 600 and Alloy 690. The Alloy 600 specimens were fabricated from 23 heats of Alloy 600 in a variety of MA and TT conditions. The Alloy 690 specimens were fabricated from 4 heats of Alloy 690 in the MA, TT (1150^{o}F), and TT(1300^{o}F) conditions. The Alloy 690 heat chemical compositions are listed in Table C-1. The tests were conducted in four once-through (refreshed) high-pressure autoclaves with AVT water at 550, 630, 650, and 680^{o}F. The autoclave pressure were kept above the water-steam equilibrium pressures at the respective test temperatures, so the test environment was water, not steam. The water chemistry and test duration are listed in Table C-2.

During the testing, 78 of the 520 Alloy 600 specimens developed cracking. Most of the cracked specimens were the RUB type and fabricated from Alloy 600 heat treated to produce a susceptible condition. Alloy 600 cracking occurred much more rapidly and frequently at 680^{o}F and at 650^{o}F than at the lower temperatures. Examination of some cracked Alloy 600 RUB specimens indicated that the IGSCC cracks started as short longitudinal cracks at the apex, then became longer and wider, and eventually propagated through-wall with exposure time. Destructive metallographic examination revealed the presence of blunt and shallow (on the order of 0.02 mm) crack indications on the I.D. surface of the RUB apex. These defects were not typical IGSCC. Further examination showed that some IGSCC initiated from the base of these defects. However, most IGSCC cracks did not initiate from these shallow defects.

None of the 113 Alloy 690 specimens failed in a typical IGSCC manner. The Alloy 690 C-ring specimens were exposed up to 72,000 hours. The maximum exposure time for Alloy 690 RUB specimens was approximately 37,200 hours, significantly less than the maximum exposure time for Alloy 600 RUB specimens. However, longitudinal shallow and blunt defects were found on the I.D. surface of the Alloy 690 RUB apex. These defects were not typical of IGSCC. Metallographic examinations showed that some of these defects appeared to be like mechanical grooves while others appeared to be separation along the grain boundaries. No evidence of further IGSCC cracking emanating from the base of these defects were found. SEM examinations of archive Alloy 690 RUB specimens found similar longitudinal defects, but they were shorter in length than those detected after the AVT autoclave exposure (0.1 to 0.35 mm long in archive Alloy 690 RUB vs. ~1.0 mm in Alloy 690 RUB after the AVT exposure).

Miglin et al. offered two explanations for the apparent longitudinal growth of the defects. The first explanation was the defect growth was a stress relaxation process. Once the defects grew to a sufficient length to relieve the stress at elevated temperature, no further growth would occur. The second explanation by Miglin et al. was that the defects did not grow at all during the AVT exposure. The growth in length observed was due to an opening process of closed or partially closed defects. During the high temperature exposure, the surface oxide growth (in the defects) would enhance an opening process by a wedging effect to give an appearance of longitudinal growth. The less strained leg portions of the RUB specimens were free from these defects. Similar SEM examinations of archive Alloy 600 RUB specimens also found the apex to be relatively free of these defects. It is noted that Framatome ANP, France noted similar longitudinal defects in the roll-transition areas of the Alloy 690 SG tube mock-ups (see Appendix B). The cause of these defects was attributed to mechanical strain from the roll expansion and a shallow cold worked layer of SG tubing surface. These defects also did not affect the PWSCC resistance Alloy 690 SG mock-ups in the 680°F deaerated water for up to 100,000 hours. In the end, Miglin et al. concluded that these defects were due to mechanical strain rather than due to IGSCC.

C.2 Deaerated Caustic Solution With or Without Contamination

Intergranular attack (IGA) and IGSCC has been experienced on the secondary side of Alloy 600MA SG tubings within the drilled tube support plate and the tubesheet crevices in PWR steam generators. Table C-3 is a summary of past laboratory tests of Alloy 690 in a high temperature deaerated NaOH solution by Crum et al.[89]

C.2.1 Sedricks et al.

Sedricks et al. tested Alloy 690 in deaerated 10% and 50% NaOH solutions. [9] When the temperature of a layer of water at a heat transfer surface exceeds the temperature of the main body of slightly alkaline water by a temperature difference of ΔT, a high concentration of NaOH can develop in this layer. A 50% NaOH solution used in some laboratory tests corresponds to a ΔT of 80°F (27°C). The maximum ΔT attainable on the secondary side the SG was not known. However, a 50% NaOH solution was considered as representing a theoretical extreme. After 2 weeks exposure in 600°F deaerated 50% NaOH solution, Alloy 690 had a slightly higher descaled weight loss than Alloy 600 and a slightly lower descaled weight loss than Alloy 800. Results from the U-Bend specimens showed that, at 600°F, Alloy 690 had a slightly lower SCC

resistance than Alloy 600 in the deaerated 50% NaOH solution while Alloy 690 had a slightly higher SCC resistance than Alloy 600 in 10% NaOH solution.

Sedricks et al. also tested Alloy 690 U-bend specimens in non-deaerated 50% NaOH solutions at 600°F.[9] After 27 days exposure, except for one cold rolled specimen, none of the Alloy 690 specimens developed cracks irrespective of the heat treatment, cold work, or the presence of welds. On the other hand, most of the Alloy 600 U-bend specimen developed cracks. Hence, it was concluded that in the non-deaerated caustic solution, Alloy 690 had a higher SCC resistance than Alloy 600.

C.2.2 A. Smith et al.

A. Smith et al. reported stress corrosion tests on commercially produced Alloy 690 SG tubes.[32, 33] C-ring stress corrosion test specimens were fabricated per ASTM G 38[90] from Alloy 690TT. The C-ring specimens were tested in a variety of environmental conditions at 340°C (644°F). No intergranular attack or stress corrosion cracking was noted after 1,500 hours of exposure in deaerated pure water (see Section 3.1). However, All C-ring specimens developed intergranular attack (IGA) when tested in deaerated caustic environments. These C-ring specimens were fabricated from Alloy 690 SG tubes "A" and "E" and "F" and were tested in 50% NaOH solution and/or 30% NaOH + 10% Na_2SO_4 solution at 340°C (644°F). The chemical composition of tubes "A", "E", and "F" and their mechanical properties are summarized in Table 3-15.

Results in deaerated 50% NaOH solution are listed in Table C-3. Figure C-1 shows the IGA in the C-ring specimen E3 after 1,200 hours exposure in deaerated 50% NaOH. Results of C-ring specimen from tubes "A" and "E" in deaerated 50% NaOH and 30% NaOH + 10% Na2SO4 are summarized in Table C-4. The results showed that 50% NaOH was a more aggressive environment than 30% NaOH + 10% Na_2SO_4. Unexpectedly, tube "E" with a lower carbon content had a lower IGA resistance than tube "A". This was attributed to the higher aluminum content in tube "E" than in tube "A" (0.13% vs. 0.03%). It was suggested that aluminum increased the propensity for IGA in Alloy 690. However, IGA growth rate in Alloy 690 appeared to decrease rapidly with continued exposure. In deaerated 30% NaOH + 10% Na_2SO_4, it appeared that the tip of the advancing IGA became blunted by corrosion products after a short distance. Further intergranular attack was in a direction parallel to the surface (or perpendicular to the original IGA direction), resulting in a general corrosion (or wastage) across the exposed surface. C-ring specimens from tube "F" were given different thermal treatment (at 650 – 750°C for 1 – 15 hours). These specimens were tested in 30% NaOH + 10% Na_2SO_4 at 350°C (662°F) for 1,500 hours. The specimens showed comparable IGA depth.

C.2.3 K. Smith et al.

K. Smith et al. tested the SCC resistance of Alloy 690TT and Alloy 600 in deaerated NaOH solutions at elevated temperatures.[11] The Alloy 690 chemical composition and mechanical properties are listed in Table 3-3. Table C-5 summarizes the K_{ISCC} obtained from wedge-opening-loading (WOL) specimens of Alloy 690 and Alloy 600 in deaerated NaOH solutions. Figure C-2 shows the crack propagation rates obtained from C-ring specimens of Alloy 690TT and Alloy 600 tested in deaerated 10% NaOH solution at temperatures between 315 and 343°C

(600 and 650°F). The C-rings were loaded to different percentages of the yield strength and Alloy 690TT had the lowest crack propagation rate regardless of the loading levels.

Table C-6 summarizes the results of C-ring specimens stressed to 50, 75, 90, 150% of the yield strength and C-ring specimens strained until the legs touch (14% strain, TLT) after 1,000 hours of exposure to 10% NaOH deaerated solution at 315°C (600°F). The potential was maintained at the active-passive transition (140 mV vs. Ni) to accelerate any SCC propensity during the 1,000 hours exposure. The Alloy 690TT C-ring specimens, except for the TLT specimens, did not develop cracking. Based on these results, K. Smith et al. concluded that Alloy 690TT was more SCC resistant than Alloy 600 in low concentration of deaerated NaOH solution at 600°F and in all concentrations of deaerated NaOH solution at 650°F. The improvement of Alloy 690TT over Alloy 600 was attributable to a higher SCC threshold stress level and a lower crack propagation rate.

C.2.4 Sarver et al.

Sarver et al. investigated the effect of thermal treatment on the Alloy 690 SG tubing in 10% and 30% NaOH solutions.[91] The chemical compositions of the Alloy 690 and Alloy 600 used in these tests are listed in Table C-7. The Alloy 690 U-bend specimens were stressed well beyond the yield stress and tested in 10% and 30% NaOH solution at 228°C (550°F) held at different potential levels. In the 10% NaOH solution, only the Alloy 690TT (1/2 hour at 1200°F) specimens held at +170 mV vs. Ni developed cracking approximately 15% through-wall. In the 30% NaOH solution, the Alloy 690MA specimens held at +170, +190, and +210 mV experienced through-wall cracking. Compared to Alloy 600, the Alloy 690 has a narrower range of potential which produces SCC in 10% NaOH. This is attributed to the greater stability of the oxide film formed on the Alloy 690 than on the Alloy 600 due to the higher Cr content.

At higher NaOH concentration levels, the stability of Cr-rich oxide films is reduced and the SCC potential range is expanded. In addition to U-bend specimens, Sarver et al. tested Alloy 690 C-ring specimens with varying thermal treatment conditions 228°C (550°F). The specimens were first put in the 10% NaOH solution held at +170 mV potential for two months. Cracking was only observed in the Alloy 600MA C-ring specimens. Subsequently, the solution concentration was increased to 30% NaOH and held at +210 mV for two additional months. The C-rings specimens were metallographically examined at the end of the test and the results are summarized in Table C-8. The cracking in the Alloy 690 C-ring specimens was less than anticipated based on the Alloy 690 U-bend results. This was attributed to the lower stress level in the C-ring specimens than the U-bend specimens. Sarver et al. concluded that continuous grain boundary carbides from thermal treatment is insufficient in itself to prevent caustic SCC in Alloy 690 material.

C.2.5 Vaillant et al.

Vaillant et al. tested Alloy 690, Alloy 600, and Alloy 800 SG tubing in a variety of deaerated caustic solutions.[92] The Alloy 600 and Alloy 690 material properties used in the testing are summarized in Table C-9. The IGSCC test results in 350°C (662°F) deaerated NaOH solutions are listed in Table C-10. The tests were stopped after a given duration (minimum time: 720 hours on C-rings; some tests of Alloy 690 were extended to 11,000 hours). However, the test duration

for the test results listed in Table C-10 was not listed. Table C-10 shows that the Alloy 600 was susceptible to IGSCC in 4 to 500 g/L NaOH solutions, with a maximum at 100 g/L. The Alloy 690 was susceptible to IGSCC in 40 to 400 g/L NaOH solutions, with a maximum also at a concentration of 100 g/L.

The Alloy 690TT condition was found to have the highest resistant to IGSCC. Vaillant et al. observed that the SCC threshold stress for Alloy 600 increases with increasing yield strength at 350°C (644°F). The Alloy 600 heats with the lowest yield strength at 350°C were the most susceptible to caustic IGSCC. However, no correlation was found between caustic IGSCC in the Alloy 690 and the yield strength at 350°C. The IGA of Alloys 600 and 690 was investigated in a deaerated 100g/L NaOH solution at 350°C (662°F) with or without the addition of magnetite. After 8,000 hours, the IGA depth was 150 μm in the Alloy 600MA and 30 μm in the Alloy 600TT. No IGA was identified in the Alloy 690TT, which had an oxide layer 50 μm thick. Adding magnetite significantly increased the IGA of the Alloy 600 while only slightly increasing the Alloy 690 oxide thickness without any IGA.

C.2.6 Mertz et al.

Mertz et al. performed SCC testing of Alloy 690 materials in high temperature caustic solutions.[93] However, no Alloy 600 specimens were included in the testing program. The materials tested were two heats of Alloy 690 SG tubing and one heat of Alloy 690 plate. The chemical composition, heat treatment, and mechanical properties in the as-received state are listed Table C-11. The RUB specimens were fabricated from the Alloy 690 SG tubing with the 12.70 mm O.D. dia. bent around a 25.4 mm dia. mandrel and the 6.35 mm O.D. dia. bent around a 12.70 mm dia. mandrel. The U-bend specimens were fabricated from the Alloy 690 plate that had been reduced to 2.8 mm in thickness. The U-bend specimens were bent around a 25.4 mm dia. mandrel. The Alloy 690 materials were given different processing and heat treated to produce a variety of grain boundary carbide morphology as summarized in Table C-12 and Table C-13.

The RUB specimens were placed in a 25% NaOH solution and the U-bend specimens were placed in a 10% NaOH solution. Both caustic solutions contained <100 ppb oxygen and <100 ppb chloride and were held at 307+/– 6°C (585+/–11°F). The crack depth in the Alloy 690 U-bend specimens (from the plate) after 500 hours of exposure is listed in Table C-13. Cracking was generally intergranular, although transgranular cracking was also observed. The crack depth was clearly related to the grain boundary carbide morphology. Specimens with a continuous network of intergranular carbides (in the HRA+SA+WQ+TT condition) had the smallest depth while specimens without intergranular carbides (in the HRA+SA+WQ) had the maximum depth. Hence, it was concluded that thermal treatment improved caustic SCC resistance of the Alloy 690 plate as it did for the Alloy 690 SG tubing material. The cracking depth after an exposure of 200 to 2,100 hours in the Alloy 690 RUB specimens (from the SG tubing) is shown in Figure C-3. Cracking in the Alloy 690 RUB specimens was both intergranular and transgranular. Figure C-3 shows that the crack depth was very small (from 0 to 0.11 mm) and had a specific correlation among the three types of grain boundary carbide morphology. Therefore, it was concluded that caustic SCC resistance of thermally treated Alloy 690 was independent of grain boundary carbide decoration. Mertz et al. suggested that the thermal treatment improves caustic SCC resistance by removing carbon from the grain interior, hence also reducing the yield

strength. The reduction in yield strength was thought to shift the stress distribution to the grain interior from the grain boundaries.

C.2.7 Kawamura et al.

Kawamura et al. investigated caustic IGA and SCC of Alloy 690TT along with Alloy 800 (shot peened) and Alloy 600.[94] C-ring specimens were fabricated from SG tubing while double cantilever beam (DCB) specimens were fabricated from plate of these materials. Details of the heat chemical composition, heat treatment, and mechanical properties are listed Table C-14. The Alloy 690 and Alloy 600 C-ring specimens had a dimension of 22.23 mm O.D. dia. by 1.27 mm thick by 15 mm wide. All C-ring specimens were stressed to 1.63 times the yield strength at the apex. Each material condition had 30 C-ring specimens and was exposed to a deaerated 10% NaOH + 2% Na_2CO_3 solution at 350°C (662°F). The dissolved oxygen was kept to below 5 ppb. The Alloy 600MA specimens developed through-wall IGA/SCC after 1,000 hours of exposure. The Alloy 600FS specimens had an average IGA/SCC depth of 40 mm after 500 hours of exposure. In contrast, the Alloy 690TT specimens had neither developed IGA nor SCC after 10,000 hours of exposure. The IGA/SCC crack propagation rates were determined using DCB specimens. The DCB specimens had a dimension of 58 mm (length) by 20 mm (height) by 8 mm (thickness) and was given a fatigue pre-crack prior to the testing. The DCB tests were conducted in a deaerated 20% NaOH + 4% Na_2CO_3 solution at 320°C (608°F).

The results of the DCB tests are shown in Figure C-4. The stress dependency of Alloy 690TT and Alloy 600MA are similar. The SCC crack growth rate dependence on stress intensity factor can be divided into two regions, Region I and Region II. In Region I, the crack growth rate increases rapidly with increasing stress intensity factor. In Region 2, the crack growth rate is mostly unaffected by increasing stress intensity factor. At the same stress intensity factor (up to 75 MPa$\sqrt{m}$), the crack growth rate of Alloy 690TT is approximately 1/100th of Alloy 600MA. Hence, the improvement in IGA/SCC resistance of the Alloy 690TT over the Alloy 600MA in a deaerated caustic solution was derived from a combination of a longer crack initiation time and a lower crack propagation rate.

C.2.8 H.P. Kim et al.

H.P. Kim et al. conducted caustic SCC testing of both Alloy 600 and Alloy 690 materials.[95] C-ring specimens were fabricated from archive heats of Alloy 600 and Alloy 690 SG tubing that were used in Korean nuclear power plants. The chemical composition and the mechanical properties are listed in Table C-15. The Alloy 600 and the Alloy 690 C-ring specimens were stressed to 565 MPa at the apex and placed in a deaerated 10% NaOH solution at 315°C (600°F). The corrosion potential was kept at 200 mV vs. Ag/AgCl reference. After 15 days of exposure, the Alloy 690TT showed no IGA/SCC while all four of the Alloy 600 heats showed varying degrees of cracking. The Alloy 600 with a low mill anneal temperature (LT600) had the deepest cracking.

C.3 Lead Contaminated Secondary Water

C.3.1 Castano-Marin et al – Acidic, Caustic, AVT Water + Lead

Castano-Marin et al. performed C-ring tests of Alloy 690TT and Alloy 600MA SG tubing in a variety of PbO-doped water environments.[96] Table C-16 and Table C-17 list the chemical composition, mechanical properties, and size of these SG tubing materials. The environmental conditions and metallographic examination results are summarized in Table C-18. In caustic water un-doped by PbO at 350 and 320°C, the Alloy 690TT was resistant to IGA/IGSCC while the Alloy 600MA was susceptible to IGSCC. In PbO doped caustic waters at 350°C (662°F), the Alloy 690TT developed TGSCC cracks (see Figure C-5) more quickly than the Alloy 600MA developed IGA/IGSCC cracks. In acidic water with or without PbO doping, the Alloy 600TT was resistant to SCC while the Alloy 600MA failed by IGSCC irrespective of PbO doping. In PbO doped caustic water and in AVT water with or without PbO doping at 320°C, the Alloy 690TT was immune from IGA/SCC. Both the Alloy 600TT and the Alloy 600 MA were susceptible to IGA/SCC under these conditions, although the Alloy 600TT was slightly more resistant than the Alloy 600MA.

C.3.2 Vaillant et al. – Deaerated Caustic Water + Lead

Vaillant et al. tested Alloys 690 and 600 in lead-contaminated deaerated solutions containing 100 g/L NaOH at 350°C (662°F).[92] Lead in the form lead oxide (PbO) was added to a concentration of 10 g PbO /L. The test showed that lead significantly increased both IGA and SCC of the Alloy 600 and the Alloy 690 in caustic solutions at 300-350°C (572-662°F). The cracking was found to be both transgranular and intergranular SCC. The Alloy 600TT has the highest SCC resistance in the lead-contaminated caustic solution while the Alloy 600MA and the Alloy 690TT were similar. The Alloy 600TT lost the beneficial effect of intergranular carbides observed in pure NaOH solution after lead introduction. The IGA rate in PbO doped water was increased by 10 times for the Alloy 600MA and by 6 times for the Alloy 600TT. The growth rate of the Alloy 690TT oxide thickness was increased by 8-10 times.

C.3.3 Helie – Non-deaerated Acidic Water + Lead

Helie performed CERT and RUB tests of Alloy 600MA and Alloy 690TT in non-deaerated pure water doped either with PbO or PbS to a concentration of 10g/L.[97] The CERT and RUB specimens were cut from the SG tubing. The chemical composition and the heat treatment of the Alloy 600 and Alloy 690 materials are listed Table C-19. The Alloy 690TT CERT tests were performed at 360°C (680°F) and at a strain rate of 5×10^{-8} s^{-1}. The Alloy 600MA CERT tests were performed at 320°C (608°F) and at a strain rate of 2.7×10^{-7} s^{-1}.

The CERT test results showed that the Alloy 690TT did not develop SCC, except for some indentations less than 20 μm deep. The Alloy 600MA specimens showed extensive cracking. Compared to the previous test results in the undoped water, the addition of PbO drastically increased the Alloy 600MA CERT cracking propensity and changed the SCC mode from IGSCC to predominantly TGSCC. The RUB tests were performed at 325°C (617°F) for 5000 hours in two autoclaves, respectively doped with PbO and PbS. Testing in one of the two autoclaves was interrupted after 1,000 hours and then resumed. None of the Alloy 690TT RUB specimens in the

two autoclaves showed any SCC. In contrast, the Alloy 600MA RUB specimens showed extensive SCC cracks in both autoclaves. The SCC was predominantly TGSCC in the PbO doped water and predominantly IGSCC in the PbS doped water.

C.4 Chloride and Sulfate Containing Secondary Water

C.4.1 Berge et al. – Acidic Chloride Containing Solutions

Berge et al. investigated SCC resistance of Alloy 600 and Alloy 690 materials in various chloride containing solutions.[98] Table C-20 is a summary of past laboratory tests of both Alloys 600 and 690 in various chloride-containing solutions at low elevated temperatures ranging from room temperature to 180°C (356°F). These tests indicate that Alloys 600 and 690 are not susceptible to cracking in chloride-containing media at lower elevated temperatures. This is consistent with the fact that alloys with greater than 40% nickel are immune to cracking in standard boiling $MgCl_2$ solution. At high elevated temperature, Alloy 600 material is known to develop SCC when both chloride and oxygen are present.

Table C-21 is a summary of past laboratory tests of Alloy 690 in various chloride-containing solutions at high elevated temperatures by Berge et al. These results showed that Alloy 690 is resistance to SCC in chloride containing solutions with or without dissolved oxygen. Berge et al. tested RUB specimens fabricated from Type 304L stainless steel, Alloy 600, and Alloy 690 in boiling $MgCl_2$ solution, whose pH was adjusted with addition of HCl acid to 2.3, 1.6 , and 1.0. The chemical composition and heat treatment of these materials are listed in Table C-22. The results of the boiling MgCl2 tests are listed in Table C-23. The Type 304L specimens cracked in less than 24 hours in all three pH solutions. Alloy 600MA developed intergranular crack after 1500 hours at pH of 1.6. Alloy 690MA developed intergranular crack after 288 hours in the strongest acidic (pH = 1.0) boiling $MgCl_2$ solution. Berge et al also perform SCC tests of Alloy 600 in many acidified chloride-containing solutions at temperatures ranging from 100 to 360°C (212 to 680°F). The results showed that Alloy 600 is susceptible to SCC in acidified chloride-containing media. However, Alloy 690 was not among these tests.

C.4.2 Cullen et al. – Acidic Sulfate and Chloride Containing Solutions

Cullen et al. tested Alloys 600 and 690TT SG tubing materials for wastage, IGA, and IGSCC in acid chloride and sulfate environments at various pH levels, temperatures, and applied potential.[99, 100] C-ring specimens were fabricated from Alloy 690TT and Alloy 600 materials in low and high temperature MA, TT, and sensitized conditions. The chemical composition and heat treatment are listed in Table C-24. The C-ring specimens were strained to 0.1%, 0.2%, 0.5%, and fully closed (4% to 5% strain). The autoclave water chemistry was adjusted to simulate the concentration of species in secondary water based on the computer program MULTEQ. The solutions for some of the tests are listed in Table C-25. The test results showed that the Alloy 690TT material wastage measured from weight loss in the C-ring specimens was as much or more than the Alloy 600 material in any heat treatment condition. However, the Alloy 690TT had the highest IGSCC resistance in these solutions and was considered to be relatively immune to IGSCC in the acidified sulfate and chloride environments.

C.4.3 Bouvier et al. – Neutral to Slightly Caustic Sulfate Solutions

Bouvier et al. tested C-ring specimens fabricated from Alloy 690 and Alloy 600MA&TT materials in neutral to slightly caustic sulfate solutions.[101] The chemical composition, heat treatment, and mechanical properties of the Alloys 600 and 690 SG tubing tested are listed in Table C-26. In order to be representative of the creviced areas in the SG, a calculation was performed. The calculation showed the maximum soluble sulfate concentration obtained with a ΔT of 50°C (90°F) between primary and secondary temperature was 0.6M (57000 ppm). Because the actual sulfate concentration value was considered to be less, the three deaerated solutions selected for the testing contained 0.6M, 0.05M, and 0.001M sulfate, respectively. The C-ring specimens were stressed to 0.8 YS (only for the Alloy 600), YS, and until the C-ring was closed. The C-ring specimens were tested at 320°C (608°F) for 2000 to 3000 hours. The pH at elevated temperature was adjusted to between 5 and 9.5 with sulfuric acid and sodium hydroxide. The neutral pH at 320°C (608°F) is about 5.5. Hence, the test solutions were neutral to slightly alkaline at these pH values.

The test results showed that the Alloy 600MA material had a maximum IGSCC susceptibility at a pH of 5 and that the susceptibility decreased with increasing pH values. The crack growth rate increased by a factor of 10 when the sulfate concentration was increased from 0.001M to 0.05M and from 0.05M to 0.6M. The stress level was not a factor in crack growth rate when the Alloy 600MA specimens were loaded above the yield stress. The Alloy 600TT responses paralleled those of the Alloy 600MA, except the Alloy 600TT crack growth rate decreased by a factor of two. The Alloy 690TT material was not affected in any of the solutions.

C.4.4 Bouvier et al. – Neutral Sulfate Solution + Copper

Bouvier et al. tested C-ring specimens fabricated from Alloy 690TT and Alloy 600MA&TT materials in neutral to sulfate solutions containing copper.[102] Among the large number of chemical elements present in the secondary side deposit, copper has been found on numerous pulled SG tubes. This copper may become oxidized during a lay-up and/or a shutdown in the presence of air and stagnant water. The copper oxide could have a detrimental effect on SG tubing IGSCC. The Alloy 690TT used was the same as listed in Table C-26, which was used in a previous study by Bouvier et al. The C-ring specimens were stressed to 0.8 YS (only for the Alloy 600), YS, and until the C-ring was closed. The C-ring specimens were tested at 320°C (608°F) for 2000 to 3000 hours. In order to study the copper influence, the following solutions were also used.

1. R – the reference solution, deaerated and containing 0.05M sulfate (SO_4);
2. R + mixed copper oxides ($CuO + Cu_2O$) both at 0.01% and 1%;
3. R + metallic copper (13 g/L)
4. R + metallic copper deposit on C-ring samples (electrolytic deposit);
5. R without copper but with electrochemical polarization.

The test results showed that copper or copper oxides were in general not detrimental to IGSCC of Alloy 600 material. The copper or copper oxides were beneficial in some cases as the measured crack growth rate was sometimes lower than in the reference solution. High amounts of copper oxide were found to be detrimental to the Alloy 600 material, especially to sensitized

Alloy 600 material. However, the Alloy 690 material was never affected by the addition of copper or copper oxides.

C.5 Summary of Secondary Water Corrosion

1. In an AVT water environment, the laboratory tests have demonstrated that Alloy 690 (MA or TT) is very highly resistant to IGSCC.

2. In deaerated caustic solutions, various laboratory tests consistently showed that Alloy 690TT material usually has significantly higher IGA/SCC resistance than Alloy 600MA and Alloy 600TT materials, although it may have a slightly lower SCC resistance in highly caustic water (50% NaOH) at 600^{o}F. The observed improvement for Alloy 690 is derived from longer crack initiation times and lower crack propagation rates compared to the Alloy 600 materials. However, these tests also showed that Alloy 690TT material can undergo IGA/SCC in deaerated caustic environments.

3. In neutral or acidic water, or AVT water doped with lead, Alloy 690TT material is more resistant to IGA/SCC than Alloy 600TT material, which is more resistant than Alloy 600MA material. However, all of these materials are considered to be susceptible in neutral or acidic environments containing lead.

4. In caustic water doped with PbO, Alloy 690 TT material has a somewhat lower resistance than Alloy 600MA and Alloy 600TT, but all three materials are susceptible to IGA/SCC.

5. In chloride-containing solutions in the absence of oxygen, laboratory test data confirm that both Alloy 600 and Alloy 690 materials possess very high SCC resistance. However, they can be susceptible to SCC in highly acidified chloride solutions, or when both oxygen and chloride are present. Alloy 690 material has a higher SCC resistance than Alloy 600 material under such extreme conditions.

6. In acidic solutions containing sulfate and chloride, laboratory tests show that Alloy 690TT material has a much higher IGSCC resistance than Alloy 600TT&MA materials.

7. In deaerated neutral, or slightly caustic, sulfate solutions, laboratory tests indicate that Alloy 690TT is highly resistant to IGA/IGSCC, even when copper or copper oxides are present.

In summary, even though it cannot be considered immune to IGA/SCC, Alloy 690TT material has nevertheless demonstrated far superior IGA/SCC resistance compared to Alloy 600MA or Alloy 600TT materials under most conditions pertinent to faulted secondary water. Lead-doped caustic water is an exception here. Furthermore, Alloy 690 appears to be just as resistant to IGSCC in AVT water as it is to PWSCC in primary water.

Table C-1 Alloy 690 Heats Tested in AVT Water by Miglin et al. [88]

Alloy	Ni	Cr	Fe	C	Mn	Si	S	Ti	Nb + Ta	Cu	P	Al	Mo	Other
NX4457H	62.44	28.01	8.81	0.01	0.19	0.14	0.007	0.23				0.14		
NX4458H	62.58	27.93	8.81	0.01	0.19	0.10	0.007	0.23				0.12		
NX4459H	62.01	28.25	8.86	0.06	0.20	0.10	0.007	0.32				0.17		
NX4460H	62.07	28.25	8.86	0.06	0.20	0.10	0.007	0.26				0.17		

(a) All tubes are 12.7 mm O.D x 1.35 mm wall from Huntington Alloys.

Table C-2 Alloys 600 and 690 Corrosion Test in AVT Water by Miglin et al.[88]

Test Duration			AVT Water	
^{o}C	^{o}F	Hour	SiO_2	< 0.002 ppm
360	680	17,917	Cl^-	< 0.05 ppm
343	650	93,750	Fe	< 0.01 ppm
332	630	52,343	O_2	O (excess hydrazine)
288	550	95,960	Conductivity	4 – 10 μΩ/cm
			pH	9.3 – 9.5 (NH_3 at 25 ^{o}C)

Table C-3 Summary of Alloy 690 SCC Results in Deaerated 50% NaOH Solution [89]

Test	Strain	NaOH Conc.	Temp		Time,	SCC Results [a]		TT Condition
	%	%	°C	°F	Hour	MA	TT	
U-Bend		10	307	585	500		NC	10-hour at 1325°F
U-Bend		10	307	585	500		C	7-hour at 1125°F + 7-hour at 1050°F
U-Bend		10	316	600	1176	C		
U-Bend		10	316	600	1296	C	NC	10-hour at 1200°F
U-Bend		10	316	600	1008	C	C	2-hour at 1200-1250°F
U-Bend		10	325	617	500	C	NC	15-hour at 1292°F
U-Bend		10	350	662	5976	C	NC	>0.2-hour at >1300 °F
U-Bend		50	284	543	336	C	C	2-hour at 1200-1250°F
U-Bend		50	300	572	840	C	C	2-hour at 1200-1250°F
U-Bend		50	315	599	Unknown	C		
U-Bend		50	316	600	72	C		
U-Bend		50	316	600	336	C		
U-Bend		50	316	600	1680	C	C	2-hour at 1200-1250°F
U-Bend		50	332	630	1680	C	C	2-hour at 1200-1250°F
RUB		10	360	680	10000	C		
C-Ring	0.5	4	323	613	2000		NC	5-hour at 1300-1328°F
C-Ring	< 0.4	10	288	550	480	NC	NC	10-hour at 1300°F
C-Ring	> 0.2	10	315	599	144	C		Unknown
C-Ring	0.3	10	316	600	4800	NC	NC	10-hour at 1200°F
C-Ring	0.3	10	316	600	2000	NC	NC	16-hour at 1292°F
C-Ring	2	10	316	600	1920	C, NC	NC	4-hour or 15-hour at 1300°F
C-Ring	0.2	10	320	600	2000		NC	Unknown
C-Ring	0.2	10	332	630	5592	NC	NC	10-hour at 1200°F
C-Ring	0.3	10	343	650	2000	C	NC	16-hour at 1292°F
C-Ring	0.3	10	343	650	1500	NC	NC	15-hour at 1292°F
C-Ring	2	10	350	662	2000		NC	
C-Ring	0.2	50	316	600	336	NC		
C-Ring TLT[b]	14	10	316	600	2000	C	NC	16-hour at 1292°F
C-Ring TLT[b]	14	10	343	650	2000	C	NC	16-hour at 1292°F
C-Ring TLT[b]		30	288	550	2900	NC	NC	<10-hour at 1200-1600 °F
C-Ring TLT[b]		50	340	644	8000	C	C	12-hour at 1220°F

(a) NC – Not cracked; C - Cracked.
(b) C-Ring until the legs touched.

Table C-4 IGA in Alloy 690TT C-Rings in Deaerated Caustic Solutions at 644°F by A. Smith et al.[32]

Alloy	Environment	Mean IGA Depth (μm)	Standard Dev.	Maximum IGA Depth (μm)	Test Time (hour)
E1	50% NaOH	38.4	17	157	8000
A1	50% NaOH	26.1	10	56	8000
E4	30% NaOH + 10% Na_2SO_4	29.4	9	75	8000
A5	30% NaOH + 10% Na_2SO_4	17.4	8	59.2	8000
A5	30% NaOH + 10% Na_2SO_4	10.9	5	41	1200
E3	30% NaOH + 10% Na_2SO_4	26.0	12	88	1200

Table C-5 K_{iscc} of Alloys 600 and 690 in Deaerated NaOH Solution by K. Smith et al.[11]

Alloy	NaOH Concentration (gram/liter)	K_{ISCC}, MPa$\sqrt{m}$
600MA	100	9.2
600TT	100	12.8
690MA	100	16.4
690TT	100	23.2
600MA	4	20.4
600TT	4	21.6
690MA	4	No SCC
690TT	4	No SCC

(a) TT – thermally treated, 15-hour at 1292°F.

Table C-6 Alloys 600 and 690 C-Rings in Deaerated 10% NaOH at 315°C by K. Smith et al.[11]

Alloy	Crack Depth, μm				
	50%YS	75%YS	90%YS	150%YS	TLT (14% Strain)
600MA	0	25	Thru-wall	Thru-wall	Thru-wall
600TT	10	10	10	Thru-wall	Thru-wall
690MA	0	10	10	30	Thru-wall
690TT	0	0	0	0	5

(a) Corrosion potential was kept in the active-passive transition, 140mv vs. Ni.

Table C-7 Alloys 690 and 600 Tested in Deaerated 10% and 30% NaOH Solutions by Sarver et al.[91]

Heat	Ni	Cr	Fe	C	Mn	Si	S	Ti	Nb + Ta	Cu	P	Al	Mo	Co
753234 Alloy 690	59.2	29.9	9.8	0.02										
96834 Alloy 600	75.0	15.8	8.0	0.04										

Table C-8 Results of C-Ring Specimens in Deaerated NaOH Solution by Sarver et al. [91]

	Heat Treatment	Depth of Attack (% through-wall)	Form of Attack
Alloy 690MA	5-min at 2000°F	3.6	Pits, Heavy Oxide
Alloy 690TT	5-min at 2000°F + 30-min at 1200 °F	6.4	Intergranular Penetration, Pits, Heavy Oxide
Alloy 690TT	5-min at 2000°F + 10-hour at 1218 °F	3.6	Intergranular Penetration
Alloy 690TT	5-min at 2000°F + 1-hour at 1300 °F	4.5	Intergranular Penetration
Alloy 690TT	5-min at 2000°F + 5-hour at 1300 °F	4.5	Intergranular Penetration
Alloy 690TT	5-min at 2000°F + 10-hour at 1300 °F	2.7	Intergranular Penetration
Alloy 690TT	5-min at 2000°F + 1-hour at 1400 °F	2.7	Intergranular Penetration, Heavy Oxide
Alloy 690TT	5-min at 2000°F + 1-hour at 1500 °F	3.6	Intergranular Penetration, Heavy Oxide
Alloy 690TT	5-min at 2000°F + 10-min at 1600 °F	3.6	Intergranular Penetration
Alloy 600MA	5-min at 1900°F	100	Intergranular Penetration
Alloy 600TT	5-min at 1900°F + 15-hour at 1300 °F	100	Intergranular Penetration

(a) At 550°F for 2-month in 10% NaOH solution with 170mV potential an 2-month in 30% NaOH solution with 210 mV potential.

Table C-9 Alloys 690 and 600 SG Used by Vaillant et al. [92]

Heat [(a)]	%C	Heat Treatment	YS 20°C	YS 350°C	UTS 350°C	Grain Size	Inter-granular Carbides	Intra-granular Carbides
			MPa	MPa	MPa	ASTM		
6C, Ind, Alloy 600	0.025	1000-1020°C	310	690	240	7-8	Low	Low
6D, Exp, Alloy 600	0.045	1070°C	340-353	700-710	270-300	8-9	Low	Heavy
6I1, Exp, Alloy 600	0.021	Not listed	305	698	258	9	Medium	Low
6J, Ind, Alloy 600	0.038	980°C	396	752	369	10	Medium	Low
6M, Ind, Alloy 600	0.039	980°C	380	720	340	10	Heavy	Low
6P, Ind, Alloy 600	0.016	980°C	320-340	702-720	275-300	9	Low	Low
		980°C + 700°C	329	719	254	9	Low	Heavy
SL, Ind, Alloy 600	0.014	950-990°C	286	691	227	6	Low	Low
6V, Exp, Alloy 600	0.030	1150°C	175	613	125	2	Low	Medium
9E1, Exp, Alloy 690	0.028	1040°C	370	760	280	8-9	Heavy	Low
		1040°C+ 700°C	350	750	270	9	Heavy	Low – medium
9E2, Exp, Alloy 690	0.032	1010°C	360	710	290	7-8	Heavy	Low
		1010°C+ 700°C	330	690	270	7-8	Heavy	Low – medium
9G3, Exp, Alloy 690	0.012	1045°C	319	722	241	7-8	Medium	Low
		1045°C+ 700°C	314	730	244	7	Medium	Heavy
9G4, Exp, Alloy 690	0.012	980°C	409	806	331	10	Medium	Low
		980°C+ 700°C	407	792	323	10	Medium	Medium
9P1, Exp, Alloy 690	0.028	980°C+ 700°C	497	848	423	11	Medium – heavy	Medium
9P2, Exp, Alloy 690	0.028	1040°C+ 700°C	419	825	358	9-10	Medium	Low – medium
9I1, Ind, Alloy 690	0.015	1040-1080°C+ 700°C	304	727	244	7	Low	Medium – heavy
9I2, Ind, Alloy 690	0.021	1040-1070°C+ 700°C	360	755	287	7-8	Low	Low – medium

(a) Ind – industrial heat SG tube; Exp – experimental heat of SG tubes.

Table C-10 IGSCC in 350°C Deaerated NaOH Solution Used by Vaillant et al. [92]

Stress Level > Yield Strength (C-Ring at 2YS, U-Bend, RUB, WOL)

	NaOH Concentration,					
	1 g/L	4g/L	10 g/L	40g/L	100 g/L	500 g/L
Alloy 600MA		Crack (C-Ring)	Crack (C-Ring)	Crack (C-Ring)	Crack (C-Ring)	Crack (C-Ring)
Alloy 600TT			Crack (C-Ring)	Crack (C-Ring)	Crack (C-Ring)	
Alloy 690 intergranular carbides			No Crack (RUB)		Crack (WOL)	
Alloy 690 with intragranular carbides		No Crack (C-Ring)	No Crack (RUB)		Crack (WOL)	Very Short crack (C-Ring)

Stress Level <= Yield Strength (C-Ring)

	NaOH Concentration,					
	1 g/L	4g/L	10 g/L	40g/L	100 g/L	500 g/L
Alloy 600MA		Crack (C-Ring)	Crack (C-Ring)	Crack (C-Ring)	Crack (C-Ring)	Crack (C-Ring)
Alloy 600TT		No Crack (C-Ring)	Crack (C-Ring)		Crack (C-Ring)	No Crack (C-Ring)
Alloy 690 intergranular carbides			No Crack (C-Ring)		No Crack (C-Ring)	
Alloy 690 with intragranular carbides		No Crack (C-Ring)	No Crack (C-Ring)		Crack (C-Ring)	

Table C-11 Properties of Alloy 690 in the As-Received Condition [93]

Matl.	Ni	Cr	Fe	C	Mn	Si	S	Ti	Nb + Ta	Cu	P	Al	**Co**	**Mg**
SG Tubing A	59.03	29.93	10.0	0.025	0.16	0.19	0.001	0.34		0.03	0.006	0.25	0.005	0.004
SG Tubing B	59.12	30.05	10.11	0.029	0.07	0.14	0.001	0.33		0.05	0.005	0.18	0.01	
Plate	59.38	29.98	9.41	0.028	0.11	0.32	0.001	0.32		0.03	0.015	0.38	0.03	0.02

Matl.	Size	Final Anneal	Thermal Treatment	ASTM Grain Size	Mechanical Properties
SG Tubing A	6.30 mm O.D. x 0.46 mm	< 4-min at >1093°C	10-hour at 718°C	6-7	YS = 302 MPa UTS = 680 MPa Elong. = 46.8%
SG Tubing B	12.70 mm O.D. x 1.45 mm	< 4-min at >1093°C	10-hour at 718°C	5-7	
Plate	38.1 mm thick	4-hour at 1038°C, air cool	None	6	YS = 324 MPa UTS = 691 MPa Elong. = 46%

Table C-12 Alloy 690 SG Tubing Heat Treatments Used by Mertz et al. [93]

Final Grain Boundary Carbide	Reference (Continuous)	Modified (Semi-continuous)	Local Grain Growth (None to discontinuous)
SG Tubing Heat	A, B	A, B	A
Mill Annealed (MA) 1107°C	X	X	X
Thermal Treatment (TT) 10-hour at 718°C	X	X	X
Thermal HIP [(a)] 6-hour at 995°C		X	
Deformation HIP [(a)] 0.25-hour at 995°C			X
Thermal HIP [(a)] 5.75-hour at 995°C			X

(a) HIP – hot isostatic pressing performed 995°C. The treatment was used to cause strain-induced grain boundary migration without dissolving the carbides. Hence the migrated grain boundary would be undecorated by carbides.

Table C-13 Alloy 690 Plate Heat Treatments Used by Mertz et al. [93]

Condition	Final Grain Boundary Carbide	Maximum Crack Depth, after 500 hours in 10% NaOH at 585+/–11°F
HRA – as received hot rolled plate + 4-hour at 1038°C, air cool	Semi-continuous	0.043
HRA + TT (10-hour at 718°C)	Semi-continuous	0.025
HRA + SA (2-hour at 1177°C solution anneal) + WQ (water quench)	Un-decorated	0.508
HRA + SA + WQ + TT	Continuous	0.010

Table C-14 Properties of Alloys 600 and 690 Used by Kawamura et al. [94]

Matl.	Ni	Cr	Fe	C	Mn	Si	S	Ti	Nb + Ta	Cu	P	Al	Mo	Other
Alloy 600 SG Tube	74.90	15.90	8.20	0.026	0.29	0.29	0.001			0.01	0.007			
Alloy 690 SG Tube	59.85	30.50	8.60	0.02	0.28	0.31	0.001				0.009			
Alloy 600 Plate	76.66	15.40	7.24	0.021	0.34	0.33	0.002			0.002	0.004			
Alloy 690 Plate	60.75	29.95	8.42	0.018	0.29	0.28	0.001			0.03	0.009			

Test	Matl.	Mill Anneal Treatment	Thermal Heat Treatment	0.2% YS, MPa	UTS, MPa	Elong, %
C-Ring, from SG Tube	600MA	2-min at 1025°C, H_2 cool		284	667	52
	600FS	2-min at 1025°C, H_2 cool	1-hour at 700°C			
	600TT	2-min at 1025°C, H_2 cool	15-hour at 700°C			
	690TT	3-min at 1075°C, H_2 cool	15-hour at 700°C	333	735	50
DCB, from Plate	600MA	30-min at 925°C, air cool				
	690TT	5-hour at 1050°C, H_2 cool	15-hour at 700°C	263	637	41

Table C-15 Properties of Alloys 600 and 690 Used by Kim et al. [95]

Matl.	Ni	Cr	Fe	C	Mn	Si	S	Ti	Nb + Ta	Cu	P	Al	N	B
HT600A	72.5	16.85	9.00	0.025		0.31	0.003	0.28		0.01	0.008	0.015	0.016	0.001
HT600B	74.76	15.63	8.62	0.025		0.14	<0.001	0.34		0.03	0.007	0.21	0.01	0.004
HT600C	76.11	15.29	7.57	0.026		0.15	0.001	0.32		0.015	0.008	0.23	0.004	0.004
HT600D	75.08	15.38	8.56	0.023		0.20	0.001	0.26		<0.01	0.006	0.24	0.01	0.003
HT600	75.14	15.46	8.42	0.025		0.16	0.001	0.29		0.011	0.008	0.21	0.0042	0.0039
LT600	74.66	15.21	9.16	0.022		0.2	0.001	0.29		0.01	0.003	0.24		
TT690E	58.9	29.57	10.54	0.02		0.22	0.001	0.26		0.01	0.009	0.019	0.017	0.004
HT690	60.39	29.66	8.90	0.017		0.14	0.001	0.26		0.007	0.005	0.35	0.009	0.0007

Matl.	Mill Anneal Treatment	YS, MPa	UTS, MPa	Elong, %	ASTM Grain Size
HT600A	High temperature mill anneal	275	689	44	5.5
HT600B	High temperature mill anneal	244	647	47	5.0
HT600C	High temperature mill anneal	258	675	43	6
HT600D	High temperature mill anneal	255	661	44	6
HT600	High temperature mill anneal	255	669	44	
LT600	Low temperature mill anneal	310	679	44	
TT690E	High temperature mill anneal + 10-hour at 715°C	330	730	44	
HT690	High temperature mill anneal	293	698	52.2	

Table C-16 Chemical Composition of Alloys 600 and 690 Used by Castano-Marin et al. [96]

Matl.	Ni	Cr	Fe	C	Mn	Si	S	Ti	Nb + Ta	Cu	P	B	N	Co
690TT, A	59.42	29.05	10.49	0.022	0.33	0.29	0.001	0.24		0.007	0.008	0.001	0.037	0.011
690TT, B	60.10	30.10	8.51	0.019	0.26	0.40	0.002	0.32		0.010	0.012	0.001	0.027	0.010
600MA, G	73.84	16.16	9.34	0.045	0.18	0.18	0.007	0.21		0.260	0.007	0.002		0.050
600TT, H	74.64	14.81	9.80	0.044	0.21	0.24	0.009	0.21		0.260	0.009	0.003		0.050

Table C-17 Mechanical Properties of Alloys 600 and 690 Used by Castano-Marin et al. [96]

Matl.	YS, MPa	UTS, MPa	Elong., %	Tube Size, mm
690TT, A	359	754	42.2	19.05 x 1.09
690TT, B	332	731	45.0	17.45 x 1.02
600MA, G	386	793	36.5	19.05 x 1.09
600TT, H	386	772	36.5	17.45 x 1.02

Table C-18 C-Ring Test Condition and Results by Castano-Marin et al. [96]

Test Temperature 350°C (662°F)

Solution		10%NaOH	10%NaOH + 0.1M(2%)PbO	10%NaOH + 0.01M(0.2%)PbO	4%NaOH + 0.002M(0.04%)PbO	0.75M Na_2SO_4 + 0.25M $FeSO_4$	0.75M Na_2SO_4 + 0.25M $FeSO_4$ +0.1M(2%)PbO
Matl.	pH [(a)]	13.77	13.76	13.80	13.57	3.99	6.49
690TT, A	500-h 750-h 1000-h Mode	0% 0% <2.0%	100% TGSCC	100% TGSCC	50% -- 88% TGSCC	0% 0% 0%	0%
690TT, B	500-h 600-h 750-h 1000-h Mode	0% -- 0% <1.4%	100% TGSCC	0% 63% TGSCC	0% -- -- 0%	0% -- 0% 0%	0%
600MA, G	500-h 600-h 750-h 1000-h Mode	45% -- 70% 80% IGSCC	10% IGA+IGSCC	50% 53% IGA+IGSCC	12% -- -- 70% IGA+IGSCC	82% IGSCC	100% IGSCC

Test Temperature 320°C (608°F)

Solution		4%NaOH	4%NaOH + 0.01M(0.2%)PbO	4%NaOH + 0.002M(0.04%) PbO	4%NaOH + 0.0004M(0.008%) PbO	AVT + 0.01M(0.2%) PbO [(b)]	AVT + 0.002M (0.04%) PbO [(b)]
Matl.	pH [(a)]	13.80	13.79	13.82	13.69	9.52	7.06
690TT, B	500-h 1000-h 1500-h 2000-h Mode	-- 0%	-- 0% -- 0%	-- 0% -- 0%	-- 0% -- 0%	-- 0% -- 0%	-- 0% -- 0%
600MA, G	500-h 1000-h 1500-h 2000-h Mode	-- 20% IGSCC	-- 10% -- 17% IGA	-- 2% 4% 9% IGA	-- 5% -- 12% IGA	-- 40% 43% 37% IGSCC	-- 11% 23% 25% IGSCC
600TT, H	500-h 1000-h 1500-h 2000-h Mode		-- 2% -- 2% IGA	-- 1% -- 6% IGA	-- 2% -- 3% IGA	-- 26% -- 27% TG+IGSCC	-- 13% -- 34% TG+IGSCC

(a) Room temperature pH value.
(b) AVT – Deionized and deaerated water + 500 ppb N_2H_4.

Table C-19 Properties of Alloys 600 and 690 Used by Helie [97]

Matl.	Ni	Cr	Fe	C	Mn	Si	S	Ti	Nb + Ta	Cu	P	Al	N	Co
600 (a)	73.74	15.83	8.69	0.036	0.82	0.27	<0.005	0.31		0.005	0.009	0.26		0.021
690b (b)	58.93	29.25	10.58	0.016	0.32	0.29	<0.001	0.21		0.01	0.008	0.13	0.034	0.010
690c (C)	59.65	28.92	10.36	0.020	0.31	0.31	<0.005	0.24		0.006	<0.005	0.16	0.035	0.014

(a) Alloy 600 was mill annealed at 965°C (1769°F).
(b) Alloy 690b was thermally treated at 700°C (1292°F) for 5 hours. Alloy 690b was only used for CERT specimens in PbO doped water.
(c) Alloy 690c was thermally treated at 700°C (1292°F) for 5 hours. Alloy 690c was only used for RUB specimens in PbO and PbS doped water.

Table C-20 Summary of Alloys 600 and 690 in Chloride Solutions at Low Temperatures [98]

Material	Chloride-containing Solution	Temperature, °C	Duration	IGSCC/TGSCC
600	3.5%NaCl + 0.5% CH_3CO_2H + H_2S	30	5040	None
	50% H_2SO_4 + 3%NaCl	30	5040	None
	NaCl	100	5040	None
	NaCl saturated (pH 4)	109	5040	None
	42% $MgCl_2$	154	1680	None
	85% $ZnCl_2$	180	1680	None
690	$MgCl_2$ U-bend	154	2325	None

Table C-21 Summary of Alloy 690 in Chloride Solutions at High Temperatures [98]

Solution	Temperature		Test Type	Duration (hour)	Results
	°C	°F			
500 ppm Cl-	260	500	Double U-Bend	3024	Not cracked
875 ppm Cl-	260	500	Double U-Bend	1344	Not cracked
600 ppm Cl- + 150 ppm Na2HPO4, un-deaerated	260	500	Double U-Bend	1344	Not cracked
100 ppm Cl- (CuCl2 + NiCl2 + Seawater)	288	550	Double U-Bend Double C-Ring	4000	Not cracked
500 ppm Cl-	300	572	Double U-Bend	1000	Not cracked
Deaerated water + 500 ppm Cl-	316	600	Double U-Bend	16128	Not cracked
100 ppm Cl- + 50 ppb O2	320	608	Capsules	14000	Not cracked
AVT + 400g NaCl (pH 3 – 9)	333	631	Not listed	2000	Not cracked
AVT + 200g NaCl + 200g FeCl2 (pH 3 – 5)	333	631	Not listed	840	Not cracked
100 ppm Cl-	350	662	Capsules	21000	Not cracked
100 ppm Cl- + 300 ppb O2	350	662	Capsules	15000	Not cracked

Table C-22 Materials Tested in Boiling $MgCl_2$ by Berge et al. [98]

Matl.	Identification	Heat Treatment	SCC Specimens	C	Cr	Ni	Fe	Mo
600	U572, tube	MA, Sensitized (1-h at 700°C)	RUB	0.028	15.25	74.5	9.25	--
690	U455, tube	MA	RUB	0.018	28.90	59.3	10.95	<0.01
304L	U118, tube	MA (1040°C)	RUB	0.023	18.15	11.4	67.4	0.50

Table C-23 RUB Test Results in Boiling $MgCl_2$ by Berge et al. [98]

Matl.	Identification	Heat Treatment	pH 1	pH 1.6	pH 2.3
600	U572, tube	MA	Not cracked after 1500-hour	Intergranular crack after 1500-hour	Not cracked after 1500-hour
		Sensitized (1-h at 700°C)	Not cracked after 1500-hour	Not cracked after 1500-hour	Not cracked after 1500-hour
690	U455, tube	MA	Intergranular crack depth 60 μm after 288-hour	Not cracked after 1200-hour	Not cracked
304L	U118, tube	MA (1040°C)	Fail < 24-hour	Fail < 24-hour	Fail < 24-hour

Table C-24 Chemical Composition of Alloys 600 and 690 Used by Cullen et al. [99, 100]

Alloy	Ni	Cr	Fe	C	Mn	Si	S	Ti	Nb + Ta	Cu	P	Al	Co
600, LTMA & Sensitized	74.26	14.46	9.47	0.024	0.39	0.17	0.004			0.40			0.074
600, HTMA	74.29	14.41	9.40	0.025	0.39	0.17	0.001			0.40			0.074
600, TT	Bal.	16.00	9.00	0.046	0.24	0.100	0.004	0.26				0.26	
690, TT	59.80	28.58	10.50	0.021	0.36	0.34	0.001	0.28		0.005	0.008	0.13	0.013

Alloy	Heat	Heat Treatment	Surface Finish
600, LTMA	NX3587	Low-temperature MA, 3 to 5-min. at 927°C (1700°F)	As ground
600, HTMA	NX3587	High-temperature MA, 3 to 5-min. at 1024°C (1875°F)	As ground
600, TT	NX1054	MA + 15-hour at 705°C (1300°F), air cool	As Heat treated
690, TT	WF657	MA + 5.75-hour at 700°C (1292°F), air cool	As Heat treated
600 Sensitized	NX3587	3 to 5-min at 1024°C (1875°F), 11-hour at 621°C (1150°F), air cool	As Heat treated

Table C-25 Autoclave Solutions Used for C-Ring Tests by Cullen et al. [100]

Alloy	Heat Treatment	pH at 315°C
Test 3.1	0.00946m NH_4HSO_4, 0.0045m $(NH_4)_2SO_4$	3.16
Test 3.2	0.0045m NH_4HSO_4, 0.0046m $(NH_4)_2SO_4$, 0.005m NaCl	3.34
Test 3.5	0.1m $(NH_4)_2SO_4$	4.33
Test 3.6	1.0m $(NH_4)_2SO_4$	3.90

Table C-26 Properties of Alloys 600 and 690 Used by Bouvier et al. [101]

Alloy	Ni	Cr	Fe	C	Mn	Si	S	Ti	Nb + Ta	Cu	P	Al	N	B
600	Bal.	16.01	6.59	0.044	0.25	0.40	0.007				0.007			
690	Bal.	28.9	10.9	0.018	0.34	0.32	0.002				0.004			

Matl.	Mill Anneal Treatment	YS, MPa	UTS, MPa	Elong, %
600MA	2-min at 1070°C (1958°F)	350	280	36
600TT	MA + 16-hour at 700°C (1292°F)	330	280	33
690TT	MA + 5-hour at 700°C (1292°F)	306	245	50

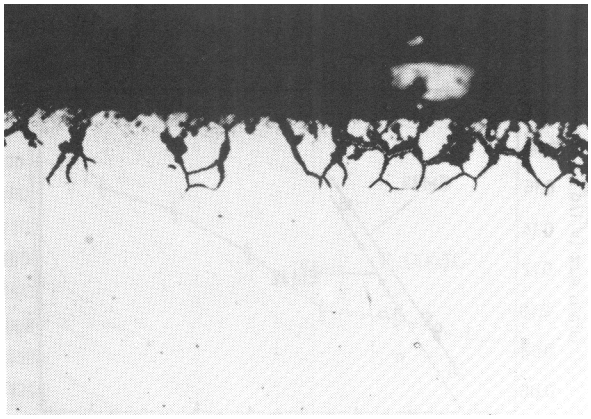

Figure C-1 Intergranular attack (IGA) in Alloy 690TT C-ring (specimen E3) after 1,200 hours in deaerated 50% NaOH at 340°C (644°F). Magnification 500X.[32]

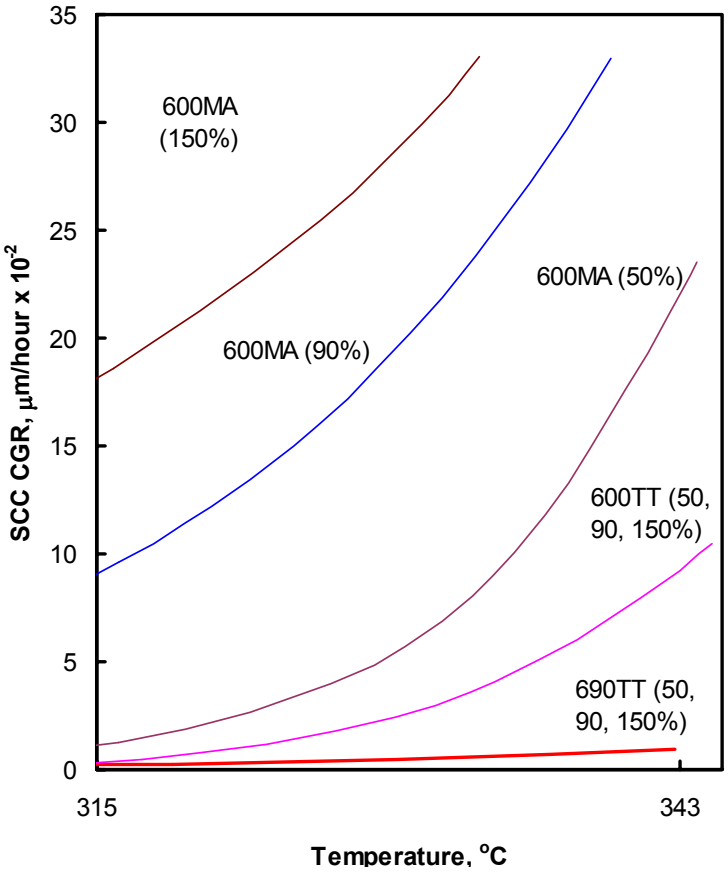

Figure C-2 Crack growth rate of Alloy 690TT and Alloy 600MA&TT from C-Ring specimens in deaerated 10% NaOH solution. (x%) indicate the loading stress to x% of the yield strength. After Ref. 11.

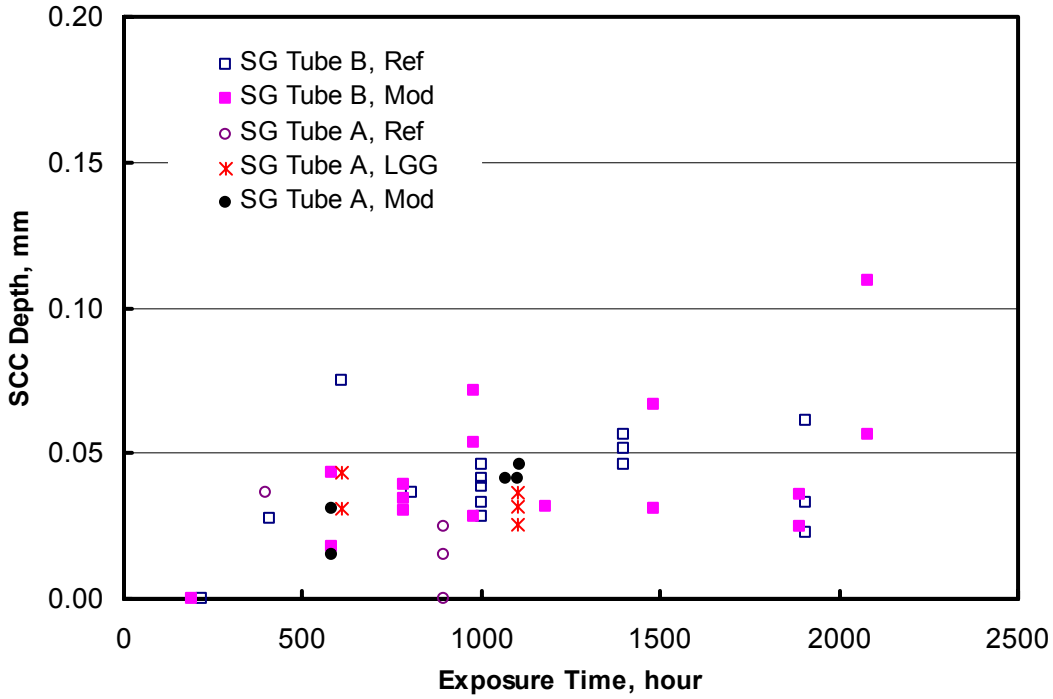

Figure C-3 Caustic SCC crack depth of Alloy 690 SG tubing thermally heat treated to produce different intergranular carbide morphology. The results indicate that there is little additional improvement in caustic SCC resistance from a continuous intergranular carbide coverage in thermally heat treated Alloy 690. After Ref. 93.

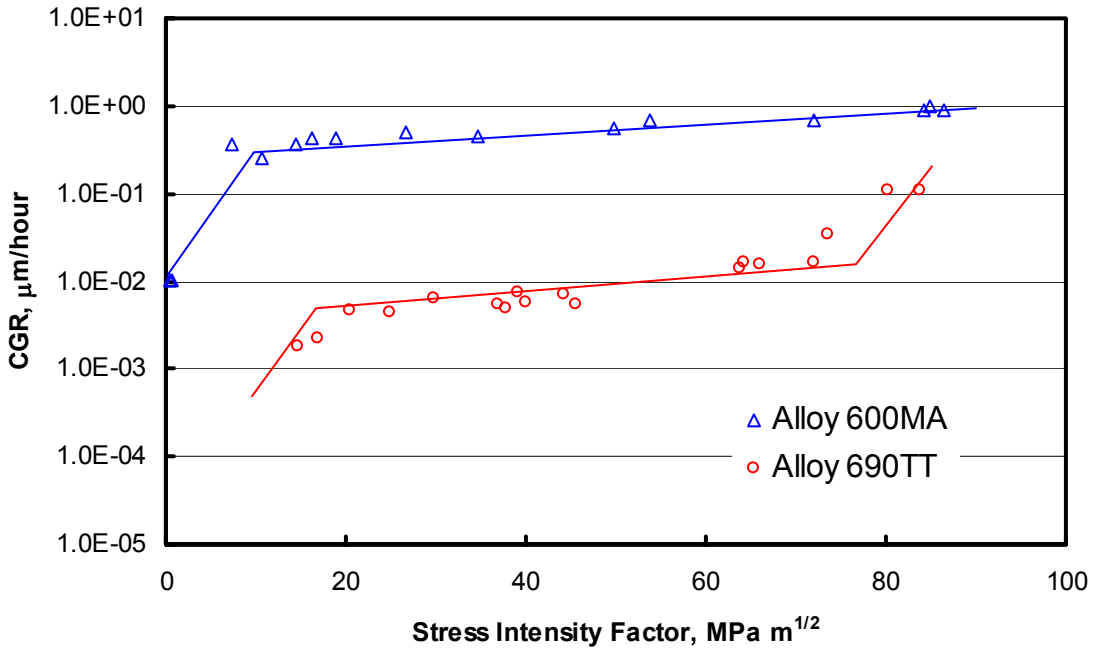

Figure C-4 Caustic SCC crack growth rate as a function of stress intensity factor by DCB tests in deaerated caustic solution. After Ref. 94.

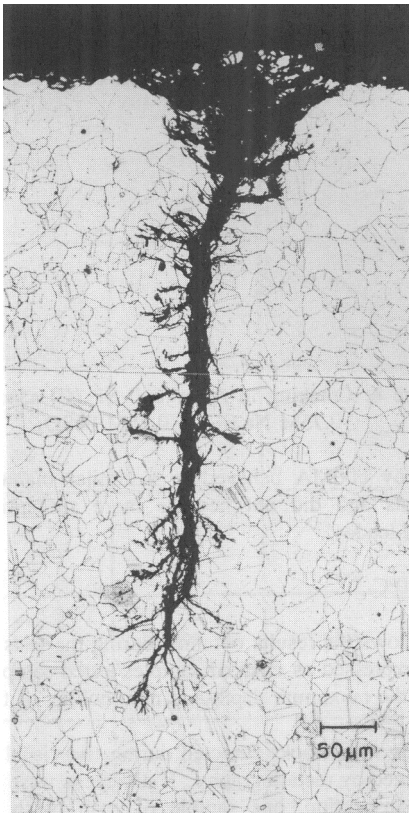

Figure C-5 TGSCC in Alloy 690TT after 500 hours in 10% NaOH + 0.1M PbO at 350°C (662°F).[96]

D REFERENCES

1. H. Coriou, et al., “High Temperature Stress Corrosion Cracking of Inconel in Water,” Third Metallurgical Symposium on Corrosion (Aqueous and Gaseous),1959, North Holland Publishing Co., Amsterdam, published in 1960, pp. 161-169.

2. F. Champigny, F. Chapelier, et al., “Maintenance Strategy of Inconel Components in PWR Primary System in France,” paper presented NRC/ANL Conference on Vessel Head Penetration Inspection, Cracking, and Repair in Gaithersburg, MD from September 29 – October 2, 2003 (to be published).

3. B. Gronwall, L. Ljungberg, et al., “Intercrystalline Stress Corrosion Cracking of Inconel 600 Inspection Tubes in the Agesta Reactor,” Atomenergi, (Rapp.) AE, AE-245, 1966.

4. C.A. Campbell and S. Fyfitch, “PWSCC Ranking Model for Alloy 600 Components,” Proceedings of 6th International Conference on Environmental Degradation of Materials in Nuclear Power Systems—Water Reactors, TMS, 1993, p. 863.

5. INCONEL Alloy 600, Publication Number SMC-027, Special Metals Corporation, 2002 (Sept. 02).

6. INCONEL Alloy 690, Publication Number SMC-079, Special Metals Corporation, 2002 (Sept. 02).

7. Datasheet for “INCONEL Filler Metal 52M,” Special Metals Corporation, 2003

8. EPRI Report TR-016743-V2R1 “Guidelines for PWR Steam Generator Tubing Specification and Repair,” Vol. 2, Rev. 1: Guidelines for Procurement of Alloy 690 Steam Generator Tubing, Final Report, April 1999.

9. A.J. Sedricks, J.W. Schultz, and M.A. Cordovi, “Inconel Alloy 690 – A New Corrosion Resistant Material,” Corrosion Engineering (Boshoku Gijutsu), vol. 28, pp. 82-95, 1979, Japan Society of Corrosion Engineering.

10. H. Xu and S. Fyfitch, “Aging Embrittlement Modeling of Type 17-4PH at LWR Temperatures,” the 10th International Conference on Environmental Degradation of Materials in Nuclear Power Systems – Water Reactors, NACE International, Houston, Texas (2001).

11. K. Smith, A. Klein, P. Saint-Paul, J. Blanchet, “Inconel 690, A Material with Improved Corrosion Resistance for PWR Steam Generator Tubes,” Proceedings of 2nd International Symposium on Environmental Degradation of Materials in Nuclear Power Systems – Water Reactors, Monterey, CA, 1985 pp. 319-328.

12. T. Larsson, J. O. Nilsson, and J. Frodigh, “On the Possibility of Forming Ordered Ni_2Cr in Alloy 690,” Proceedings of 9th International Symposium on Environmental Degradation of Materials in Nuclear Power Systems – Water Reactors, Newport Beach, CA, 1999, pp. 143 to 147.

13. S.M. Bruemmer and C.H. Henager, “Microstructure, Microchemistry, and Microdeformation of Alloy 600 Tubing,” Proceedings of 2nd International Symposium on Environmental Degradation of Materials in Nuclear Power Systems – Water Reactors, Monterey, CA, 1985 pp. 293-300.

14. K. Norring, K. Stiller, and J. Nilsson, “Grain Boundary Microstructure, Chemistry, and IGSCC in Alloy 600 and Alloy 690,” Proceedings of 5th International Symposium on Environmental Degradation of Materials in Nuclear Power Systems – Water Reactors, Monterey, CA, 1991.

15. K. Stiller, J. Nilsson, and K. Norring, “Structure, Chemistry and Stress Corrosion Cracking of Grain Boundaries in Alloys 600 and 690,” Metallurgical and Materials Transactions, Vol. 27A-No.2, February, 1996.

16. J.M. Sarver, J.R. Crum, and W.L. Mankins, “Carbide Precipitation and the Effect of Thermal Treatments on the SCC Behavior of Inconel Alloy 690,” Proceedings of 3rd International Symposium on Environmental Degradation of Materials in Nuclear Power Systems – Water Reactors, Traverse City, MI, 1987. pp. 581-586.

17. T. Yonezawa, K. Onimura, N. Sasaguri, T. Kusakabe, H. Nagano, K. Yamanaka, T. Minami, M. Inoue, “Effect of Heat Treatment on Corrosion Resistance of Alloy 690,” Proceedings of 2nd International Symposium on Environmental Degradation of Materials in Nuclear Power Systems – Water Reactors, Monterey, CA, 1985 pp. 593-600.

18. G.P. Airey, “Effect of Processing Variables on the Caustic Stress Corrosion Resistance of Inconel Alloy 600,” Corrosion, vol. 36(1), 1980, pp. 9-17.

19. J.R. Crum, “Effect of Composition and Heat Treatment on Stress Corrosion Cracking of Alloy 600 Steam Generator Tubes in Sodium Hydroxide,” Corrosion, vol. 36(1), 1982, pp. 40-45.

20. EPRI report NP-4665M-SR, “Proceedings: Workshop on Thermally Treated Alloy 690 Tubes for Nuclear Steam Generators,” July 1986.

21. ASTM Standard A 262, “Standard Practices for Detecting Susceptibility to Intergranular Attack in Austenitic Stainless Steels,”.

22. O.K. Chopra and H.M. Chung, “Aging Degradation of Cast Stainless Steels: Effects on Mechanical Properties,” Proceedings of the 3rd Environmental Degradation of Materials in Nuclear Power Systems – Water Reactors,” pp. 737-748, September 1987, Traverse City, Michigan.

23. ASME SB-163, “Specification for Seamless Nickel and Nickel Alloy Condenser and Heat-Exchanger Tubes,” ASME Boiler and Pressure Vessel Code, Section II Part B, Nonferrous Material Specifications, 2001.

24. ASME SB-166, “Specification for Nickel-Chromium-Iron Alloys (UNS N06600, N06601, N06603, N00690, N06025, and N06045) and Nickel-Chromium-Cobalt-Molybdenum Alloy (UNS N06617) Rod, Bar, and Wire,” ASME Boiler & Pressure Vessel Code, Section II Part B, Nonferrous Material Specifications, 2001.

25. ASME SB-167, “Specification for Nickel-Chromium-Iron Alloys (UNS N06600, N06601, N00690, N06025, and N06045) Seamless Pipe and Tube,” ASME Boiler & Pressure Vessel Code, Section II Material Specifications, Part B, 2001.

26. ASME SB-168, “Specification for Nickel-Chromium-Iron Alloys (UNS N06600, N06601, N06603, N00690, N06025, and N06045) and Nickel-Chromium-Cobalt-Molybdenum Alloy (UNS N06617) Plate, Sheet, and Strip,” ASME Boiler & Pressure Vessel Code, Section II Material Specifications, Part B, 2001.

27. ASME SFA-5.11, “Specification for Nickel and Nickel-Alloy Welding Electrodes for Shielded Metal Arc Welding,” ASME Boiler & Pressure Vessel Code, Section II, Part C, Specifications for Welding Rods, Electrodes, and Filer Metals, 2001.

28. ASME SFA-5.14, “Specification for Nickel and Nickel-Alloy Welding Bare Electrodes and Rods,” ASME Boiler & Pressure Vessel Code, Section II, Part C, Specifications for Welding Rods, Electrodes, and Filer Metals, 2001.

29. Data Sheet for Inconel Welding Electrode 152 and 182, Inconel Filler Metal 52 and 82, Special Metals Welding Products Company.

30. ASME Boiler & Pressure Vessel Code, Section II Part D, Materials Properties, 2001.

31. J.N. Esposito, G. Economy, W.A. Byers, J.B. Esposito, F.W. Pement, R.J. Jacko, C.A. Bergmann, “The Addition of Zinc to Primary Reactor Coolant for Enhanced PWSCC Resistance,” Proceedings of 5th International Symposium on Environmental Degradation of Materials in Nuclear Power Systems – Water Reactors, Monterey, CA, 1991. pp. 495-501.

32. A. Smith and R. Stratton, “Relationship between Composition, Microstructure and Corrosion Behavior of Alloy 690 Steam Generator Tubing for PWR Systems,” Proceedings of 4th International Symposium on Environmental Degradation of Materials in Nuclear Power Systems – Water Reactors, Jekyll Island, GA, 1989. pp.5-33 to 5-46.

33. A. Smith and R. Stratton, “Thermal Treatment, Grain Boundary Composition and Intergranular Attack Resistance of Alloy 690,” Proceedings of 5th International Symposium on Environmental Degradation of Materials in Nuclear Power Systems – Water Reactors, Monterey, CA, 1991. pp. 855-860.

34. ASTM Standard G 38 – 73 (Reapproved 1979), “Standard Practice for Making and Using C-Ring Stress-Corrosion Test Specimens,” ASTM.

35. K. Norring, J. Engstrom, and P. Norberg, “Intergranular Stress Corrosion Cracking in Steam Generator Tubing, Testing of Alloy 690 and Alloy 600 Tubes,” Proceedings of 3rd International Symposium on Environmental Degradation of Materials in Nuclear Power Systems – Water Reactors, Traverse City, MI, 1987. pp. 587-593.

36. K. Norring, J. Engstrom, and H. Tornblom, “Intergranular Stress Corrosion Cracking Steam Generator Tubing. 25,000 hours Testing of Alloy 690 and Alloy 600,” Proceedings of 4th International Symposium on Environmental Degradation of Materials in Nuclear Power Systems – Water Reactors, Jekyll Island, GA, 1989. pp.12-1 to 12-10.

37. K. Norring, K. Stiller, and J. Nilsson, “Grain Boundary Microstructure, Chemistry, and IGSCC in Alloy 600 and Alloy 690,” Proceedings of 5th International Symposium on Environmental Degradation of Materials in Nuclear Power Systems – Water Reactors, Monterey, CA, 1991. pp. 482-487.

38. T.M. Angeliu, J.K. Sung, and G.S. Was, “The Role of Carbon and Chromium on the Mechanical and Oxidation Behavior of Nickel-Based Alloys in High Temperature Water,” Proceedings of 5th International Symposium on Environmental Degradation of Materials in Nuclear Power Systems – Water Reactors, Monterey, CA, 1991. pp. 475-481.

39. J.K. Sung and G.S. Was, “The role of Grain Boundary Chemistry in Pure Water Intergranular Stress Corrosion Cracking of Ni-16Cr-Fe Alloys,” Proceedings of 4th International Symposium on Environmental Degradation of Materials in Nuclear Power Systems – Water Reactors, Jekyll Island, GA, 1989. pp.6-25 to 6-37.

40. Nakayama, H. Tomari, K. Fujiwara, K. Shimogori, H. Hamada, and K. Takaishi, “GC/IGSCC and General Corrosion Behavior of Alloy 800 As a PWR S/G Tube Material," Corrosion 87, Paper No. 82, NACE, March 1987.

41. M.J. Psaila-Dombrowski, J.M. Sarver, P.E. Doherty, W.G. Schneider, “Evaluation of Weld Metal 82 and Weld Metal 152 Stress Corrosion Cracking Susceptibility,” Proceedings of 7th International Symposium on Environmental Degradation of Materials

in Nuclear Power Systems – Water Reactors, Breckenridge, Colorado, 1995, pp. 81 to 91.

42. M.J. Psaila-Dombrowski, C.S. Wade, J.M. Sarver, W.A. Van Der Sluys, and P.E. Doherty, “Evaluation of Weld Metals 82, 152, 52, and Alloy 690 Stress Corrosion Cracking and Corrosion Fatigue Susceptibility,” Proceedings of 8th International Symposium on Environmental Degradation of Materials in Nuclear Power Systems – Water Reactors, Amelia Island, FL, 1997. pp. 412 to 421.

43. N. Ogawa, T. Nakashiba, R. Umehara, S. Okamoto, and T. Tsuruta, “PWSCC Susceptibility Tests for Improving Primary Water Chemistry Control,” Proceedings of 8th International Symposium on Environmental Degradation of Materials in Nuclear Power Systems – Water Reactors, Amelia Island, FL, 1997. pp. 395 to 401.

44. M.G. Angell, S.J. Allan, and G.P. Airey, “The Effect of Primary Coolant Zinc Addition on the SCC Behavior of Alloy 600 and 690,” Proceedings of 9th International Symposium on Environmental Degradation of Materials in Nuclear Power Systems – Water Reactors, Newport Beach, CA, 1999, pp. 97 to 102.

45. C. Raquet, C. Dufour, G. Watilliaux and D. Besnard, CEA Technical Report RT-SCCME 618 Rev. A, 2002, "Résistance a la CSC en milieu primaire REP de matériaux tubulaires en alliage 690 soumis to une déformation globale constante", (English translation of the title, "Resistance of Alloy 690 Tubular Products to Stress Corrosion Cracking in PWR Primary Water at Constant Deformation").

46. F. Vaillant, EDF Report HT-44/95/013/A, 1996, "Résistance a la corrosion sous contrainte en milieu primaire des alliages 690 et 800 – Point des résultats en Décembre 1995", (English translation of the title, "Resistance of Alloys 690 and 800 to Stress Corrosion Cracking in PWR Primary Water – Status of Results Available to December 1995").

47. J-D. Mithieux and F. Vaillant, EDF Report HT-44/97/020/A, 1997, "Influence de la teneur en chrome et de la structure des alliages de nickel sur leur comportement en corrosion sous contrainte en milieu primaire de REP", (English translation of the title, " Influence of Chromium Content and Microstructure of Nickel Base Alloys on Their Stress Corrosion Behavior in PWR Primary Water").

48. J-P Saulay and J-M Boursier, EDF Report HT-29/02/001/A, 2002, "Influence des états de surface sur la propagation lente des fissures de corrosion sous contrainte: Comportement des alliages 600 et 690 en milieu primaire REP", (English translation of the title "Influence of Surface Condition on the Slow Propagation Stage of Stress Corrosion Cracking: Behavior of Alloys 600 And 690 in PWR Primary Water".

49. F. Vaillant, J.D. Mithieux O. de Bouvier, D. Vancon, G. Zacharie, Y. Brechet, and F. Louchet “Influence of Chromium Content and Microstructure on Creep and PWSCC

Resistance of Nickel Base Alloys," Proceedings of 9th International Symposium on Environmental Degradation of Materials in Nuclear Power Systems – Water Reactors, Newport Beach, CA, 1999, pp. 251 to 260..

50. J.M. Boursier, F. Vaillant, , P. Saulay, Y. Brechet, and G. Zacharie, "Effect of the Strain Rate on the Stress Corrosion Cracking in High Temperature Primary Water: Comparison Between the Alloys 690 and 600," Proceedings of the 11th International Symposium on Environmental Degradation of Materials in Nuclear Power Systems – Water Reactors, American Nuclear Society, 2003.

51. F. Vaillant, " EDF Report HT-44/98/016/A, 1998, "Métaux déposés base nickel contenant 15 to 30% de chrome: bilan des essais de corrosion en milieu primaire", (English translation of the title "Nickel Base Weld Deposits Containing 15 To 30% Chromium: Status of Corrosion Tests In Primary Water").

52. G. Sui, G.B. Heys, and J. Congleton, "Stress Corrosion Cracking of Alloy 600 and Alloy 690 in Hydrogen/Steam and Primary Water Side Water," Proceedings of 8th International Symposium on Environmental Degradation of Materials in Nuclear Power Systems – Water Reactors, Amelia Island, FL, 1997. pp. 274 to 281.

53. G. Sui, J.M. Titchmarsh, G.B. Heys, and J. Congleton, "Stress Corrosion Cracking of Alloy 600 and Alloy 690 in Hydrogen/Steam at 380^{o}C," Corrosion Science, Vol. 39, No.3, pp. 565-587, 1997.

54. R.J. Jacko, R.E. Gold, and A. Kroes, "Accelerated Corrosion Testing of Alloy 52M and Alloy 182 Weldments," Proceedings of the 11th International Symposium on Environmental Degradation of Materials in Nuclear Power Systems – Water Reactors, American Nuclear Society, 2003.

55. G.V. Rao, R.J. Jacko, and A.R. McIlree, "An Assessment of the CRDM Alloy 600 Reactor Vessel Head Penetration PWSCC Remedial Techniques", Proceedings, Contributions of Materials Investigation to the Resolution of Problems Encountered in Pressurized Water Reactors, Fontevraud V, pp. 93-105, SFEN, September 2002.

56. C.M. Brown and W.J. Mills, "Fracture Toughness, Tensile and Stress Corrosion Cracking Properties of Alloy 600, Alloy 690, and Their Welds in Water," paper 90, Corrosion 96, NACE, 1996.

57. C.M. Brown and W.J. Mills "Effect of Water on Mechanical Properties and Stress Corrosion Behavior of Alloy 600, Alloy 690, EN82H Welds, and EN52 Welds," Corrosion, v55(2), February 1999.

58. W.J. Mills and C.M. Brown, "Fracture Behavior of Nickel-based Alloys in Water," Ninth International Conference on Environmental Degradation of Materials in Nuclear Power Systems--Water Reactors, August 1-5, 1999, Newport Beach, CA, TMS/NACE.

59. D.M. Symons, “The Effect of Carbide Precipitation on the Hydrogen-Enhanced Fracture Behavior of Alloy 690,” Met. Trans. A, Vol. 29A, pp. 1265-1277, April 1998.

60. I. Lenartova, "Fragilisation par hydrogène et corrosion sous contrainte d'alliages de nickel et d'un acier inoxydable utilisés dans les générateurs de vapeur: influence de la composition chimique et de la microstructure" (English translation: "Hydrogen Embrittlement of Nickel Base Alloys And A Stainless Steel Used in Steam Generators: Influence of Chemical Composition and Microstructure"), PhD thesis, Ecole Centrale de Paris, 1996,

61. NUREG/CR-6335, “Fatigue Strain-Life Behavior of Carbon and Low-Alloy Steels, Austenitic Stainless Steels, and Alloy 600 in LWR Environments,” by J. Keisler, O.K. Chopra, and W.J. Shack of Argonne National Laboratory (ANL-95/15), 1995.

62. EPRI Report TR-105714-V1R4, “PWR Primary Water Chemistry Guidelines, Volume 1 and 2”, revision 4, March 1999.

63. G.P. Airey, ”The Stress Corrosion Cracking (SCC) Performance of Inconel Alloy 600 in Pure and Primary Water Environments”, Proceedings of the (1st) International Symposium on Environmental Degradation of Materials in Nuclear Power Systems – Water Reactors, pp. 462-478, NACE, 1983.

64. EPRI Report 1006695, “Materials Reliability Program Crack Growth Rates for Evaluating Primary Water Stress Corrosion Cracking (PWSCC) of Thick-Wall Alloy 600 Materials (MPR-55) Revision 1,” Final Report, November 2002.

65. EPRI Report TR-111993, “Crack Growth of Alloy 182 Weld Metal in PWR Environments,” Final Report, January 1999.

66. “The New Weibull Handbook,” 2nd Ed., Dr. Robert .B. Abernethy, Author and Publisher, July 1996.

67. “Steam Generator Reference Book,” EPRI TR-103824s-V1R1, December 1994.

68. “Experience of U.S. and International Steam Generators with Alloy 600TT and Alloy 690TT Tubes and Sleeves,” EPRI Document No. 1003589, 2002.

69. “NRC Bulletin No. 89-01: Failure of Westinghouse Steam Generator Tube Mechanical Plugs,” U.S. Nuclear Regulatory Commission, Washington, D.C. May 15, 1989.

70. Turluer, G., et al., “The French Regulatory Experience and Views on Nickel-Base Alloy PWSCC Prevention and Treatment,” Conference on Vessel Head Penetration Inspection, Cracking and Repairs Sponsored by U.S. Nuclear Regulatory Commission

and Argonne National Laboratory, Sept. 29 to Oct. 2, 2003; Marriott Washingtonian Center, Gaithersburg, Maryland.

71. J.I. Bennetch, G.E. Modzelewski, L.L. Spain, and G.V. Rao, “Root Cause Evaluation and Repair of Alloy 82/182 J-Groove Weld Cracking of Reactor Vessel Head Penetrations at North Anna Unit2,” PVP2002-1189, PVP-Vol. 437, Service Experience and Failure Assessment Applications, ASME 2002.

72. W.H. Bamford, et al., “The Embedded Flaw Process for Repair of Reactor Vessel Head Penetrations and Its Application at North Anna Unit 2,” WCAP-15986, Westinghouse Electric Company LLC, 2003.

73. NRC Information Notice 2003-11, Supplement 1, “Leakage Found on Bottom-Mounted Instrumentation Nozzles,” US NRC, January 8, 2004.

74. G.A. Young, N. Lewis, and D.S. Martin, “The Stress Corrosion Crack Rate of Alloy 600 Heat Affected Zone Exposed to High Temperature Purity Water,” Conference on Vessel Head Penetration Inspection, Cracking and Repairs Sponsored by U.S. Nuclear Regulatory Commission and Argonne National Laboratory, Sept. 29 to Oct. 2, 2003; Marriott Washingtonian Center, Gaithersburg, Maryland.

75. Coriou, H. et al.: Proc. Conf. Fundamental Aspects of SCC ; ed. By R.W. Staehle et al.; NACE Houston 1977; p. 352.

76. Coriou, H. et al.: Third Metallurgy Symposium on Corrosion; Amsterdam; 1960; pp. 161-166.

77. Coriou, H. et al.: Corrosion NACE 22; 1966; pp. 280-290.

78. Shah, V.N.; Lowenstein, D.B.; Turner, A.P.L.; Ward, S.R.; Gorman, J.A.; MacDonald, P.E.; Weidhammer, G.H.: Assessment of Primary Water Stress Corrosion Cracking of PWR SG Tubes; Nuclear Engineering and Design134; 1992; pp 199-215.

79. Bouecke R., Odar S., Stellwag B.: Operating Experience with SGs ; Service Report Power Plants, December 1989, p 4-10.

80. Latanison R.M., Staehle R.W.: Stress Corrosion Cracking of Iron-Nickel-Chromium Alloys, Proc. Symposium on Fundamental Aspects of Stress Corrosion Cracking, NACE, Houston 1969, pp 214-296.

81. Shen Y., Shewmon P.G.: A Mechanism for Hydrogen Induced Stress Corrosion Cracking In Alloy 600, Metal Trans A. 21A (1990), pp 2161 – 1271.

82. Szklarzka-Smialowska Z., Xia Z., Valbuena R.P.: Mechanism of Crack Growth in Alloy 600 In High Temperature Deaerated Water, Corrosion, 50 (1994), pp 676 – 681.

83. Sung J., Was G.S.: The Role of Grain Boundary Chemistry in Pure Water Intergranular Stress Corrosion Cracking Of Ni-16Cr-9Fe Alloys, Proc Fourth International Symposium On Environmental Degradation Of Materials In Nuclear Power Systems – Water Reactors, NACE; Jekyll Island, Georgia 1989, Pp 625 – 636.

84. Scott P.M., Le Calvar M.: Some Possible Mechanisms of Intergranular Stress Corrosion Cracking of Alloy 600 in PWR Primary Water, Proc Sixth International Symposium on Environmental Degradation of Materials in Nuclear Power Systems – Water Reactors, The Metallurgical Society, San Diego, CA, 1993, pp 657 – 665.

85. G. Economy; R.J. Jacko; J.A. Begley; F.W.: Pement; Westinghouse Corporation EPRI Workshop, Mechanisms of Primary Eater IGSCC; Alexandria, VA; April 1987.

86. Gimond, C.: Recent Corrosion Results; from Proceedings1989 EPRI Alloy 690 Workshop, New Orleans, 12-14 April 1989; EPRI NP-6750M (1990).

87. McIlree, A.; Ruud, C.O.; Pement, F.W.; Ed: Theus, G.J.; Weeks, J.R.: The Description of Residual and Applied Stresses and SCC of Row 1 Steam Generator U-Bends; Proc. of 3rd Int. Symposium on Environmental Degradation of Materials in Nuclear Power Systems - Water Reactors, The Metallurgical Society, Inc., Warrendale, PA,1988, p. 555.

88. B.P. Miglin, and C.E. Shoemaker, “A Comparison of the Stress Corrosion Cracking Behavior of Alloys 600 and Alloy 690 in AVT Water,” Corrosion 86, Paper Number 255, NACE, 1986.

89. J.R. Crum and T. Nagashima, “Review of Alloy 690 Steam Generator Studies,” Proceedings of 8th International Symposium on Environmental Degradation of Materials in Nuclear Power Systems – Water Reactors, Amelia Island, FL, 1997. pp. 127 to 137.

90. ASTM Standard G 38 – 73 (Reapproved 1979), “Standard Practice for Making and Using C-Ring Stress-Corrosion Test Specimens,” ASTM.

91. J.M. Sarver, J.V. Monter, B.P. Miglin, “The Effect of Thermal Treatment on the Microstructure and SCC Behavior of Alloy 600,” Proceedings of 4th International Symposium on Environmental Degradation of Materials in Nuclear Power Systems – Water Reactors, Jekyll Island, GA, 1989. pp.5-47 to 5-63.

92. F. Vaillant, D. Buisine, and B Prieux, “Comparative Behavior of Alloys 600, 690, and 800 in Caustic Environments,” Proceedings of 7th International Symposium on Environmental Degradation of Materials in Nuclear Power Systems – Water Reactors, Breckenridge, Colorado, 1995, pp. 219 to 231.

93. D.A. Mertz, P.T. Duda, P.N. Pica, G.L. Spahr, “Role of Microstructure in Caustic

Stress Corrosion Cracking of Alloy 690," Proceedings of 7th International Symposium on Environmental Degradation of Materials in Nuclear Power Systems – Water Reactors, Breckenridge, Colorado, 1995, pp. 477 to 494.

94. H. Kawamura, H. Hirano, S. Shirai, H. Takamatsu, T. Matsunaga, K. Yamaoka, K. Oshinden, and H. Takiguchi, "Role of Grain Boundary Characteristics in Caustic IGA/SCC Resistance of Thermally-Treated Alloy 690 and Shot-Peened Alloy 800," Proceedings of 9th International Symposium on Environmental Degradation of Materials in Nuclear Power Systems – Water Reactors, Newport Beach, CA, 1999, pp. 601 to 610.

95. H.P. Kim, Y.S. Lim, and J.S. Kim, "Stress Corrosion Cracking of Alloy 600 in 0.1M $NaHSO_4$ and NaOH Solution," Proceedings of 10th International Symposium on Environmental Degradation of Materials in Nuclear Power Systems – Water Reactors, Lake Tahoe, NV, 2001.

96. M.L. Castano-Marin, D. Gomez-Briceno, and F. Hernandez-Arroyo, "Influence of Lead Contamination on the Stress Corrosion Resistance of Nickel Alloys," Proceedings of 6th International Symposium on Environmental Degradation of Materials in Nuclear Power Systems – Water Reactors, San Diego, CA, 1993, pp. 189 to 196.

97. M. Helie, "Lead Assisted Stress Corrosion Cracking of Alloys 600, 690, and 800," Proceedings of 6th International Symposium on Environmental Degradation of Materials in Nuclear Power Systems – Water Reactors, San Diego, CA, 1993, pp. 179 to 188.

98. P. Berge, D. Noel, J-M Gras, and B. Prieux, "Chloride Stress Corrosion Cracking of Alloy 600 in Boric Acid Solution," Proceedings of 8th International Symposium on Environmental Degradation of Materials in Nuclear Power Systems – Water Reactors, Amelia Island, FL, 1997, pp. 189 to 199.

99. W.H. Cullen, M.J. Patridge, J.A. Gorman, and J.P.N. Paine "IGA/IGSCC of Alloy 600 in Acidic Sulfate and Chloride Solutions," Proceedings of 5th International Symposium on Environmental Degradation of Materials in Nuclear Power Systems – Water Reactors, Monterey, CA, 1991. pp. 780-788.

100. W.H. Cullen, M.J. Patridge, and J.P.N. Paine "Corrosion of Alloy 600 & 690 in Acidified Sulfate and Chloride Solutions" Proceedings of 6th International Symposium on Environmental Degradation of Materials in Nuclear Power Systems – Water Reactors, San Diego, CA, 1993, pp. 197 to 203.

101. O.D. Bouvier, B. Prieux, and F. Vaillant, "Nickel Alloy Stress Corrosion Cracking in Neutral and Lightly Alkaline Sulfate Environments," Proceedings of 9th International Symposium on Environmental Degradation of Materials in Nuclear Power Systems – Water Reactors, Newport Beach, CA, 1999, pp. 695 to 701.

102. O.D. Bouvier, F. Vaillant, M. Bouchacourt, and P. Lemaire “Effect of Copper Species on IGA/SCC of Alloy 600 in Neutral Sulfate Environments,” Proceedings of 10th International Symposium on Environmental Degradation of Materials in Nuclear Power Systems – Water Reactors, Lake Tahoe, NV, 2001.

About EPRI

EPRI creates science and technology solutions for the global energy and energy services industry. U.S. electric utilities established the Electric Power Research Institute in 1973 as a nonprofit research consortium for the benefit of utility members, their customers, and society. Now known simply as EPRI, the company provides a wide range of innovative products and services to more than 1000 energy-related organizations in 40 countries. EPRI's multidisciplinary team of scientists and engineers draws on a worldwide network of technical and business expertise to help solve today's toughest energy and environmental problems.

EPRI. Electrify the World

1009801

Printed on recycled paper in the United States of America

EPRI • 3412 Hillview Avenue, Palo Alto, California 94304 • PO Box 10412, Palo Alto, California 94303 • USA
800.313.3774 • 650.855.2121 • askepri@epri.com • www.epri.com